Department of Molecular and Clinical Pharmacology

Institute of Translational Medicine

University of Liverpool

&

Inflammation and Immunology Research Unit

Pfizer Worldwide Research and Development

"A study of the molecular pharmacological properties of C5a and C5a des Arg: defining their biased agonist profile and contrasting biological function".

Thesis submitted in accordance with the requirements of the University of Liverpool for the degree of Doctor in Philosophy by:

Simeon Jon Ramsey

October 2017

Declaration

This thesis is the result of my own work. The material contained within this thesis has not been presented, nor is currently being presented, either wholly or in part for any degree or other qualification.

All research was conducted in the laboratories at Pfizer Worldwide Research and Development, 610 Main Street, Cambridge, Massachusetts, USA.

Simeon Ramsey

Student number: 201001573

Table of contents

List of figures

Chapter 1. Introduction

Chapter 3. The characterization of reagents and pharmacological tools to enable accurate interrogation of C5a, C5a des Arg and their receptors, $C5a_1$ and $C5a_2$

Chapter 4. Characterization of a C5a sensitive biological test system, the human isolated neutrophil

Chapter 5. Assessing the relative functional activity of the complement system peptides, C5a and C5a des Arg

Chapter 6. Defining the mechanism of C5a des Arg induced biased agonism

Chapter 7. Final discussion

List of tables

List of equations

Abstract

The complement system provides an essential role in the orchestration of an effective immune response against microbial infection. Activation leads to the generation of C5a which activates receptors expressed on immune cells promoting microbial clearance. Dysregulation of the complement system that results in the excessive production of C5a can lead to host tissue damage. This has fuelled drug discovery efforts to therapeutically block the actions of C5a to treat diseases associated with dysregulation of the complement system. C5a is rapidly degraded to C5a des Arg, a mechanism which is considered to inactivate its effector functions, however, there is incomplete understanding of precise functions of C5a and C5a des Arg on the cognate C5a receptors, $C5a_1$ and $C5a_2$. The research conducted here attempted to improve upon this understanding as well as fuel future drug discovery efforts that target this component of the complement system.

Functional assays using human isolated neutrophils or engineered cell lines along with $C5a_1$ and $C5a_2$ receptor selective antagonists were employed to assess the contribution of each C5a receptor to functional responses elicited by human purified C5a and C5a des Arg. For each functional endpoint investigated, the relative activity of C5a des Arg was compared with C5a using the $\Delta Log(E_{max}/EC_{50})$ transformation. Single point mutagenesis was performed on the $C5a_1$ receptor to relate differences in agonist functional activity to mode of agonist binding.

The data presented here supports the hypothesis that C5a des Arg behaves as a biased agonist in relation to C5a. Via the $C5a_1$ receptor, C5a des Arg produces neutrophil phenotypes that are involved in the orchestration of immune cell recruitment to sites of infection. However, unlike C5a, C5a des Arg does not induce a respiratory burst response that leads to the generation of hypochlorous acid. The biased agonism of C5a des Arg appears to be brought about by its inability to interact with amino acid residues within the seventh transmembrane domain of the $C5a_1$ receptor, which prevents the receptor recruitment of β-arrestins. Furthermore, data presented here also show that the $C5a_2$ receptor does not directly contribute to C5a

or C5a des Arg mediated activation of the human isolated neutrophil. Taken together, the data support a hypothesis whereby the generation of C5a des Arg, through $C5a_1$ receptor, limits the ability of C5a to promote the production of potentially damaging respiratory burst while still enabling immune cell extravasation.

Acknowledgements

I would like to thank several colleagues, mentors, friends and family members who made the completion of this project possible.

Firstly, I would like to express my sincere gratitude to my original industry advisor, Dr Cara Williams. Her passion for developing others and her enthusiasm for science was instrumental in helping me identify this opportunity to fulfil both a life and career goal.

I would like to thank my friend and industry advisor Dr Nicholas Pullen. His scientific rigor and timely feedback helped me stay on track and finish this project in a respectable timeframe.

Thanks to my University of Liverpool advisors. Professor David MacEwan, who provided continual support and encouraged me to follow the science that excited me the most. Dr Jean Sathish, whose efforts were pivotal in establishing this transatlantic relationship between the University of Liverpool and Pfizer.

My friend and collaborator Dr Terry Kenakin, who provided a great deal of support and encouragement during the course of this project and enabled me to express my ideas with mathematical equations.

My Pfizer colleagues; Michael Cain, Tim Chamberlain, Ye Che, Julia Guzova, Scott Jelinsky, Peter Jones, Elizabeth Murphy, Michael Primiano, Julia Shin, Jean-Baptiste Telliez and Aaron Winkler for their technical support, scientific discussion and review of this thesis.

My parents Janice and Malcolm Ramsey, for their continual love and support. My mother who encourages me to believe “it’s not where you start it where you finish” and my father who continually reminds me that “there is no excellence without difficulty”. Also my parents-in-law, Tony and Lesley Lill, for offering words of encouragement throughout the course of this project.

I dedicate this thesis to my beautiful wife, Suzy, and two wonderful children Ruby and Olivia. They packed me off to work every Sunday with love, smiles and words of encouragement and were my rock of support in completing these studies.

Finally I would like to thank Pfizer as the sponsor of this project who, for the second time, have enabled me to continue my professional education.

Abbreviations

aHUS: Atypical haemolytic uremic syndrome

Ala: Alanine (A)

AMD: Age related macular degeneration

ANCA: Anti-neutrophil cytoplasmic antibody

ANOVA: Analysis of variance

APC: Allophycocyanin

Arg: Arginine (R)

Asp: Aspartic acid (D)

AUC: Area under the curve

BCA: Bicinchoninic acid

BSA: Bovine serum albumin

C1INH: C1 inhibitor

C3GN: C3 glomerulonephritis

C4BP: C4 Binding protein

Ca^{2+}: Calcium ion

$CaCl_2$: Calcium chloride

cAMP: Cyclic adenosine monophosphate

CD: Cluster of differentiation

cDNA: complementary DNA

CFH: Complement factor H

CFHL1: CFH-like protein 1

CFHRP: Complement factor H related protein

Cha: Cyclohexylalanine

CHO: Chinese hamster ovary

Ci: Curie

CLP: Cecal ligation and puncture

CP: Carboxypeptidase

CPM: Counts per minute

CR: Complement receptor

CRD: Carbohydrate recognition domain

DAF: Decay accelerating factor

DAG: Diacylglycerol

DAMP: Damage associated molecular pattern

DDD: Dense deposit disease

DHR: Dihydrorhodamine

DNA: Deoxyribonucleic acid

DPM: Disintegrations per minute

EC_{50}: Concentration of agonist that produced 50% of it maximal response

EDTA: Ethylenediaminetetraacetic acid

E_{max}: Maximum response induced by an agonist in relation to the full agonist for that receptor

ERK: Extracellular signal-regulated kinases

FB: Factor B

FBG: Fibrinogen-like domain

FBS: Foetal bovine serum

FD: Factor D

FI: Factor I

FITC: Fluorescein Isothiocyanate

FP: Factor P (properdin)

FPR1: Formyl peptide receptor 1

GAPDH: Glyceraldehyde-3-phosphate dehydrogenase

GFP: Green fluorescent protein

Gln: Glutamine (Q)

Glu: Glutamic acid (E)

Gly: Glycine (G)

GM-CSF: Granulocyte macrophage colony stimulating factor

GPCR: G-protein coupled receptor

H_2O: Water

H_2O_2: Hydrogen peroxide

HAE: Hereditary angioedema

HBSS: Hanks balanced salt solution

HEPES: 4-(2-hydroxyethl)-1-piperazineethanesulfonic acid

HOCl: Hypochlorous acid

IC_{50}: Concentration of antagonist that reduces the effect of an agonist by 50%

IgAN: IgA nephropathy

IP_3: Inositol trisphosphate

K: Equilibrium dissociation constant for a ligand-receptor interaction.

K_A: Agonist equilibrium dissociation

K_B: Antagonist equilibrium dissociation

K_d: Equilibrium dissociation constant for a ligand determined directly (directly labelled ligand usually quantified in a receptor ligand binding assay

K_i: Equilibrium dissociation constant for a ligand determined in inhibition studies.

L: Litre

LDS: Lithium dodecyl sulphate

Leu: Leucine (L)

LN: Lupus nephritis

LPS: Lipopolysaccharide

Lys: Lysine (K)

m: Milli

M: Molar

mAb: Monoclonal antibody

MAC: Membrane attack complex

MAPK: Mitogen-activated protein kinase

MASP: Mannose binding lectin associated serine protease

MBL: Mannose binding lectin

MCP: Membrane co-factor protein

Met: Methionine

$MgCl_2$: Magnesium chloride

mM: Millimolar

MOPS: 3-(N-morpholino) propanesulfonic acid

MPO: Myeloperoxidase

NADPH: Nicotinamide adenine dinucleotide phosphate

nM: Nanomolar

Orn: Ornithine

pA_2: The negative logarithm of the concentration of antagonist which produces a twofold shift of the agonist dose-response curve

PAMP: Pathogen associated molecule pattern

PBS: Phosphate-buffered saline

PCR: Polymerase chain reaction

PE: Phycoerythrin

PEI: Polyethylenimine

Phe: Phenylalanine (F)

PI3K: Phosphatidylinositide 3-kinases

PKA: Protein kinase A

PKC: Protein kinase C

PLC: Phospholipase C

pM: Picomolar

PNH: Paroxysmal Nocturnal Hemoglobinuria

PRM: Pattern recognition molecule

Pro: Proline (P)

PRR: Pattern recognition receptor

RA: Rheumatoid arthritis

RIPA: Radioimmunoprecipitation assay

RNA: Ribonucleic acid

ROS: Reactive oxygen species

RT-PCR: Reverse transcription polymerase chain reaction

S.D.: Standard deviation of the mean

S.E.M.: Standard error of the mean

Ser: Serine (S)

SLE: Systemic lupus erythematosus

SNP: Single nucleotide polymorphism

SOD: Superoxide dismutase

Thr: Threonine (T)

TM: transmembrane

TNFα: Tumour necrosis factor alpha

Trp: Tryptophan (W)

U2OS: Human osteosarcoma cell line

v/v: volume/volume

WT: Wild type

µ: Micro

µM: Micromolar

^{125}I: Iodine-125

^{3}H: Tritium

Chapter 1

Introduction

1. Introduction

Multicellular organisms have developed highly sophisticated defence mechanisms to combat the effects of pathogens and microbial infection that threaten normal homeostasis. These defence mechanisms are collectively known as the immune system and consist of a complex network of cells and chemical mediators, each with a specialized role to defend against microbial infection (Delves *et al.*, 2000).

For an infection to occur, a microbe must first breach the organism's anatomical barriers that face the external environment and subsequently evade destruction by host derived antimicrobial substances located on or within these physical surfaces. If entry is successful, the microbe will encounter the next level of defence, the immune system which can be broadly divided into two components depending on the speed and specificity of the response that is launched (Parkin *et al.*, 2001). The rapidly responding innate immune system launches an immediate assault through the recognition of generic microbial patterns. In contrast, the adaptive immune system, although slower to respond, delivers a tailored response to specific microbial antigens, a response which becomes imprinted within the memory of the immune system (figure 1.1).

The innate immune system consists of cells of myeloid origin which possess germline-encoded receptors which detect highly conserved molecular patterns that are shared by a broad set of pathogenic microbes. Activation of these pattern recognition receptors (PRRs) by pathogen associated molecular patterns (PAMPs) orchestrates microbial clearance by promoting an inflammatory response. Basophils, mast cells and eosinophils release inflammatory mediators, including cytokines, which promote the activation and recruitment of effector cells including macrophages, monocytes, neutrophils and natural killer cells which phagocytose and destroy the microbe, restoring sterility (Janeway *et al.*, 2002).

The adaptive immune system consists of cells of lymphoid origin including T and B lymphocytes. Unlike the cells of the innate immune system, lymphocytes are not preprogramed to respond to generic pathogen associated molecular patterns.

Instead each lymphocyte expresses a unique antigen specific receptor which was somatically generated by the random rearrangement of genes encoding the variable region of these receptors. B cells are responsible for the humoral adaptive response involving the production of highly specific antibodies while T cells are responsible for the cell-mediated adaptive response. Although this random generation of receptors leads to the detection of an almost infinite number of antigens, these receptors alone, unlike those of the innate immune system, are unable to determine the origin of their ligands. This biological context is provided by antigen presenting cells (dendritic cells and macrophages) which present self and non-self antigens to T cells using the major histocompatibility complex (MHC) class of proteins along with either co-stimulatory or co-inhibitory signal. T-cell activation leads to the clonal expansion of that T-cell, orchestration of antigen specific antibody production from B-cells and results in long term immunological memory to that antigen (Janeway, 2001).

The key attributes of an effective immune response are discrimination between foreign and self surfaces and the speed of the response, so that an infection is adequately contained. Although the cellular components of the immune system produce an antimicrobial response within minutes to hours of an infection occurring, there is a component of the innate immune system which has the ability to respond within seconds. This immediately acting element is known as the complement system. An evolutionary conserved stalwart of the innate immune system, its routes can be traced as far back as echinoderms with origins over 600 million years ago (Smith *et al.*, 1996). This facet of the innate immune system consists of a tightly regulated network of proteins that orchestrate the rapid clearance of pathogens by opsonisation, recruiting phagocytic cells to the site of infection and inducing the rapid lysis of microbes through the complement derived membrane attack complex (MAC) (Patel *et al.*, 1987).

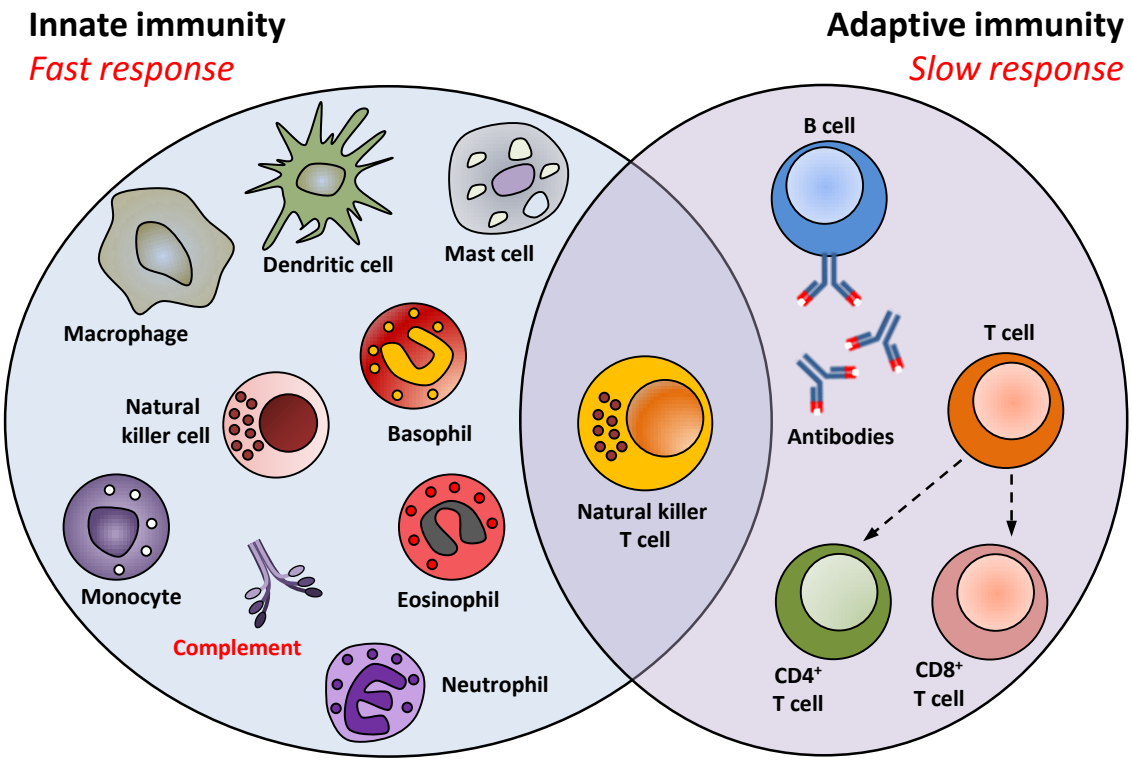

Figure 1.1. Components of the innate and adaptive immune responses

The immune system can be broken down into two components based on the speed and specificity of the response that is launched. The rapid and generic innate immune response is orchestrated by cells of myeloid origin which include monocytes, macrophages, dendritic cells, basophils, eosinophils, neutrophils and natural killer cells. The innate immune response also includes the complement system which consists of a network of soluble and membrane bound proteins that facilitate the actions of the innate immune response. The adaptive immune response, which is slower to respond, launches a tailored, specific immune response with memory. It consists of cells of lymphoid origin including B cells which release antigen specific antibodies and $CD4^+$ and $CD8^+$ T cells which possess antigen specific receptors. Natural killer T cells, which share properties of both natural killer cells and T cells, contribute to both innate and adaptive immune responses. Figure recreated from Dranoff (2004).

1.1. Overview of the complement system

The discovery of the complement system is attributed to a Belgian scientist, Jules Bordet, who, while working at the Pasteur Institute in the late 1890's, demonstrated that bacteriolysis only occurred in the presence of two serum factors. A thermo-stable factor present in the serum of immunized animals (antibodies), and a thermo-labile factor that had been earlier discovered and named Alexin (Greek - 'to ward off') by Hans Buchner (Morrison, 1922). Later the term Komplement, originally coined by Paul Ehrlich, the renowned German physician scientist, gained greater traction among research scientists and has survived to this day in its anglicized form, complement (Kaufmann, 2008). Nonetheless, it would be several decades before scientists realized that complement exists as a complex mixture of labile and stable constituents that act in succession to induce an immune response.

The complement system is now recognized to comprise more than 30 soluble plasma proteins and glycoproteins as well as membrane bound receptors and regulatory proteins (Walport, 2001). A number of these proteins exhibit protease activity but are secreted as inactive zymogens that are activated locally, at sites of infection. These, in turn, cleave and activate other complement zymogens to trigger a series of potent pro-inflammatory events. This triggered response, which is initiated by the activation of a small number of complement proteins at the start of the pathway, leads to an amplification of enzymatic activity at each successive stage, resulting in the rapid generation of a disproportionately large inflammatory response. Ultimately, a set of complement effector proteins are produced that can 1) opsonize pathogens for uptake by phagocytes, 2) cause direct lysis of cells through the assembly of a membrane attack complex (MAC) or 3) recruit additional phagocytic cells to the site of infection through the chemoattractant properties of certain liberated complement peptides (McCaughan et al., 2013).

1.2. The pathways of complement activation

The complement system consists of a set of inactive proteins that are sequentially linked in a cascading manner. Upon stimulation of the complement system, zymogens become active, causing the cleavage of substrates which yield effector molecules and opsonisation factors, leading to the activation of the next enzyme in the cascade. Activation of the complement system occurs through three main pathways: 1) the classical pathway activated by antigen-antibody complexes and so named because it was the first complement activation pathway to be described in detail (Dodds, 2002), 2) the lectin-binding pathway, initially described in the 1980's by Kawakami *et al.* (1982) that is initiated by soluble carbohydrate-binding proteins and 3) the alternative pathway, that is initiated by spontaneous hydrolysis and activation of the complement component C3 (Pillemer *et al.*, 1954) (figure 1.2). Since complement activation occurs in a sequential manner, involving proteins that are secreted as inactive zymogens, the system is finely tuned to rapidly and selectively activate at sites of pathogen invasion (Sarma *et al.*, 2011). This sequential manner of complement system activation can be divided into 4 main steps: 1) initiation of complement activation, 2) generation of C3 convertase and system amplification, 3) generation of C5 convertase leading to the production of C5a and 4) terminal pathway activity producing the MAC (Zipfel *et al.*, 2009). Although activation of the complement system leads to the indiscriminate delivery of effector molecules to both host and microbial surfaces, system amplification is tightly controlled by a series of regulatory and inhibitory proteins (figure 1.2).

While the initial activation of each pathway occurs via a different mechanism, all three pathways converge at the point of C3 convertase as highlighted below.

1.2.1. The Classical pathway

The classical activation pathway, so named because it was the first complement pathway to be discovered, is built upon nine central components, C1-9 which were

numbered in the order in which they were discovered and not the order in which they feature in the system. It is primarily activated through the binding of the C1q protein to a pathogen surface or to antigen bound immunoglobulin (Ig) IgG or IgM. The tail of the C1q protein binds two copies of the serine proteases C1r and C1s which, together, form the C1 complex. Binding to antigen bound antibody induces a conformational change in C1q which activates C1r. C1r then cleaves C1s to generate an active serine protease which splits C4 into a smaller C4a fragment and a larger C4b fragment (Lorincz *et al.*, 2000). C4b, which contains a labile thioester bond, subsequently attaches to the pathogen surface (Law et al., 1997). The C2 protein binds to C4b and is split by the C1 complex. The smaller fragment, C2b, dissociates leaving C2a bound to C4b generating the classical pathway C3 convertase, C4bC2a.

The nomenclature of the proteins that make up the classical pathway C3 convertase can often cause confusion. This comes from the inconsistency in the designation of the fragments of the C2 protein. The smaller of the two fragments generated from the cleavage of C3, C4 and C5 is typically given the designation 'a' and the larger 'b' however this nomenclature is not maintained in the naming of the C2 fragments. The cleavage of C2 by activated C1s was first demonstrated by Stroud *et al.* (1966) with guinea pig C2 and Muller-Eberhard *et al.* (1967) with human C2. Since their initial attempts failed to detect the smaller C2 fragment, the designation of C2a was given to the detected cleaved protein. Further work by Nagasawa *et al.* (1977) and Kerr *et al.* (1978) saw the successful identification of both large and small fragments of the cleaved C2 protein with apparent molecular weights of 74,000 and 34,000 Da respectively. Remaining consistent with the previous nomenclature of C2a, the smaller identified fragment was referred to as C2b. However, both C4bC2a and C4bC2b are frequently used to refer to the classical C3 convertase and there does not seem to be correlation between naming convention and the author's geographical location. Throughout the remainder of this thesis I will use the original nomenclature for the classical complement system C3 convertase of C4bC2a.

C3 convertase cleaves C3 into two fragments. The smaller fragment, C3a, acts as a potent anaphylatoxin via activating the cell surface C3a receptor, while the larger C3b fragment acts as an opsonin. Through the transient exposure of a reactive

thioester bond, C3b covalently binds to hydroxyl groups present on cell surfaces, immune complexes and complex carbohydrates. Microorganisms decorated with C3b are detected by phagocytic cells via the complement receptors, engulfed and then destroyed. If no covalent bond is formed, the thioester is rapidly hydrolysed resulting in the inactivation of C3b (Sahu *et al.*, 2001).

As well as its opsonisation function, C3b also complexes with the previously formed C3 convertase to produce the multimeric complex, C5 convertase (C4bC2aC3b) (Pangburn *et al.*, 2002). C5 convertase cleaves C5 to yield the small peptide fragment, C5a and the large fragment C5b. Like C3a, C5a is a potent anaphylatoxin which mediates an inflammatory response through binding and activating C5a receptors expressed on structural cells and cells of the immune system. C5b initiates the late events of complement activation by complexing with complement proteins C6 and C7. The C5bC6C7 scaffold contains hydrophobic phospholipid-binding sites and upon attachment to cellular membranes acts as a receptor for the subsequent binding of C8. The tetramolecular complex containing C5bC6C7C8 induces the binding of several C9 monomers which polymerize to form the lytic pore known as the MAC. The function of the MAC is to promote rapid microbial lysis. (Podack et al., 1982; Muller-Eberhard, 1985).

1.2.2. The Lectin pathway

The lectin pathway is functionally similar to the classical pathway. It is activated when conserved carbohydrates on the surfaces of pathogens are detected by a set of soluble pattern recognition molecules (PRMs). These include members of the collectin family, such as mannose-binding lectin (MBL) and the ficolin family, including H-ficolin, L-ficolin and M-ficolin (Kjaer *et al.*, 2013). Collectins are characterized by a collagen-like region and a C-type carbohydrate recognition domain (CRD) in their C-terminus that specifically recognizes monosaccharides exposing OH groups, present in mannose. Likewise, the polypeptide chain of ficolins contains a short N-terminal and a collagen-like domain, but in this case, the C-

terminal recognition domain is a fibrinogen-like domain (FBG) instead of the CRD. The FBG has affinity for N-acetylated carbohydrate structures as seen in N-acetyl-D-glucosamine (GlcNAc), but will also bind other acetylated molecules, such as acetylated-albumin or acetylated glycine (Lu *et al.*, 2002).

These PRMs associate with mannose binding lectin associated serine protease (MASP) family members, MASP-1, MASP-2 and MASP-3. MASPs are secreted as inactive zymogens and bind to collectins and ficolins at which point they become activated. Although MASP-1 cannot initiate the lectin pathway on its own, it plays a crucial role in the activation of MASP-2 which, in turn cleaves C4 into C4a and C4b facilitating exposure of the C4b thioester bond. As a result C4b covalently binds to surfaces within the immediate vicinity where it then binds one molecule of C2. C2 is in turn cleaved by MASP-2, producing C2a, which remains bound to C4b, forming the lectin mediated C3 convertase, C4bC2a. As a consequence, the C3 convertase of the lectin pathway is identical to that generated by the classical pathway (Matsushita *et al.*, 2001).

1.2.3. The Alternative pathway

The alternative pathway is evolutionally the oldest facet of the mammalian complement system (Nonaka *et al.*, 2006). It was first discovered by Pillemer *et al.* (1954) who named it the Properdin system, after one of the fundamental proteins that makes up this part of the complement system. However, it later became known as the alternative system due to the alternative activation mechanism that initiates this pathway compared with the classical pathway. This pathway exhibits two unique features; its ability to be spontaneously activated and its distinct C3 convertase. It also contains some components that are not found in the classical and lectin pathways such as factor B (FB), factor D (FD) and properdin (factor P, FP).

The alternative pathway is capable of auto-activation due to a low level of constitutive generation of a hydrolysed C3 product, C3(H_2O), a process that is referred to as 'tick over' (Lachmann *et al.*, 1975). The hydrolysis of the thioester

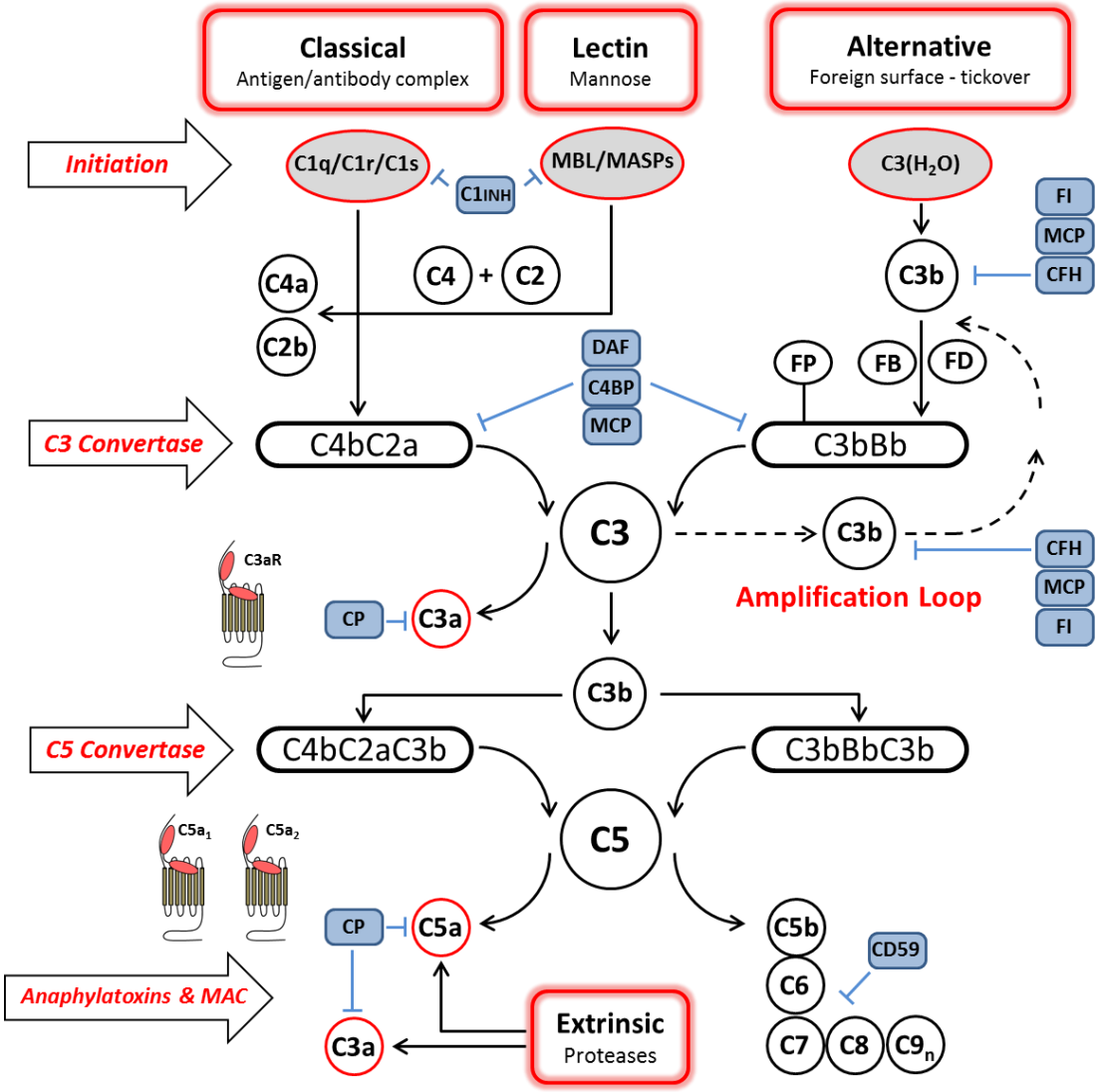

Figure 1.2. The pathways of the complement system

Activation of the Classical pathway occurs via the detection of antibody bound antigen complexes by the C1-complex of proteins. Similarly, the Lectin pathway is activated upon the detection of conserved carbohydrates on the surfaces of pathogens by mannose binding lectin (MBL) and associated serine protease (MASP) complex. This results in the cleavage of C4 and C2 to form C3 convertase. The Alternative pathway is activated by a spontaneous 'tick-over' mechanism which leads to the generation of C3(H_2O). Factor B (FB), factor D (FD) and properdin (FP) promote the generation of the alternative pathway C3 convertase which cleaves C3 into C3a and C3b. C3a binds the C3a receptor while C3b binds to C3 convertase to form C5 convertase which cleaves C5 into C5a and C5b. C5a binds to and activates C5a receptors while C5b initiates the formation of the membrane attach complex (MAC). Proteases of the coagulation and fibrinolysis systems and those release by cells can cleave C3 and C5 and represent an Extrinsic pathway. Regulatory proteins (shown in blue) direct the activation of the complement system to microbial and damaged host cell surfaces; (C1 inhibitor - C1INH, C4 binding protein - C4BP, CD59 - protectin, complement factor H - CFH, factor I - FI, membrane cofactor protein - MCP, decay accelerating factor - DAF, carboxypeptidase - CP).

within C3 promotes the recruitment of FB, in a Mg^{2+}-dependent manner, which consequently becomes susceptible to cleavage by the serine protease, FD. This causes the release of the peptide fragment Ba and the generation of the fluid phase C3 convertase, C3(H_2O)Bb (Williams *et al.*, 1994). This fluid phase C3 convertase splits C3 into C3a and C3b, the latter of which covalently binds to adjacent cells surfaces though its exposed thioester bond. Surface bound C3b again recruits FB which is also cleaved by FD generating the surface bound alternative pathway C3 convertase, C3bBb. On its own this alternative pathway C3 convertase is very short lived. However, it can be stabilized by binding to FP, a plasma protein that is synthesized and stored in the granules of neutrophils and released upon their activation (Wirthmueller *et al.*, 1997). Stabilized C3 convertase is able to cleave more C3, leading to further surface accumulation of C3b and the production of more C3 convertase. This positive feedback cycle involving the exponential production of C3 convertase is known as the 'amplification loop' of the complement system (Lachmann, 2009). Excess production of C3b gradually leads to the formation of the alternative pathway C5 convertase (C3bBbC3b) and shifts the substrate specificity away from C3 and towards C5. As with the classical and lectin pathways, C5 convertase cleaves C5, yielding the potent anaphylatoxin C5a and C5b which initiates the formation of the MAC.

This remarkable amplification of the complement system involving proteins for the alternative pathway has been shown to account for 80-90% of C5 activation even when the initial activation is highly specific for the classical pathway (Harboe *et al.*, 2008).

1.2.4. The Extrinsic mechanism of complement activation

The intrinsic mechanisms of complement system activation via the classical, lectin and alternative pathways are considered to be the main biochemical routes leading to the release of amplification and effector molecules from C3 and C5. However, in recent years it has become apparent that non-complement serine proteases residing

in the plasma or released from cells, are able to directly cleave these proteins and contribute to the so called extrinsic complement pathway. Huber-Lang *et al.* (2002), demonstrated that activated phagocytic cells (human neutrophils or rat alveolar macrophages), in the presence of exogenous C5, were able to generate a biologically active C5a. With the use of specific protease inhibitors (soybean trypsin inhibitor and secretory leukocyte protease inhibitor), they determined that serine proteases, released from these cells, were responsible for the cleavage of C5. Work performed by others suggests that the enzyme released from leukocytes responsible for the cleavage of C5 is human leukocyte elastase (Ward *et al.*, 1970; Wetsel *et al.*, 1983).

There is a reasonable amount of evidence to suggest that serine proteases of the coagulation and fibrinolysis systems are also able to induce the local complement activation. In the absence of C3, Huber-Lang *et al.* (2006) demonstrated that thrombin, the coagulation pathway serine protease responsible for fibrin production and thrombus formation, is able to generate a biologically active C5a in the presence of C5. Similarly Amara *et al.* (2010) found that plasmin, the serine protease of the fibrinolysis pathway, responsible for breaking down the thrombus fibrin matrix, is also able to generate biologically active anaphylatoxins in the presence of C3 and C5. This apparent cross talk between the complement, coagulation and fibrinolysis pathways is thought to be critical in regulating thrombus formation. The localized production of complement by thrombin and plasmin provides a role in both thrombus formation and thrombus resolution. Neutrophils and monocytes recruited to the site of tissue damage by C5a release mediators such as proteases and nucleosomes which provide a scaffold for platelet aggregation and thrombus stabilization. C5a also promotes the release of other chemotactic factors that recruit phagocytic cells to assist in thrombus breakdown and clearance (Foley *et al.*, 2016). In the thrombotic microangiopathy disorder, atypical hemolytic uremic syndrome (aHUS), the production of C5a appears to be out of balance leading to excessive renal capillary and arteriole inflammation. This over production of C5a may be due, in part, to the actions of thrombin and plasmin but may also be exacerbated by plasmin's ability to locally generate C3b. Failure to regulate C3b, which is also generated from the tick-over of the alternative pathway, is a genetic phenotype of

many aHUS patients and contributes to excessive C5a production, leading to extreme capillary and arteriole inflammation which often results in acute renal failure (Noris *et al.*, 2015).

1.3. Regulatory proteins of the complement system

Activation of the complement system leads to the potentially deleterious, non-specific deposition of effector molecules onto local surfaces. To discriminate between self and non-self surfaces, the complement system also consists of numerous regulatory proteins. Regulation of the complement system occurs at different stages of activation by molecules that are present in both the fluid phase and on the surface of cells. These regulators work in a tight balance to precisely control the location and degree of complement activation. Changes in the function or expression of any one of the regulatory components can lead to complement dysregulation and disease.

With the exception of properdin, which is the only known positive regulator of the complement system, all regulatory proteins reduce complement system propagation and potency of effector molecules. Starting at the activation stage of the complement system, C1-inhibitor (C1INH), an acute phase protein, limits pathway initiation by binding to the serine proteases C1r and C1s of the classical pathway and MASP-1 and MASP-2 of the lectin pathway (Hansen *et al.*, 2015). If pathway activation progresses beyond this point, the formation of C3 convertase can be inhibited by C4-binding protein (C4BP). This soluble protein binds to C4b and facilitates its cleavage by acting as a cofactor for the serine protease, factor I (FI) (Blom *et al.*, 2004).

A similar brake is applied to the functions of C3b of the alternative pathway by complement factor H (CFH) family of proteins. This group of soluble plasma proteins includes CFH, CFH-like protein 1 (CFHL1) and the complement factor H related proteins (CFHR1-5). A common feature of these proteins is their composition of individual domains called short consensus repeat domains (SCR), with the C-terminal

domains recognizing and anchoring to host surfaces, and the N-terminal domains recognizing C3b, promoting its destabilization. All proteins contain heparin binding regions (Skerka *et al.*, 2013). CFH and CFHL1 are the only two proteins to possess a four SCR regulatory region at their N-terminus. This regulatory region provides two functions; to act as a co-factor for FI, which cleaves C3b to the inactive iC3b, C3dg or C3d, and to promote the destabilization and decay of C3 convertase.

The five CFHR proteins lack this regulatory region and based on their sequence homology are divided into two groups. Group one contains CFHR1, 2 and 5 which display a highly conserved N-terminus and circulate as dimers, and group two includes CFRH3 and 4, which lack the ability to form dimers, yet share sequence homology with CFH in a heparin binding region of the protein (Skerka *et al.*, 2013). CFHR1 can not only bind to C3b of C5 convertase and prevent the cleavage of C5, but it can also disrupt the formation of the MAC. CFHR2 binds to C3b and prevents the formation or C3 convertase and inhibits the amplification loop. The complete actions of CFHR5 are not fully understood but it appears to bind to C3b and iC3b in a similar fashion to CFH and provide cofactor activities to FI (Goicoechea de Jorge *et al.*, 2013). Similarly, the complete actions of CFHR3 and CFHR4 are not fully characterized. They are believed to bind both C3b and C3d and provide cofactor activity to FI and CFH (Hellwage *et al.*, 1999). Interestingly, CRHR1, 3 and 5 have been shown to bind C3b in a competitive manner to CFH promoting its displacement from C3b (Fritsche *et al.*, 2010).

Two other proteins can also regulate the actions of the complement system at the level of C3b. Membrane cofactor protein (MCP, CD46) binds to C3b and C4b providing cofactor activity to FI facilitating their cleavage and inactivation (Liszewski *et al.*, 1991). Similarly decay accelerating factor (DAF, CD55), binds to both C3b and C4b preventing the formation of new and accelerates the decay of preformed C3 and C5 convertases (Lublin *et al.*, 1989).

There are four cell surface bound regulatory receptors that, upon recognition of cell deposited complement products, induce responses by effector cells. Complement receptor 1 (CR1, CD35) expressed on erythrocytes and phagocytic cell promotes the

clearance of C3b opsonized immune complexes. Activation of CR1 expressed on lymphocytes has been shown to regulate their proliferation and differentiation (Jozsi *et al.*, 2002; Wagner *et al.*, 2006). Complement receptor 2 (CR2, CD21) is expressed primarily on B cells where it forms a complex with CD19 and CD81. Activation of CR2 by fragments of C3 which include iC3b, C3dg and C3d, enhances B cell receptor activation (Asokan *et al.*, 2013). Both CR3 (CD11b/CD18) and CR4 (CD11c/CD18) belong to the β2 integrin family of adhesion molecules and are expressed on the surface of monocytes and many other phagocytic cells. Activation by iC3b or C3dg mediates the binding and phagocytosis of complement bound cells (Vik *et al.*, 1987; Law, 1988).

Finally, two other proteins that can regulate the effects of the complement system are Protectin (CD59) and carboxypeptidases (CP). Protectin is expressed on the surface of many host cells including erythrocytes and epithelial cells where it prevents the formation of the MAC, inhibiting its lytic activity (Meri *et al.*, 1990). CPs, specifically CPN, hydrolyse a bond at the carboxy-terminal of C3a and C5a that leads to the removal of the terminal arginine resulting in their inactivation (Skidgel *et al.*, 2007).

The majority of the soluble components of the complement system are synthesized and secreted into the bloodstream by hepatocytes (Morris *et al.*, 1982). However, hepatocytes are not the only source of complement protein production. Figure 1.3 highlights some of the cellular and tissue gene expression patterns of many soluble and membrane bound proteins of the complement system.

1.4. Disorders associated with the complement system

The extensive set of regulatory proteins ensures that the complement system focuses its actions on invading pathogens or damaged host cells. However, if the expression or function of any of these proteins is altered in any way, the effector functions of the complement system may damage host cells and lead to disease

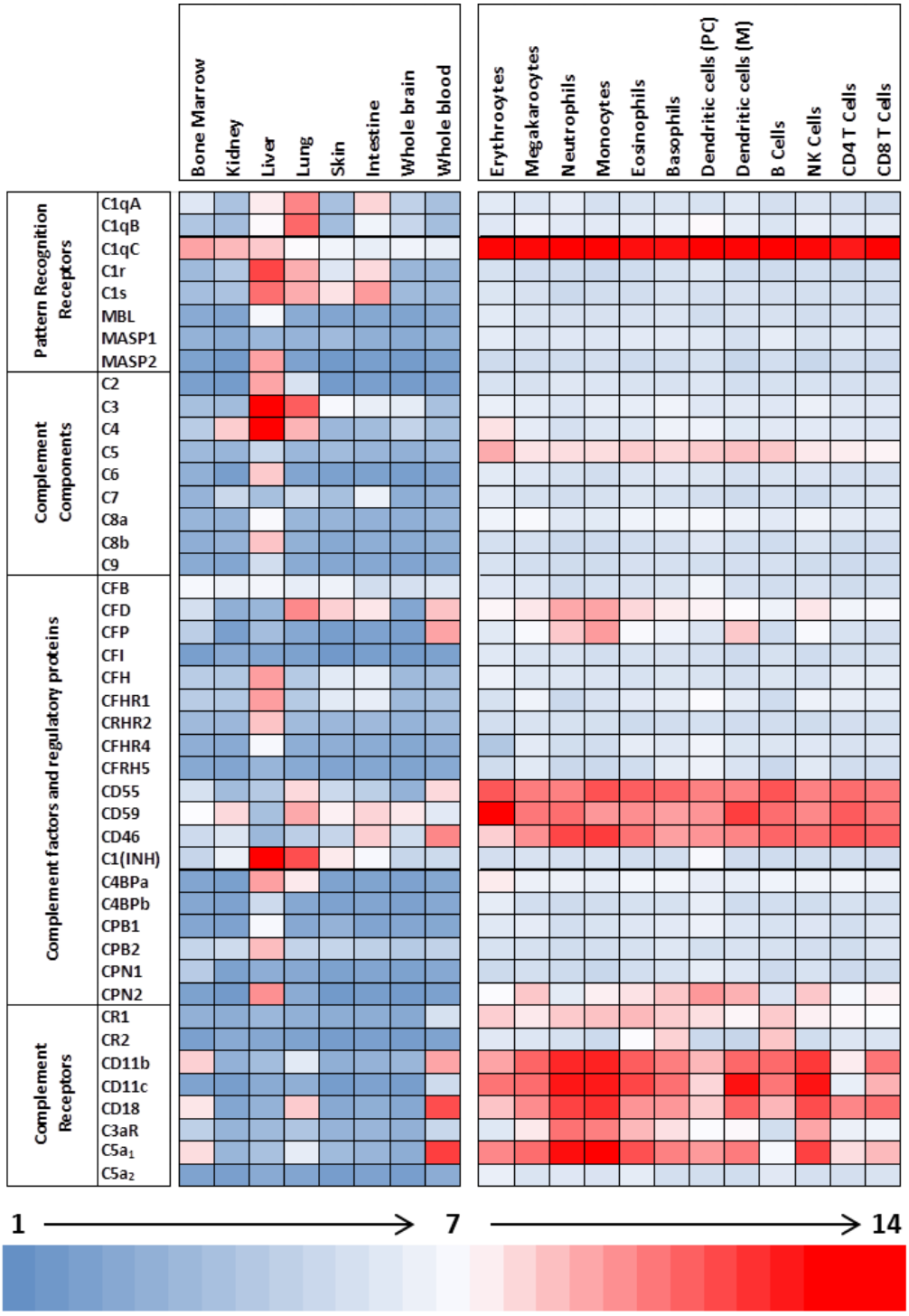

Figure 1.3. Cellular and tissue gene expression of complement proteins

Table represent mRNA expression values of proteins of the complement system. Normal tissue expression is derived from BioGPS (Wu *et al.*, 2009). Normal human hematopotic cell expression is derived from the DMAP database (Huang *et al.*, 2015). Scale represents $\log_2$ gene expression values.

(Morgan *et al.*, 2015). A dysfunctional complement response can occur due to inherited genetic mutations, that alter complement protein expression or function, or because of acquired auto-antibodies, that either neutralize or stabilize complement proteins. In some instances, the genetic deficiency of non-complement proteins, that provide a supporting role to complement system proteins, can also lead to disease. This is evident from the genetic mutation of the glycosylphosphatidylinositol anchor in hematopoietic stem cells which leads to paroxysmal nocturnal hemoglobinuria (PNH). Mutations in this protein prevent the attachment of protectin and DAF to the surface of erythrocytes, resulting in the failure to regulate MAC formation which leads to their lysis (Rother *et al.*, 2007). There are many examples in the literature of inherited or acquired alterations of complement proteins that cause disease (Morgan et al., 2015), some of which are outlined in table 1.1.

There is a great deal of evidence to suggest that over activation or dysregulation of the complement systems is involved in the pathogenesis of rheumatoid arthritis (RA) and the syndrome of sepsis. These two disorders have received a great deal of attention from the pharmaceutical industry and the role of the complement system in driving these disorders is outlined below.

1.4.1. Complement and rheumatoid arthritis

RA is a chronic autoimmune disease which is characterized by synovial inflammation, autoantibody production, cartilage and bone destruction leading to joint deformity, and systemic features, including cardiovascular, pulmonary, psychological, and skeletal disorders. Affecting over 1% of the western population (Alamanos et al., 2006) RA is regarded as a common multi-factorial chronic inflammatory disorder that involves an interaction between genetic and environmental factors (McInnes et al., 2011). Over activation of the complement system and excessing joint recruitment of neutrophils is implicated in the pathogenesis of RA.

Several studies investigating the presence of complement activation products in the joint fluid of RA patients have observed significant increases in C5a concentrations compared with fluid taken from healthy volunteers and osteoarthritis patients (Jose et al., 1990; Hogasen et al., 1995b). Production of C5a enhances the recruitment of neutrophils into the joint space where they propagate the inflammatory response and exacerbate joint destruction. This is achieved through the release of degrading enzymes, reactive oxygen species, cytokines and chemokines which enhances the recruitment of other immune cells (Wright et al., 2014). Evidence for the role of the complement system driving the pathogenesis of RA also comes from experimental models of arthritis. Antibodies to either C5 or $C5a_1$ receptor both produce disease amelioration in mouse, collagen induced arthritis models (Wang et al., 1995; Andersson et al., 2014).

There are several genetic variations in complement proteins which appear to predispose patients to RA. Single nucleotide polymorphisms (SNP) of the C1q gene are associated with increased protein levels and appear to be linked to a greater susceptibility for developing RA (Trouw et al., 2013). From genome wide association studies, identification of a TRAF1-C5 locus on chromosome 9 has been associated with an increased risk for RA (Plenge et al., 2007). Focusing on a coding SNP within this locus, which causes a mutation at V802I in C5, Giles et al. (2015) noted this mutant C5 was more susceptible to cleavage by elastases found within the joints of RA patients. This in turn would lead to enhanced joint C5a levels and lead to greater neutrophil recruitment maintaining joint inflammation.

1.4.2. Complement and sepsis

Sepsis is defined as life-threatening organ dysfunction caused by a dysregulated host response to infection (Singer et al., 2016). Sepsis is a syndrome where patients can present with a constellation of different physiological, pathological, and biochemical symptoms. If unregulated and allowed to progress, the syndrome can develop from initial systemic inflammation to septic shock and on to organ dysfunction, eventually

leading to death. With around 600,000 cases of sepsis in the US each year, this syndrome places a huge burden on the health care system and accounted for more than $20 billion of total US hospital costs in 2011 (Singer et al., 2016). There have been more than 100 clinical trials conducted to test the efficacy of agents designed to modify systemic inflammation, many of which have targeted microbial endotoxin, their innate receptors or the slew of cytokines that are released during sepsis (TNF, IL-1). However, none of these trials have resulted in new treatments for this devastating syndrome (Marshall, 2014).

There is a large body of evidence from human investigations and experimental models suggesting that over activation of the complement system is implicated in the pathophysiology of sepsis. The excessive systemic production of C5a rapidly activates neutrophils resulting in tissue damage and subsequent paralysis immune system. In preclinical models of sepsis, systemic C5a concentrations have been shown to increase, which correlates with a loss in in $C5a_1$ receptor expression on neutrophils (Riedemann et al., 2002a; Guo et al., 2003). Prophylactic administration of neutralizing antibodies to either C5a or $C5a_1$ receptor, or $C5a_1$ receptor small molecule antagonist have all improved animal survival in these models (Czermak et al., 1999; Huber-Lang et al., 2002b).

Activation of the complement system during sepsis has also been demonstrated in a clinical setting. Circulating concentrations of C5a in septic patients have been reported to be as high as 5 nM (Younger et al., 2010). Similar to preclinical observations, Unnewehr et al. (2013) noted that in a clinical setting, circulating concentrations of C5a increased 5 fold during severe sepsis, which correlated with a loss of neutrophil $C5a_1$ receptor expression. Interestingly, these authors noted that the degree of $C5a_1$ receptor loss from neutrophils correlated with mortality, suggesting that over stimulation of the C5a-$C5a_1$ receptor axis on neutrophils promotes immune system paralysis and results in death. These experimental model and clinical data provide a strong body of evidence suggesting that modulators of the C5-$C5a_1$ receptor axis could provide benefit to patients who develop sepsis.

Complement component	Abnormality	Complement system consequence	Associated disorders	Reference
Loss of function				
C1INH	Genetic deficiency	Failure to regulate CS and coagulation pathways preventing vascular homeostasis.	HAE/AMD	(Carugati *et al.*, 2001; Ennis *et al.*, 2008)
C1q/r/s	Genetic deficiency	Failure to activate CP and clear immune complex	SLE	(Pickering *et al.*, 2000)
	Anti-C1q antibody	Failure to activate CP and clear immune complex	SLE/LN	(Orbai *et al.*, 2015)
C2	Genetic deficiency	Failure to activate CP and clear immune complex	SLE/RA/Infection	(Glass *et al.*, 1976; Hussain *et al.*, 2007)
C4	Genetic insufficiency	Failure to activate CP and clear immune complex	SLE	(Yih Chen *et al.*, 2016)
MBL	Genetic deficiency	Failure to activate LP and opsonize microbes	Infection	(Super *et al.*, 1989)
FH	Genetic deficiency	Loss of FH mediated C3b regulation – excessive activation of AP leading to inflammation	C3GN, DDD, AMD, IgAN	(Hageman *et al.*, 2005; Maillard *et al.*, 2015; Zhu *et al.*, 2015)
	Anti-FH antibody	Neutralization of FH preventing C3b regulation – excessive activation of AP leading to inflammation	aHUS	(Blanc *et al.*, 2012)
FI	Genetic deficiency / insufficiency	Failure to inactivate C3b – excessive CS activation leading to inflammation	aHUS	(Bienaime *et al.*, 2010)
MCP	Genetic insufficiency	Reduced affinity for C4b and C3b - excessive CS activation leading to inflammation	aHUS	(Liszewski *et al.*, 2015)
FP	Genetic deficiency	Failure to activate AP and opsonize microbes	Infection	(Linton *et al.*, 1999)
Gain of function				
C3bBb (C3 convertase)	Anti-C3 convertase (C3 nephritic factor)	Stabilization of C3 convertase – excessive AP activation	DDD	(Servais *et al.*, 2012)
FB	Genetic gain of function	Stabilization of C3 convertase – excessive AP activation	DDD, aHUS	(Goicoechea de Jorge *et al.*, 2007)
	Anti-FB antibody	Stabilization of C3 convertase – excessive AP activation	DDD	(Strobel *et al.*, 2010)
C3	Genetic gain of function	Reduced regulation by MCP – excessive CS activation	aHUS	(Lhotta *et al.*, 2009)

Table 1.1. Inherited and acquired dysfunctions of complement system proteins

Examples of inherited and acquired alterations on complement system proteins. In many incidences, the gain or loss of complement system protein function is associated with the pathogenesis of disease. (Complement system – CS, Classical pathway – CP, Lectin pathway – LP Alternative pathway – AP, Hereditary angioedema – HAE, Age related macular degeneration – AMD, Systemic lupus erythematosus – SLE, Lupus nephritis – LN, Rheumatoid arthritis – RA, C3 glomerulonephritis – C3GN, Dense deposit disease – DDD, IgA nephropathy – IgAN, Atypical hemolytic uremic syndrome – aHUS).

1.5. C5a and the cleaved isoform C5a des Arg

As described above, all three complement pathways lead to the generation of C5 convertase (Rawal *et al.*, 2001). Proteolytic cleavage of an arginine-leucine bond at position 74-75 in the α-chain of C5 leads to the generation of the potent anaphylatoxin C5a and C5b, which initiates the formation of MAC. (DiScipio *et al.*, 1983). C5a consists of four alpha helices linked by peptide loops and contains three disulphide bridges between cysteine residues at positions 21-47, 22-54 and 34-55. (Manthey *et al.*, 2009). The C-terminal residues 69-74, are considered to contain all of the agonist properties of C5a (Ember *et al.*, 1992). C5a binds to and activates two members of the G protein-coupled receptor (GPCR) family of cell surface proteins, the $C5a_1$ and $C5a_2$ (Alexander *et al.*, 2013). Activation of C5a receptors orchestrates a plethora of leukocyte actions which contribute to the immune response. These include; integrin up regulation (Weber *et al.*, 1996), chemotaxis (Snyderman *et al.*, 1971), respiratory burst (Sacks *et al.*, 1978b), NETosis (Martinelli *et al.*, 2004), enhanced cytokine release (Riedemann *et al.*, 2002), phagocytosis (Mollnes *et al.*, 2002) and cell degranulation leading histamine release, the latter of which contributes to the anaphylactic properties of C5a (Regal *et al.*, 1983).

The potent inflammatory effects of C5a are regulated as described earlier, by members of the CP family of enzymes, specifically CPB and CPN, which remove the C-terminal arginine by hydrolysis, generating C5a des Arg. The inactivation of C5a is very rapid and has been reported to be complete within two minutes in human serum (Bokisch *et al.*, 1970). With this in mind, although the majority of analytical methods used to quantify concentrations of the peptide fragments of C5 are unable to distinguish between C5a and C5a des Arg, the vast majority of C5a in the circulation is considered to be that of the des arginated isoform (Fernandez *et al.*, 1976; Mueller-Ortiz *et al.*, 2009). Removal of C5a and C5a des Arg from the circulation is believed to be mediated through binding to C5a receptors expressed on leukocytes (Oppermann *et al.*, 1994).

Original methods employed to assess the functional activity of C5a and C5a des Arg, focused on the contraction of guinea pig ileum, release of histamine from mast cells

and the wheal and flare response (Vogt *et al.*, 1969; Vallota *et al.*, 1973). It was not until researchers directly compared the activity of these two C5 derived peptides in other cell based assay systems, that it became apparent that C5a des Arg retains a significant degree of activity. Fernandez *et al.* (1978b) demonstrated that C5a des Arg, although approximately 10 fold weaker than C5a at inducing a chemotactic response of human isolated neutrophils, was able promote the migration of a larger number of cells. Using an *in vitro* assay to measure the adhesion of human isolated neutrophils to human umbilical vein endothelial cells, Tonnesen *et al.* (1984) discovered that C5a des Arg was able to promote a comparable response to that of C5a. Interestingly, in contrast to C5a, this group also observed that C5a des Arg was unable to induce the release of myeloperoxidase (MPO) from human neutrophils, a mechanism which may be comparable with the release of histamine from mast cells.

With these data in mind, it appears that, although the anaphylactic properties of C5a are lost when the C-terminal arginine is removed, C5a des Arg retains certain functional activities. Given the plethora of cellular responses that have been described for C5a and the increasing availability of biochemical and phenotypic assays, an extensive investigation characterizing the full signalling potential of C5a des Arg in relation to C5a would be a worthwhile endeavour. Such data would help the scientific community better understand the functional role of C5a des Arg and its contribution to the pathogenesis of diseases that are associated with over activation of the complement system.

1.6. The two C5a receptors

As previously mentioned, C5a and C5a des Arg mediate their actions through binding to and activating two members of the GPCR superfamily of receptors, the $C5a_1$ (formerly known as CD88 and C5aR) and the $C5a_2$ (formerly known as GPR77 and C5a-like receptor 2, C5L2). Both of these receptors belong to the rhodopsin-like (class A) sub-family and are encoded by adjacent genes in cluster q13.3 of chromosome 19. The $C5a_1$ receptor is the larger of the two consisting of 350 amino

acids compared with 337 for the $C5a_2$ receptor. Although originally considered to be confined to cells of myeloid lineage, including neutrophils, monocytes and mast cells, the expression of the C5a receptors has been demonstrated in many other cell and tissue types including brain, lung, heart and kidney (Monk *et al.*, 2007). However, their expression on lymphocytes still remains controversial (Dunkelberger *et al.*, 2010). Although the $C5a_1$ receptor was cloned in 1991 (Boulay *et al.*, 1991; Gerard *et al.*, 1991), it was not until 2000 that the $C5a_2$ receptor was discovered (Ohno *et al.*, 2000). Despite these two receptors sharing a low overall sequence homology of 35%, both peptide ligands are able to bind these two receptors with relatively high affinity. Researchers at the University of Sheffield (Cain *et al.*, 2002) reported that the binding affinity of C5a to $C5a_1$ and $C5a_2$ is comparable (IC_{50} values of 19 and 10 nM respectively) and while C5a des Arg has a much reduced affinity for $C5a_1$, it retains high affinity for $C5a_2$ (IC_{50} values of 412 and 37 nM respectively).

One key difference between the $C5a_1$ and $C5a_2$ receptors is in their ability to couple to G-proteins. The $C5a_1$ receptor has been shown to couple to heterotrimeric G-proteins leading to changes in intracellular cAMP and calcium (Buhl *et al.*, 1993). However, activation of the $C5a_2$ receptor does not lead to productive coupling of G-proteins which is thought to be due to lack of the highly conserved aspartic acid-arginine-tyrosine/phenylalanine (DRY/F) motif found in the third transmembrane domain (Okinaga *et al.*, 2003).

1.6.1. The multi domain interaction between C5a and its receptors

The mechanism by which C5a and C5a des Arg interact with the $C5a_1$ receptor has been revealed to be highly complex involving multiple ligand-receptor domains. Like many peptidergic GPCRs, the binding of the peptide ligand to the receptor involves both the hydrophilic N-terminal and a binding pocket formed by the transmembrane domains (TM) of the receptor. With the use of N-terminal specific antibodies (Oppermann *et al.*, 1993) and receptor mutagenesis (DeMartino *et al.*, 1994), researchers were able to demonstrate that this negatively charged, aspartic acid rich

region of the $C5a_1$ receptor contributes to greater than 45% of the total binding energy for C5a. The work also concluded that this region of the receptor did not control receptor activation, as truncated peptides, resembling the C-terminal of C5a, and a N-terminal truncated receptor were still able to promote receptor activation and G-protein coupling. With the data suggesting the involvement of a second site on the receptor, further research focused on the interactions of C5a with the TM region of the receptor.

Several residues within the TM region of the $C5a_1$ receptor have been identified as being critical for the binding and functional responses associated with C5a. Using hexapeptides that resemble the six terminal amino acids of C5a and both calcium mobilization and degranulation assays, DeMartino *et al.* (1995) demonstrated the terminal arginine of C5a contributes heavily to the binding affinity and is essential for receptor activation. Using receptor mutagenesis and altering the charge of the hexapeptide terminal arginine, they were able to demonstrate an electrostatic interaction between this residue and the receptor residue Arg-206, which appears to control the activation state of the receptor.

Subsequent research to map the ligand interaction sites on the $C5a_1$ receptor highlighted the importance of the aspartic acid residue at position 282. Using full length peptides and mutating Asp-282 to alanine, Cain *et al.* (2001) observed a reduction in receptor activation by C5a but not C5a des Arg. Similarly, mutating the terminal arginine on C5a to alanine resulted in the reduction in activation of the wild type receptor. These data confirm the importance of the interaction between Asp-282 and the terminal arginine of C5a and provides an explanation for the typical reduction in potency observed with C5a des Arg at the $C5a_1$ receptor.

A more extensive study to characterize the TM binding regions of the $C5a_1$ receptor was performed by Higginbottom *et al.* (2005). Using both receptor-ligand binding and functional assays, they confirmed the importance of the C5a-arginine and $C5a_1$-Asp-282 interaction. Their work also discovered important ligand interactions with residues Arg-175, Glu-199 and Arg-206 on the $C5a_1$ receptor. This cluster of residues

towards the top of TM 4 and 5 was demonstrated to have minimal impact on the affinity and function of C5a but dramatically affected C5a des Arg.

The interactions of C5a and C5a des Arg with the $C5a_2$ receptor are less well characterized. The inability of peptides that resemble the C-terminus of C5a, to interact with the $C5a_2$ receptor suggests that the core of C5a is most relevant for binding to this receptor. Both mutagenesis and antibody neutralization of the N-terminus of the $C5a_2$ receptor has highlighted amino acid residues that are important for C5a des Arg binding but do not contribute to the affinity of C5a. These data suggest that, similar to the $C5a_1$ receptor, there are probably multiple domains involved in ligand binding to the $C5a_2$ receptor (Klos *et al.*, 2013).

1.6.2. Functional signalling of the $C5a_1$ receptor

Upon binding, C5a induces a change in the conformation of the $C5a_1$ receptor that results in the re-orientation of the transmembrane (TM) domains. The movement of TM7 relieves a constraint on TM6 allowing it to move away from TM3 and the core of the receptor, resulting in the exposure of intracellular receptor binding sites (Gerber *et al.*, 2001). The appearance of these new binding sites promotes the recruitment of heterotrimeric guanine nucleotide-binding proteins (G-proteins), composed of α, β and γ subunits, leading to the activation of the G-protein cycle which comprises the following events. Prior to receptor activation, the G-protein complex exists in an inactive state with the α-subunit bound to GDP. Upon activation, the receptor functions as a guanine nucleotide exchange factor, promoting the exchange of GDP for GTP on the α-subunit. The GTP bound α-subunit dissociates from the $G_{\beta\gamma}$ complex and both elements are able to regulate the activity of intracellular signalling pathways. The G-protein cycle is terminated via intrinsic GTPase activity of the α-subunit, which hydrolyses the terminal phosphate of GTP. The GTPase activity is enhanced by the regulators of G-protein signalling family of proteins promoting re-association of GDP bound α-subunit with the $G_{\beta\gamma}$ complex, completing the G-protein

cycle. Restoration of the inactive G-protein complex allows the cycle to undergo further activation upon receptor stimulation (Milligan *et al.*, 2006).

The $C5a_1$ receptor displays high expression on cells of myeloid origin, including neutrophils, where it has been demonstrated to couple to both pertussis toxin sensitive $G_{\alpha i/o}$-proteins and pertussis toxin insensitive $G_{\alpha 16}$-proteins (Rollins *et al.*, 1991; Amatruda *et al.*, 1993). Activation of $G_{\alpha i/o}$-proteins leads to the negative regulation of adenylate cyclase resulting in a lowering of intracellular cAMP concentration and the regulation of protein kinase A activity. The dissociated $G_{\beta\gamma}$ complex activates phospholipase Cβ (PLCβ) which cleaves phosphatidylinositol 4,5-bisphosphate into inositol trisphosphate (IP_3), which induces the release of Ca^{2+} from intracellular stores, and diacylglycerol (DAG), which activates protein kinase C. The $G_{\beta\gamma}$ complex is also able to activate phosphatidylinositide 3-kinase (PI3K)/Akt (protein kinase B) pathway which is considered to play an important role in cell migration (Hirsch *et al.*, 2000). Both $G_{\alpha i/o}$-protein and $G_{\beta\gamma}$ complex have also been shown to activate the mitogen-activated protein kinase pathway. This pathway includes the protein kinases, Ras, Raf, MEK and eventually leads to the phosphorylation and activation of extracellular signal-related kinase (ERK), regulating gene transcription (Inglese *et al.*, 1995; Mochizuki *et al.*, 1999).

Unlike the $G_{\alpha i/o}$-protein, the $G_{\alpha 16}$-protein, which is a $G_{\alpha q}$ family member and almost exclusively expressed in cells of hematopoietic lineage, couples directly to PLC leading to the generation of IP_3 and DAG (Buhl *et al.*, 1993).

After G-protein activation, the intracellular domain of the $C5a_1$ receptor is phosphorylated by G-protein coupled receptor kinases which promote the recruitment of β-arrestins. The physical presence of these molecules prevents further G-protein association and initiates receptor internalization via clathrin-coated vesicles. However, β-arrestins do not only act to regulate GPCR activity and have been shown to activate ERK in a non G-protein manner (Ahn *et al.*, 2004) (figure 1.4).

As briefly mentioned above, C5a and C5a des Arg orchestrate many cellular functions of human leukocytes including adhesion molecule regulation and chemotaxis. With the use of selective receptor antagonists, researchers have determined that most of

these cellular responses are mediated through the $C5a_1$ receptor (Sumichika *et al.*, 2002; Brodbeck *et al.*, 2008). It is often reported that activation of the $C5a_1$ receptor expressed on neutrophils can also lead to the respiratory burst response. The purpose of the respiratory burst response is to enable phagocytic cells to destroy engulfed microbes and involves a multi-step process. Once a microbe has been engulfed, nicotinamide adenine dinucleotide phosphate-oxidase (NADPH) assembles and leads to the production of superoxide which is subsequently converted to hydrogen peroxide (H_2O_2) by super oxide dismutase. Although H_2O_2 is a reactive oxygen species, its oxidizing capabilities are mild (Halliwell *et al.*, 2000). The full potential of the respiratory burst response is not fully realized until hypochlorous acid (HOCl) is produced from H_2O_2 and chloride anions by myeloperoxidase. HOCl, is highly reactive and has the power to destroy pathogenic microbes via oxidation.

Although the $C5a_1$ receptor is often cited as driving the neutrophil respiratory burst response, the mechanism by which this is achieved is not well understood (Lee *et al.*, 2008). Although receptor activation does lead to MPO release, there is little evidence to suggest that the $C5a_1$ receptor couples directly to the generation of reactive oxygen species. Some data in the literature point to the fact that neutrophils need to be primed before $C5a_1$ receptor can induce certain effector functions (Bajaj *et al.*, 1992; Brodbeck *et al.*, 2008). Further work to elucidate the exact contribution of the $C5a_1$ receptor to the respiratory burst response would help scientist better understand this cellular event, which, when excessively activated can result in tissue damage leading to disease (Jeitner *et al.*, 2016).

1.6.3. The enigmatic role of the $C5a_2$ receptor

Although discovered over 15 years ago, the precise contribution of the $C5a_2$ receptor to C5a and C5a des Arg signalling still remains unclear. Devoid of the capacity to couple to G-proteins, the $C5a_2$ receptor has been shown to be phosphorylated at intracellular domains after C5a activation (Okinaga *et al.*, 2003). Since its discovery, there have been numerous claims as to the precise role of this receptor with both

pro and anti-inflammatory functions being suggested (Li *et al.*, 2013). A summary of the proposed functions of the $C5a_2$ receptor can be found in figure 1.5.

There are several lines of evidence suggesting an anti-inflammatory role for the $C5a_2$ receptor. Using cell lines engineered to overexpress the $C5a_2$ receptor and human isolated neutrophils, Scola *et al.* (2009) suggested that the main function of $C5a_2$ was to act as a recycling decoy receptor, sequestering C5a and preventing the pro-inflammatory activation of the $C5a_1$ receptor. They observed that the majority of $C5a_2$ receptors primarily reside at an intracellular location and undergoes rapid constitutive recycling from the membrane to the intracellular compartment of the cell by a clathrin-dependent mechanism which is agonist independent. With use of a ligand uptake assay, using radiolabelled C5a and C5a des Arg, they observed that the $C5a_2$ receptor was able to remove both ligands from the extracellular space. This uptake into intracellular compartments led to ligand degradation. The majority of their work was performed using engineered or differentiated HL-60 cells. When switching to human isolated neutrophils they observed that although expressed at a very low level at the cell surface, the $C5a_2$ receptor preferentially removed and degraded C5a des Arg with minimal effect on C5a.

An alternative mechanism by which the $C5a_2$ receptor provides an anti-inflammatory role was proposed by Bamberg *et al.* (2010). With their research focused on human isolated neutrophils, they reported that the $C5a_2$ receptor is confined to an intracellular location with no detectable expression at the cell surface. In contrast to the work performed by (Scola *et al.*), they were unable to detect $C5a_2$ receptor mediated ligand uptake, although they only investigated the uptake of C5a. Neutrophil activation by C5a led to both chemotactic activity and ERK phosphorylation, both of which were enhanced in the presence of $C5a_2$ receptor blocking antibody. Using confocal microscopy, they observed that when neutrophils were activated with C5a, the $C5a_1$ and $C5a_2$ receptors co-localized at an intracellular location and that each receptor associated with β-arrestin 1. The $C5a_1$-β-arrestin complex promoted the phosphorylation of ERK while the $C5a_2$-β-arrestin complex did not. Based on these data they proposed that upon activation of the $C5a_1$ receptor,

the $C5a_2$ receptor acts as negative regulator of $C5a_1$ receptor function by competing for β-arrestin, with the net signal being a result of the balance of the two pathways.

In a rat cecal ligation and puncture (CLP) sepsis model, Gao *et al.* (2005) observed an increase in neutrophil $C5a_2$ receptor expression, which was in contrast to the reduction in $C5a_1$ receptor expression. *In vivo* blockade of the $C5a_2$ receptor using a receptor specific antibody resulted in a fourfold increase in IL-6 levels compared with IgG control animals, an observation that was consistent with *in vitro* findings. Similar results were obtained by Gerard *et al.* (2005) who investigated the *in vivo* effects of both C5a and C5a des Arg in a lung injury model. They observed that the targeted deletion of $C5a_2$ receptor dramatically enhanced neutrophil influx into the lung. This finding was further supported with the demonstration that neutrophils from $C5a_2$ knock out animals displayed enhanced chemotactic activity *in vitro.*

There appears to be an equal number of research efforts that have provided evidence for a pro-inflammatory role for the $C5a_2$ receptor as well. In the mouse CLP sepsis model, Rittirsch *et al.* (2008) showed that the selective antibody blockade or targeted deletion of either the $C5a_1$ or $C5a_2$ receptor improved animal survival in mid-grade sepsis. The *in vivo* appearance of the damage associated molecular pattern (DAMP), high mobility group box 1 protein, in this study was solely due to the activation of the $C5a_2$ receptor. In more severe sepsis, protection was only achieved with the blockade of both C5a receptors.

Chen *et al.* (2007) demonstrated that leukocytes obtained from mice with the targeted deletion of the $C5a_2$ receptor displayed both reduced upregulation of surface adhesion molecules and chemotactic responsiveness to C5a. These leukocytes also displayed a reduced ability to regulate LPS stimulated TNFα and IL-6 production. Contrary to the data generated by Bamberg *et al.* (2010), they showed that the deletion of $C5a_2$ receptor reduced C5a induced ERK activation. In an *in vivo* model of airway hyper-sensitivity, $C5a_2$ receptor knock out mice displayed reduced airway inflammation which correlated with a reduced influx of immune cell infiltration.

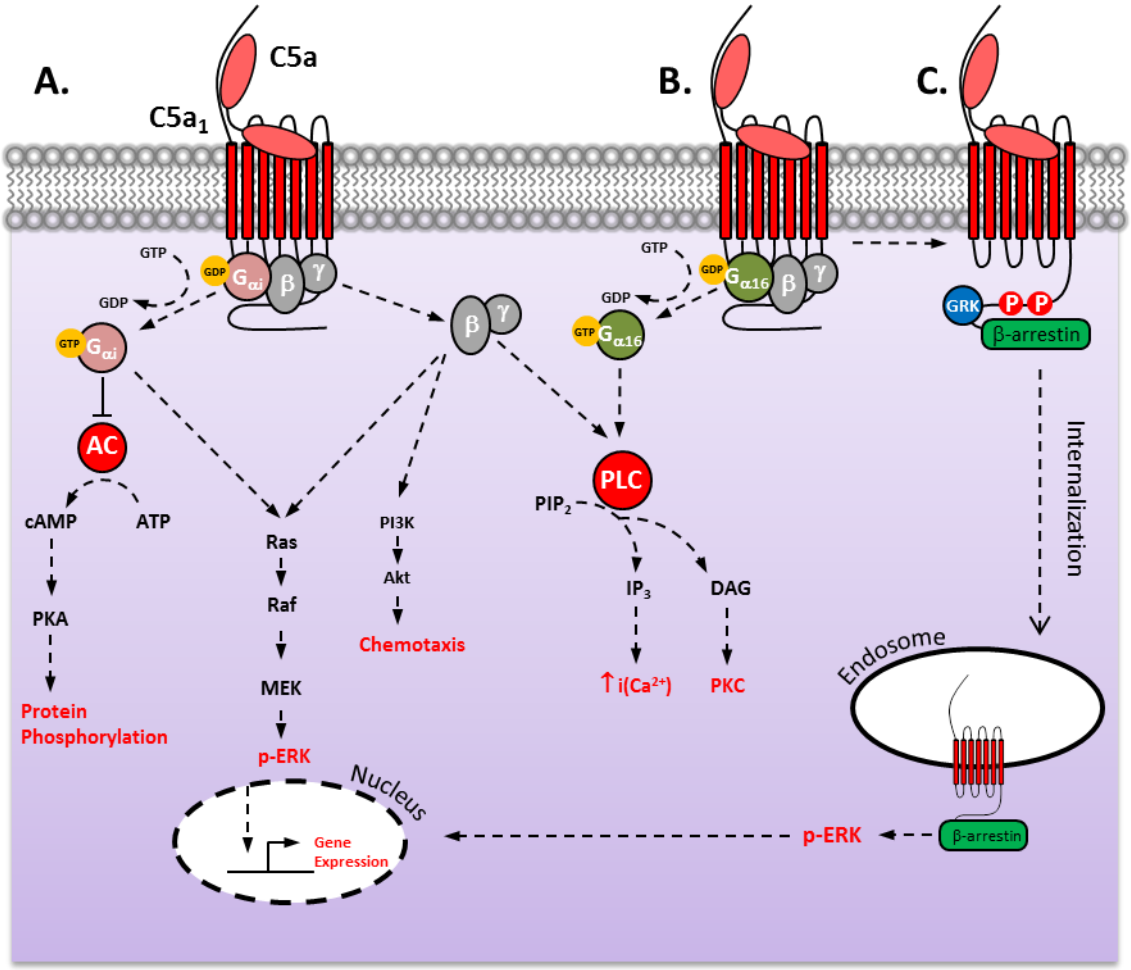

Figure 1.4. The mechanistic functions of the C5a$_1$ receptor

Activation of the C5a$_1$ receptor inhibits adenylate cyclase (AC) via $G_{\alpha i}$-proteins resulting in a lowered intracellular cAMP concentration which alters protein kinase A activation and protein phosphorylation (A). Receptor activation also stimulates phospholipase C (PLC) via $G_{\alpha 16}$-proteins and the $\beta\gamma$ complex (B). This results in the cleavage of phosphatidylinositol 4,5-bisphosphate (PIP_2) generating inositol 1,4,5-trisphosphate (IP_3) which regulates intracellular calcium and diacylglycerol (DAG) which activates protein kinase C (PKC). The $\beta\gamma$ complex activates the mitogen activated protein kinase pathway leading to the phosphorylation of extracellular signal–regulated kinases (ERK) and gene transcription. The $\beta\gamma$ complex can also activate the phosphoinositide 3-kinase (PI3K)/Akt (protein kinase B) pathway which regulates cell motility. After G-protein activation, G-protein receptor kinases (GRKs) phosphorylate intracellular domains of the C5a$_1$ receptor leading to the recruitment of β-arrestin and receptor internalization (C). The Internalized C5a$_1$-β-arrestin complex can induce ERK phosphorylation.

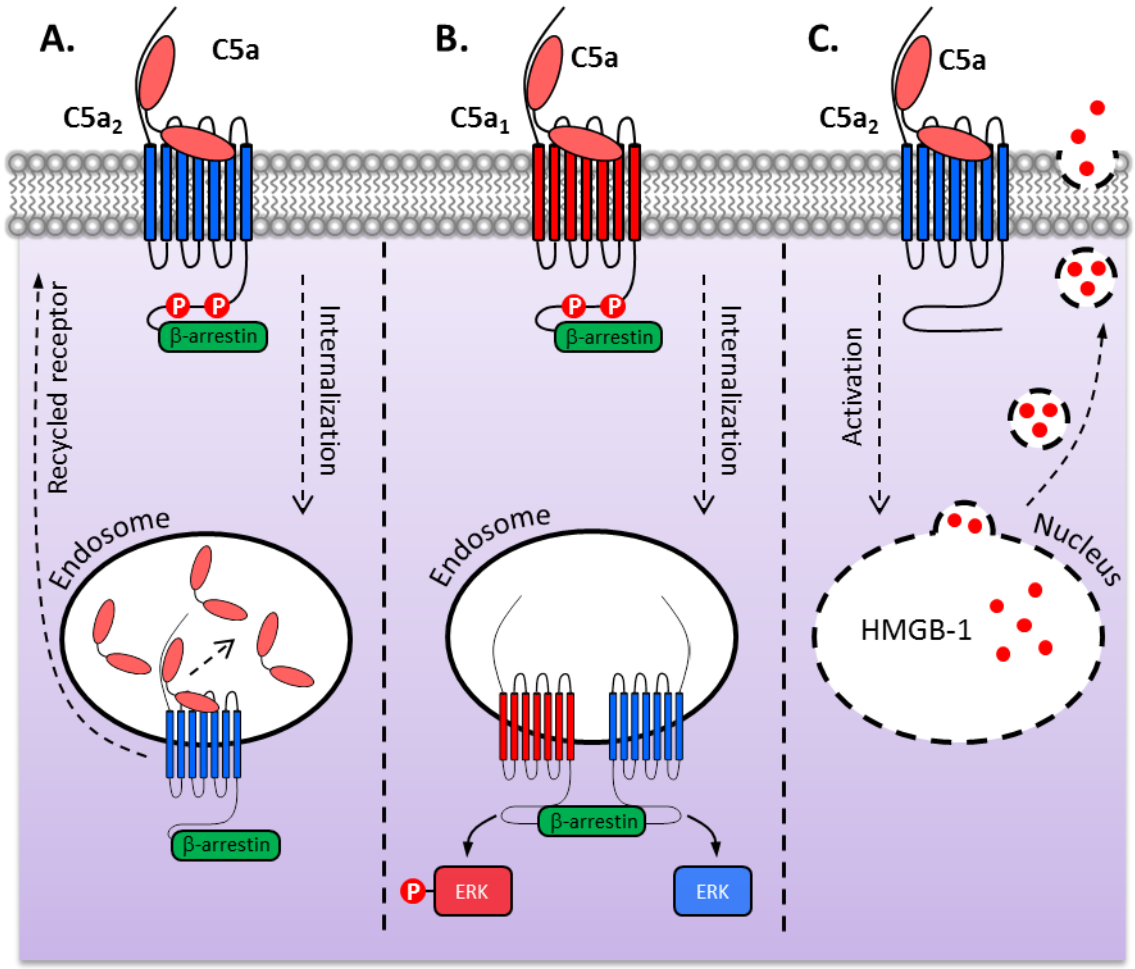

Figure 1.5. The proposed mechanistic functions of the $C5a_2$ receptor

A recycling decoy receptor (A); The $C5a_2$ receptor binds C5a or C5a des Arg and sequesters it from the extracellular space via β-arrestin mediated receptor internalization. Peptide agonists dissociate from the receptor in the endosome, after which the $C5a_2$ receptor recycles back to the surface. An intracellular regulator of $C5a_1$ receptor function (B); Activation of the $C5a_1$ receptor by C5a or C5a des Arg promotes the activation of the $C5a_2$ receptor. Post activation, both receptors are phosphorylated and recruit β-arrestin. The $C5a_1$-β-arrestin complex activates ERK whereas the $C5a_2$-β-arrestin complex does not. An independent signalling receptor (C); Activation of cell surface $C5a_2$ receptor leads to the direct release of the nuclear damage associated molecular pattern, high mobility group box 1 protein (HMGB-1).

Finally, Hao *et al.* (2013) investigated the role of $C5a_2$ receptor during C5a-priming of neutrophils prior to anti-neutrophil cytoplasmic antibody (ANCA) induced neutrophil activation. In C5a primed neutrophils, subsequent activation with MPO-ANCA or mPR3-ANCA led to neutrophil degranulation and respiratory burst which was significantly reduced in the presence of the $C5a_2$ receptor antibody. With the lack of any inhibition of neutrophil response achieved with a $C5a_1$ receptor antagonist, the authors proposed that $C5a_2$ receptor plays a pro-inflammatory role in C5a-primed neutrophils for ANCA-induced activation.

Although the data described above highlight the interesting mechanisms by which the $C5a_2$ receptor can regulate the actions of the complement system, the precise function of this receptor still remains enigmatic. A potential reason for the conflicting roles of this receptor could be due to the situation in which the receptor was investigated. The majority of the data that support an anti-inflammatory role, were generated using either engineered cells or using quiescent systems where only C5a or C5a des Arg were present. However, in more complex settings, where additional inflammatory mediators were present, the $C5a_2$ receptor was described as having a pro-inflammatory role. Also, the majority of the work described focused on the same leukocyte functions, mainly chemotaxis and cytokine release. An assessment of the impact that different inflammatory mediators have on the cellular expression profile of the $C5a_2$ receptor and an investigation as to the contribution of $C5a_2$ receptor in different cellular events may help better define the role of the $C5a_2$ receptor.

1.7. Therapeutically targeting the complement system

Over the past 30 years there have been numerous attempts to therapeutically target the complement system to treat disease. Many of these attempts have targeted the serine proteases of the complement system. Ruconest®, Cinryze and Berinert are all human recombinant versions of nature's own serine protease inhibitor, C1-inhibitor, and are approved in the US for the treatment of hereditary angioedema.

Lampalizumab, a monoclonal antibody from Roche/Genentech, targets FD and is currently in Ph3 clinical trials for age related macular degeneration (AMD). There is currently a great deal of activity to demonstrate the clinical benefit of targeting the amplification loop of the complement system. This is being investigated by Amyndas Pharmaceuticals and Apellis Pharmaceuticals with analogues of the cyclic peptide inhibitor of C3, Compstatin (Morgan *et al.*, 2015).

During this time, there has also been a large degree of activity to design therapies that target the distal part of the complement system, the C5-C5a-C5a$_1$ receptor axis. Examples of which will be discussed below and are represented in figure 1.6.

1.7.1. Preventing C5 cleavage

With all pathways of the complement system signalling though C5, inhibiting the cleavage of this protein is an attractive therapeutic strategy as it will stop pathway progression regardless of the stimuli. This is exactly what is achieved with the humanized anti-C5 monoclonal antibody Eculizumab. Sold by Alexion Pharmaceuticals Inc, under the trade name Soliris®, this agent was approved by the FDA in 2007 for the treatment of paroxysmal nocturnal hemoglobinuria (PNH). PNH is a rare haemolytic disease caused by somatic mutations that result in the loss of expression of glycosylphosphatidylinositol anchors that link complement regulator proteins DAF and CD59 to hematopoietic stem cells. The absence of this protein allows the formation of the MAC on erythrocytes, leading to complement mediated hemolysis, which, if not treated becomes a progressive illness with an increased risk of death (Rother *et al.*, 2007). Eculizumab functions by binding to C5 in such a way that it sterically hinders C5 convertase from cleaving it. More recently Eculizumab has received FDA approval for the treatment of aHUS and is currently in clinical trials for several other clinical indications.

The success of Eculizumab has spurred other biotechnology companies to generate agents that target the C5 protein. Ra Pharma is currently developing RA101495, a subcutaneous, self-administered macrocyclic peptides that binds C5 in a very

different location to Eculizumab. Alynylam is attempting to silence the production of C5 with their liver targeted C5 RNAi, ALN-CC5. Both agents are currently in Ph2 clinical trials for PNH and provide hope for patients with C5 polymorphisms that make them resistant to Eculizumab.

1.7.2. Neutralizing C5a

With experimental model data suggesting blocking the actions of C5a would be protective in the syndrome of sepsis, InflaRx GmbH have recently completed a Ph2 clinical trial investigating the efficacy of their anti-C5a monoclonal antibody IFX-1 in patients suffering from early sepsis associated organ failure. A key advantage of targeting C5a is that the actions of this peptide are blocked at both C5a receptors while maintaining the function of the MAC. Although the data from this clinical study demonstrated that IFX-1 showed positive trends in various clinically relevant endpoints such as organ dysfunction score, need for ventilator support and length of stay on the ICU, the development of this agent for sepsis associated organ failure has been put on hold. The graveyard of sepsis clinical trial failures and investor fear have prompted InflaRx to reposition IFX-1 to other complement driven disorders including the debilitating systemic skin disease hidradenitis suppurativa and ANCA-vasculitis (www.inflarx.de).

1.7.3. Antagonizing the $C5a_1$ receptor

Targeting the $C5a_1$ receptor to treat complement system related disorders has received a great deal of attention since the early 1990s. Neutralizing antibodies (NNC0215-0384) and several small and large molecule antagonists (MP-435, NGD 2000-1 and PMX53) have all entered clinical trial for the treatment of RA. However, all efforts with these molecules have been abandoned due to either compound toxicity or lack of clinical efficacy (Lee *et al.*, 2008). More recently ChemoCentryx has

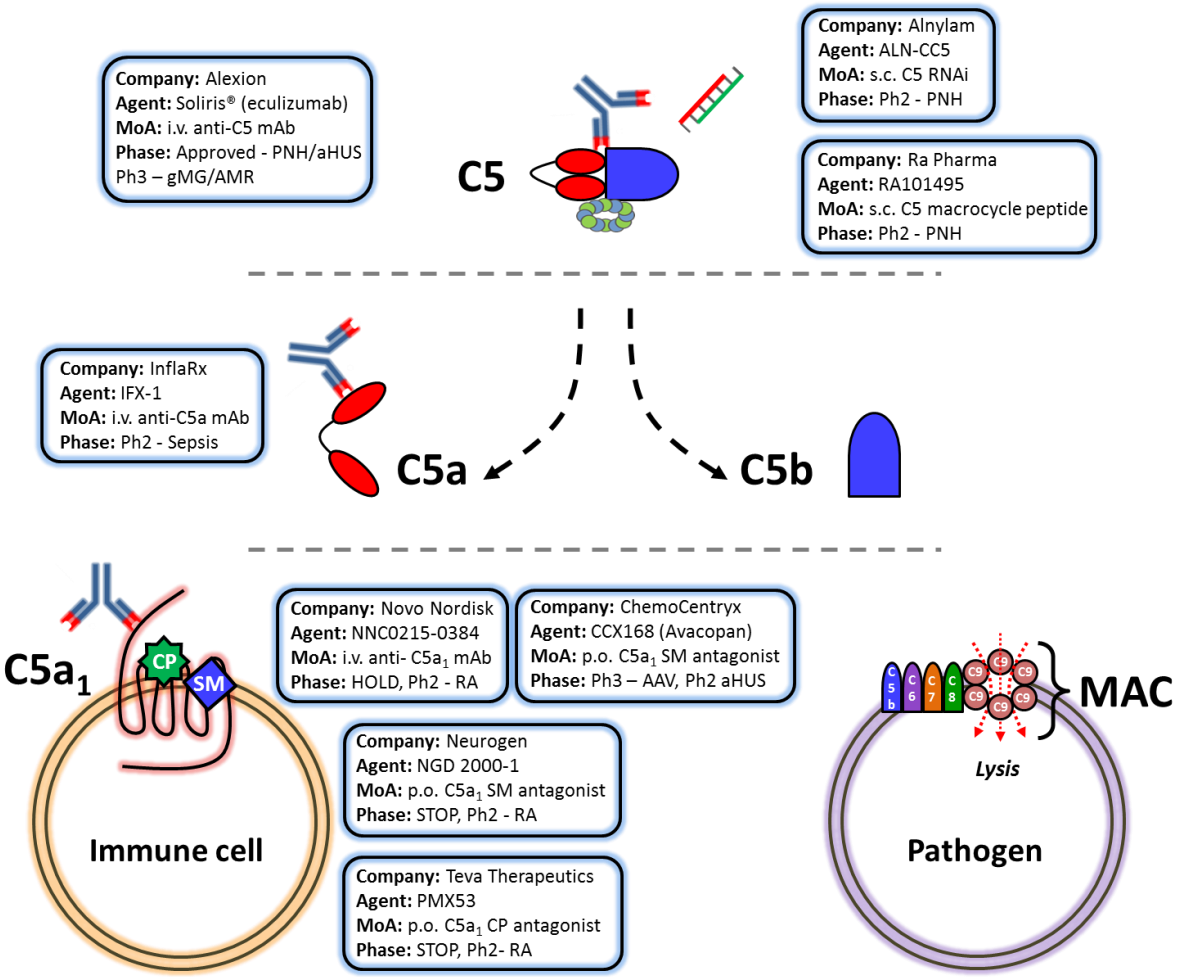

Figure 1.6. Therapeutically targeting the C5-C5a$_1$ receptor axis

Marketed or investigational drugs that target the distal part of the complement system. Alexion's Solaris®, a C5 monoclonal antibody (mAb) is approved for the treatment of paroxysmal nocturnal hemoglobinuria (PNH) and atypical hemolytic uremic syndrome (aHUS) and is currently in clinical trials for generalized Myasthenia Gravis (gMG) and antibody mediated rejection (AMR). Alnylam Pharmaceuticals and Ra Pharma are currently developing agents that neutralize C5 by other mechanisms. InflaRx are developing the C5a mAb IFX-1, which recently completed a Ph2 clinical trial investigating its efficacy in sepsis associated organ dysfunction. Numerous attempts have been made to antagonize the C5a$_1$ receptor. Novo Nordisk's mAb, Neurogen's small molecule (SM) antagonist and Teva Therapeutics cyclic peptide (CP) antagonist all entered clinical trials for rheumatoid arthritis (RA) but their development has been stopped. ChemoCentryx are currently developing the C5a$_1$ receptor antagonist CCX168 for the treatment of ANCA associated vasculitis and aHUS.

received greater success with CCX168 (Avacopan), which has progressed to Ph3 clinical trials for ANCA vasculitis (Bekker *et al.*, 2016).

One particular molecule that has received a great deal of attention since its discovery is the peptide antagonist, PMX53. This cyclic hexapeptide resembles the last six amino acids of C5a and was generated from a culmination of work by three separate teams of researchers. In 1992 researcher at Abbot Laboratories discovered that the analogues of the C-terminus of C5a were able to bind to and activate the $C5a_1$ receptor (Kawai *et al.*, 1992). Two years later colleagues at Merck made further modifications to these truncated peptides which removed all agonist properties, generating potent antagonists with nanomolar affinity for the $C5a_1$ receptor (Konteatis *et al.*, 1994). Scientists at the University of Queensland continued this research and using NMR spectroscopy they determined that in solution these peptide antagonists naturally adopted a cyclic conformation. Stabilizing the peptides conformation via cyclization generated AcF[OPdChaWR] (PMX53), which displays an IC_{50} of 20 nM for the $C5a_1$ receptor (Finch *et al.*, 1999). This orthosteric, competitive receptor antagonist has been extensively characterized both *in vitro* and *in vivo* and has demonstrated efficacy in numerous experimental animal models (Seow *et al.*, 2016).

In 2006 PMX53 entered into a double-blind, placebo controlled, orally administered clinical trial to assess its efficacy in patients with active RA. Unfortunately PMX53 did not show any benefit in this patient population and the study sponsors (Teva Pharmaceuticals Ltd) concluded that antagonism of the $C5a_1$ receptor does not result in reduced synovial inflammation in RA patients (Vergunst *et al.*, 2007). However, on closer inspection of the reported clinical data, it appears the clinical exposures of PMX53 in this study were very low and perhaps not enough to sufficiently antagonize the actions of C5a at the $C5a_1$ receptor. It is therefore a matter of a debate as to whether this clinical trial truly tested the hypothesis that antagonizing the $C5a_1$ receptor would ameliorate joint inflammation associated with RA. Further research, focused on quantifying the degree of antagonist-receptor occupancy required to block the actions of both C5a and C5a des Arg would provide a great deal of benefit to future clinical studies investigating this axis in disease.

1.8. Rationale, aims, hypotheses and experimental strategy.

Rationale

The complement system is an integral component of the body's immune system and provides an essential role in clearance of microbial infections. Appropriate activation of the complement system leads to the generation of potent inflammatory mediators, including C5a, which through ligation of C5a receptors guide neutrophils to the site of infection and help orchestrate its clearance. However, dysregulation or over activation of the complement system can lead to the continual and excessive production of these inflammatory mediators which can result in disease.

The precise role of the $C5a_1$ and $C5a_2$ receptors in orchestrating neutrophil functions and true signalling signature of both C5a and its cleaved isoform C5a des Arg are still not fully understood. A better understanding of the function and signalling capabilities of C5a, C5a des Arg and the role of the C5a receptors will help inform future drug discovery efforts that aim to treat disorders associated with this part of the complement system.

With the above in mind, I plan to focus my research to address the following aims and hypothesis.

Aims

1. To investigate the impact of inflammatory mediators, present during states of disease, on the expression of neutrophil C5a receptors.
2. To perform an extensive characterization of the signalling signatures of both C5a and C5a des Arg in cell base functional assays and define the contribution of the $C5a_1$ and $C5a_2$ receptors in agonist mediated neutrophil responses.
3. At receptor and G-protein level, determine the mechanism that controls the biased signalling profile of C5a des Arg.

Hypothesis and experimental strategies:

1. There are conflicting data as to the precise role of the $C5a_2$ receptor mediating the actions of C5a and C5a des Arg. *I hypothesised that pro inflammatory mediators around during states of inflammation alter the human neutrophil surface expression of this receptor which controls $C5a_1$ receptor function.* **Experimental strategy: I compared the effects of stimulating unactivated neutrophils with LPS, TNFα, C5a or C5a des Arg on the surface expression of $C5a_1$, $C5a_2$ and other innate immune receptors.**

2. Experimental evidence suggests that C5a des Arg retains some but not all of the signalling activity of C5a. *I hypothesised that C5a des Arg retains certain signalling properties that enable it to orchestrate the extravasation of neutrophils to sites of infection while minimizing damage to surrounding tissue.* **Experimental strategy: I compared the potency and efficacy of C5a and C5a des Arg in a panel of human neutrophil and engineered cell based assays to determine the functional signature of each peptide agonist. Using receptor specific antagonists I determined the contribution of each C5a receptor to the agonist responses observed in human isolated neutrophils.**

3. Certain amino acid residues on the $C5a_1$ receptor have been identified as being important for the binding and function of C5a and C5a des Arg. *I hypothesised that the removal of the C-terminal arginine from C5a causes C5a des Arg to bind the $C5a_1$ receptor in such a way that it induces a receptor conformation that only allows the activation certain G-protein mediated pathways.* **Experimental strategy: I used receptor mutagenesis and a functional cell based assay to confirm the key receptor amino acid residues involved in C5a and C5a des Arg binding and function. I worked with a collaborator, Domain Therapeutics, to determine the G-protein signalling signature of C5a and C5a des Arg at the $C5a_1$ receptor.**

Chapter 2

Materials and methods

Materials and methods

2.1. Reagents and assay kits

Unless otherwise stated, all reagents and assay kits were purchased from either Complement Technology, Sigma-Aldrich, PerkinElmer, Life Technologies, Thermo Fisher Scientific, Biolegend, BD Biosciences, R&D Systems, Tocris, Qiagen, Integrated DNA Technologies, Miltenyi Biotec, DiscoverX or Cisbio.

2.2. Assay buffer

Unless otherwise stated, all *in vitro* assays were conducted using the following assay buffer: HBSS containing $CaCl_2$ and $MgCl_2$ (Life Technologies, Cat. 14025) supplemented with 20 mM HEPES (Life Technologies, Cat. 15630) and 0.1% BSA (Miltenyi Biotec, Cat. 130-091-376) at pH 7.4.

2.3. $C5a_1$ and $C5a_2$ receptor expressing cell lines

To investigate the selectivity, specificity and functional responses of ligands at either the human $C5a_1$ or $C5a_2$ receptor, historical Pfizer cell lines expressing either of the C5a receptors were used. CHO-K1 cells engineered to express the $C5a_1$ receptor and the $G_{\alpha16}$ protein were cultured in a Dulbecco's Modified Eagle Medium/F-12 growth media (Life Technologies Cat. 11320) containing 10% heat inactivated FBS (Sigma-Aldrich, Cat. F4135), 1mg/mL Geneticin® (Life Technologies, Cat. 11811) and 250 µg/mL ZeocinTM (Life Technologies, Cat. R25001). U2OS cells engineered to express the $C5a_2$ receptor and GFP tagged β-arrestin 2 were cultured in Minimum Essential Medium (Life Technologies, Cat. 11095) containing 10% heat inactivated FBS, 400 µg/mL Geneticin® and 400 µg/mL Zeocin™ (Life Technologies Cat. R25001). Cells were cultured in humidified conditions at 37°C, 5% CO_2.

2.3. Assessment of recombinant $C5a_1$ and $C5a_2$ receptor sequences

Genomic DNA was isolated from CHO-K1 $C5a_1$ and U2OS $C5a_2$ receptor cells using the Qiagen DNAeasy kit. In brief the method was as follows: Approximately 2 x 10^6 of each cell type was thawed and dispensed into a fresh micro-centrifuge tube and centrifuged at 300 x *g* for 5 minutes. Cells were suspended in PBS containing proteinase K. Cells were centrifuged again and AL buffer, without ethanol, was added to cell pellet. Cells were mixed thoroughly and then incubated at 56°C for 10 min. 100% ethanol was then added to each sample and mixed before being transferred to a DNeasy mini spin column which was placed in a micro-centrifuge tube. Samples were centrifuged at 6000 x *g* for 1 min and the flow-through was discarded. Each DNeasy mini spin column was placed in a new collection tube and AW1 buffer was added over the column. Tubes were centrifuged for 1 min at 6000 x g after which the flow-through and collection tube were discarded. DNeasy mini spin columns were placed in a new collection tube and AW2 buffer was added to each sample which were subsequently centrifuged for 3 min at 20,000 x *g* to dry the DNeasy membrane. The DNeasy mini spin columns were placed in a clean collection tube and nuclease free water was dispensed directly onto the DNeasy membrane. Incubated at room temperature for 1 min, and then centrifuged for 1 min at 6000 x *g* to elute the genomic DNA. DNA purity and concentration was determined with UV spectrophotometry using a BioTek® Synergy™ H4 plate reader (BioTek Instruments, Inc, Winooski, VT, USA).

Two sets of polymerase chain reaction (PCR) primers were designed for each gene using the known expression vector flanking sequences (Integrated DNA Technologies, Coralville, IA, USA). Forward and reverse primers were diluted to 100 nmol/mL in nuclease free dH_2O, diluted 1:2 with each other and added to the KOD hot start master mix (Sigma-Alrdich Cat. 71842-4) to achieve 100 pmol of each primer pair. 300 ng of each DNA template was added separately to each primer set, transferred to a thermal cycler and DNA amplification was achieved using 40 cycles of a protocol consisting of a 15 second 95^{o}C denaturing step, 15 second 55^{o}C annealing step and

25 second 68°C elongation step. Final elongation was achieved at 68°C for 10 minutes.

Samples were de-salted using spin columns and sent to Wyzer Biosciences (www.wyzerbio.com) for sequencing. DNA sequence analysis and alignment to NCBI nucleotide reference sequences were confirmed using Vector NTi data analysis software. Coding sequences were translated and aligned to NCBI protein reference sequences.

2.4. Quantitation of receptor gene expression

$C5a_1$ CHO-K1 cells (2×10^6), $C5a_2$ U2OS cells (2×10^6) or neutrophils (2×10^7) were harvested and lysed using QIAshredder columns (Qiagen, Cat. 79656) and total RNA was prepared using the RNeasy Plus Mini Kit (Qiagen, Cat. 74136). RNA purity (ratio of absorbance at 260 and 280 nm) and concentration was determined using a BioTek® Synergy™ H4 plate reader.

The RT-PCR reactions were performed using TaqMan® RNA-to-CT™ 1-Step Kit (Life Technologies Cat. 4392938) and the QuantStudio™ 12K Flex Real-Time PCR System (Life Technologies). Assay was performed in a 384 well plate using Taqman®, Assay on Demand™ primer probe sets for each protein of interest (see table 2.1) and 100 ng total RNA per reaction. Samples were tested in quadruplicate. RT-PCR was performed using the following protocol; 30 minutes at 48°C, 1 minute at 95°C, followed by 40 cycles of 15 seconds 95°C, 1 minute at 60°C. The fluorescence signal was measured at the annealing step of 60°C. The cycle thresholds (Ct) were manually set and the baseline was set automatically to obtain the Ct values for each target. Human or rodent GAPDH was used as an endogenous housekeeping control gene for normalization to determine a ΔCt for each target. The analysis of gene expression was performed using the Comparative Ct method ($2^{-\Delta\Delta Ct}$) of relative quantification, according to ABI/Life Technologies recommended protocols. Results were expressed as the mean difference in relative expression.

Gene target	Species	Primer probe exon mapping	Life Technologies Taqman® reagent Catalogue number
$C5a_1$ receptor	Human	Within a single exon	Hs00704891_s1
$C5a_1$ receptor	Human	Probe spans exons	Hs00383718_m1
$C5a_2$ receptor	Human	Within a single exon	Hs01933768_s1
$C5a_2$ receptor	Human	Probe spans exons	Hs00218495_m1
C3a receptor	Human	Probe spans exons	hs00377780_m1
FPR1	Human	Probe spans exons	hs00181830_m1
CXCR1	Human	Probe spans exons	hs00174146_m1
CCR2	Human	Probe spans exons	hs00356601_m1
CCR5	Human	Probe spans exons	hs00152917_m1
β-arrestin1	Human	Probe spans exons	Hs00244527_m1
β-arrestin2	Human	Probe spans exons	Hs01034132_m1
GAPDH	Human	Probe spans exons	Hs02758991_g1
GAPDH	Rodent	Probe spans exons	4308313

Table 2.1. Taqman® primer probe sets used to quantify gene expression

2.5. Detection of protein expression using gel electrophoresis and immunoblotting

$C5a_1$ CHO-K1 cells (2 x 10^6), $C5a_2$ U2OS cells (2 x 10^6) were lysed at 4^{o}C for 30 minutes in RIPA buffer (Sigma-Aldrich, Cat. R0278) supplemented with 1x protease inhibitor cocktail (Sigma-Aldrich, Cat. P8340) and 1mM PMSF (Sigma Aldrich Cat. P7626) at a concentration of 20,000 cells per µL. Lysate was then centrifuged at 15,000 x g for 15 minutes at 4^{o}C. Supernatants were harvested and protein concentrations were quantified using a BCA protein detection kit (Thermo Fisher Scientific, Cat. 23225). Protein lysates were then diluted to the appropriate concentration in the supplemented RIPA buffer and then prepared in sample loading buffer (70% (v/v)

NuPAGE LDS Sample Buffer (Life Technologies, Cat. NP0008) and 30% (v/v) NuPAGE Sample Reducing Agent (Life Technologies, Cat. NP0004)) so that 20 µL of sample contained between 5 and 10 µg of protein. The SeeBlue Plus2 pre-stained standard protein ladder (Life Technologies, Cat. LC5925) was diluted 1:10 in loading buffer. Protein samples and protein ladder were incubated at room temperature for 30 minutes. High denaturing temperatures were avoided to minimize protein aggregation. 20 µL of each protein sample was loaded to separate lanes of a 10% Bis-Tris polyacrylamide NuPAGE mini-gel (Life Technologies, Cat NP0301). Proteins were resolved by electrophoresis using a XCell SureLock™ Mini-Cell Electrophoresis System and NuPAGE MOPS SDS running buffer (Life Technologies, Cat. NP000102) at 80V for 5 minutes, 100V for 5 minutes followed by 160V for 80 minutes. The resolved proteins were transferred to a 0.45 µm pore size nitrocellulose membrane (Life Technologies, Cat. 88014) using the XCell™ Blot Module and NuPAGE Transfer Buffer (Life Technologies, Cat. NP0006) containing 10% methanol and 0.1% (v/v) NuPAGE antioxidant (Life Technologies, Cat. NP0005). Proteins were transferred at 230mA for 70 minutes. Nitrocellulose membranes were then blocked in neat Odyssey® PBS blocking buffer (Li-COR, Cat. 927-40000) for one hour. Block solution was removed and membranes were then incubated with antibody block solution (50% (v/v) PBS/Odyssey® PBS blocking Buffer), supplemented with 0.1% Tween 20 (Thermo Fisher Scientific, Cat. 28360) containing both C5a receptor and GAPDH specific detection antibodies (either 1:500 dilution of mouse anti-$C5a_1$ clone S5/1 (Thermo Fisher Scientific, Cat. MA5-16937) plus 1:2000 dilution rabbit anti-GAPDH Clone 14C10 (Cell Signaling Technology, Cat. 2118) or 1:500 rabbit anti-$C5a_2$ clone N1-50 (Thermo Fisher Scientific, Cat. PA1-41397) plus 1:2000 dilution of mouse anti-GAPDH clone ZG003 (Thermo Fisher Scientific Cat. 39-8600) for 16 hours at 4^oC. Membranes were rinsed for 5 minutes, 5 times with 10 mLs of TBS containing 0.1% Tween 20. Membranes were then incubated with antibody block solution containing 1:10,000 dilution of both Alexa Fluor® 680 conjugated donkey anti-mouse IgG (Thermo Fisher Scientific, Cat. A10038) and IRDye 800CW conjugated goat anti-rabbit IgG secondary antibodies (LI-COR. Cat. 827-08365) for one hour at room temperature. Membranes were washed again and fluorescent antibody detection

was performed using an ODYSSEY® CLx Infrared Imaging System (LI-COR Biotechnology, Lincoln, NE, USA).

2.6. Characterization of human serum derived C5a and C5a des Arg

Native human C5a and C5a des Arg, prepared from human derived C5 were obtained from Complement Technology Inc. C5a, Lot 17 (Cat. A144) was supplied at a concentration of 50 µM and C5a des Arg, Lot 15, (Cat. A145) was supplied at a concentration of 54 µM. Both peptides were reported to have an endotoxin level below < 0.1 EU/µg. Purity and characterization of each anaphylatoxin was determined by mass spectrometry as follows: 40 µL of 50 µM sample solution in HEPES buffer was injected into an LC-MS system for MS and UV analysis. After injection, analytes were separated by reversed-phase liquid chromatography with an online ACQUITY H Class UPLC (Waters, Milford, MA, USA) system coupled with MS (SQ2)/UV. The system was equipped with a 5 µm Waters XBridge C4 Protein BEH (4.6 µm × 50 mm; Waters), separation of the Proteins/peptides was conducted at room temperature and a flow rate of 2 mL/min. A linear gradient from 5% A (0.05% formic acid in water) to 25% B (0.05% formic acid in acetonitrile) was applied over 4.1min, with a wash at 100% B to 5 min. UV monitoring was conducted at 280nm. MS analysis was performed on an SQ2 (Waters) mass spectrometer equipped with an electrospray ionization source controlled by MassLynx 4.1 software (Waters). The capillary voltage was set to 3.5 kV, the cone voltage to 50 V and the source temperature to 150 °C. Mass spectra were acquired in positive ionization mode over an m/z range of 200–3000 Da at scan rate of 1.3s. Deconvoluted spectra were generated by MaxEnt1 (Waters) over the full range of scanned raw data (200-3000Da) with an output range of 10000:11000 Da, a resolution of 1Da and a minimum intensity ratio of 10%.

2.7. ^{125}I-C5a receptor-ligand binding studies

Whole cell receptor-ligand binding assays using ^{125}I human recombinant C5a (PerkinElmer, Cat. NEX250) were performed to assess the expression level of each C5a receptor, the specificity of pharmacological tools, or kinetics of C5a for each C5a receptor. Assays used use of the previously described engineered cells ($C5a_1$ CHO-K1 2500 cells/well, $C5a_2$ U2OS 1000 cells/well) or human isolated neutrophils (200,000 cells/well).

The following pharmacological reagents were tested in competition mode to assess their affinity and specificity for each C5a receptor: Anaphylatoxins (obtained from Complement Technology Inc) C3a (Cat. A118), C3a des Arg (Cat. A119), C5a (Cat. A144) and C5a des Arg (Cat. A145) anti $C5a_1$ receptor antibody clones (Thermo Fisher Scientific, P12/1 (Cat. MA1-35971), S5/1 (Cat. MA5-16937), 8D6 (Cat. MA5-17740), W17/1 (Cat. MA1-40174)), $C5a_1$ receptor antagonists PMX53 (Pfizer laboratories) and NDT9513727 (Tocris, Cat. 3333), $C5a_2$ receptor antibody clones 1D9-M12 (BioLegend, Cat. 342402), N1-50 (Thermo Fisher Scientific, Cat. PA1-41397), N1-23 (Hycult Biotech, Cat. HP9036) and species specific isotype controls (Thermo Fisher Scientific). Cells were incubated with 10 different concentrations of each test agent and a fixed concentration of ^{125}I-C5a (approximately 25 pM for $C5a_1$ receptor and 50 pM $C5a_2$ receptor) for four hours at room temperature.

To characterize the binding kinetics of ^{125}I-C5a to both C5a receptors and determine assay viability at extended incubation times, association receptor ligand binding experiments using two separate concentrations of ^{125}I-C5a ($C5a_1$ = 20 and 60 pM, $C5a_2$ = 40 and 120 pM) were performed at time points ranging from 1 to 240 minutes at room temperature. Specific ^{125}I-C5a receptor binding for each time point was calculated from duplicate total binding (assay buffer) and non-specific binding ($C5a_1$ receptor 1 µM PMX53, $C5a_2$ receptor 15µg/mL antibody clone 1D9-M12) controls.

To obtain affinity estimates (K_d values) for ^{125}I-C5a and quantify the expression of each C5a receptor in either CHO-K1, U2OS or human isolated neutrophils, saturation receptor ligand binding experiments were performed. Each cell line was incubated

with 12 different concentrations of ^{125}I-C5a, ranging from 1 nM to 1 pM, for four hours at room temperature. For each ^{125}I-C5a concentration, specific receptor ligand binding was calculated using both total binding and non-specific binding controls as described above.

All receptor ligand binding reactions were performed in assay buffer in a total volume of 200µL (160 µL cells, 20 µL test agent or control and 20 µL ^{125}I-C5a). Experiments were terminated via rapid vacuum filtration over GF/C Unifilter plates (PerkinElmer, Cat. 6005174) pre-soaked in 0.5% PEI (Sigma-Aldrich, Cat. 764647) using a Brandel Harvester (Brandel Inc. Gaithersburg, MD, USA). Filters were washed four times with 1 mL of assay buffer and then dried at 40^{o}C for two hours prior to the addition of 50 µL MicroScint™-O cocktail (PerkinElmer, Cat. 6013611) to each well. Plates were counted on a TopCount NXT™ Microplate Scintillation Counter (PerkinElmer, Waltham, MA, USA). To quantify the concentration of each diluted ^{125}I-C5a sample, 10 µL of each sample was diluted in 6 mL of Ultima Gold™ scintillation cocktail (PerkinElmer, Cat. 6013680) and counted on a Tri-Carb® liquid scintillation counter (PerkinElmer, Waltham, MA, USA) using and a ^{125}I quench curve. Radioactivity in DPM was converted to molar concentration using the constant 1 Ci = 2.22^{12} DPM and a specific activity for ^{125}I of 2200 Ci/mmol.

2.8. Isolation of neutrophils from human whole blood

Blood was collected at the Pfizer phlebotomy unit from healthy volunteers who had previously provided informed consent.

Neutrophils were rapidly isolated from human whole blood using the negative selection MACSxpress® human neutrophil isolation kit (Miltenyi Biotec, Cat. 130-104-434). Blood was collected in K_2EDTA spray-coated Vacutainer™ tubes (BD Biosciences, Cat. 366643). The lyophilized neutrophil isolation cocktail pellet was reconstituted in 2 mL of the provided buffer A and mixed gently with repeat pipetting. The final cocktail was then prepared with the addition of 2 mL of the provided buffer B. The final 4 mL of neutrophil isolation cocktail was then added to a

15 mL conical centrifuge tube containing 8 mL of human whole blood. The tube was gently inverted three times and mixed for five minutes at room temperature using the MACSmix™ Tube Rotator (Miltenyi Biotec, Auburn, CA, USA). The tube was then placed in the MACSxpress® Separator magnet (Miltenyi Biotec) for 15 minutes. With the tube still inside the magnetic field, the supernatant, containing the enriched neutrophils, was collected and transferred to a new 15 mL tube. Magnetically labelled non-target cells as well as aggregated erythrocytes are retained in the original tube. The supernatant was then centrifuged at 300 x *g* for 5 minutes, the supernatant aspirated and discarded and the neutrophil pellet suspended in 15 mL of assay buffer. Cells were centrifuged again and suspended in assay buffer to the desired concentration.

2.9. Neutrophil purity and activation state

To assess the purity of neutrophils isolated using the MACSxpress® human neutrophil isolation kit, a comparison of the percentage cells that stain for the granulocyte markers CD15 and CD16 before and after isolation from whole blood was performed. 100 µL of human whole blood was added to 2.5 mL 1x BD Phosflow™ Lyse/Fix buffer (BD Biosciences, Cat. 558049) for 10 minutes at 37^{o}C in order to lyse erythrocytes and fix leukocytes. 1 x 10^{6} isolated neutrophils were fixed in 1 mL of BD Cytofix™ (BD Biosciences, Cat. 554655) for 20 minutes at 4^{o}C. Each fixed cell population was centrifuged at 500 x *g* for 5 minutes and suspended in sterile filtered BSA based stain buffer (BD Biosciences, Cat. 554657) supplemented with the Fc receptor blocking solution Human TruStain FcX™ (Biolegend Cat. 422302) to a concentration of 1 x 10^{7} cell/mL. 100 µL of each sample was stained with 20 µL APC mouse anti-human CD15 clone HI98 (BD Biosciences, Cat. 561716) and 20 µL FITC mouse anti-human CD16 clone 3G8 (BD Biosciences, Cat. 555406) for 20 minutes in dark conditions on ice. Samples were then centrifuged at 500 x *g* for 5 minutes and washed three times in 200 µL of stain buffer. Separate neutrophil samples were stained with individual antibodies for fluorochrome compensation controls. Blank and stained samples

were analysed for FITC and APC staining using the BD LSRFortessa™ flow cytometer (BD Biosciences, San Jose, CA, USA)

To determine the activation state of the isolated neutrophils, a comparison of the expression of the cell surface adhesion molecule, CD11b, was performed between neutrophils fixed in whole blood and those isolated using the MACSxpress® isolation kit. Procedures for erythrocyte lysis and cell fixation were the same as described above. Prior to fixation, a sample of neutrophils was stimulated with 10 nM human purified C5a for 30 minutes at 37^{o}C in assay buffer. Samples were centrifuged at 300 x *g* for 5 minutes, suspended in stain buffer containing 20 µL APC mouse anti-human CD11b/Mac-1 clone ICRF44 (BD Biosciences, Cat. 550019) or isotype matching control antibody clone X40 (BD Biosciences, Cat. 354818). Staining intensity was assessed using BD LSRFortessa™ flow cytometer.

2.10. Detection of cell surface C5a receptor expression using flow cytometry

To determine the specificity and saturating concentrations of fluorophore conjugated antibodies for each C5a receptor and the presence of other immune system related receptors on the surface of the human isolated neutrophil, flow cytometry was employed. $C5a_1$ CHO-K1 cells, $C5a_2$ U2OS cells or neutrophils were suspended in stain buffer to a concentration of 1 x 10^7 cells/mL. Individual cell samples were incubated with multiple or single concentrations of fluorophore conjugated antibodies for the following receptors; $C5a_1$ receptor (Biolegend, Cat. 344305), $C5a_2$ receptor (Biolegend, Cat. 342405), FPR1 (R&D Systems, Cat. FAB3744P), CD11b (BD biosciences, Cat. 562108), TNFR1 (R&D Systems, Cat. FAB225A), TNFR2 (R&D Systems, Cat. FAB226A) and TLR4 (R&D Systems, Cat. FAB6248A). Cells were washed in stain buffer and fixed in BD Cytofix™ as previously described. Mean fluorescence intensity of each fluorophore was assessed using BD LSR Fortessa™ flow cytometer and compared to samples stained with equivalent concentrations of isotype matched control.

2.11. The impact of inflammatory agents on neutrophil receptor expression

The effects of the sepsis associated inflammatory agents, LPS (InvivoGen Cat. tlrl-ppglps), TNFα (R&D Systems, Cat. 210-TA) C5a and C5a des Arg were individually assessed on the neutrophil surface expression of $C5a_1$ receptor, $C5a_2$ receptor, CD11b and the FPR-1. Human isolated neutrophils we re-suspended in assay buffer to a concentration of 1×10^7 cells/mL and 90 µL of cell suspension was dispensed into wells of a 96 well polypropylene plate. Neutrophils were then stimulated with either LPS (5 ng/mL), TNFα (1 ng/mL), human purified C5a (5 nM) or human purified C5a des Arg (50 nM) at 37^{o}C 5% CO_2 for 60 minutes. Cells were then centrifuged at 300 x *g* for 5 minutes, assay buffer removed and cells re-suspended in the previously described stain buffer. Cells were transferred to a V-bottom polystyrene plate and further centrifuged as described above. To each well, 100 µL of either receptor specific staining cocktail containing; FITC-anti $C5a_1$ (Biolegend, Cat. 344306), APC-anti $C5a_2$ (Biolegend, Cat. 342406), PE-anti FPR-1 (R&D Systems, Cat. FAB3744P) and V450-anti CD11b (BD Biosciences, Cat. 562108) or isotype control cocktail was added. All antibodies were used at the manufacturers recommended concentrations. Cells were incubated with antibody cocktail for 20 minutes on ice in dark conditions. Cells were centrifuged and washed three times in 200 µL of stain buffer. Cells were re-suspended in 200 µL Cytofix™ (BD Biosciences, Cat. 554655) and incubated on ice in dark conditions for 20 minutes. Cells were centrifuged and washed twice in stain buffer. Each sample was filtered and the fluorescence intensity of each fluorophore was analysed using an LSR Fortessa™ flow cytometer (BD Biosciences). Single stain controls were generated to determine the degree of compensation correction required for each emission channel. Mean fluorescence intensity values of each fluorophore for each sample were expressed as a percentage of the no stimulation control.

2.12. Agonist induced intracellular calcium mobilization

$C5a_1$ CHO-K1 cells or human isolated neutrophils were suspended in assay buffer containing 1x Calcium 3 dye (Molecular Devices, Cat. R8091) to a concentration of 200,000 cells/mL. 50 µL of cell suspension was added to each well of a black, clear bottom, 384 well assay plate and incubated for 1 hour at 37^{o}C, 5% CO_2. For neutrophil experimentation, 10 µL of either assay buffer, $C5a_1$ receptor antagonist PMX53 (assay concentration of 1 µM), $C5a_2$ neutralizing antibody (clone 1D9-M12 Biolegend – assay concentration of 15 ng/mL) or isotype control antibody (clone MG2a-53, BioLegend – assay concentration of 15 ng/mL) was added to control wells. Assay plate was then incubated for a further hour at 37^{o}C, 5% CO_2. Assay plate was then stimulated with the addition of assay buffer or a concentration range of either C5a or C5a des Arg to wells that were previously treated with assay buffer. To wells pre-treated with receptor antagonists, cells were stimulated with a sub-maximal concentration of either C5a (assay concentration of 1nM) or C5a des Arg (assay concentration 3nM). Fluorescence of the Calcium 3 dye was measured from 0 seconds to 3 minutes post agonist addition using the FDSS 7000 plate reader (Hamamatsu, Japan). Maximum dye fluorescence in response to agonist addition was expressed as a ratio of dye fluorescence prior to agonist addition. All fluorescence ratio data were expressed as a percentage of the assay window defined by the basal and maximum C5a response.

2.13. Agonist induced neutrophil CD11b expression

Human isolated neutrophils were diluted in assay buffer to a concentration of 1.2 x 10^7 cells/mL. To each well of a 96 x 1 mL polypropylene block, 70 µL of cell suspension was added and the assay block was then incubated at 37^{o}C 5% CO_2 for 1 hour. 10 µL of either assay buffer, $C5a_1$ receptor antagonist PMX53 (assay concentration of 1µM), $C5a_2$ neutralizing antibody (clone 1D9-M12 Biolegend – assay concentration of 15 ng/mL) or isotype control antibody (clone MG2a-53, BioLegend –

assay concentration of 15 ng/mL) was added to respective wells. This was followed by the addition of 10 µL of 1 mg/mL APC mouse anti-Human CD11b/Mac-1 clone ICRF44 (BD Biosciences, Cat. 550019) and the assay block was incubated for 60 minutes at 37^{o}C, 5% CO_2. To each assay well treated with assay buffer, either 10 µL assay buffer or 10 µL of a concentration range of either C5a or C5a desArg was added. To wells pre-treated with antagonist, 10 µL of a sub maximal concentration of either C5a or C5a des Arg (assay concentration of 3 nM) was added. The assay block was then incubated for 30 minutes at 37^{o}C, 5% CO_2. After this time 500 µL of pre-warmed 1x BD Phosflow™ Lyse/Fix buffer (BD Biosciences) was added to each assay well and further incubated for 15 minutes at 37^{o}C 5% CO_2. Assay block was then centrifuged at 500 x g for 5 minutes, supernatant aspirated and cell pellet was re-suspended in 800 µL of assay buffer. Assay block was centrifuged again, assay buffer aspirated and cells pellets re-suspended in 200 µL of assay buffer and filtered prior to analysis. CD11b expression was assessed using a BD LSR Fortessa™ flow cytometer (BD Biosciences) and APC mean fluorescence intensity was quantified for each sample. Fluorescence values were expressed as a percentage of the basal control and maximum C5a response.

2.14. Agonist induced neutrophil respiratory burst

Human isolated neutrophils were suspended in assay buffer to a concentration of 2 x 10^7 cells/mL and 30 µL of cell suspension was added to each well of a 96 well polypropylene plate. Cells were incubated with 10 µL of either assay buffer or $C5a_1$ receptor antagonist PMX53 (assay concentration of 1µM), $C5a_2$ neutralizing antibody (clone 1D9-M12 Biolegend – assay concentration of 15 ng/mL) or isotype control antibody (clone MG2a-53, BioLegend – assay concentration of 15 ng/mL) for 45 minutes at 37^{o}C, 5% CO_2. 10 µL of either assay buffer or TNFα (assay concentration 1 ng/m, R&D Systems Cat. 210-TA) was added to each well and the assay plate was incubated for 15 minutes at 37^{o}C. Cells incubated with antagonist were stimulated with fixed concentrations of C5a (5 nM) or C5a des Arg (50 nM) and cells incubated with assay buffer were incubated with concentration ranges of either C5a or C5a des

Arg. Each agonist concentration was diluted in 2x the reactive oxygen species indicator dye, Dihydrorhodamine (DHR) 123 (Sigma-Aldrich, Cat. D1054) to a 2x concentration. Cells were stimulated with 50 µL of agonist for 15 minutes at 37^{o}C 5% CO_2. Samples were then added to a 96 well x 1.2 mL polypropylene block containing 400 µL pre-warmed Phosflow™ Lyse/Fix buffer (BD Biosciences) and incubated for 20 minutes at 37^{o}C 5% CO_2. A 200 µL sample from each well was filtered into a fresh assay plate and samples were analysed for mean fluorescence intensity on a BD LSR Fortessa™ flow cytometer (BD Biosciences). Fluorescence values for each sample were expressed as a percentage the basal and maximal C5a induced response.

2.15. Detection of intracellular ROS generation in the human isolated neutrophil

To determine the role of TNFα and C5a in the respiratory burst responses, the ability of each ligand to generate either hydrogen peroxide (H_2O_2) or hypochlorous acid (HOCl) in human isolated neutrophils was assessed. Human isolated neutrophils were re-suspended in assay buffer to a concentration of 2 x 10^6 cell/mL. For HOCl detection, experiment was performed as described above with DHR-123. Neutrophils were incubated with diluent or receptor antagonizing agents (PMX53, 1D9-M12, TNFR1 antibody (R&D Systems, Cat. MAB225), TNFR2 antibody clone (R&D Systems, Cat. MAB726), MPO inhibitor PF-1355 (Pfizer) or isotype controls antibody) for 45 minutes at 37^{o}C, 5% CO_2. Neutrophils were then incubated with TNFα (1 ng/mL R&D Systems) or diluent for 15 minutes at 37^{o}C, 5% CO_2 followed by 15 minute stimulation with either C5a (5 nM), C5a des Arg (50 nM) or diluent, all diluted in the HOCl indicator dye. Samples were then processed as described above and the mean fluorescence intensity of each sample was detected using an LSR Fortessa™ flow cytometer. Fluorescence values for each sample were expressed as a percentage of the maximal response to TNFα plus highest concentration of C5a.

For H_2O_2 detection, 30 µL cell suspension was added to wells of a 96 well polypropylene plate and incubated with the above receptor antagonizing agents for

45 minutes at 37°C, 5% CO_2. Cells were then stimulated with either TNFα (1 ng/mL), C5a or C5a des Arg for 15 minutes before hypotonic lysis with 50 µL sterile dH_2O for 30 minutes at 37°C 5% CO_2. Cell lysates were transferred to a clear flat bottom assay plate containing 100 µL of 1x Amplex® Red (Thermo Fisher Scientific, Cat. A22188). After 30 minutes incubation at room temperature, the assay plate was read on a EnVision® Multilabel plate reader (PerkinElmer) using a fluorescence protocol with excitation and emission wavelengths of 570 and 585 nm respectively.

2.16. Agonist induced human isolated neutrophil chemotaxis

Human isolated neutrophils were suspended in assay buffer containing 1.5 µM Calcein AM (Corning, Cat. 354217) at a cell concentration of 2 x 10^6 cells/mL and incubated for 30 minutes at 37°C, 5% CO_2. Cells were then centrifuged at 300 x g for 5 minutes and washed in assay buffer. Cells were then centrifuged again and suspended in assay buffer to a concentration of 2.2 x 10^6 cells/mL. Cells were then dispensed into wells of a 96 well polypropylene plate and incubated with either assay buffer, $C5a_1$ receptor antagonist PMX53 (assay concentration of 1µM), $C5a_2$ neutralizing antibody (clone 1D9-M12 Biolegend – assay concentration of 15 ng/mL) or isotype control antibody (clone MG2a-53, BioLegend – assay concentration of 15 ng/mL) for 60 minutes at 37°C, 5% CO_2. 50 µL of each cell sample was then added to the top chamber of a FluoroBlok™ multiwell plate (Corning Life Sciences) containing 3 µm polyethylene terephthalate membranes. To the bottom chamber, 200 µL of either assay buffer or concentrations of C5a or C5a des Arg were added. For cells pre-treated with antagonist a submaximal concentration of either C5a or C5a des Arg (1 nM) was added to the lower chamber. Both top and bottom chambers were assembled together and the chemotaxis plate was incubated for 60 minutes at 37°C, 5% CO_2. Chemotaxis plates were then read on an EnVision® Multilabel plate reader (PerkinElmer) using a bottom read protocol with excitation and emission wavelengths of 485 and 530 nm respectively.

2.17. Agonist induced cAMP accumulation in CHO cells expressing the $C5a_1$ receptor

CHO cells overexpressing the $C5a_1$ receptor were suspended in growth media and seeded at 10,000 cell/well into a black, clear bottom 384 well polystyrene assay plate and incubated at 37^{o}C, 5% CO_2 overnight. On the day of experimentation growth media was aspirated and replaced with 5 µL assay buffer. After equilibration for an hour at 37^{o}C, 5% CO_2, 5 µL of water soluble forskolin, NKH 477 (Tocris, Cat. 1603) was added to all assay wells to achieve an assay concentration of 10 µM. 5 µL of assay buffer or a concentration range of either C5a or C5a des Arg was added to separate assay wells and the plate was then incubated for 3 hours at 37^{o}C, 5% CO_2. Intracellular cAMP concentrations were then detected using the DiscoverX HitHunter® cAMP detection kit (Cat. 90-0075SM25). In brief, 5 µL of cAMP antibody reagent was added to all wells followed by 20 µL of cAMP working detection solution. Assay plate was equilibrated for 1 hour at room temperature in the dark to allow the immunocompetition reaction to occur. 20 µL of cAMP solution A was then added to each well and the assay plate was then incubated in the dark overnight prior to reading on a PerkinElmer Envision® Multilabel plate reader using a luminescence protocol. A cAMP standard curve was performed to ensure all cell generated cAMP was within the detection range of the assay kit.

2.18. Agonist induced ERK 1/2 phosphorylation in CHO cells expressing the $C5a_1$ receptor

C5a and C5a des Arg induced intracellular phosphorylation of extracellular signal-related kinase (ERK 1/2) was assessed using Cisbio's cell based homogeneous HTRF® assay kit (Cisbio, Cat. 64AERPEG). CHO cells overexpressing the $C5a_1$ receptor were seeded into a white, clear bottom, 384 well assay plate at 15,000 cells/well in growth media. Cells were incubated for 4 hours at 37^{o}C, 5% CO_2 to allow cells to attach. Growth media was then aspirated and replaced with growth media without FBS.

Assay plate was incubated at 37°C, 5% CO_2 overnight to minimize basal levels of phosphorylated ERK 1/2. On the day of experiment, cells were stimulated with concentration ranges of either C5a or C5a des Arg prepared in FBS deficient growth media supplemented with 0.05% BSA (Miltenyi Biotec Cat. 130-091-376). The plate was incubated at 37°C, 5% CO_2 for 5 minutes after which time the assay was terminated by the rapid removal of liquid from each well by a flicking action onto a paper towel, followed by the rapid administration of the cell lysis to all assay wells. After a 60 minute incubation on a shaker at room temperature, cell lysates were transferred to respective wells of a white, low volume 384 well detection plate containing 4 μL of pre-mixed pERK specific antibody detection reagent. The assay plate as then sealed and incubated at room temperature overnight before being read on a PerkinElmer Envision® Multilabel plate reader using a 337 nm excitation and 620/665 nm emission protocol. Emission ratio values were expressed as a percentage of assay window defined by the no stimulation control and the maximum response achieved with C5a.

2.19. Agonist induced $C5a_1$ or $C5a_2$ receptor internalization

Agonist induced receptor internalization was assessed using the DiscoverX PathHunter® Activated GPCR Internalization Assay technology. This technology monitors GPCR trafficking to the early endosome using β-galactosidase (β-gal) enzyme fragment complementation. In this system a small fragment of β-gal called the ProLink™ is localized to intracellular endosomes. The larger fragment of β-gal, called the Enzyme Acceptor is fused to β-arrestin. Receptor stimulation leads to β-arrestin recruitment to the activated GPCR followed by internalization of the receptor-arrestin complex to cellular endosomes. This results in complementation of the two enzyme fragments and the formation of a functional enzyme that is able to hydrolyse a substrate to generate a chemiluminescent signal using the PathHunter® detection reagents.

U2OS cells over expressing either the $C5a_1$ or the $C5a_2$ receptor, enzyme acceptor tagged β-arrestin and a ProLink™ tag localized to the endosomes were plated at 5000 cells per well in 20 µL in 384 well, black, clear bottom, tissue culture plates in DiscoverX proprietary cell plating media and left for 24 hours at 37°C, 5% CO_2. Cell plating media was aspirated and replaced with 20 µL assay buffer. Cells were next incubated with 5 µL of either assay buffer, the $C5a_1$ receptor antagonist PMX53 (1 µM final assay concentration), mouse anti-human $C5a_2$ receptor (15 µg/mL final assay concentration of clone 1D9-M12, BioLegend), or mouse IgG2a isotype antibody control (15 µg/mL final assay concentration of clone MG2a-53, BioLegend) for 60 minutes at 37°C, 5% CO_2. Assay buffer pre-treated cells were then stimulated with 5 µL of either assay buffer or concentrations of C5a or C5a des Arg. Cells pre-treated with antagonist or isotype control were stimulated with 5 µL of either 3 nM or 30 nM final assay concentration of C5a or C5a des Arg. Assay was incubated for 3 hours at 37°C 5% CO_2. 12 µL PathHunter® detection reagent was added to each experimental well and the assay plate was incubated for 60 minutes at room temperature. Assay plates were then read on an EnVision® Multilabel plate reader (PerkinElmer) using luminescence protocol.

2.20. Agonist induced $C5a_1$ or $C5a_2$ receptor β-arrestin recruitment

Agonist induced β-arrestin recruitment to C5a receptors was assessed using the DiscoverX PathHunter® β-arrestin recruitment assay technology. The assay principle is similar to that described above for the internalization assay, with enzyme complementation occurring when receptor and β-arrestin come together.

CHO-K1 cells over expressing either ProLink™ fused $C5a_1$ receptor or the $C5a_2$ receptor and enzyme acceptor tagged β-arrestin were plated at 5000 cells per well in 20 µL in 384 well, black, clear bottom, tissue culture plates in DiscoverX proprietary cell plating media and left for 24 hours at 37°C, 5% CO_2. The remainder of the assay

was performed in the same manner as described for the PathHunter® internalization assay.

2.21. Expression of wild type and mutant $C5a_1$ receptors in CHO cells

To determine whether specific amino acid residues, located within the transmembrane region of the $C5a_1$ receptor, contribute to either the affinity and functional potency of human purified C5a and C5a des Arg or antagonism produced by PMX53 and NDT9513727, either wild type or mutant $C5a_1$ receptor constructs (E180A, E199A, D282A, R175A and R206A) were expressed in CHO cells. pcDNA3.1 plasmids containing each $C5a_1$ receptor gene were generated by Blue Sky BioServices Inc, Worcester, MA, USA. CHO cells transformed to stably over express the $G\alpha_{16}$ G-protein under Zeocin resistance were grown to 80% confluency in media described above with the exclusion of Geneticin®. Cells were re-suspended in electroporation buffer (MaxCyte, Cat. EBR100) to a concentration of 1×10^8 cells/mL and 2×10^7 cells were mixed with 40 μg of a single plasmid. Cells and plasmid were then transferred to a processing assembly (MaxCyte Cat. OC-400R10) and cells were transfected with the MaxCyte STX® electroporation transfection system using a CHO cell specific protocol. Cells were then incubated at 37°C, 5% CO_2 for 30 minutes in electroporation buffer before being re-suspended in previously described growth media and seeded into a 384 well, black, clear bottom assay plate at a density of 10,000 cells/well. Cells were incubated over night at 37°C, 5% CO_2 before being investigated for agonist induced calcium mobilisation. The expression of each receptor was assessed using the $C5a_1$ receptor specific, FITC-S5/1 antibody (Biolegend) and flow cytometry as described above.

Chapter 3

The characterization of reagents and pharmacological tools to enable accurate interrogation of C5a, C5a des Arg and their receptors, $C5a_1$ and $C5a_2$

The characterization of reagents and pharmacological tools to enable accurate interrogation of C5a, C5a des Arg and their receptors, $C5a_1$ and $C5a_2$

3.1. Abstract

To elucidate the role of a protein macromolecule in a complex signalling pathway, scientists often use protein specific antibody, peptide and small molecule pharmacological tools to activate or neutralize the function of that protein. However, the specificity of a pharmacological tool for a single protein is concentration dependent, and using excessive amounts of that tool will invariably lead to the cross reactivity with other proteins. Selection of pharmacological tools is usually achieved through data presented in peer reviewed scientific manuscripts, where details pertaining to the purity and protein specificity of that tool are often misleading or absent. To enable the robust and accurate interrogation of the role of C5a and C5a des Arg in $C5a_1$ and $C5a_2$ signalling, here I have performed a thorough evaluation of the purity and receptor specificity of pharmacological tools that are reported to interact with the C5a receptors. Through the use of receptor specific cell lines and competition binding experiments I have been able to select pharmacological tools and concentrations that will specifically perturb the interaction of C5a and C5a des Arg at either the $C5a_1$ or $C5a_2$ receptors. These data will inform tool selection for research outlined in subsequent chapters of this thesis.

3.2. Introduction

Small molecule, peptide ligands and specific protein antibodies are essential pharmacological tools to determine the role and function of protein macromolecules in biological systems. Pharmacological tools, in conjunction with tailored experimental methods, not only enable the pharmacologist to determine the presence and abundance of a peptide or protein but also allow them to elucidate its role within a specific signalling pathway in the biological system of interest.

In order for a pharmacologist to make an accurate claim regarding the role of a peptide or protein in a biological signalling pathway they must understand the quality and true protein specificity of the pharmacological tool that is being used. No pharmacological tool is truly specific for any protein subtype and any claims regarding specificity of an agent will be related to a concentration used (Ramage, 2005).

Pharmacological tool selection is generally achieved by gathering information from peer reviewed scientific manuscripts or from information provided by the supplier. The specificity of a pharmacological tool is often determined by biochemical or pharmacological experimentation using either purified or recombinant versions of the protein of interest. However, in some instances, claims regarding the specificity of a pharmacological tool can be misleading. This can then lead the pharmacologist to make incorrect assumptions about the quality, specificity and subsequent utility of the research tool under consideration. Lack of or misleading information can present in several forms:

1. Minimal information concerning the amino acid sequence of a peptide ligand or a protein target to which the tool was designed.

2. No information pertaining to the mode of the tools action. Where on the protein target does the tool bind? Is it competitive or non-competitive with the endogenous ligand for that protein?

3. Appropriate use of pharmacological endpoints to assess the selectivity of the pharmacological tool for the protein of interest over closely related protein homologues. For instance, IC_{50} values can sometimes exaggerate the specificity of a competitive receptor antagonist for one protein over another if inappropriate concentrations stimulating agonist or tracer ligand are used.

The main aim of this chapter is to perform a thorough characterization of the biological systems that specifically overexpress either the $C5a_1$ or $C5a_2$ receptor and determine the selectivity profile of the commercially available pharmacological agents that bind to these receptors. These agents include the peptide anaphylatoxins, C5a and C5a des Arg and the reported receptor specific tools which could be used to antagonize C5a and C5a des Arg at either the $C5a_1$ or $C5a_2$ receptor. These data will enable accurate interrogation of these ligands and receptors in subsequent chapters of this thesis.

To address the concerns regarding the specificity of pharmacological tools that could be used to investigate the role of the fragment anaphylatoxin peptides C5a and C5a des Arg and the role of their receptors $C5a_1$ and $C5a_2$ in cell signalling this chapter includes the following aims:

1. Confirm the sequence of the $C5a_1$ and $C5a_2$ receptor that are overexpressed in previously generated in-house cell lines (CHO-K1 expressing $C5a_1$ receptor and the $G_{\alpha16}$ G-protein, U2OS expressing the $C5a_2$ receptor and GFP β-arrestin 2).
2. Confirm that each cell line selectively expresses the relevant C5a receptor.
3. Quantify the purity and molecular weight of commercially sourced human purified C5a and C5a des Arg by mass spectrometry.
4. Develop receptor ligand binding assays for both the $C5a_1$ and $C5a_2$ receptor using the overexpressing cells and ^{125}I-C5a to quantify the affinity and receptor specificity of reported pharmacological tools.

3.3. Chapter specific methods

3.3.1. Data analysis and model fitting

All non-linear regression models were fitted to data using GraphPad Prism version 6.00 for Windows (GraphPad Software, La Jolla California USA, www.graphpad.com).

Radioactive counts in CPM obtained from saturation binding experiments were converted to number of receptors in fmol/100,000 cells using a counter efficiency correction factor, the DPM/Ci constant 2.22 x 10^{12}, ligand specific activity of 2200 Ci/mmol and the number of cells per assay well. Saturation data were fit to a one site specific binding model. The K_d defined as the concentration of hot ligand that binds 50% of the receptor population and B_{max} defined as the maximum number of binding sites per sample.

Association kinetic data were globally fit to the association kinetic model using multiple concentrations of hot ligand to derive a single best-fit estimate for k_{on} and for k_{off}.

Concentration response data from competition binding experiments were fit using the four parameter logistic equation (equation 3.1) to obtain IC_{50} values and an estimate of Hill slope. Affinity constants (K_i) for each competitive agent were calculated from IC_{50} values using the Cheng-Prusoff equation as described by Cheng *et al.* (1973) (equation 3.2).

Equation 3.1. Four parameter logistic equation

$$y = d + \frac{a - d}{1 + \left(\frac{x}{c}\right)^b}$$

Where, y = dependent variable, x = independent variable a = lower asymptote, b = Hill slope, c = IC_{50}, d = upper asymptote.

Equation 3.2. Cheng-Prusoff equation

$$K_i = \frac{IC_{50}}{1 + \frac{[L]}{K_d}}$$

Where, K_i = equilibrium dissociation constant of a ligand for receptor, IC_{50} = concentration of pharmacological tool that inhibits 50% of tracer ligand binding to the receptor, [L] = free concentration of tracer ligand used in the experiment, K_d = equilibrium dissociation constant of the tracer ligand for receptor.

3.4. Results

3.4.1. Sequence analysis of recombinant $C5a_1$ receptor and $C5a_2$ receptor overexpressed in CHO and U2OS cells

To make accurate conclusions regarding the selectivity and specificity of pharmacological tools for each of the C5a receptors, the DNA sequence of the $C5a_1$ receptor over expressed in CHO cells and the $C5a_2$ receptor over expressed in U2OS cells was determined. Two sets of PCR primers were designed to the flanking sequences of the expression vectors for the $C5a_1$ and $C5a_2$ constructs. The PCR products were purified and sent to Wyzer Biosciences Inc (Cambridge MA, US) for double stranded sequencing.

The DNA nucleotide sequence for each recombinant gene from the initiating 'ATG' (Methionine) codon to the stop 'TAG' codon was aligned with the human DNA sequence for each gene published in the NCBI database ($C5a_1$ receptor = NM_001736, $C5a_2$ receptor = NM_018485). The $C5a_1$ receptor nucleotide sequence aligned 100% with the published nucleotide sequence. The alignment of the $C5a_2$ receptor highlighted one nucleotide difference at position 754 with the recombinant $C5a_2$ gene containing thymine and the published gene sequence containing cytosine. However the resultant nucleotide triplet (recombinant $C5a_2$ receptor = TTG) encodes for the same amino acid, leucine, as reported in the published protein sequence (published $C5a_2$ receptor = CTG), and therefore the difference is conserved. This results in 100% identity for each recombinant receptor protein sequence to the published protein sequence ($C5a_1$ receptor = NP_001727, $C5a_2$ receptor = NP_060955). Amino acid alignment of each receptor protein sequence is shown in appendix 1.

3.4.2. Quantifying the expression of each C5a receptor in the CHO and U2OS cells

A range of methods were utilized to assess the extent and selectivity of expression of each C5a receptor at both the gene and protein level.

Real-time qPCR was employed to assess the relative $C5a_1$ and $C5a_2$ receptor gene expression in each cell line compared to the endogenous control GAPDH. For each gene in each sample ΔCT were calculated by subtracting the average CT of GAPDH control gene from CT of each replicate for the test gene. Expression values were multiplied by a constant value such that genes with CT values of background (CT > 35) had an expression value of ~1. This allowed for easy determination of signals above background. Relative gene expression for the $C5a_1$ and $C5a_2$ can be seen in figure 3.1. The stably transfected CHO cell express the $C5a_1$ receptor gene to a high level with approximately 3×10^6 relative expression and as expected there was no detection of endogenous $C5a_2$ receptor in this rodent cell line. Similarly the U2OS cell line stably expressing the $C5a_2$ receptor displays a high copy number of this gene with approximately 2×10^6 relative gene expression. Using the primer probe set for the $C5a_1$ receptor gene that maps within a single exon (highest gene coverage) it can be seen that this gene is expressed at a low level in the U2OS cell. However, the expression of the $C5a_2$ receptor is more than 300 time that of the $C5a_1$ receptor which is sufficient to assess the specificity of agents towards the $C5a_2$ receptor. Quantification of endogenous $C5a_2$ gene expression with a primer probe set that spans an exon demonstrates that all of the $C5a_2$ receptor expression in the U2OS cell comes from the stable transfection of this cell line.

Whole cell protein expression of each receptor was next determined by resolving proteins from transformed CHO cell and U2OS cell lysates using gel electrophoresis followed by immunoblotting with specific receptor antibodies. GAPDH detection was used as protein loading control and lysates from GM-CSF differentiated human monocyte-derived macrophages were used as a control lysate for both C5a receptors. As can be seen in figure 3.2, a single protein band that corresponds to the approximate molecular weight of either the $C5a_1$ or $C5a_2$ receptor (45 kDa) appears

in each of the macrophage lysate lanes confirming the expression of both C5a receptors in human monocyte-derived macrophages. The detection of a $C5a_1$ receptor protein band was only observed in the CHO cell lysate while the detection of a $C5a_2$ receptor protein band was only observed in U2OS cell lysate. Unlike the single $C5a_2$ protein band identified in the macrophage lysate, two discrete bands appear in the U2OS lysate. This double band probably reflects a post translational modification of the $C5a_2$ receptor that has occurred in the U2OS cell line. These data confirm the selective protein expression of the $C5a_1$ and $C5a_2$ in the CHO and U2OS cell lines respectively.

Flow cytometry analysis was employed to ascertain the expression of each receptor at the surface of each cell line. Separate samples of each cell line were stained with fluorophore conjugated antibodies that are specific for each C5a receptor. Mean fluorescence staining intensity was compared to samples stained with matching concentrations of isotype control antibodies.

As can be seen from figure 3.3, the CHO cell line displays a high degree of staining intensity for the $C5a_1$ receptor compared to isotype control (A) with no meaningful staining intensity of the $C5a_2$ receptor (C). Whereas the U2OS cell line displays a high degree of staining intensity for the $C5a_2$ receptor (D) with no meaningful expression of the $C5a_1$ receptor (B). Saturated receptor staining was achieved with the manufactures recommended test concentration of 1 µg for the $C5a_1$ specific S5/1 antibody clone and 2 µg for the $C5a_2$ specific 1D9-M12 antibody clone.

Combined with the gene and whole cell protein expression results, these data confirm the selective cell surface expression of either the $C5a_1$ or the $C5a_2$ receptor in the CHO cells and U2OS cells respectively.

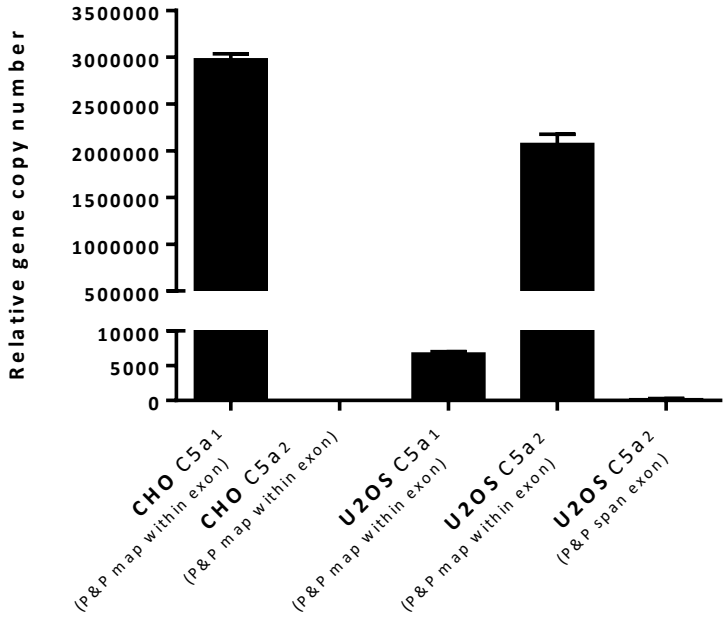

Figure 3.1. Selective gene expression of the $C5a_1$ and $C5a_2$ receptors in the transformed cell lines

$C5a_1$ and $C5a_2$ receptor gene expression quantified from RNA isolated from either CHO or U2OS cells using Real-Time PCR. Relative gene copy number was calculated using the endogenous control gene GAPDH and a comparative CT method ($2^{-\Delta Ct}$). The vertical axis represents mean + S.D. from quadruplicate wells. Data obtained from a single experiment.

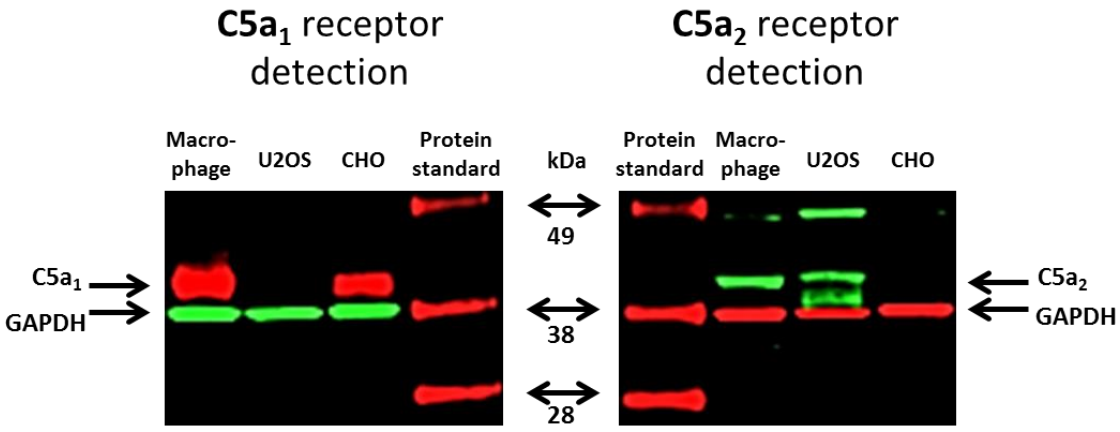

Figure 3.2. Whole cell expression of the $C5a_1$ and $C5a_2$ receptors in CHO and U2OS cells

Detection of the $C5a_1$ and $C5a_2$ receptor protein in lysates from CHO and U2OS cells by immunoblotting. GAPDH was used as the sample loading control and lysate from human monocyte-derived macrophage was used as a positive sample control. Image representative of three separate experiments.

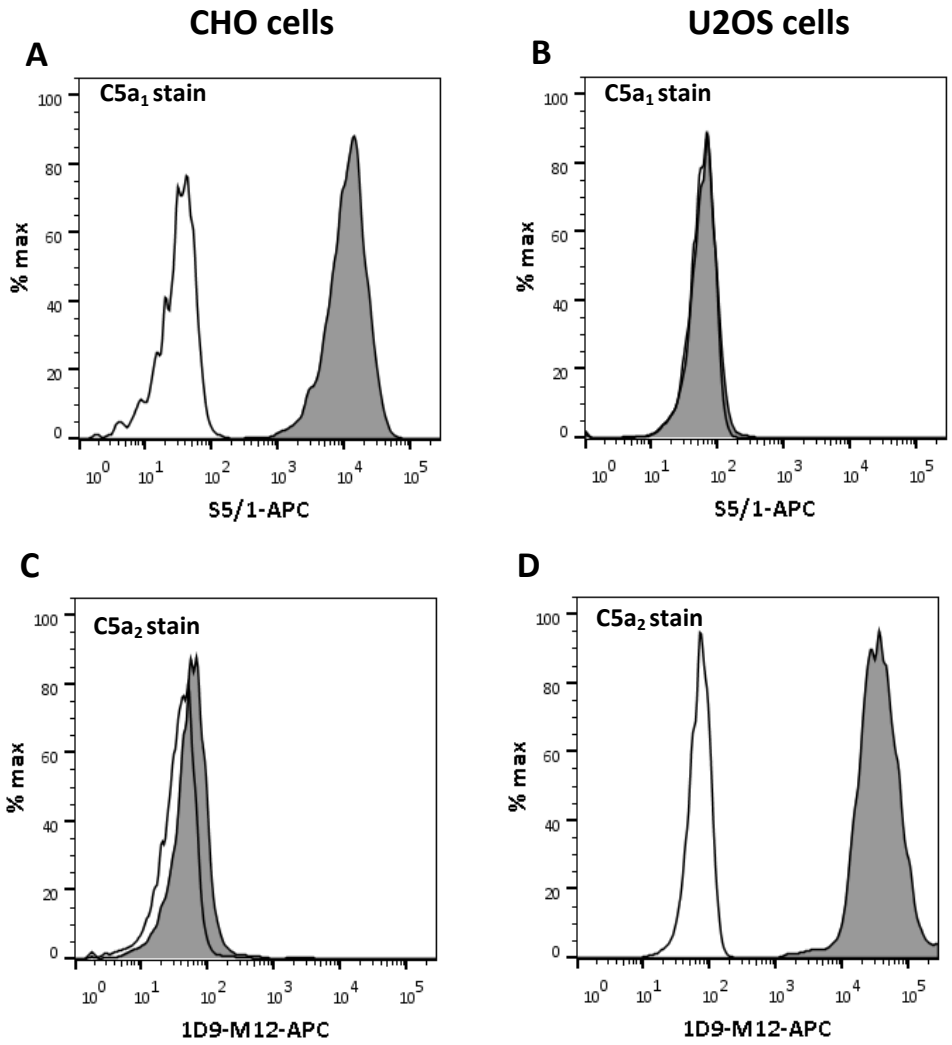

Figure 3.3. Cell line specific membrane expression of either the $C5a_1$ and $C5a_2$ receptor

Cell surface staining of CHO cells with either the (A) $C5a_1$ specific S5/1 antibody or (C) $C5a_2$ specific 1D9-M12 antibody and cell surface staining of U2OS cells with either (B) the $C5a_1$ specific S5/1 antibody or (D) the $C5a_2$ specific 1D9-M12 antibody. Receptor specific antibody staining is represented by the filled histogram and the isotype matched control staining by the open histogram. The horizontal axis represents mean fluorescence intensity. The vertical axis represents cell count as a percentage peak height at the mode of the distribution.

3.3.3. Characterisation of human purified C5a and C5a des Arg

In order to verify the purity and mass of the purchased human purified C5a and C5a des Arg, each peptide fragment was analysed using mass spectrometry. Peptide purity was assessed at an absorbance wavelength of 280 nm and revealed that C5a was 96% pure (figure 3.4A). Maximum Entropy deconvolution was applied to the raw mass spectrometry data from peak 2 (B) to determine the peptide mass in the target molecular weight range (C). The deconvoluted mass showed a parent ionization peak at 10,594 Da and a daughter peak at 10,476 Da with a molecular weight difference between these peaks of 118 Da. Similar results were observed for C5a des Arg (figure 3.5). Peptide purity was approximately 95% (A) and the devonvolution of the raw mass spectrometry peak (B) generated a parent ionizing peak at 10,438 Da and a daughter ionizing peak at 10,319 Da. The difference between parent and daughter peak was 119 Da.

The observed presence of parent and daughter ionization peaks split by a mass difference of 119 Da can be explained by cysteinylated adduct formation. C5a and C5a des Arg each contain a total of seven cysteine residues (figure 3.6 A). Reis *et al.* (2012) comment that six of the these cysteines are engaged in disulphide bridges between residues 21-47, 22-54 and 34-55. The cysteine at position 27 is therefore able to associate with free plasma cysteines in circulation forming a cysteinylated adduct via a disulphide bond. This results in the parent ionizing peak, which contains the cysteinylated adduct, having a mass increase of 119 Da compared to the daughter ionizing peak which does not (figure 3.6 B).

To determine the molecular weight difference between C5a and C5a des Arg the molecular weight of the parent ionization peak for C5a des Arg was subtracted from the molecular weight of the parent ionization peak for C5a. This revealed a molecular weight difference of 156 Da. Arginine is removed from the C-terminus of C5a via enzyme mediated hydrolysis by carboxypeptidases. The molecular weight of Arginine is 174 Da and its removal followed by the addition of water (18 Da) results in a mass difference of 156 Da (figure 3.7).

The expected mass of each peptide based on the amino acid composition is 8274 and 8117 Da for C5a and C5a des Arg respectively (determined using an online peptide mass calculator). However both peptides have generated ionization peaks between 10,600 and 10,300 Da. This extra mass is can be explained by the glycosylation pattern of each peptide. Fernandez *et al.* (1978b) demonstrated that the asparagine residue at position 64 in C5a is linked to a single oligosaccharide unit. Attachment occurs by a N-glycosidic linkage between N-acetylglucosamine and the amide nitrogen of an asparagine side chain which follows the empirical rule for N-glycosylation at an asparagine residue in that the linkage occurs in glycoproteins only at an Asn-X-Ser/Thr sequence (Jackson *et al.*, 1970).

3.3.4. Determining the specificity of ligands and pharmacological tools for the $C5a_1$ and $C5a_2$ receptors

Competition binding experiments using ^{125}I-C5a were next employed to determine the affinity and selectivity of a set of pharmacological tools at the $C5a_1$ and $C5a_2$ receptors. All receptor ligand binding experiments were constructed in a way to prevent ligand depletion (< 10% of ^{125}I-C5a or compound is bound to receptor or non-specific sites). To ensure all affinity constants (K, the equilibrium dissociation constant) were determined at equilibrium, a set of association kinetic experiments using two concentrations of ^{125}I-C5a were performed at each receptor. As can be seen in figure 3.8, the binding of ^{125}I-C5a to both C5a receptors is stable at the four hour extended incubation time. Data for both ligand concentrations were fit to the association kinetic model to derive a single best-fit estimate for k_{on} and for k_{off} from which an estimate of the K_d could be derived. ^{125}I-C5a bound to $C5a_1$ receptor with a mean average k_{on} of 6.48E+08 M^{-1} $min^{-1,}$ a k_{off} of 0.011 min^{-1} which generated a kinetically derived K_d of 18 pM. ^{125}I-C5a displayed an eight fold slower k_{on} to the $C5a_2$ receptor (7.96E+07 M^{-1} min^{-1}) but a comparable K_{off} (0.018 min^{-1}) which generated a kinetically derived K_d of 255 pM.

^{125}I-C5a saturation analysis was next performed on each C5a receptor expressing cell line at the extended four hour incubation time. This experiment allows the determination of the K_d, the concentration of ligand that binds to 50% of the receptor population at equilibrium, a value which is required for affinity constant calculation using the Cheng-Prusoff equation. ^{125}I-C5a saturated both receptor populations in a monophasic manner (figure 3.9) with average Hill slopes of 0.85 and 1.1 for $C5a_1$ and $C5a_2$ respectively and bound to $C5a_1$ receptors expressed on CHO cells with a K_d of 35.2 $\pm$ 7.41 pM (n=5) and to the $C5a_2$ receptors expressed on U2OS cells with a K_d of 169.8 $\pm$ 52.3 pM (n=4). Both receptors were expressed at a high density in their respective cells lines with the $C5a_2$ receptor expressed eight fold higher (B_{max} = 98 fmol receptor/100,000 cells) than the $C5a_1$ receptor (B_{max} = 12 fmol receptor/100,000 cells).

Eight of the pharmacological tools tested (table 3.1) bound to the $C5a_1$ receptor in a competitive manner with ^{125}I-C5a and displayed the following rank order of affinity: human purified C5a > human recombinant C5a > 8D6 > human purified C5a des Arg > P12/1 > S5/1 > NDT9513727 > PMX53. Four of the tools bound the $C5a_2$ receptor in a competitive manner with ^{125}I-C5a with the following rank order of affinity: human purified C5a > human purified C5a des Arg > human recombinant C5a > 1D9-M12.

A Purity at 280nm

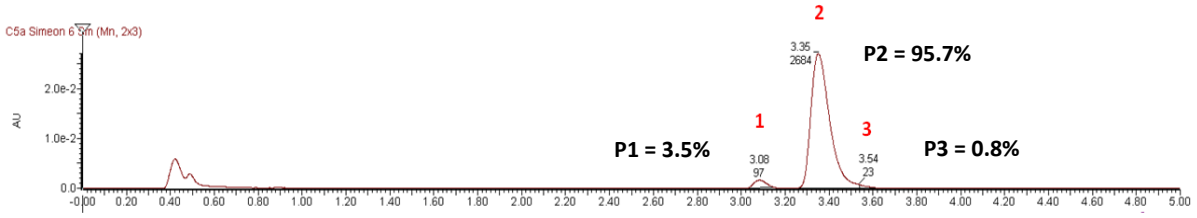

B Raw MS spectra of peak 2

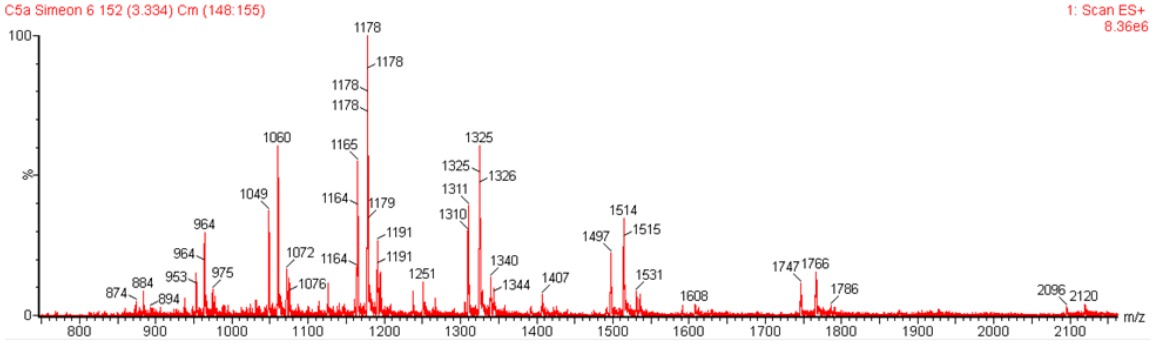

C Deconvoluted spectra of peak 2

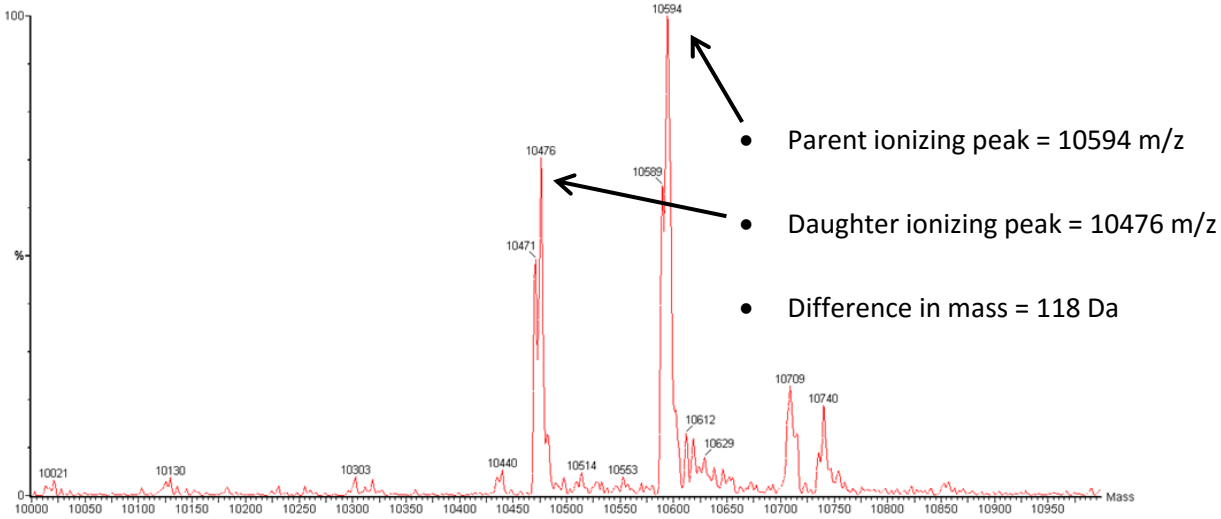

Figure 3.4. Purity assessment and mass determination of human purified C5a

Analysis of C5a peptide purity as measured at an absorbance of 280 nm (A). Raw mass spectrometry data for peak 2 (B) and deconvolution of peak 2 using MaxEnt in the anticipated molecular weight range of C5a (C).

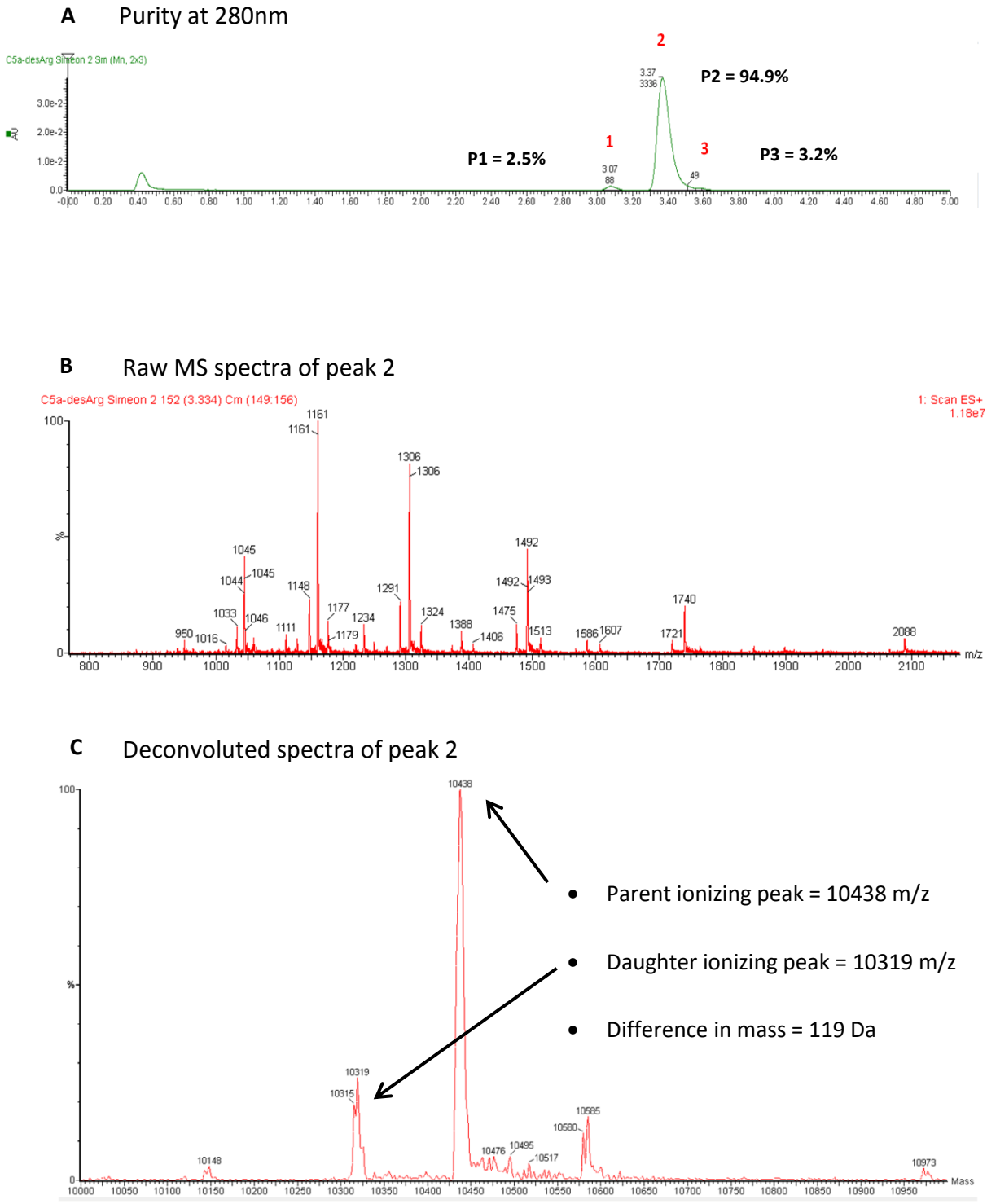

Figure 3.5. Purity assessment and mass determination of human purified C5a des Arg

Analysis of C5a des Arg peptide purity as measured at an absorbance of 280 nm (A). Raw mass spectrometry data for peak 2 (B) and deconvolution of peak 2 using MaxEnt in the anticipated molecular weight range of C5a des Arg (C).

A

B.

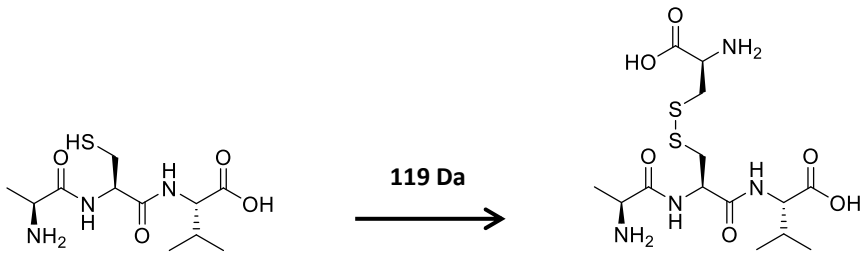

Ala-Cys-Val

MW = 291.366

Cys

Ala-Cys-Val

MW = 410.504

Figure 3.6. Location of asparagine and cysteine residues in the peptide sequence of C5a and cysteinylation of cysteine[27]

Location of the glycosylated asparagine[64] (underlined) and cysteine residues in the amino acid sequence of C5a (A). Disulphide bridges form between cysteine residues 21-47 (red), 22-54 (blue) and 34-55 (green) leaving a free cysteine residue at position 27 (orange). Cysteinylation results in a mass increase of 119 Da (B).

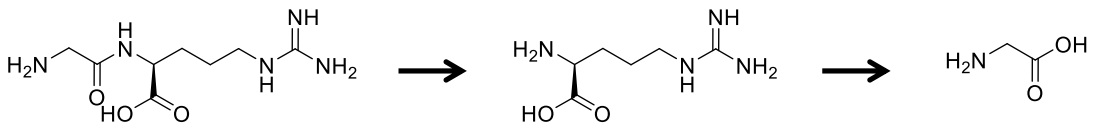

Gly-Arg MW = 231.256

Arg MW = 174.204

Gly MW = 75.067

Figure 3.7. Removal of arginine via enzyme mediated hydrolysis

Amino acid scheme detailing the molecular weight reduction in C5a when arginine is removed via enzyme mediated hydrolysis to form C5a des Arg. This results in a molecular weight difference of 156 Da between the two peptides.

Both the recombinant C5a and the ^{125}I-C5a originate from the source (Sigma Aldrich Cat# C5788) and the affinity estimates for this ligand across the association kinetic, saturation and competition binding assays are highly comparable (18, 35, & 20 pM for $C5a_1$ receptor and 255, 170 and 171 pM for the $C5a_2$ receptor).

Human purified C5a displayed very high affinity towards the overexpressed $C5a_1$ receptor in CHO cells and demonstrated a nine fold selectivity for $C5a_1$ receptor over the $C5a_2$ receptor. Similar results were obtained with human recombinant C5a. In contrast C5a des Arg displayed marginally higher affinity (two fold) for the $C5a_2$ receptor. Interestingly the competition response curves for C5a des Arg at the $C5a_1$ receptor were notably shallow (-0.54, n=4) and significantly different to the slopes at the $C5a_2$ receptor (-1, n=4) (paired Students t-test; P=0.01) (figure 3.10 B).

As expected the anaphylatoxin peptides C3a and C3a des Arg did not bind either C5a receptor in a competitive manner with ^{125}I-C5a. C3a and C3a des Arg have been reported to possess acylation-stimulation properties (Murray *et al.*, 1997) and that C3a des Arg mediates this response via binding to and activation of the $C5a_2$ receptor (Kalant *et al.*, 2003). The authors demonstrate that C3a des Arg interacts with the $C5a_2$ receptor is at discrete binding sites to those used by C5a. These data confirm that there is no competitive interaction between these two peptides at the $C5a_2$ receptor, and confirms the results obtained by Johswich *et al.* (2006).

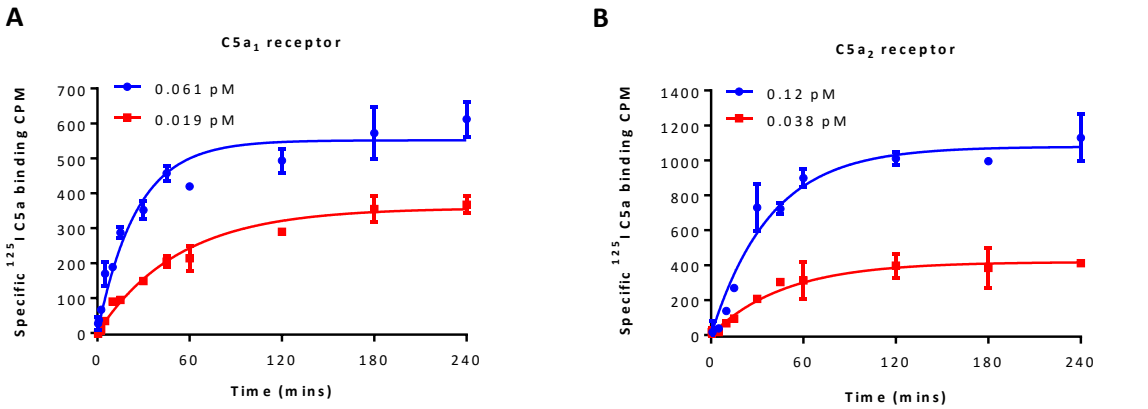

Hot ligand (nM)	K_{off} (min^{-1})	K_{on} (M^{-1} min^{-1})	K_d (M)
0.061	0.010	4.88E+08	1.98E-11
0.019	0.010	4.88E+08	1.98E-11

Hot ligand (nM)	K_{off} (min^{-1})	K_{on} (M^{-1} min^{-1})	K_d (M)
0.121	0.019	5.97E+07	3.15E-10
0.038	0.019	5.97E+07	3.15E-10

Figure 3.8. Binding kinetics of ^{125}I-C5a to the $C5a_1$ and $C5a_2$ receptors

Association of ^{125}I-C5a to (A) the $C5a_1$ receptor and (B) the $C5a_2$ receptor with two concentrations of hot ligand. A global association kinetics model was fit to each data set to obtain K_{on} (M^{-1} min^{-1}), K_{off} (min^{-1}) and K_d (M). Each data point is the mean average of two replicates ± S.D. Representative data from two separate experiments.

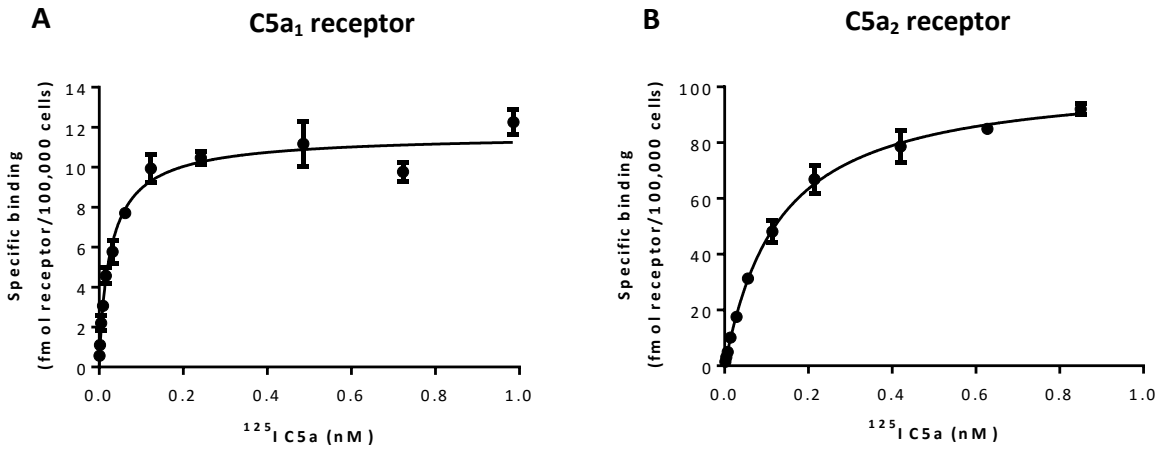

Figure 3.9. Saturation analysis of $C5a_1$ and $C5a_2$ receptors using ^{125}I-C5a

Specific binding of ^{125}I-C5a to (A) $C5a_1$ receptors on CHO cells and (B) $C5a_2$ receptors on U2OS cells. Plateau of the non-linear regression curve defined the maximal receptor expression (B_{max}). Affinity (K_d) was defined as the concentration of ^{125}I-C5a that bound 50% of the receptor population. Each data point is the mean average of two replicates. Data representative of four separate experiments.

The cyclic peptide antagonist PMX53 and small molecule antagonist NDT9513727 displayed high affinity for the $C5a_1$ receptor inhibiting the binding of ^{125}I-C5a to the $C5a_1$ receptor in a concentration dependent manner. Neither agent inhibited the binding of ^{125}I-C5a to the $C5a_2$ receptor. Similar $C5a_1$ receptor selective inhibition profiles were observed with the antibody clones P12/1, S5/1 and 8D6. The P12/1 and S5/1 mouse monoclonal antibodies were both generated through peptide immunization using a 31 amino acid peptide fragment of the N-terminus of the $C5a_1$ receptor (Met^1-Asn^{31}). Vendors of this antibody (Abcam and Novus Biologicals) both claim in their product literature that clone P12/1 does not inhibit C5a binding to the $C5a_1$ receptor. However, data in this report clearly demonstrate this claim to be false. Interestingly, unlike clone 8D6 which was raised using a rat basophilic leukemia cell line (RBL-2H3) transfected with the human $C5a_1$ receptor, both P12/1 and S5/1 cannot fully displace ^{125}I-C5a from binding to the $C5a_1$ receptor with approximately 15-20% residual ^{125}I-C5a binding at receptor saturating concentrations of these two antibodies. Antibody clone W17/1 demonstrated weak inhibition of ^{125}I-C5a at the $C5a_1$ receptor with no apparent affinity for $C5a_2$.

Of all the antibody clones tested, only 1D9-M12 inhibited the binding of ^{125}I-C5a to the $C5a_2$ receptor. As anticipated from the flow cytometry results this antibody does not bind the $C5a_1$ receptor in a competitive manner with C5a.

	$C5a_1$ receptor			$C5a_2$ receptor			
Agent	**Mean pK_i**	**95% CI**	**Mean K_i (M)**	**Mean pK_i**	**95% CI**	**Mean K_i (M)**	**Fold selectivity**
hp C5a	11.08	10.91 - 11.25	8.29E-12	10.11	9.90 – 10.32	7.75E-11	9.3 for $C5a_1$
hp C5a des Arg	9.47	9.25 - 9.70	3.35E-10	9.84	9.61 – 10.07	1.45E-10	2.3 for $C5a_2$
hrec C5a	10.68	10.51 - 10.85	2.08E-11	9.77	9.61 – 9.91	1.71E-10	8.2 for $C5a_1$
hp C3a	X			X			X
hp C3a des Arg	X			X			X
PMX53	8.02	7.94 - 8.11	9.46E-09	X			Specific for $C5a_1$
NDT9513727	8.37	8.18 - 8.57	4.25E-09	X			Specific for $C5a_1$
P12/1	8.89	8.74 - 9.03	1.30E-09	X			Specific for $C5a_1$
8D6	10.09	9.93 - 10.25	8.16E-11	X			Specific for $C5a_1$
S5/1	8.72	8.56 - 8.89	1.89E-09	X			Specific for $C5a_1$
W17/1	X			X			X
1D9-M12	X			8.35	8.19 – 8.51	4.45E-09	Specific for $C5a_2$
N 1-50	X			X			X
N 1-23	X			X			X
Mouse Isotype	X			X			X
Rabbit Isotype	X			X			X

Table 3.1. Affinity of pharmacological tools for the $C5a_1$ and $C5a_2$ receptors

Affinity estimates for pharmacological tools that are reported to bind the C5a receptors. Affinity estimates (K_i) calculated from IC_{50} curves using the Cheng-Prusoff equation. Mean K_i and 95% CI calculated from four separate experiments. X = less than 50% inhibition achieved at highest concentration tested.

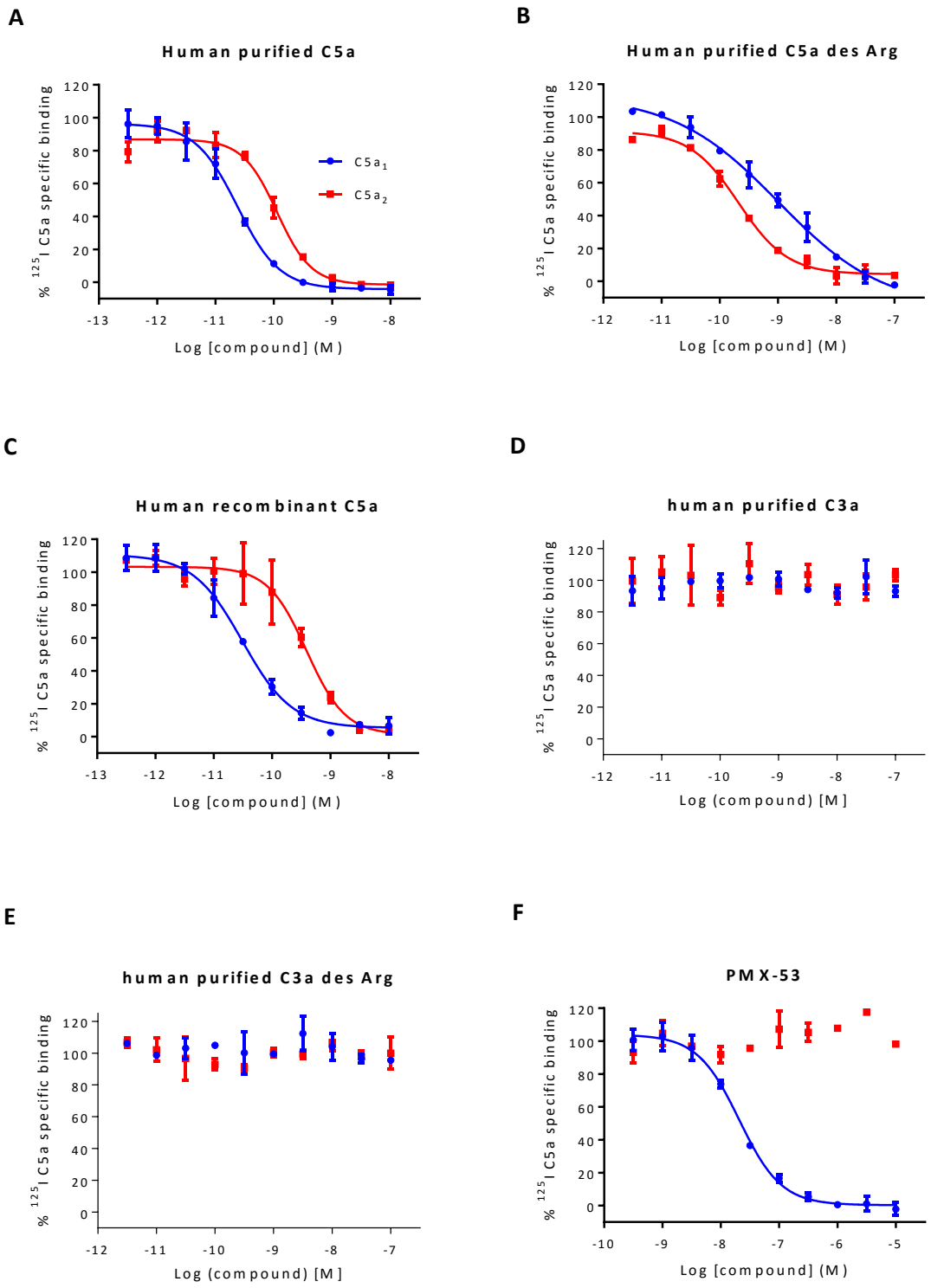

Figure 3.10. Competition binding of pharmacological tools at the $C5a_1$ and $C5a_2$ receptors

Inhibition of specific ^{125}I-C5a binding to the human $C5a_1$ receptor (blue) or human $C5a_2$ receptor (red) by human purified C5a (A), human purified C5a des Arg (B), human recombinant C5a (C), human purified C3a (D), human purified C3a des Arg (E), small molecule receptor antagonists PMX53 (F), NDT-9513727 (G) and antibody clones P12/1 (H), 8D6 (I), S5/1 (J), W17/1 (K), 1D9-M12 (L). Data points represent mean ± S.D. and are representative of four separate experiments.

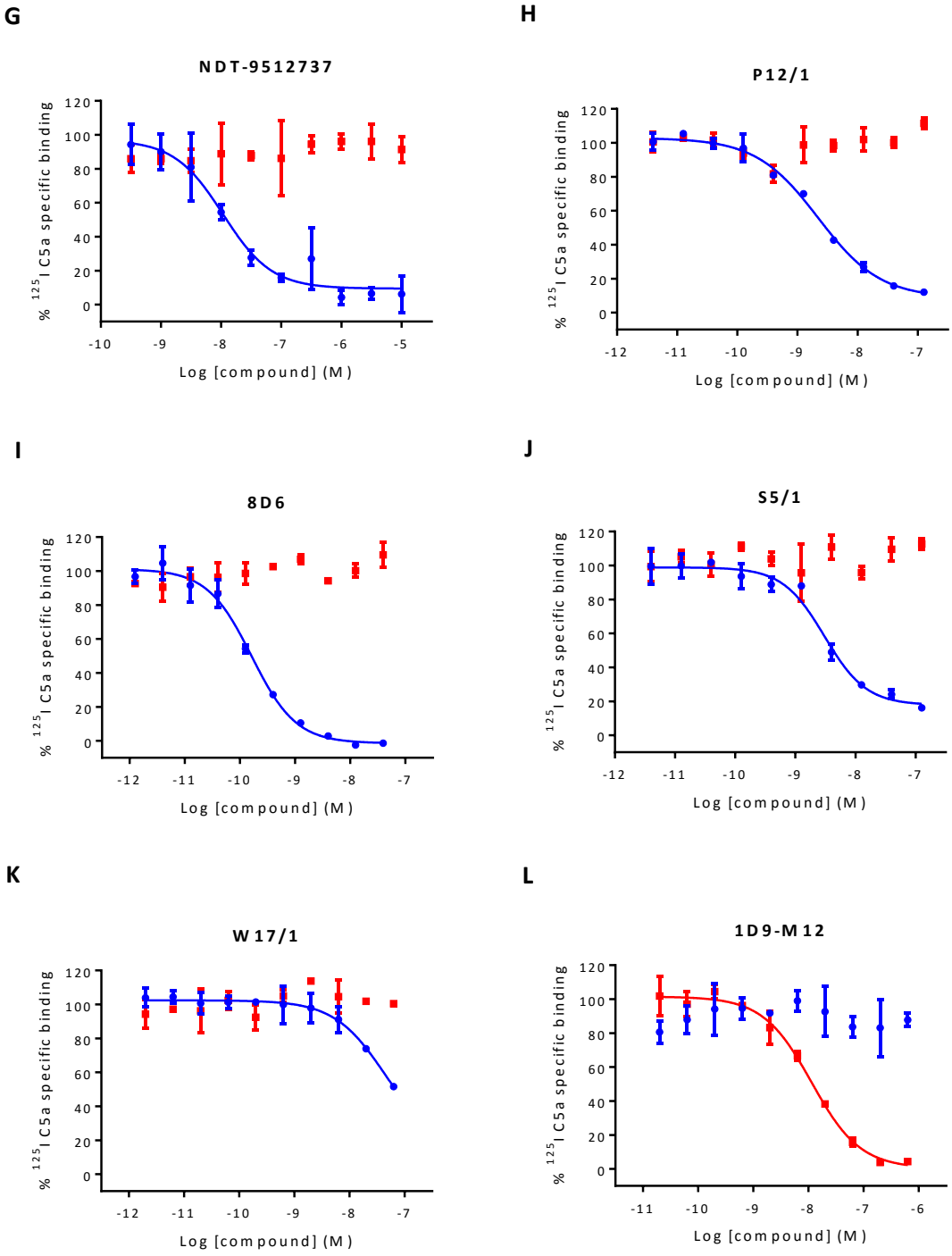

Figure 3.10. Continued

3.5. Discussion

The data generated in this research chapter have provided important information regarding the quality and specificity of pharmacological tools to enable the interrogation of C5a, C5a des Arg and their receptors, $C5a_1$ and $C5a_2$.

Confirmation of the molecular mass and purity of human C5a and C5a des Arg has generated confidence that any similarities or differences observed in the pharmacology of these two peptides can be attributed to their molecular properties. Receptor-ligand binding assays enabled the quantification of the affinity of pharmacological tools for both C5a receptors which subsequently enabled the selection of agents that were both receptor specific and C5a competitive.

The differences in affinity estimates for C5a and C5a des Arg for each of the C5a receptors reported here follow a similar trend to the affinity estimates generated by others. However, the absolute estimates of affinity are quite different (table 3.2). Cain *et al.* (2002), Okinaga *et al.* (2003) and Scola *et al.* (2007) all report affinities in the nanomolar range whereas affinity estimates reported here are in the picomolar range. This could be due to a number of reasons. The cited reports all used recombinant versions of the peptide ligand which, as demonstrated here, are less potent that the human purified peptides. Also, Cain and Okinaga report IC_{50} values which, unlike K_i values, are not affinity constants and are influenced by the concentration of competing ligand.

The experimental factor that is probably contributing the most to the differences in absolute affinity estimates is that of the biological test system. C5a and C5a des Arg are receptor agonists and there are four factors that make up receptor agonism (Kenakin, 2009a). Two of these factors, affinity and intrinsic efficacy, are related to the agonist. The other two factors, receptor density (R_t) and receptor-pathway coupling efficiency are related to the cell based system. If an agonist possesses affinity for a receptor it will bind to the ligand binding-domain and induce a change in the receptor conformation. This leads to a change in reactivity of the allosteric, cytosolic portion of the receptor resulting in intracellular pathway activation via G-

	Cain (2002) IC_{50} nM		Okinaga (2003) IC_{50} (nM)		Scola (2007) EC_{50} (nM)		Ramsey K_i (nM)	
	$C5a_1$	**$C5a_2$**	**$C5a_1$**	**$C5a_2$**	**$C5a_1$**	**$C5a_2$**	**$C5a_1$**	**$C5a_2$**
C5a	19.0	9.50	3.4	2.5	5.52	6.92	0.008	0.075
C5a des Arg	412	36.5	660	12	527	36	0.335	0.145
Experimental details	1. Competition binding with recombinant ^{125}I-C5a 2. Transfected RBL cells 3. Recombinant His_6-tagged peptides		1. Competition binding with recombinant ^{125}I-C5a 2. Transfected L1.2 cells 3. Recombinant peptides		1. Direct binding – antibody detection of peptides 2. Transfected CHO cells 3. Recombinant His_6-tagged peptides		1. Competition binding with recombinant ^{125}I-C5a 2. Transfected CHO & U2OS cells with intracellular proteins 3. Human purified peptides	

Table 3.2. A comparison of the affinity estimates for C5a and C5a des Arg at the $C5a_1$ and $C5a_2$ receptors

Mean estimates of affinity for C5a and C5a des Arg at wild type $C5a_1$ and $C5a_2$ receptors. The table details the aspects of the experimental method employed for each data set namely competing ligand, cell background for receptor overexpression and source of C5a and C5a des Arg. Mean affinity estimates were obtained from a minimum of four experiments.

protein coupling and β-arrestin recruitment. This vectorial transfer of energy or information from allosteric sites is considered to be bi-directional (Kenakin, 2009b). As much as an agonist can promote an increase in the reactivity of a receptor with intracellular proteins and pathways, increasing the cellular components that make up these pathways can increase the likelihood that a receptor exists in an active conformation, a conformation that an agonist will display higher affinity for. Both cell lines used in this research have a high degree of receptor expression and were both transformed to overexpress intracellular signalling pathway proteins. The impact of G-protein overexpression on agonist affinity has been observed by others (Azzi *et al.*, 2001).

The clinically tested receptor antagonists PMX53 and NDT9513727 both displayed high affinity for the $C5a_1$ receptor and complete specificity over the $C5a_2$ receptor. Both of these antagonists, which bind to the transmembrane domain of the $C5a_1$ receptor (Waters *et al.*, 2005), were able to antagonize the binding of ^{125}I-C5a to the same degree as unlabelled C5a. This observation was not consistent with the antibody clones P12/1 and S5/1 that were raised against the N-terminus of the $C5a_1$ receptor using a peptide sequence from Met^1- Asn^{31} as the immunogen. At receptor saturating concentrations, there is 10-20% residual ^{125}I-C5a binding to the $C5a_1$ receptor. This residual C5a binding is consistent with the multi binding-domain hypothesis by which C5a binds the $C5a_1$ receptor (Mery *et al.*, 1993). Both Siciliano *et al.* (1994) and DeMartino *et al.* (1994) demonstrated that partial or complete truncation of the N-terminus of the $C5a_1$ receptor resulted in a significant reduction in the affinity of C5a (~600 fold). However, C5a and C-terminal peptides of C5a, are still able to bind the receptor through interactions with the transmembrane domain. These observations suggest that agents that interact with the transmembrane domain of the receptor bind in such a way that the full steric hindrance with C5a occurs. However, agents that bind the N-terminus of the receptor only partially hinder the binding of C5a to the $C5a_1$ receptor. With that said, the antibody clone 8D6, which was generated using the full length of the $C5a_1$ receptor, is able to fully displace C5a binding. These data suggest that this antibody achieves its antagonising effects through interactions with the transmembrane domain of the receptor.

The only agent to inhibit the binding of C5a to the $C5a_2$ receptor was the antibody clone 1D9-M12 that was generated using the full length receptor as the immunogen. This antibody was able to inhibit ^{125}I-C5a binding to the $C5a_2$ receptor to the same degree as unlabelled C5a, suggesting that this inhibition is achieved via interactions in the transmembrane region of the receptor. This observation is consistent with data generated by Scola *et al.* (2007) who demonstrated using N-terminus targeting antibodies that C5a only interacts with the transmembrane domain of the $C5a_2$ receptor. A scheme of the proposed mechanisms by which the different antibodies, cyclic peptides and small molecules antagonize the actions of C5a and C5a des Arg at the $C5a_1$ and $C5a_2$ receptors can be seen in figure 3.11.

In summary, the research outlined in this chapter has verified the molecular weight and purity of the complement system peptides C5a and C5a des Arg and enabled the selection of receptor specific agents that will antagonize the actions of C5a and C5a des Arg at the $C5a_1$ or $C5a_2$ receptor. In subsequent research within this thesis 1μM of PMX53 or NDT9513727 will be used to antagonize the $C5a_1$ receptor and 300nM (45 μg/mL) 1D9-M12 will be used to antagonize the $C5a_2$ receptor.

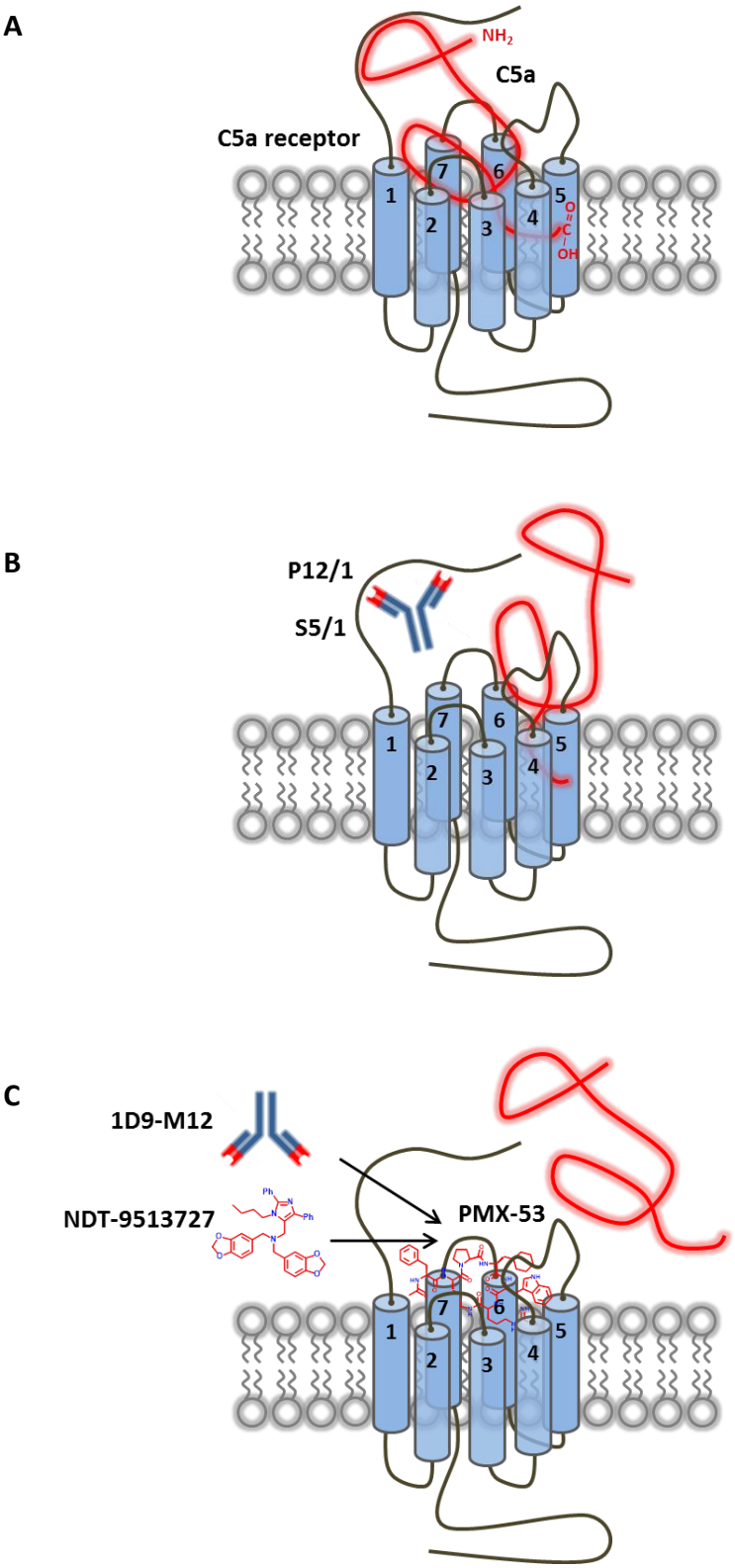

Figure 3.11. Inhibition of C5a binding to C5a receptors by pharmacological tools

A sheme showing the machanism of A. C5a bindigng to C5a receptors, B. the antagonism of C5a at the $C5a_1$ receptor by antibody clones P12/1 and S5/1 and C. the antagonism of C5a at the $C5a_1$ receptor by PMX53 and NDT9513727 and C5a at the $C5a_2$ receptor by antibody clone 1D9-M12.

Chapter 4

Characterization of a C5a sensitive biological test system, the human isolated neutrophil

Characterization of a C5a sensitive biological test system, the human isolated neutrophil

4.1. Abstract

Biochemical and pharmacological assay systems employed to study the role of specific receptors on the surface of a neutrophil often require the use of purified neutrophils isolated from human whole blood. Procedures to isolate human neutrophils are often lengthy and cumbersome involving many different reagents, some of which have the potential to activate this fragile population of myeloid cells. Using a range of molecular biology, biochemical and pharmacological assay techniques I have investigated the suitability of the new MACSxpress® neutrophil isolation kit offered by Miltenyi Biotec Inc to study the role of both the $C5a_1$ and $C5a_2$ receptors in regulation of neutrophil function. The rapid, negative selection MACSxpress® kit yielded a uniform, quiescent population of neutrophils from human whole blood with minimal erythrocyte contamination. Gene expression studies, receptor ligand binding experimentation and flow cytometry analysis all demonstrate that human neutrophils express both the $C5a_1$ and $C5a_2$ receptors on the surface of the neutrophil. Neutrophil activation induced by C5a, C5a des Arg or TNFα leads to a reduction or loss in surface expression of the two C5a receptors but enhances the expression of another innate immune system receptor, the formylpeptide receptor 1 (FPR1). This work demonstrates the high performance of the MACSxpress® human neutrophil isolation kit, which offers several advantages over more traditional neutrophil isolation methods, for the detection and investigation of the role of the $C5a_1$ and $C5a_2$ receptors in neutrophil function.

4.2. Introduction

During pathogenic microbial infection, activation of the complement system leads to the rapid and localized generation of C5a which ligates receptors expressed on parenchymal cells and leukocytes (Haviland *et al.*, 1995). Activation of C5a receptors expressed on these myeloid cells leads to a series of cellular events that orchestrates their role in the inactivation and clearance of microbes. These cellular events include selectin shedding, integrin up regulation (Jagels *et al.*, 2000) and chemotaxis (Shin *et al.*, 1968) promoting cellular margination and extravasation from the circulatory system to the site of infection. Once myeloid cells have arrived at the site of infection, C5a facilitates the phagocytosis (Craddock *et al.*, 1976) and destruction of pathogenic microbes via respiratory burst (Sacks *et al.*, 1978a) and the release of antimicrobial proteins from intracellular granules. High activation of C5a receptors on neutrophils can also lead to the generation of neutrophil extracellular traps (NETs), which are composed of nuclear chromatin, histones and granular antimicrobial proteins that are designed to trap and kill large scale microbial infections (Urban *et al.*, 2009).

Neutrophils are the most abundant leukocyte in human blood. They represent approximately 60% of the total white blood cell population and are considered to be the fastest responding immune cell to infection (Kolaczkowska *et al.*, 2013). Neutrophils are short-lived leukocytes that have a peripheral blood life span of approximately 6-10 hours (Tofts *et al.*, 2011), after which they undergo apoptosis (Payne *et al.*, 1994).

The role of the $C5a_1$ receptor in mediating anaphylatoxin induced neutrophil activation is well understood (Guo *et al.*, 2005), however the role of $C5a_2$ receptor is still largely enigmatic. Scola *et al.* (2009) demonstrated that the $C5a_2$ receptor primarily resides at an intracellular location when overexpressed in RBL and CHO cells. They also showed that expression of the $C5a_2$ receptor on the surface of the human isolated neutrophil, as identified by C5a binding capacity, is weak compared with the $C5a_1$ receptor. This low level of $C5a_2$ receptor expression is capable of internalizing a small proportion of C5a, but is almost exclusively responsible for the

internalization and degradation of C5a des Arg. Similar patterns of C5a receptor localization were observed by Bamberg *et al.* (2010) who showed that the $C5a_1$ and $C5a_2$ receptors were exclusively expressed in the human isolated neutrophil at surface and intracellular locations respectively. Contrary to the anaphylatoxin internalization capacity of $C5a_2$, Bamberg and co-workers demonstrated that the $C5a_2$ receptor expressed in neutrophils did not contribute to the internalization of C5a from the extracellular space and that the main role of this receptor was to act as an intracellular regulator of the C5a activated $C5a_1$ receptor.

To investigate the role of receptors and other cellular proteins in neutrophil function, many biochemical and functional assay systems require the use of purified neutrophil preparations. Traditional methods used in the isolation on neutrophils from human whole blood involve many reagents (dextran sedimentation erythrocytes, ficoll separation of mononuclear cells from neutrophils and lysis of residual erythrocytes) and rely on lengthy centrifugation steps. These complex and lengthy procedures increase the potential for neutrophil activation, reduces the time a researcher has to investigate this short lived cell type and potentially leads to incorrect conclusions being made about the functional role of a cellular protein, (Glasser *et al.*, 1990).

With this in mind, the main focus of this research chapter is to investigate the performance of a MACSxpress®, rapid, negative selection, neutrophil isolation method offered by Miltenyi Biotec Inc. This assessment will determine the suitability of this kit for the isolation of human neutrophils in subsequent chapters of this thesis. The main objectives of this research chapter are:

1. Determine the purity and activation state of neutrophils isolated from human whole blood using the Miltenyi Biotec Inc. MACSxpress® negative isolation kit.
2. Assess the gene expression of C5a receptors in context to other innate immune system GPCRs, pattern recognition receptors, cytokine receptors and the intracellular pathway proteins β-arrestin 1 and 2.

3. Using receptor specific, C5a competitive pharmacological tools, assess the contribution of each C5a receptor to the neutrophil surface binding capacity of C5a.
4. Investigate whether sepsis associated inflammatory mediators (LPS, TNFα, C5a and C5a des Arg) activate and alter the surface expression of each C5a receptor on human isolated neutrophil.

4.3. Chapter specific methods

Concentration response data from competition binding experiments were fitted using the four parameter logistic equation outlined in chapter 3.

4.3.1. Isolation of neutrophils from human whole blood using the Miltenyi Biotec MACSexpress® kit

Figure 4.1 outlines the steps and apparatus used to isolate untouched neutrophils from human whole blood using the MACSxpress® protocol. In brief, 8 mL of venous human whole blood, collected in EDTA coated BD Vacutainers, was added to 4 mL of reconstituted MACSxpress® neutrophil isolation cocktail in a 15 mL tube. Tube was inverted three times and incubated for five minutes at room temperature using the MACSmix® Tube Rotator at a speed of 12 rpm. Tube was then placed in the magnetic field of a MACSxpress® separator for 15 minutes with tube lid removed. After this time, with the tube still in the magnetic separator, the supernatant containing the neutrophils was collected and placed in a fresh tube, leaving behind the magnetically labelled cells and aggregated erythrocytes settled at the bottom of the tube. Collected neutrophils were spun at 300 x *g* for five minutes, supernatant aspirated and cell pellet suspended in 10 mLs of assay buffer. Cell concentration and viability was determined using a Beckman Vi-CELL™ cell counter.

4.3.2. Statistical analysis.

Statistical significance differences between population means was assessed using either the Student's *t* test or the one way analysis of variance (ANOVA) followed by a Tukey's multiple comparison test. All significance tests were performed using Graphpad Prism.

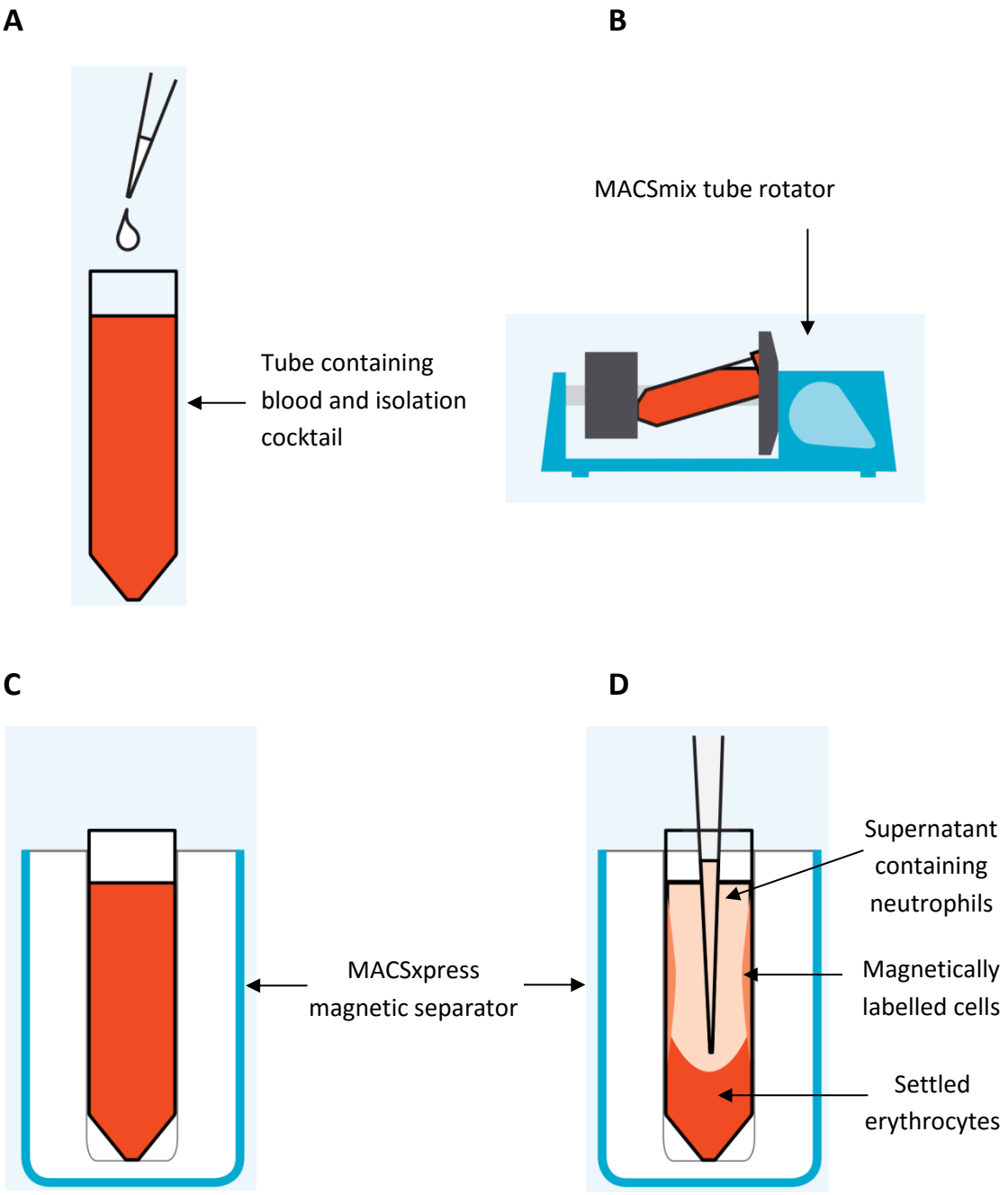

Figure 4.1. Untouched isolation of neutrophils from human whole blood using the MACSxpress® neutrophil isolation kit

EDTA collected human blood was added to the MACSxpress® neutrophil isolation cocktail (A) and mixed for 5 minutes on the MACSmix tube rotator for 5 minutes (B). Tubes containing the blood/cocktail mix was then placed in MACSxpress magnetic separator with lid removed for 15 minutes (C). Supernatant containing untouched neutrophils was then collected and dispensed into a fresh tube, leaving behind the settled aggregated erythrocytes and magnetically labelled cells (D). Figure generated with images obtained from the Miltenyi Biotec Inc website.

4.4 Results.

4.4.1. The MACSxpress® kit isolates a pure population of neutrophils from human whole blood with minimal erythrocyte contamination

To assess the performance of the MACSxpress® neutrophil isolation method, the purity of isolated neutrophils was compared with the purity of neutrophils within human whole blood. Both lyse fixed whole blood and fixed isolated neutrophils were labelled with fluorophore conjugated antibodies for the granulocyte cell surface proteins CD15 and CD16. Staining fluorescence intensity was assessed using flow cytometry. Cells staining positive for both CD15 and CD16 were identified as neutrophils. Figure 4.2 shows the different cell populations, based on forward (FSC) and side (SSC) scatter, found in either (A) human whole blood or (B) supernatant collected after neutrophil isolation. As expected, whole blood generated a typical forward and side scatter plot, from which different cell populations (lymphocytes, monocytes and neutrophils) could be identified. In comparison, the forward and side scatter plot of cells isolated using the MACSxpress® method appeared to only contain neutrophils and were devoid of monocytes and lymphocytes. In human whole blood (C), approximately 57% of gated cells (lymphocytes, monocytes and neutrophils) showed positive staining for the two granulocyte markers. After isolation (D), greater than 95% of cells stained positive for the two markers. Interestingly, based on surface expression of a cell activation marker, the integrin receptor CD11b, isolated neutrophils display the same activation state as neutrophils in whole blood. Activation of isolated neutrophils with 10 nM human purified C5a increased CD11b surface expression, demonstrating the functional viability of neutrophils isolated using the MACSxpress® method. From routine assessment of neutrophil yields, between 1.5 to 4 x 10^6 neutrophils were obtained per mL of human whole blood.

MACSxpress® neutrophil isolation method was also assessed visually by microscopy. Isolated cells were mounted on to glass slides using a cytospin method followed by Wright-Giemsa staining. Figure 4.3 shows an image of the isolated cells acquired on

a Zeiss Axio Imager microscope using a 20x objective. Neutrophils, identified by their multi-lobed nucleus, are the only leukocyte isolated using the MACSxpress® method. Routine visual examination of isolated cell fraction revealed that there was between 15-40% erythrocyte contamination. This level of red blood cell contamination was considered acceptable and preferable over erythrocyte removal via hypotonic lysis which may cause neutrophil activation.

4.4.2. Gene expression of neutrophil C5a receptors and other proteins associated with the innate immune system

Next, gene expression analysis of the C5a receptors in conjunction with other innate G-protein coupled receptors (GPCR) was performed on purified RNA from the human isolated neutrophils using Real-Time, reverse transcription qPCR. RNA purified from neutrophils was determined to be of high quality with absorbance ratios at 260/280 nm being greater than 2. Figure 4.4 shows the relative gene expression of the $C5a_1$ and $C5a_2$ receptors compared with the C3aR, FPR1, CXCR1, CCR2 and CCR5 receptors determined from neutrophil RNA obtained from four different donors. These data demonstrated that, at the gene level, human neutrophils express both the $C5a_1$ and $C5a_2$ receptors. Assuming the efficiency of all primer-probe sets are the same it can be suggested that the $C5a_1$ receptor appears to have twice the level of expression of the $C5a_2$ receptor. Expression of the C3aR, CCR2 and CCR5 receptors was barely detectable. This was in contrast to the expression of FPR1 and the interleukin-8 receptor, CXCR1, which display approximately 10 fold and 3 fold the expression of the $C5a_1$ receptor respectively.

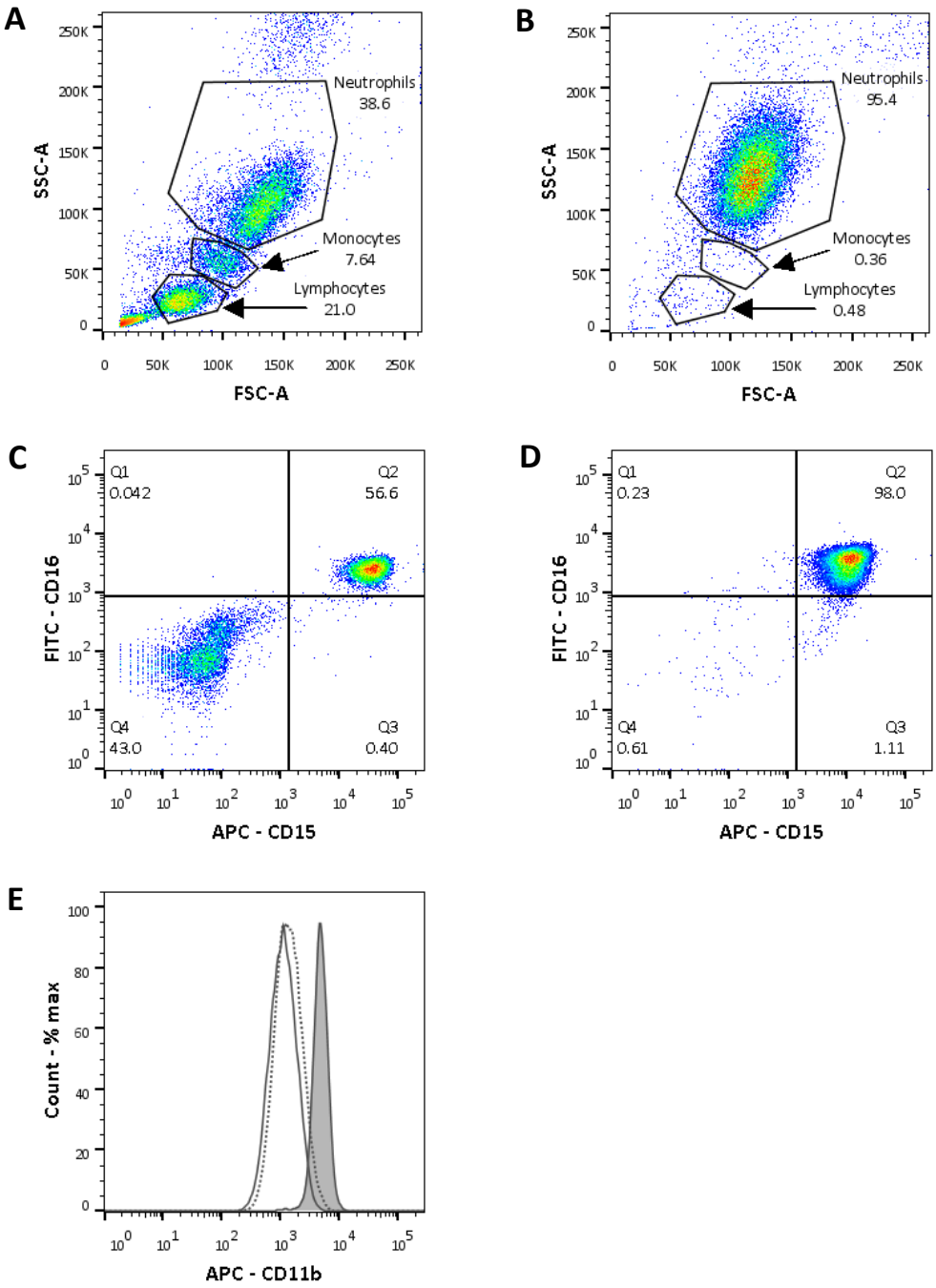

Figure 4.2. MACSxpress® Neutrophil Isolation Kit delivers a highly pure population of un-activated neutrophils from freshly drawn human blood

Forward and side scatter of (A) lyse/fixed human whole blood and (B) fixed human isolated neutrophils separated from human whole blood using the MACSxpress® kit. Neutrophil population identified by APC-CD15 and FITC-CD16 staining in (C) lyse/fixed human whole blood and (D) fixed human isolated neutrophils. Activation state of neutrophils as identified by CD11b up-regulation before and after isolation (E). Dotted histogram represents neutrophils in whole blood, solid histogram represents isolated neutrophils, filled histogram represents isolated neutrophils stimulated with 10 nM human purified C5a. Data representative of three different experiments.

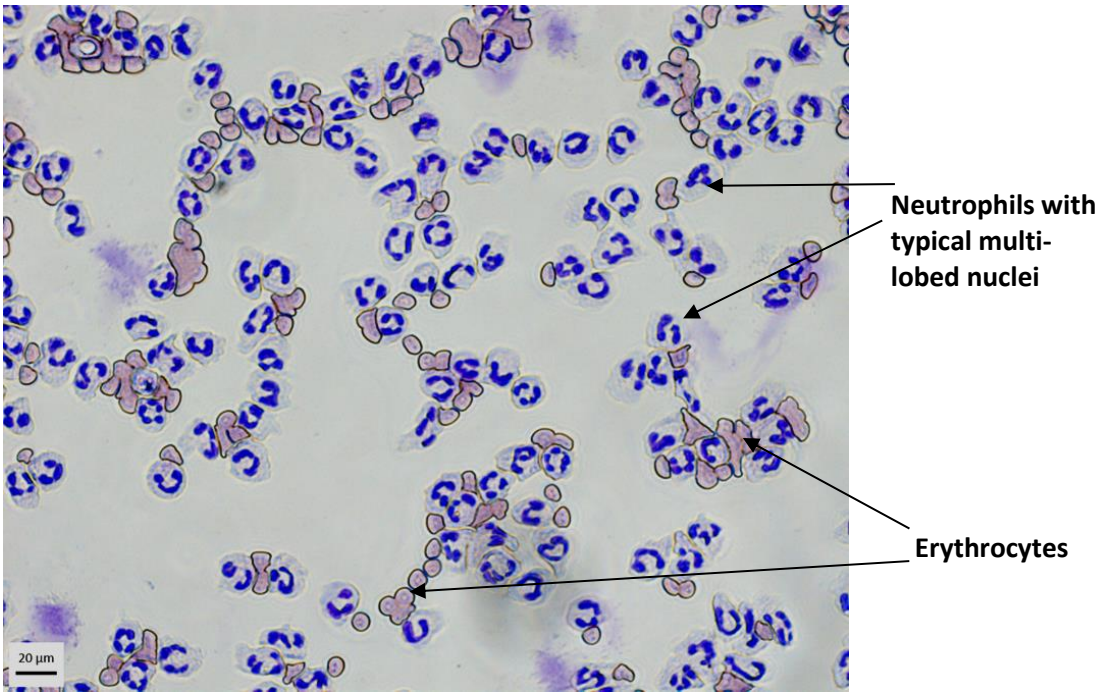

Figure 4.3. MACSxpress® isolation method only isolates neutrophils from human whole blood

Supernatant, collected from the MACSxpress® neutrophil isolation method, was cytospun onto a glass slide and stained with a Wright-Giemsa reagent. Image, collected on Zeiss AxioImager with a Plan-Apochromat 20x/0.8 objective with image capture on an AxioCam MRc digital camera, shows that the neutrophils, identified by their multi-lobed nucleus, are the only leukocyte to be isolated from human whole blood using this method. Routine visual analysis shows that the collected supernatant contains a degree of erythrocyte contamination which represents between 15-40% of the total cells isolated.

The relative gene expression of other proteins associated with the innate immune system and GPCR function was also assessed using the same purified neutrophil RNA used in the above experiment (figure 4.5A). The toll-like receptor 4 protein (TLR-4), tumour necrosis factor receptor 1 (TNFR1), Interleukin-6 receptor (IL-6R) all displayed comparable levels of expression in the human isolated neutrophil. The gene expression of two integrin proteins, integrin alpha M (ITGAM, CD11b) and integrin beta 2 (ITGB2) was also assessed. Together these two proteins form the heterodimeric integrin alpha-M beta-2 (ITGAMB2) also known as complement receptor 3 (CR3), a pattern recognition receptor involved in the detection and clearance of pathogenic bacteria. ITGB2 displayed approximately 10 fold greater expression than ITGAM. This seemed appropriate as, unlike ITGAM which only forms a complex with ITGB2, ITGB2 complexes with many other integrin proteins including integrin alpha L (ITGAL), integrin alpha X (ITGAX) and integrin alpha D (ITGAD) forming important molecules for leukocyte migration and cellular interactions (Barczyk *et al.*, 2010).

To determine the suitability of the DiscoverX β-arrestin PathHunter® assay system, which uses β-arrestin-2, for functional assessment of C5a receptor pharmacology, the neutrophil, expression of two members of the β-arrestin family of signalling proteins, β-arrestin 1 and 2, was also assessed. As can be seen from figure 4.5B the expression of β-arrestin 2 was approximately 40 fold greater than β-arrestin 1 ($P < 0.0001$ determined by an unpaired Student's *t* test). These data are comparable with those obtained by Croker *et al.* (2014) who demonstrated that β-arrestin 2 displays a significantly higher level of expression (17 fold) than β-arrestin 1 in the human monocyte derived macrophage.

The gene expression of TLR4 does not translate into detectable neutrophil surface expression (figure 4.6). This is in contrast to the TNFα receptors TNFR1 and TNFR2, which are both detected on the surface of a neutrophil by flow cytometry.

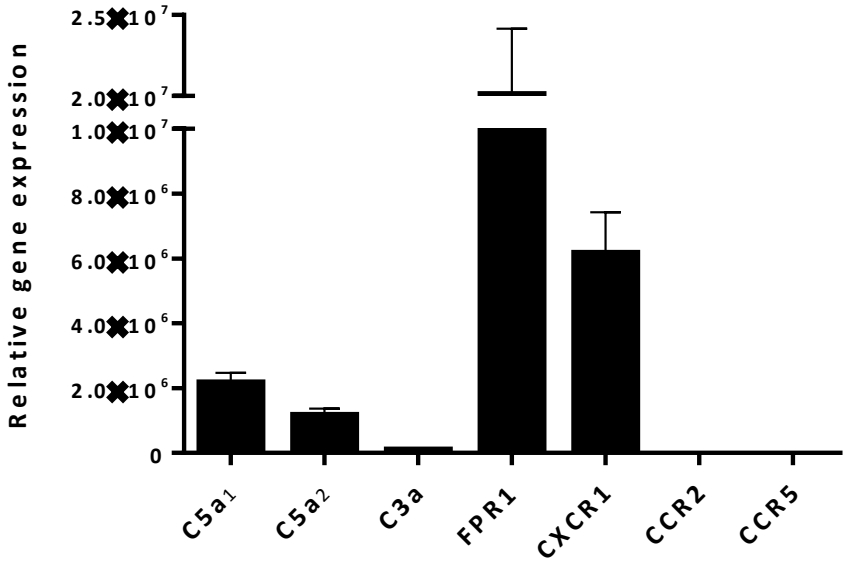

Figure 4.4. Gene expression of the C5a receptors and other innate G-protein coupled receptors in the human isolated neutrophil

Gene expression of the C5a receptors and other innate immune system GPCRs determine by qRT-PCR on RNA isolated from neutrophils using the MACSxpress® isolation method. Relative gene expression was calculated using the endogenous control gene GAPDH and a comparative CT method ($2^{-\Delta Ct}$). The vertical axis represents mean gene expression + S.D. from neutrophil RNA isolated from four healthy donors.

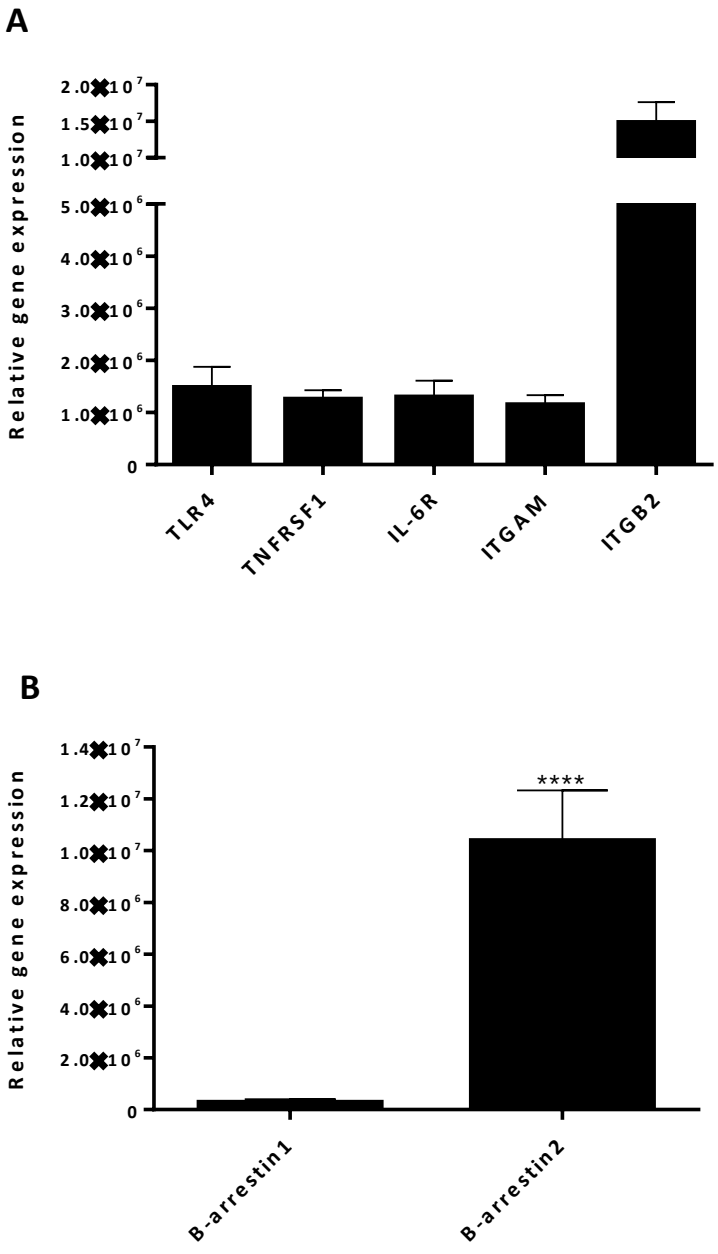

Figure 4.5. Gene expression of innate immune system receptors and intracellular signalling proteins in the human neutrophil

Gene expression of (A) TLR-4, TNFRSF1, IL-6R, ITGAM and ITGB2 and (B) β-arrestin 1 and 2 determined by qRT-PCR on RNA isolated from neutrophils using the MACSxpress® isolation method. Relative gene expression was calculated using the endogenous control gene GAPDH and a comparative CT method ($2^{-\Delta Ct}$). The vertical axis represents mean gene expression + S.D. from neutrophil RNA isolated from four healthy donors. **** represents $P < 0.0001$ determined by an unpaired Student's *t* test.

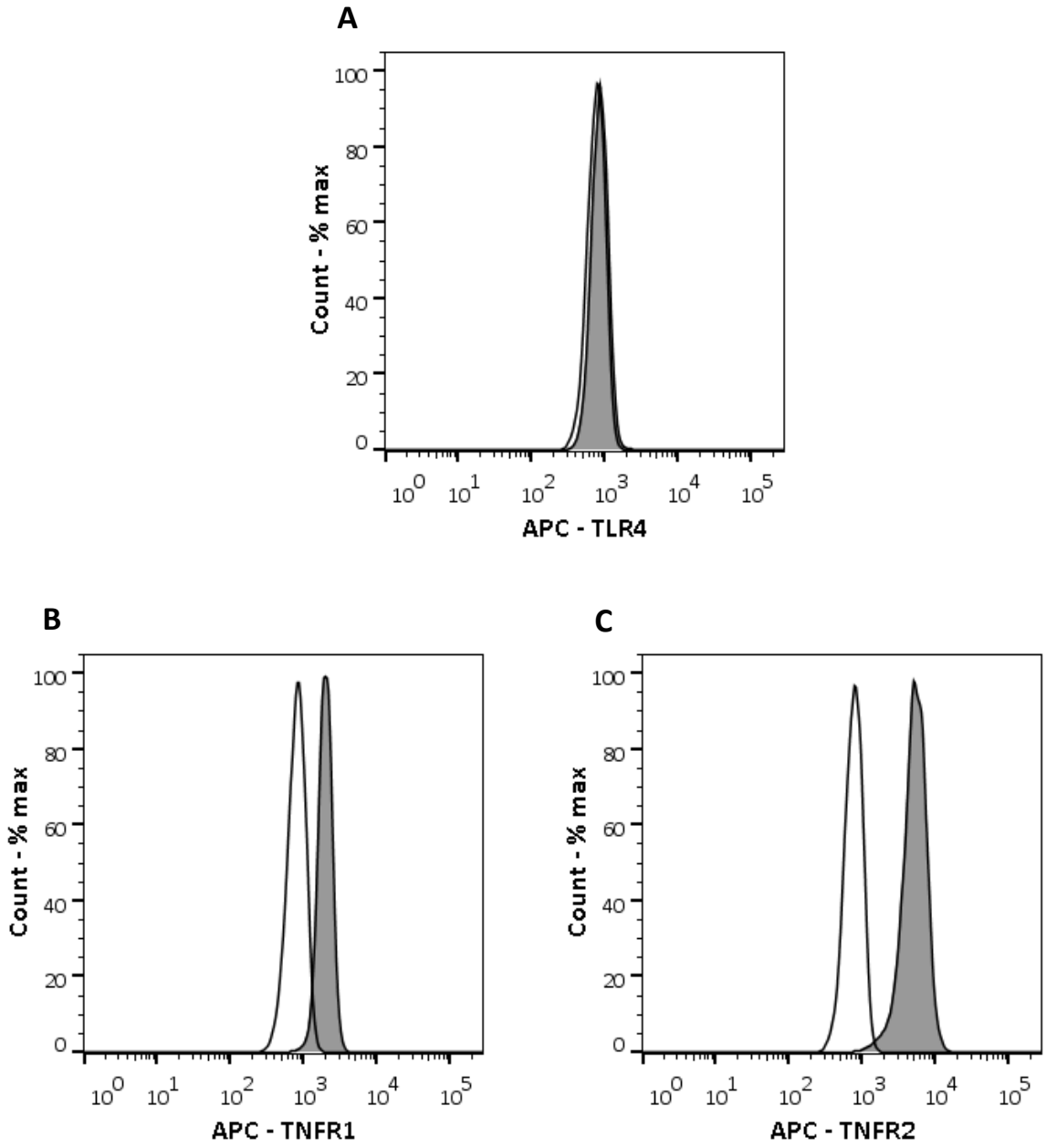

Figure 4.6. Neutrophil surface expression on the TLR4 and the TNFα receptors TNFR1 and TNFR2

Surface expression of (A) TLR4, (B) TNFR1 and (C) TNFR2 as detected by flow cytometry on the quiescent neutrophils isolated from human whole blood using the MACSxpress® isolation method. Open histogram represents concentration matched isotype control antibody staining, shaded histogram represents receptor specific antibody staining. Data representative of four separate donors.

4.4.3. Both C5a receptors are expressed on the surface of the human isolated neutrophil

To determine the relative surface expression of each C5a receptor on the human isolated neutrophil, the contribution of each C5a receptor to the cell surface binding capacity of ^{125}I-C5a was investigated. Neutrophils were incubated with 140 pM ^{125}I-C5a, a concentration of C5a expected to label both C5a receptors, at 4^{o}C in the absence and presence of receptor specific, C5a competitive, inhibitors. Specific ^{125}I-C5a receptor binding was determined using maximum (diluent) and minimum (100 nM C5a) binding controls and all inhibitor treated wells were expressed as a percentage of the specific binding for each donor. The $C5a_1$ receptor specific antagonist, PMX53, significantly ($P < 0.0001$) reduced ^{125}I-C5a specific binding to 15.6% suggesting that the $C5a_1$ receptor contributes to 84.4% of the surface C5a binding capacity of a neutrophil. The $C5a_2$ receptor specific antibody clone 1D9-M12 significantly ($P < 0.0001$) reduced ^{125}I-C5a specific binding to 87.1% suggesting that the $C5a_2$ receptor contributes only 12.9% of the surface C5a binding capacity of a neutrophil. The use of both receptor inhibitors together significantly ($P < 0.001$) reduced C5a binding over PMX53 alone but this dual receptor inhibition was not significantly different ($P > 0.05$) to the minimum ^{125}I-C5a binding control (figure 4.7).

To quantify the surface expression of C5a receptors on human neutrophils, saturation binding analysis was performed at 4^{o}C using a concentration range of ^{125}I-C5a in the absence and presence of 100 nM unlabelled human purified C5a. ^{125}I-C5a saturated neutrophils in a monophasic manner with an average Hill slope of 1.2 (figure 4.8A). The average maximum number of C5a binding sites (B_{max}) was 0.58 fmol/100,000 cells ($\pm$ 0.24, 95% CI, n=4) and ^{125}I-C5a bound to these receptors with a K_d of 150 pM ($\pm$ 60, 95% CI, n=4). In comparison with the expression of C5a receptors in the transformed cell lines described in chapter 3, C5a receptors are expressed at a low level in the human neutrophil, with 20 and 170 fold lower expression than the $C5a_1$ (CHO) and $C5a_2$ (U2OS) receptors respectively (figure 4.8B) .

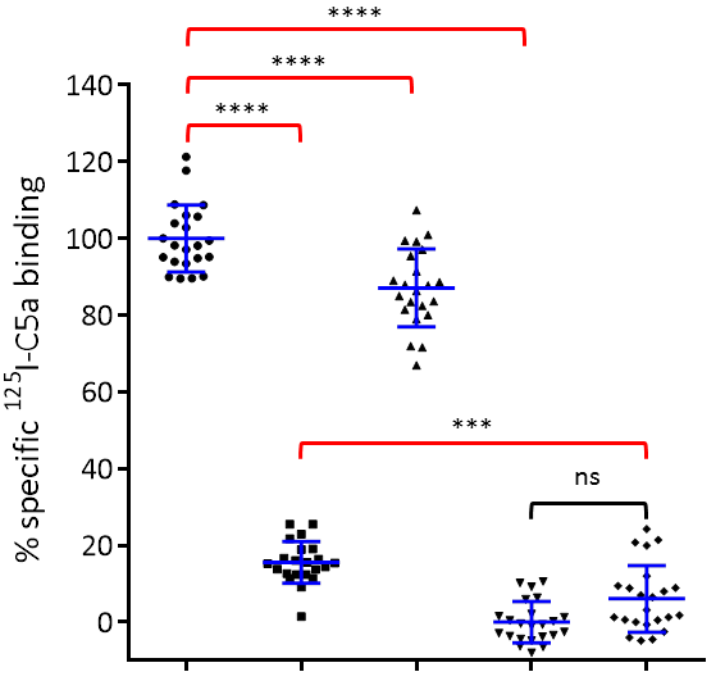

^{125}I C5a (140 pM)	+	+	+	+	+
Diluent	+				
PMX-53 (1 µM)		+			+
1D9-M12 (300 nM)			+		+
Human purified C5a (100 nM)				+	
Mean % specific ^{125}I-C5a binding (SD)	**100** (8.7)	**15.6** (5.5)	**87.1** (10.2)	**0** (5.3)	**6.1** (8.7)

Figure 4.7. Both C5a receptors contribute to the neutrophil surface binding capacity of ^{125}I-C5a

Neutrophils isolated from human whole blood using the MACSxpress® method were incubated with 140 pM ^{125}I-C5a in the absence or presence of receptor specific, C5a competitive inhibitors ($C5a_1$ - PMX53, $C5a_2$ - 1D9-M12, or dual receptor - C5a). Specific ^{125}I-C5a binding for each condition was represented as a percentage of the diluent and C5a controls for each donor. Bars represent mean % specific ^{125}I binding +/- S.D. Statistical analysis was performed using one-way analysis of variance (ANOVA) and Tukey's multiple comparison test (**** = $P < 0.0001$, *** = $P < 0.001$, ns = not significant $P > 0.05$). Data obtained with neutrophils isolated from four healthy donors.

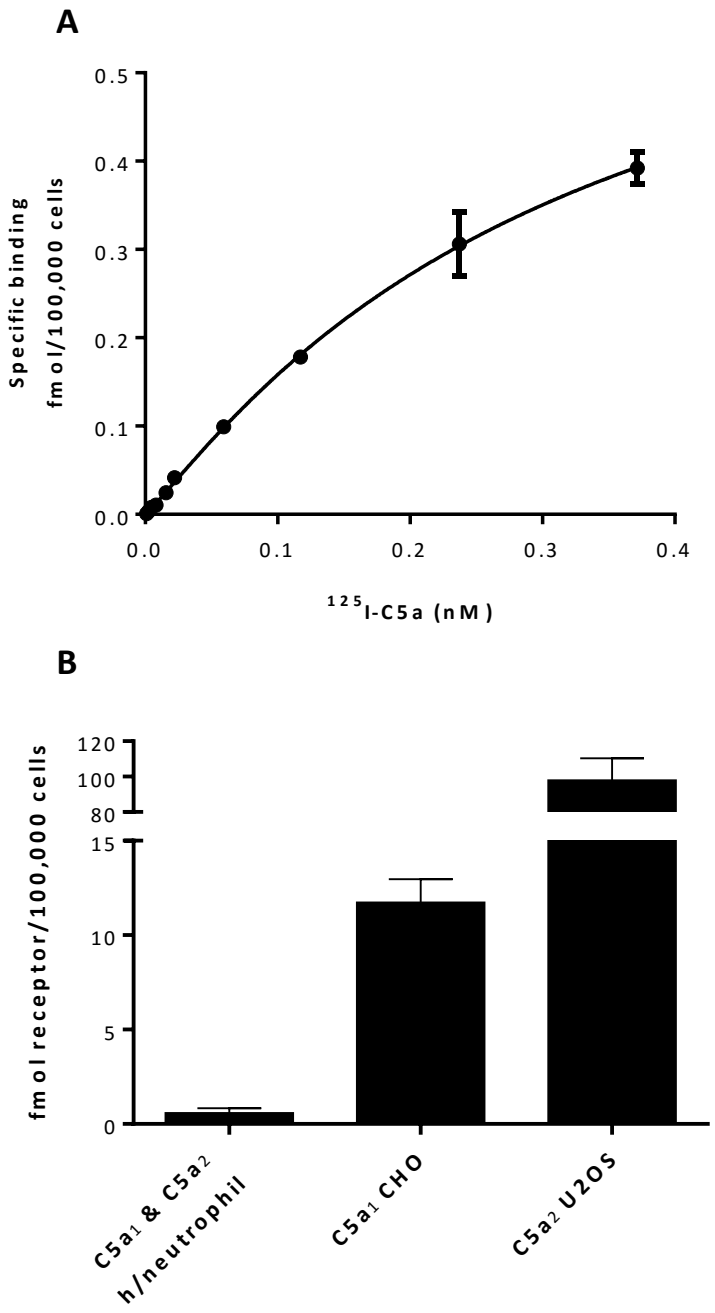

Figure 4.8. C5a receptor expression on the human isolated neutrophil compared with transformed cell lines

^{125}I-C5a saturation binding of C5a receptors expressed on the surface of human isolated neutrophils (A). A nonlinear regression model was fit to the specific ^{125}I-C5a receptor binding determined for each ligand concentration. The maximum C5a binding sites (B_{max}) and ^{125}I-C5a affinity (K_d) were extrapolated from the nonlinear fit. Representative data from neutrophils isolated from four healthy donors (A). Neutrophil C5a receptor expression compared with $C5a_1$ and $C5a_2$ receptor expression on the transformed cell lines described in chapter 3. Bars represent mean B_{max} values in fmol receptor/100,000 cells + S.D obtained from four separate experiments.

Next, competition binding experiments were employed to determine the affinity of human purified C5a and C5a des Arg for the receptors on the surface of human isolated neutrophils. Both C5a and C5a des Arg fully inhibited a fixed concentration (190 pM) of ^{125}I-C5a in a monophasic manner with Hill slopes close to unity (figure 4.9). IC_{50} values for each peptide ligand were extrapolated from the nonlinear regression fits and subsequently converted to system independent K_i values using the Cheng-Prusoff equation and the K_d for ^{125}I-C5a described above. Table 4.1 shows the calculated K_i values of both C5a and C5a des Arg for the C5a receptors expressed on the neutrophil compared with K_i for each ligand at the overexpressed receptors described in chapter 3. Human purified C5a displayed 150 fold greater affinity for neutrophil C5a receptors than C5a des Arg. This measured difference in affinity between the two peptide ligands was far greater than the fold difference that was observed at the overexpressed $C5a_1$ (40 fold) or $C5a_2$ receptor (2 fold). Interestingly, the absolute measures of affinity for each peptide agonist are noticeably weaker at the neutrophil C5a receptors than their overexpressed counterparts. C5a, displayed a 25 and 3 fold increase in affinity for the overexpressed $C5a_1$ and $C5a_2$ receptors respectively compared with the neutrophil C5a receptors while C5a des Arg displayed an 87 and 200 fold increase in affinity for the two overexpressed receptors. Due to the consistency in experimental parameters between neutrophil and overexpressed competition binding assay systems, such as probe ligand, assay incubation time and assay buffer, differences in peptide affinity are probably not due to experimental bias but due rather to differences in the cellular systems.

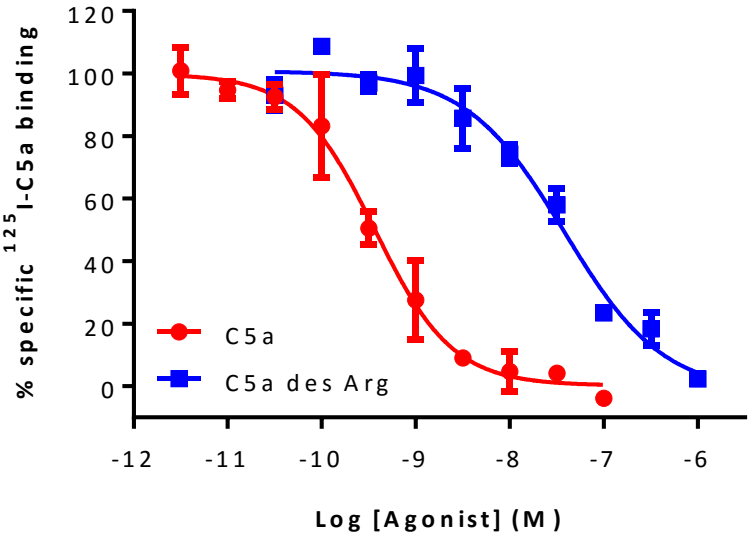

Figure 4.9. Characterizing the binding affinity of human purified C5a and C5a des Arg at neutrophil C5a receptors

Competition binding experiment performed on human isolated neutrophils using a fixed concentration (190 pM) of ^{125}I-C5a and increasing concentrations of human purified C5a or C5a des Arg. Experiments were performed at 4^{o}C and under equilibrium conditions. IC_{50} values were extrapolated from the four parameter logistic equation fit of the data. Points represent mean % specific ^{125}I-C5a binding ± S.D. Data representative of four separate experiments.

	$C5a_1$ & $C5a_2$ (Human neutrophil) K_i nM (pKi ± 95% CI)	**$hrC5a_1$** (CHO + Gα16) K_i nM	**$hrC5a_2$** (U2OS + β-arrestin2) K_i nM
C5a	0.196 (9.72 ± 0.14)	0.008	0.075
C5a des Arg	29.3 (7.54 ± 0.07)	0.335	0.145

Table 4.1. Human purified C5a and C5a des Arg display a reduced affinity for neutrophil C5a receptors

Mean average affinity estimates (K_i) of human purified C5a and C5a des Arg for C5a receptor expressed on the surface of the human isolated neutrophil determined by competition binding experiments using ^{125}I-C5a. Neutrophil C5a receptor affinity estimates compared with those derived at the overexpressed receptors in chapter 3. Mean values derived from at least 4 different experiments.

4.4.4. Regulation of C5a receptor expression on human isolated neutrophils

To validate the ^{125}I-C5a detection of both $C5a_1$ and $C5a_2$ receptors on the surface of the human isolated neutrophil, flow cytometry analysis was employed using saturating concentrations of the previously described receptor specific, fluorophore conjugated, antibody clones S5/1 and 1D9-M12. As shown in figure 4.10, both C5a receptors are present on the surface on the human isolated neutrophil. The $C5a_1$ receptor antibody significantly ($P < 0.01$) stained the surface of neutrophils with approximately 25 fold the intensity of the isotype control antibody. The staining of the $C5a_2$ receptor, although significant ($P < 0.001$), was less pronounced with only a fourfold increase in staining over the isotype control. Human neutrophils also stained positively for the formyl peptide receptor, FRP1, and the integrin molecule CD11b.

To determine whether activation of neutrophils could lead to a change in the surface expression of C5a receptors, neutrophils were incubated with either LPS (3 ng/mL), TNFα (1 ng/mL), C5a (5 nM) or C5a des Arg (50 nM) in the absence or presence of a C5/C5a neutralizing antibody. To determine the degree of neutrophil activation induced by each inflammatory agent, changes in the surface CD11b expression were measured. Changes in FPR1 expression were also measured to assess the impact of each inflammatory agent on a non-complement system neutrophil receptor. From figure 4.11 it can be seen that LPS did not activate neutrophils with respect to changes in cell surface expression of CD11b or alter the expression of the three receptors. In contrast, TNFα induced profound activation of neutrophils as measured by an increase in CD11b expression ($P < 0.0001$) and significantly reduced ($P < 0.0001$) the expression of both the $C5a_1$ and $C5a_2$ receptors. TNFα induced activation of neutrophils caused an opposing effect on the FRP1 receptor, significantly increasing ($P < 0.0001$) its surface expression. The C5/C5a neutralizing antibody had no effect on the neutrophil responses observed to TNFα suggesting that TNFα did not cause neutrophil activation and receptor regulation through the localized production of C5a. As expected both C5a and C5a des Arg activated human

isolated neutrophils and significantly reduced ($P < 0.0001$) the cell surface detection of both the $C5a_1$ and $C5a_2$ receptors. This reduced receptor detection was probably caused by receptor activation and internalization but it cannot be ruled out that the loss in receptor detection was cause by antibody displacement as a result of a competitive interaction with C5a. Regardless of the reason for the reduced detection of each C5a receptor, these data demonstrate the presence of the $C5a_2$ receptor on the surface of the human isolated neutrophil. Comparable with TNFα, C5a significantly increased ($P < 0.01$) the neutrophil surface expression of the FPR1 receptor. However, although C5a des Arg activated neutrophils to a comparable degree as C5a, it did not significantly regulate ($P > 0.05$) the expression of the FRP1 receptor.

Interestingly, the C5a neutralizing antibody was able to inhibit the actions of both C5a and C5a des Arg at the $C5a_1$ receptor but not the $C5a_2$ receptor. Although the neutralizing antibody was able to inhibit the ability of C5a to upregulate CD11b expression, it had no impact on ability of C5a des Arg to induce an increase in CD11b expression. These data support the argument that the $C5a_2$ receptor mediates C5a des Arg induced up-regulation of CD11b. These data also suggest that both C5a and C5a des Arg bind the $C5a_2$ receptor in a very different manner compared with how they bind the $C5a_1$ receptor, involving peptide-receptor contact points which are not blocked by the C5a neutralizing antibody.

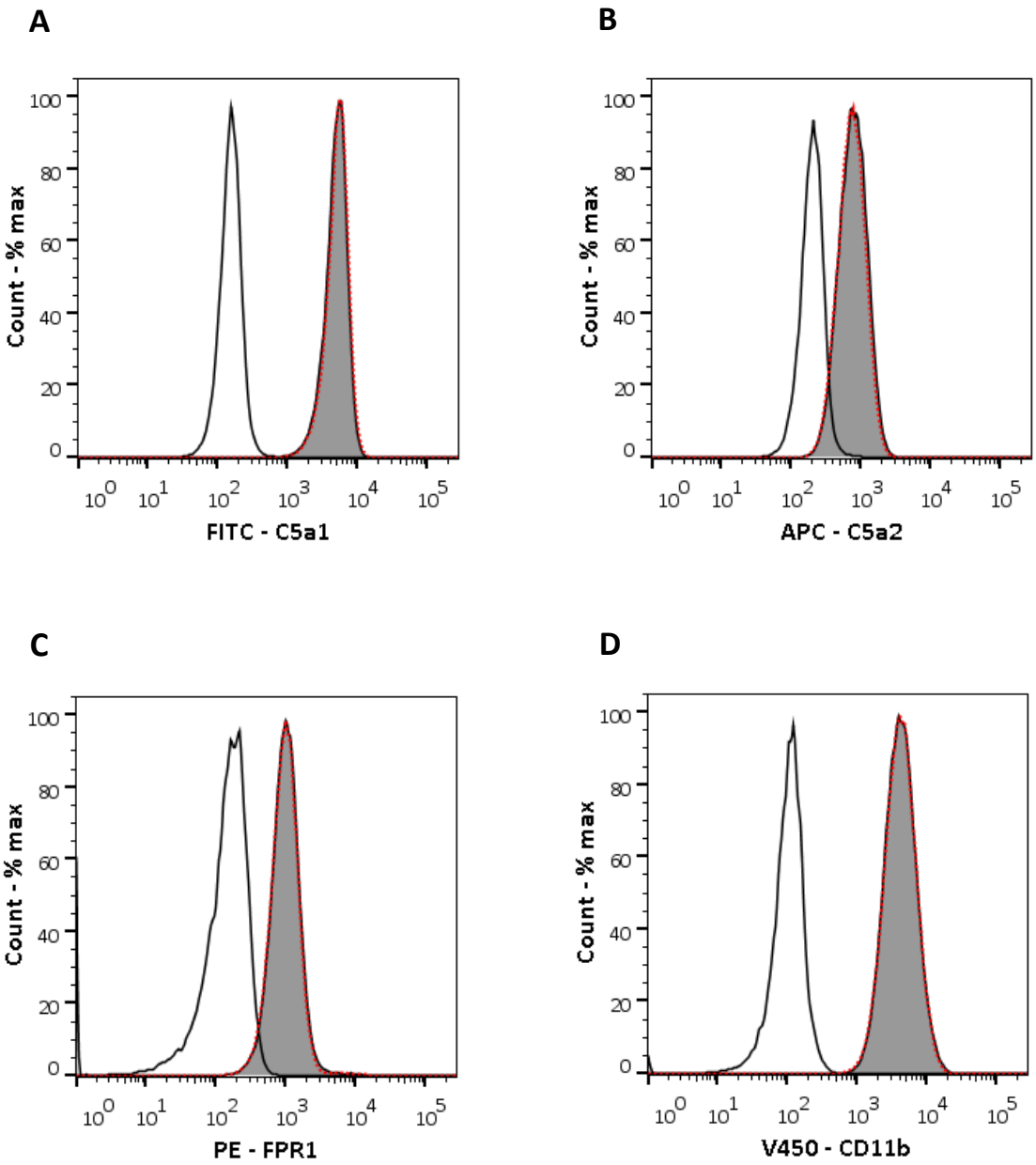

Figure 4.10. Both C5a receptors are expressed on the surface of the human isolated neutrophil

Flow cytometry detection of fluorescence intensity staining of the (A) $C5a_1$ receptor, (B) $C5a_2$ receptor, (C) FRP1 receptor and (D) the integrin molecule CD11b on neutrophils isolated from human whole blood using the MACSxpress® isolation method. Black open histogram represents concentration matched isotype control antibody staining, shaded histogram represents receptor specific antibody staining, red dotted histogram represents receptor specific antibody staining in the presence of the C5a neutralizing antibody. Data representative of four separate donors.

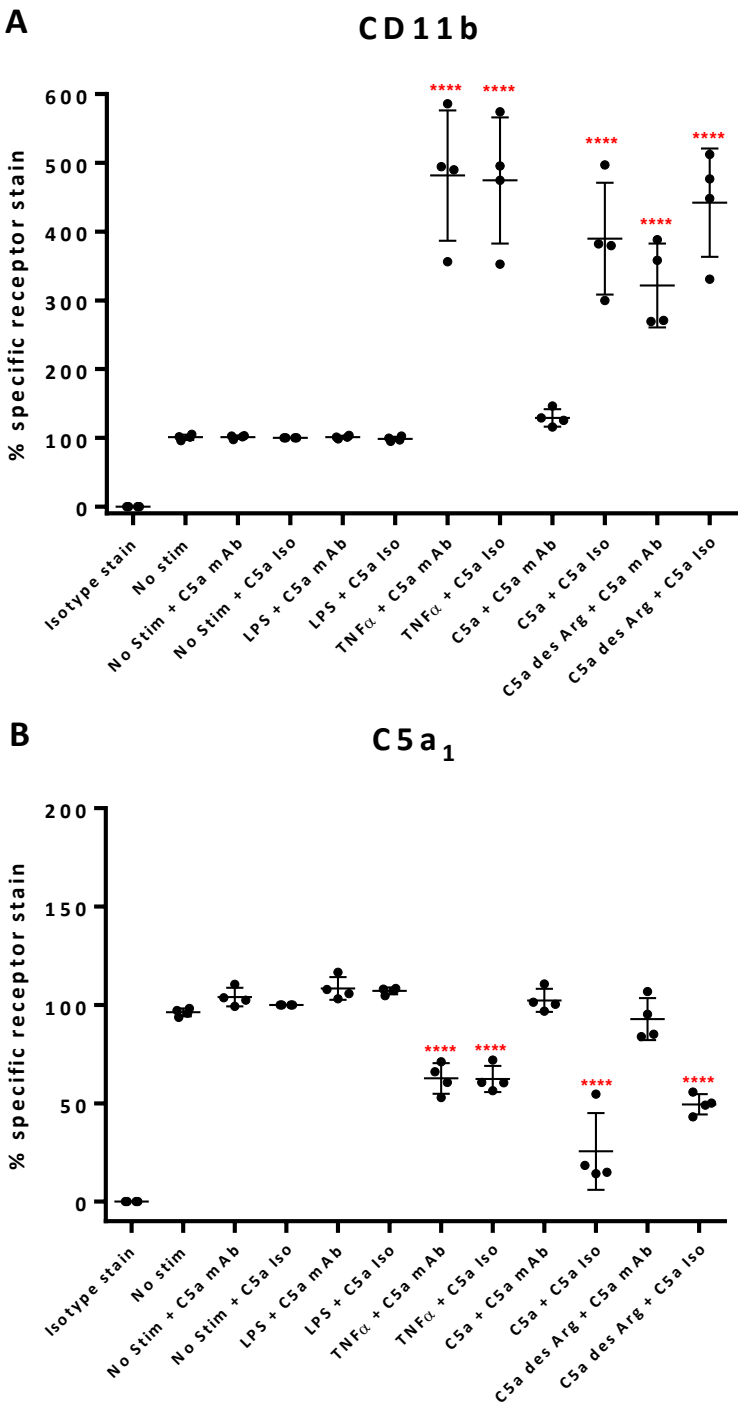

Figure 4.11. TNFα, C5a and C5a des Arg activate neutrophils and regulate surface receptor expression

Flow cytometry detection of cell surface receptors (A – CD11b, B – C5a1, C – $C5a_2$, D – FPR1) on the human isolated neutrophil after stimulation by either LPS (3 ng/mL), TNFα (1 ng/mL), C5a (5 nM) or C5a des Arg in the absence or presence of a neutralizing antibody to C5/C5a. Vertical axis represents % specific receptor staining. Bars represent mean and S.D. using neutrophils isolated from four separate healthy donors. Statistical analysis was performed using one-way analysis of variance (ANOVA) and Tukey's multiple comparison test (**** = $P < 0.0001$, ** = $P < 0.01$). All comparisons were made to no stimulation controls containing C5a or isotype antibody.

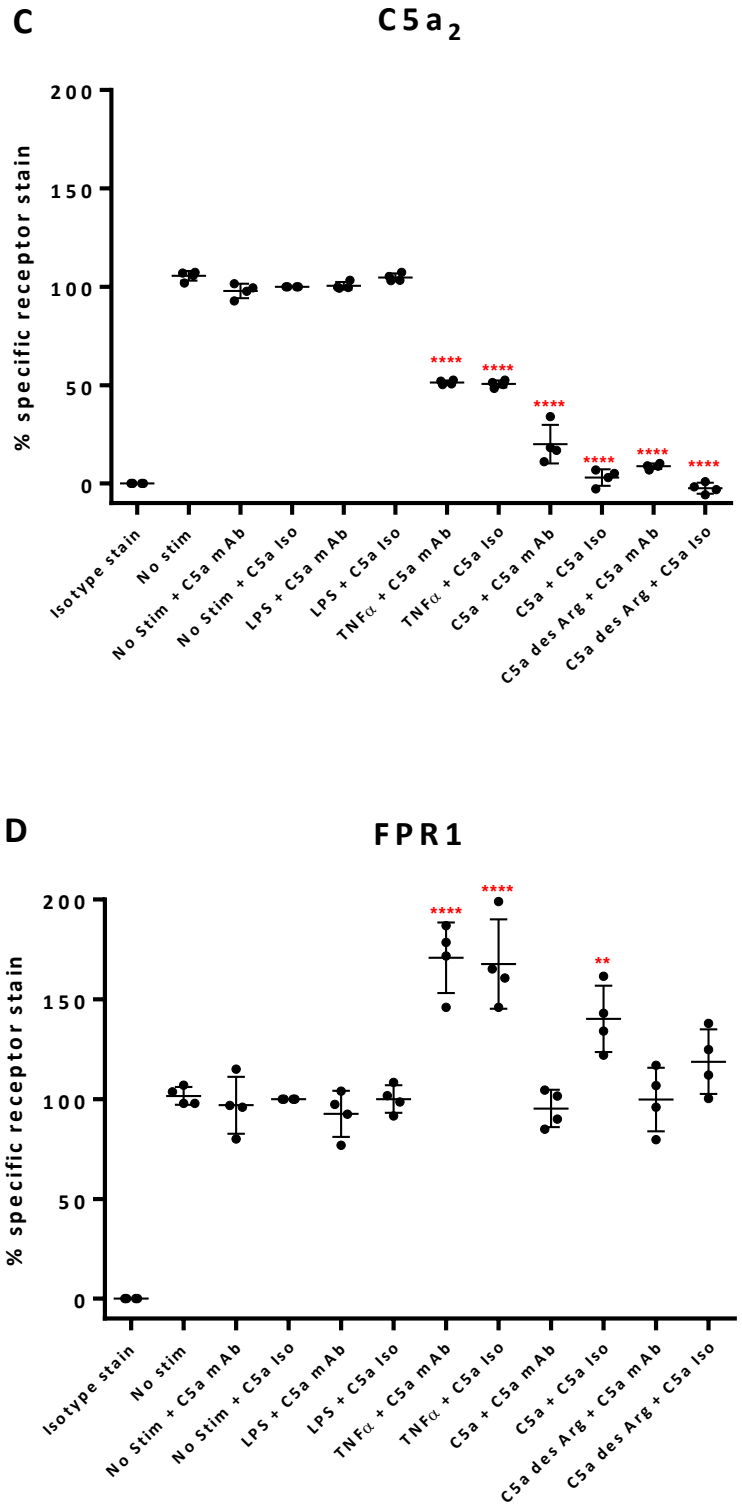

Figure 4.11. Continued

4.5. Discussion

The results described in this research chapter demonstrate the quality in performance of a new, negative selection, human neutrophil isolation kit offered by Miltenyi Biotec. The MACSxpress® kit enabled the untouched isolation of a pure, high viability, non-activated population of neutrophils from human whole blood in 20 minutes with minimal erythrocyte contamination. This method offers several advantages over more traditional neutrophil isolation techniques that require multiple steps (ficoll density gradient centrifugation, dextran sedimentation of erythrocytes and lysis of residual erythrocytes with a hypotonic solution), all of which increase the likelihood of neutrophil activation (Bland *et al.*, 2001; Maqbool *et al.*, 2011).

The quantification of the relative gene expression level of each C5a receptor demonstrated that the $C5a_1$ receptor is expressed at twice the level of the $C5a_2$ receptor in the human isolated neutrophil, a finding similar to those reported by others (Chen *et al.*, 2007). Both C5a receptors appear to have far greater neutrophil expression than the other complement system receptor, C3aR, but far reduced expression compared with the FPR1 and the CXCR1, GPCRs which control similar neutrophil functions to the C5a receptors (Sun *et al.*, 2012). The significant increase in β-arrestin-2 gene expression over β-arrestin-1 confirms the suitability of the DiscoverX PathHunter® platform for investigating interactions between the C5a receptors β-arrestins.

Gene expression translated into neutrophil surface protein expression of both C5a receptors as detected by both competition binding studies and flow cytometry analysis. This is an important finding as it contrasts the observations made by Bamberg *et al.* (2010), who, using the same $C5a_2$ specific antibody, clone 1D9-M12, were unable to detect expression of this receptor on the surface of a neutrophil. The presence of the $C5a_2$ receptor on the surface of a neutrophil is further supported by the fact that this receptor can be desensitized, or its detection antagonized by both C5a and C5a des Arg. In fact neutrophil activation, via TNFα stimulation, leads to down regulation of both C5a receptors and in the case of the $C5a_2$ receptor this

down regulation is close to the point of zero detection. Minimal information is provided in the aforementioned manuscript as to how neutrophils were isolated from human whole blood. Ficoll purification is mentioned which was presumably followed with a hypotonic lysis of erythrocytes. As discussed above, these lengthy isolation procedures may lead to cellular activation which, as we have shown here, can result in loss of cell surface expression of C5a receptors.

The neutrophil stimulation data described in this research chapter have highlighted a possible role for $C5a_2$ and C5a des Arg in orchestrating the function of neutrophils. When bound by the C5a neutralizing antibody, both C5a and C5a des Arg are unable to bind, and presumably activate the $C5a_1$ receptor. However, even when bound by the C5a neutralizing antibody, C5a and C5a des Arg are still able to bind to the $C5a_2$ receptor. Although antibody bound C5a is unable to activate neutrophils with respect to CD11b up-regulation, antibody bound C5a des Arg is still able to induce neutrophil activation. These data suggest that C5a mediated neutrophil activation is via the $C5a_1$ receptor and C5a des Arg activation is through $C5a_2$.

Unlike TNFα and the isoforms of C5a, exposure to 3 ng/mL LPS did not induce neutrophil activation, as observed by changes in surface CD11b expression, or alter the expression of either of the three receptors that were measured. This concentration of LPS is close to the range detected in clinical sepsis (Opal *et al.*, 1999) and a concentration that I have shown to maximally induce IL-6 and TNFα production in human whole blood (data not shown). This lack of LPS induced neutrophil activation is perhaps not that surprising based on the negligible TLR4 expression on the surface of the non-activated neutrophil shown both here and by others (Hayashi *et al.*, 2003).

In contrast to the down regulation of C5a receptors, which presumably occurs to tightly regulate neutrophil activation once they have migrated along a C5a/C5a des Arg gradient to the site of microbial infection, TNFα induced an increase in the expression of the formylpeptide receptor, FRP1. These data corroborate the findings by O'Flaherty *et al.* (1991) who showed that specific binding of ^{3}H-fMLP to human isolated neutrophils is increased in the presence of TNFα. Formylated peptide

ligands that bind and activate the FPR1 are secreted by invading pathogens and released from dying cells that are injured during inflammation (Dorward *et al.*, 2015). Presumably this switching in neutrophil receptor emphasis orchestrates a more direct detection and clearance of pathogens and necrotic cells than the initial, indirect recruitment neutrophils to the site of infection that is orchestrated by toll-like receptors and anaphylatoxins of the complement system.

In summary, the research outlined in this chapter has demonstrated the high performance of the MACSxpress® kit to isolate a uniform population of non-activated neutrophils from human whole blood with minimal erythrocyte contamination. Based on the detection of both C5a receptors at the cell surface this isolation method appears to offer an advantage over more traditional neutrophil isolation methods for studying both C5a receptors. The MACSxpress® method will be used to isolate neutrophils for functional assessment of the $C5a_1$ and $C5a_2$ in the next research chapter of this thesis.

Chapter 5

Assessing the relative functional activity of the complement system peptides, C5a and C5a des Arg

Assessing the relative functional activity of the complement system peptides, C5a and C5a des Arg

5.1. Abstract

Activation of the complement system leads to the generation of the 74 amino acid peptide C5a which possesses potent anaphylactic and chemotactic properties. C5a is rapidly metabolized to C5a des Arg by serum carboxypeptidases, a process considered to render this complement peptide inactive. However many groups have demonstrated that C5a des Arg retains a strong capacity to induce the chemotaxis of leukocytes. With the majority of, if not all, serum C5a thought to be the des arginated form, I decided to perform an in-depth characterization of the functional ability of C5a des Arg using a range of *in vitro* cell based assay systems. From concentration responses to C5a and C5a des Arg in each experimental system, E_{max} and EC_{50} values were extrapolated. A system independent expression of agonism was obtained for each peptide by taking the $Log(E_{max}/EC_{50})$. The relative activity of C5a des Arg to C5a was determined using $\Delta Log(E_{max}/EC_{50})$. C5a des Arg displayed biased agonism towards promoting a phenotype required for extravasation of neutrophils from the vasculature to sites of infection but away from an antimicrobial phenotype. These results demonstrate that C5a des Arg retains potent cell adhesion and chemotactic properties required for migration of leukocytes from the blood to sites of infection. However, the reduced capacity to induce a neutrophil respiratory burst response has possibly evolved to minimise the damage to blood vessels and surrounding tissue that can be caused by the highly reactive oxygen species generated during the respiratory burst response.

5.2. Introduction

Activation of the complement system leads to the generation of the biologically active, 74 amino acid peptide, C5a. Upon ligation of the C5a receptors, C5a induces a range of cellular responses in both immune and parenchymal cells including increased vascular permeability, selectin shedding, integrin upregulation, chemotaxis, phagocytosis, respiratory burst and cytokine release (Guo *et al.*, 2005; Amara *et al.*, 2008). While the bulk of C5a, between amino acid residues 1-69, contributes to the majority of the binding affinity between C5a and the C5a receptors, all of the agonist properties of C5a are contained in the C-terminal between residues 69-74 (Monk *et al.*, 2007). C5a is rapidly metabolized by cell surface and serum carboxypeptidases that remove the C-terminal arginine, generating C5a des Arg (Bokisch *et al.*, 1970; Skidgel *et al.*, 2007). Although the majority of analytical methods used to quantify concentrations of the peptide fragments of C5 are unable to distinguish between C5a and C5a des Arg, the vast majority of C5a in the circulation is considered to be that of the des arginated isoform (Fernandez *et al.*, 1976; Mueller-Ortiz *et al.*, 2009).

C5a des Arg is often referred to as inactive C5a. It has a greatly reduced affinity for the $C5a_1$ receptor compared with C5a, as demonstrated by data in this thesis, and is devoid of anaphylactic properties. Fernandez *et al.* (1978a) showed that when injected intradermally into guinea pigs, only C5a was able to increase vascular permeability whereas C5a des Arg was not. Similarly, Gerard *et al.* (1981) showed that C5a des Arg exhibited $1/1000^{th}$ of the activity of C5a at inducing both smooth muscle contraction of guinea pig ileum and vascular permeability of guinea pig skin. Interestingly these authors discovered that removal of the oligosaccharide unit from asparagine^{64} enhanced the activity of C5a des Arg in both of these assay endpoints.

Workers at the New York University Medical Center identified a serum anionic polypeptide 'helper factor' that enhances the chemotactic activity of low concentrations C5a des Arg (Perez *et al.*, 1980). Originally referred to as cochemotaxin (Perez *et al.*, 1986) and later identified as vitamin D-binding protein, this protein specifically enhances the actions of C5a des Arg and not C5a.

There is a wealth of data in the literature highlighting the ability of C5a des Arg to induce a chemotactic response of leukocytes. Fernandez *et al.* (1978b) determined that C5a des Arg, although approximately 10 fold weaker than C5a at inducing chemotactic response of human isolated neutrophils, was able promote the migration of a larger number of cells. Similarly, Webster *et al.* (1980) demonstrated that human purified C5a des Arg was able to induce the same degree of chemotactic activity as C5a albeit at 50 times higher concentration. Interestingly Marder *et al.* (1985) observed that human isolated monocytes exhibit identical chemotactic responses to C5a and C5a des Arg although their observation with human neutrophils were in line with those reported above. Using a label-free technology to measure dynamic mass redistribution cellular responses, Reis *et al.* (2012) observed that C5a des Arg was 10 fold more potent than C5a at inducing morphological changes of RBL cells transformed to express the human $C5a_1$ receptor. Using the same technology they also observed that C5a des Arg was more potent than C5a at inducing cellular responses of human isolated neutrophils.

There appears, therefore, to be a separation of biological activities between C5a and C5a des Arg and it has previously been postulated that anaphylatoxin and chemotactic properties of C5a reside in different regions of the peptide molecule (Muller-Eberhard, 1969). Removal of the C-terminal arginine of C5a appears to generate an agonist that preferentially induces a chemotactic phenotype. It is now widely accepted that agonists of G protein coupled receptors do not uniformly activate all cellular signalling pathways linked to a specific receptor and agonists can stabilize specific receptor conformation leading to the activation of different pathways (Kenakin, 2002). Agonists that are able selectively activate a specific intracellular signalling pathway are often referred to as functionally selective or biased agonists (Kenakin *et al.*, 2013).

The response of an agonist is made up of two disparate parameters. Efficacy or E_{max}, the maximal response induced by an agonist and potency or EC_{50}, the concentration of agonist that produces 50% of its maximal response. Methods to determine biased agonism rely on the quantification of the relative activity between agonists in a test system and require agonism be reduced to a single parameter (Ehlert, 2008; Kenakin

et al., 2012). The most commonly used method to quantify the relative agonist activity lends from operational model of agonism where a system independent expression of agonism can be obtained from values of $Log(\tau/K_A)$. From explicit expressions of maximal response and EC_{50}, it has also been shown that a surrogate of $Log(\tau/K_A)$ value is provided by a value of $Log(E_{max}/EC_{50})$ for dose-response curves with slopes not significantly different from unity (Black et al, 1985; Kenakin, 2012).

As C5a des Arg, rather than C5a, appears to be the predominant form of the C5 fragment isolated form in serum and displays signalling bias, I have decided to focus the research in this chapter on understanding the relative functional activity of human purified C5a des Arg and C5a in a range of cell based assay systems. The main objectives of are:

1. Perform concentration response curves of both C5a and C5a des Arg in a range of functional assay systems using both neutrophils and transformed cell lines.
2. For each agonist response curve fit the four parameter logistic equation and extrapolate both E_{max} and EC_{50} values.
3. Using the $Log(E_{max}/EC_{50})$ transformation, determine the relative efficacy of C5a des Arg compared with C5a.

5.3 Chapter specific methods

5.3.1. Functional assays

Concentration response curves were generated for both human purified C5a and C5a des Arg and tested in the following 12 functional cell based assay systems; neutrophil calcium mobilization, neutrophil chemotaxis, neutrophil integrin up regulation, neutrophil respiratory burst (with and without TNFα prime), CHO $C5a_1$ receptor calcium mobilization, CHO $C5a_1$ receptor cAMP accumulation, CHO $C5a_1$ receptor ERK phosphorylation, CHO $C5a_1$ receptor β-arrestin2 recruitment, CHO $C5a_2$ receptor β-arrestin2 recruitment, U2OS $C5a_1$ receptor internalization and U2OS $C5a_2$ receptor internalization.

5.3.2. Minimizing test system bias

Test system bias is the impact a specific biological assay can have on the absolute potency of each agonist tested. Undoubtedly each biological assay will impart a degree of system bias, either in the form of receptor sensitivity (via differential receptor expression and receptor pathway coupling efficiencies), kinetics of assay response and the temperature which the assay was performed at. For this reason, the absolute potency of each agonist should not be solely used to determine pathway bias. To minimize observational bias, the same assay buffer (Hanks Balanced Salt Solution with calcium and magnesium, supplemented with 20mM HEPES and 0.1% BSA, pH7.4) was used in all assay systems.

5.3.3. Quantifying the relative efficacy of C5a and C5a des Arg

The four parameter logistsic equation, described in chapter 3, was used to fit the concentration response data obtained for C5a and C5a des Arg in each experimental

endpoint. Data for each agonist were expressed as a percentage of the maximal response obtained in the test system to C5a. E_{max}, EC_{50} and Hill slopes were extrapolated from each sigmoidal curve. The activity of each agonist was reduced to a single parameter using the $Log(E_{max}/EC_{50})$ ratio and the relative activity of C5 des Arg was compared with C5a by subtracting the ratio obtained for C5a des Arg from the ratio obtained for C5a to generate $\Delta Log(E_{max}/EC_{50})$. The fold relative activity of C5a compared with C5a des Arg was calculated by taking the reciprocal of the inverse-Log of the $\Delta Log(E_{max}/EC_{50})$ determined for each assay endpoint. A minimum of four curves were performed for each agonist. In experiments using human isolated neutrophils, cells were tested from a minimum of four healthy donors.

5.3.4. Statistical analysis

To determine statistical differences between treatment groups, data were initially assessed for normal distribution after which parametric one-way ANOVA followed by a Tukey's multiple comparison test was performed. All statistical tests were performed using Graphpad Prism

5.4. Results

5.4.1. Assessing neutrophil functional responses to C5a and C5a des Arg

Initial experiments investigating the relative activity of human purified C5a and C5a des Arg were focused on functional responses in the human isolated neutrophil. Neutrophils were isolated from human whole blood using the Miltenyi Biotec Inc MACSxpress® kit previously described in chapter 4.

Both human purified C5a and C5a des Arg produced robust calcium mobilization in human neutrophils as detected with the Molecular Devices Calcium 3 indicator dye (figure 5.1A). C5a was approximately 100 fold more potent than C5a des Arg producing an average EC_{50} value of 87 pM compared with 8.3 nM for C5a des Arg. As calculated from the upper asymptote of the non-linear regression, C5a des Arg was less efficacious than C5a, generating an E_{max} value that was, on average 15% lower than the maximum response produced by C5a. Using $\Delta Log(E_{max}/EC_{50})$, the relative activity of C5a des Arg compared with C5a was -1.62 with C5a possessing 42 fold greater activity than C5a des Arg at inducing calcium mobilization in the human isolated neutrophil. The selective antagonism of either the $C5a_1$ receptor with PMX53 ($P < 0.001$) or the $C5a_2$ receptor with the antibody clone 1D9-M12 demonstrated that only the $C5a_1$ receptor mediates C5a and C5a des Arg induced calcium mobilization in human neutrophils. This finding is consistent with the reported inability of the $C5a_2$ receptor to couple to G-proteins due to a sequence modification in the DRY motif at the end of the third transmembrane domain (Okinaga *et al.*, 2003) (figure 5.1B).

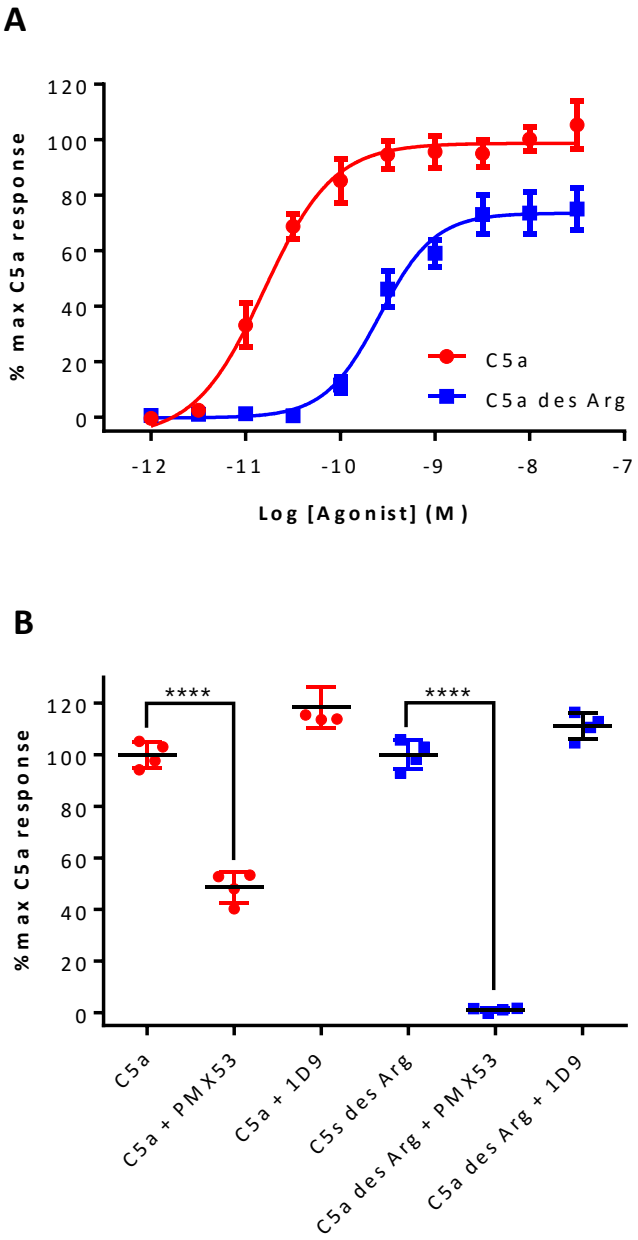

Figure 5.1. C5a and C5a des Arg induced calcium mobilization in the human isolated neutrophil

Concentration response curves of human purified C5a and C5a des Arg at inducing calcium mobilization within human isolated neutrophils (A). From the non-linear regression E_{max} and EC_{50} values were extrapolated. All data points were expressed as a percentage of the maximal response observed to C5a. Each datum point represents the mean average ±S.D. of two replicates. Data are representative of eight separate experiments. Inhibition of neutrophil calcium mobilization induced by a fixed concentration of human purified C5a or C5a des Arg with either the $C5a_1$ receptor antagonist PMX53 or the $C5a_2$ receptor antagonist 1D9-M12 (B). Data are expressed as a percentage of the C5a response. Bars represent mean average ±S.D. of four replicates. Data are representative of two separate experiments.

Next, I investigated the ability of each peptide to induce chemotaxis of human isolated neutrophils (figure 5.2). Both C5a and C5a des Arg induced a strong chemotactic response of human neutrophils at concentrations less than 1 nM. Interestingly, C5a des Arg, unlike C5a, did not produce the typical 'bell shaped' concentration response profile, often see with chemotactic agents (figure 5.2A). Instead of the typical concentration dependent desensitization of cellular migration, C5a des Arg produced a sustained response at concentrations greater than 1 nM. The degree of desensitization induced by C5a (comparing the response of each peptide at the top concentration tested, 100 nM, with the peak response at 1 nM) was significantly different to the same response produced by C5a des Arg (figure 5.2B). To determine whether the lack of desensitization response to C5a des Arg was due to agonist induced enhancement of the fluorescence intensity of the cell tracking dye Calcein-AM, cells were stimulated with a concentration range of each peptide (figure 5.2C). Neither C5a or C5a des Arg, up to the maximal concentration of 100 nM, enhanced the fluorescence intensity of the Calcein-AM loaded neutrophils.

After removal of the assay points related to the desensitization response, a non-linear regression was fit to the chemotaxis data. Human purified C5a and C5a des Arg were equipotent at inducing chemotaxis of human neutrophils with average EC_{50} values of 486 and 277 pM respectively (figure 5.3A). Although C5a des Arg displayed a 15% reduced E_{max} compared with C5a ($P < 0.01$), the $\Delta Log(E_{max}/EC_{50})$ comparison generated a value of 0.12. This reveals that C5a des Arg possesses a slightly greater relative activity than C5a at inducing chemotaxis of human neutrophils. As with calcium mobilization, the use of selective receptor antagonists demonstrated that all of the neutrophil chemotactic response induced by C5a and C5a des Arg is mediated via the $C5a_1$ receptor (figure 5.3B).

Fundamental to the extravasation of neutrophils from the blood to sites of infection is the up regulation of neutrophil cell surface adhesion molecules. One such molecule is integrin alpha M or CD11b. Both C5a and C5a des Arg potently induced an increase in cell surface expression of CD11b as detected by flow cytometry. At the highest concentrations tested, both C5a and C5a des Arg appeared to desensitize

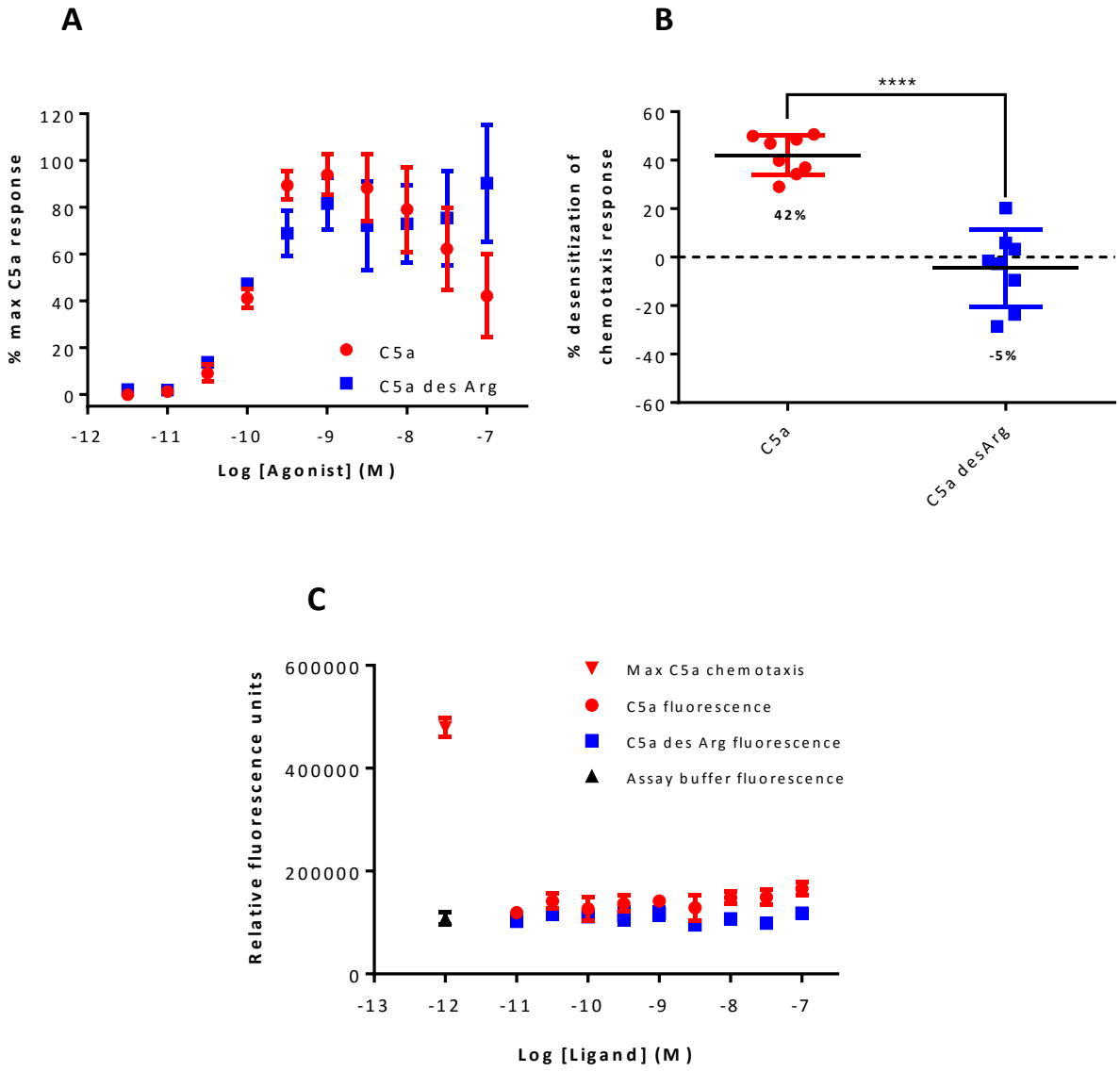

Figure 5.2. C5a and C5a des Arg induced chemotaxis of the human isolated neutrophil

Human purified C5a and C5a des Arg mediated chemotaxis of human isolated neutrophils using the Corning Fluoroblok™ system (A). Data are expressed as a percentage of the maximum response observed to C5a and each point represents the mean average ±S.D. of two replicates, data are representative of eight separate donors. Percentage desensitization of chemotaxis response between maximal response (at 1 nM) and top concentration tested (100nM) for all eight donors (B). Data were analysed using one-way ANOVA (**** = $P < 0.0001$). The impact C5a and C5a des Arg stimulation on the fluorescence of human neutrophils loaded with the calcein-AM cell indicator dye used in chemotaxis experiments (C). Data were expressed in relative fluorescence units and points represent mean average ±S.D. of two replicates. Data were obtained from a single experiment.

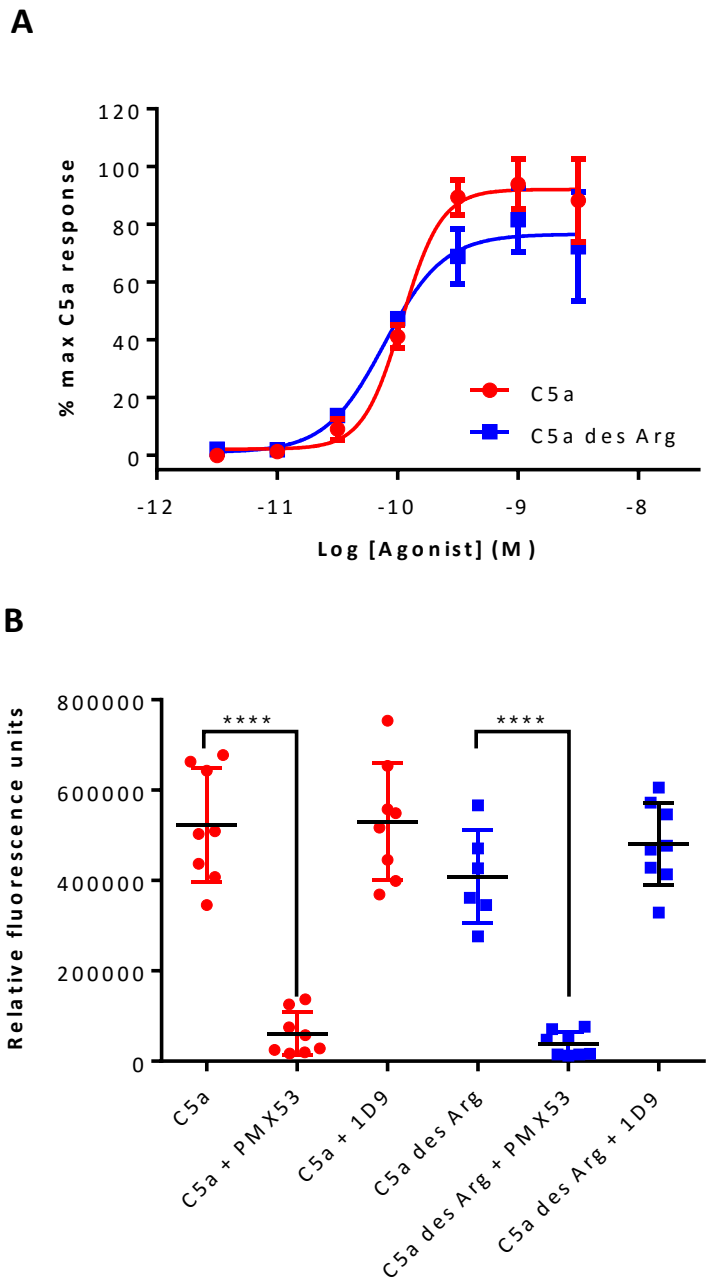

Figure 5.3. The neutrophil chemotactic response induced by C5a and C5a des Arg is mediated through the $C5a_1$ receptor

Non-linear regression fit to the human purified C5a and C5a des Arg neutrophil chemotaxis response data after desensitization point were removed (A). Data are expressed as a percentage of the maximum response observed to C5a and each point represents the mean average ±S.D. of two replicates, data are representative of eight separate donors. Inhibition of 1 nM C5a or C5a des Arg with saturating concentrations of either PMX53 or 1D9-M12 (B). Data are expressed in relative fluorescence units and points are the average of two replicates per experiment. Bars represent mean average ±S.D. from eight donor experiments. Statistical significance was determined using one-way ANOVA (**** = $P < 0.0001$).

the integrin up regulation response. Subsequent removal of the desensitization assay points allowed for a non-linear regression to be fit to the data which generated EC_{50} values of 244 pM and 357 pM for C5a and C5a des Arg respectively. C5a des Arg was less efficacious than C5a and produced an average maximum response that was 70% of that produced by the parent peptide (figure 5.4A). The $\Delta Log(E_{max}/EC_{50})$ produced a value of -0.35 which translates to C5a having a 2.2 fold greater relative activity than C5a des Arg at inducing CD11b up regulation in the human isolated neutrophil. Again, the use of the selective C5a receptor inhibitors demonstrated that C5a and C5a des Arg mediate neutrophil CD11b up regulation via the $C5a_1$ receptor. Activation of the $C5a_2$ receptor by either peptide agonist does not appear to regulate the integrin response in either a positive or negative manner (figure 5.4B).

The final neutrophil response I investigated was that of respiratory burst. Upon bacterial infection, neutrophils engulf pathogenic microbes by phagocytosis and respiratorily destroy them by generating hypochlorous acid (HOCl). The cell permeable reactive oxygen species (ROS) indicator, dihydrorhodamine 123, is rapidly oxidised to the fluorescent rhodamine 123 by HOCl and not by other ROS. As detected by flow cytometry, activation of non-primed neutrophils by either C5a or C5a des Arg led to only a very small respiratory burst response with C5a des Arg being approximately 20% less efficacious than C5a (figure 5.5A). The des arginated peptide also displayed a reduced potency to C5a, producing an average EC_{50} of 13 nM compared with 2.4 nM. A determination of the relative activity using $\Delta Log(E_{max}/EC_{50})$ generated a value of -0.81, translating to C5a possessing a 6.5 fold greater relative activity than C5a des Arg at inducing respiratory burst in the non-primed human neutrophil.

To determine whether cytokines provide a priming role to enhance the respiratory burst response to C5a and C5a des Arg, neutrophils were pre-incubated for 15 minutes prior to stimulation with a concentration of TNFα (1 ng/mL). TNFα had a profound impact on the magnitude of the respiratory burst response to both C5a and C5a des Arg (figure 5.5B), significantly enhancing their actions by 8 and 5 fold respectively compared with their non-primed respiratory burst response ($P < 0.001$).

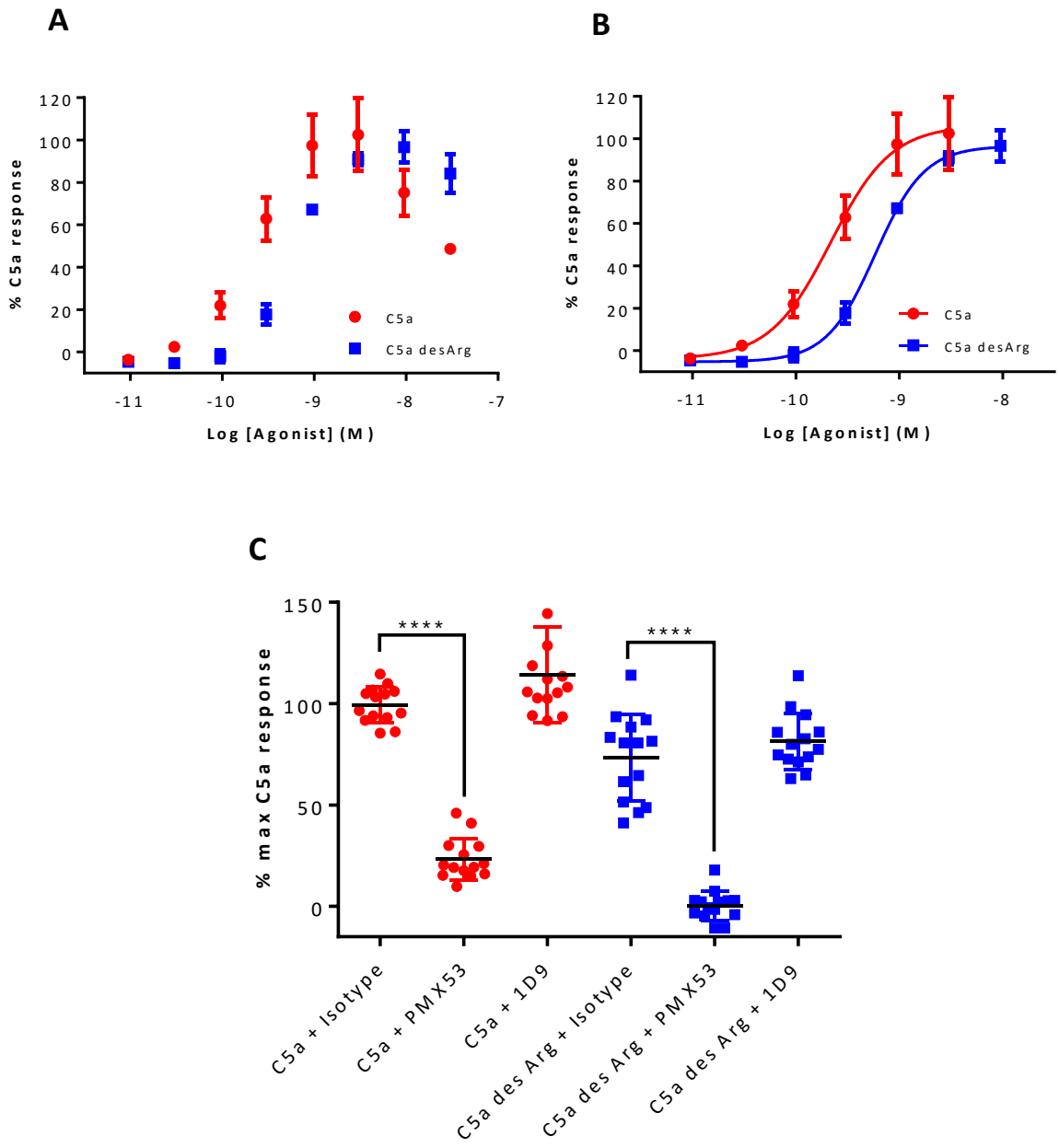

Figure 5.4. C5a and C5a des Arg induced neutrophil integrin up regulation is mediated via the $C5a_1$ receptor

Human purified C5a and C5a des Arg induced CD11b up regulation on human isolated neutrophils (A). Non-linear regression fit to the data after the removal of the desensitized response points (B). Each point represents the mean average ±S.D of two replicates, data are representative of seven separate donors. Inhibition of C5a or C5a des Arg induced CD11b up regulation by either the $C5a_1$ receptor antagonist PMX53 or the $C5a_2$ receptor antagonist 1D9-M12 (C). Data are expressed as a percentage of the C5a response and each datum point reflect a test replicate. Bars represent the mean average response ±S.D from seven separate experiments.

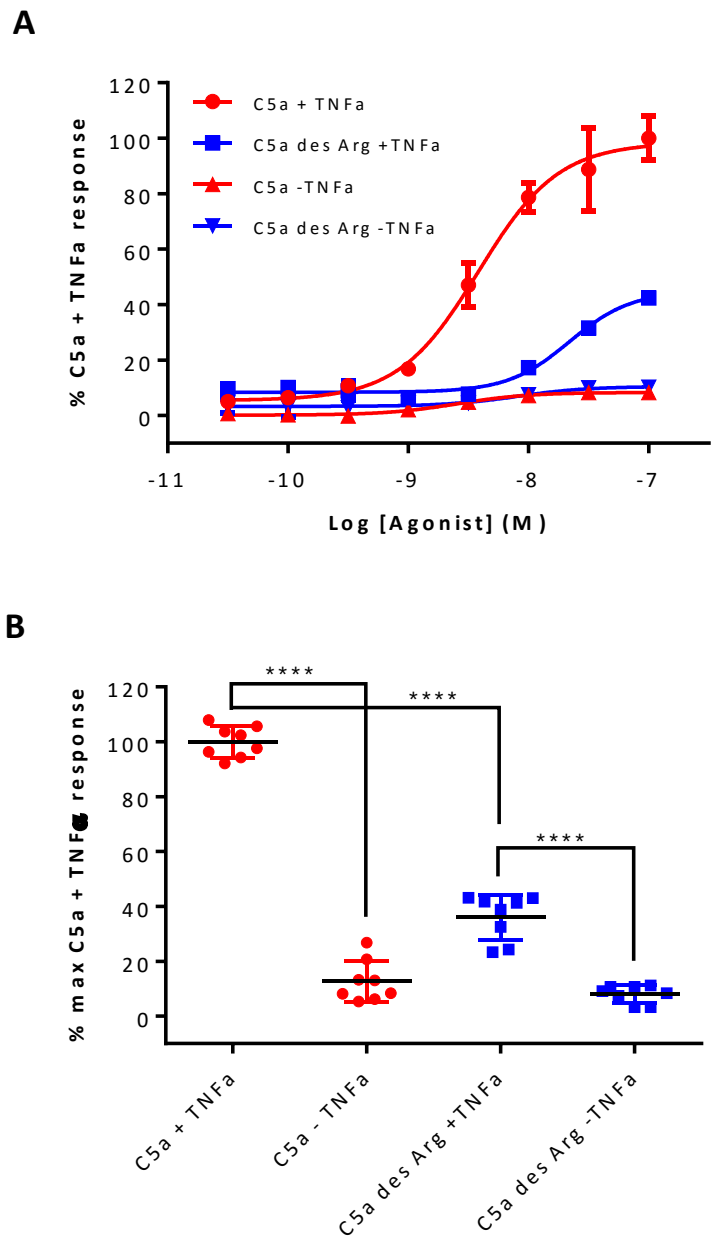

Figure 5.5. Neutrophils require a cytokine prime to generate a maximum respiratory burst response

Concentration response of human purified C5a and C5a des Arg induced respiratory burst in the human isolated neutrophils, as detected by dihydrorhodamine-123 fluorescence using flow cytometry, in the absence and presence of 1 ng/mL TNFα (A). Data are expressed as a percentage of the maximum respiratory burst response achieved with C5a + TNFα for each donor. Each point represents the mean average ±S.D of two replicates, data are representative of four separate donor experiments. Maximal respiratory burst response achieved with C5a or C5a des Arg (100 nM) in the absence or presence of 1 ng/mL TNFα. Each datum point reflects a test replicate and bars represent mean average response ±S.D from four separate donor experiments.

As with the non-primed respiratory burst response, C5a des Arg was less efficacious, producing a maximal response that was only 40% of that produced by C5a. EC_{50} values were comparable with those generated in the non-primed neutrophil with values of 2.4 nM and 18 nM for C5a and C5a des Arg respectively. The $\Delta Log(E_{max}/EC_{50})$ comparison generated a value of -1.33 indicating that C5a has a 21 fold greater relative activity than C5a des Arg at inducing respiratory burst in the TNFα primed neutrophil.

5.4.2. Activation of both the $C5a_1$ receptor and TNFR1 is required for a complete neutrophil respiratory burst response

With the data suggesting that activation of two cellular mechanisms is required to achieve maximal respiratory burst response, I next decided to focus my research on elucidating the contribution of TNFα, C5a and their associated receptors to this neutrophil event. To do this, I measured the effect of TNFα (1 ng/mL) and or C5a (5 nM) on the neutrophil production of HOCl and hydrogen peroxide (H_2O_2), a precursor to the formation of HOCl. Experiments were performed in the absence and presence of TNF and C5a receptor specific, ligand competitive agents. As can be seen in figure 5.6A, only TNFα was capable of inducing H_2O_2 production in the human neutrophil as measured by the H_2O_2 specific indicator Amplex® Red. Selective antagonism of each TNFα receptor (TNFR) demonstrated that only TNFR1 mediates TNFα induced production of H_2O_2 in a human neutrophil. C5a or its receptors do not appear to contribute to the H_2O_2 component of the neutrophil respiratory burst response. As observed in the concentration response experiments, C5a was unable to induce a profound respiratory burst on its own. This is also the case for TNFα. Not until the neutrophil is sequentially exposed to both agents, is a full HOCl respiratory burst response generated (figure 5.6B). As expected, selective antagonism of either TNFR1 or the $C5a_1$ receptor resulted in complete inhibition of the HOCl response. Interestingly, whereas the TNFR2 did not contribute to the generation of H_2O_2, blockade of this receptor significantly inhibited ($P < 0.001$) the generation of HOCl. As observed with other neutrophil responses, antagonism of the $C5a_2$ receptor did

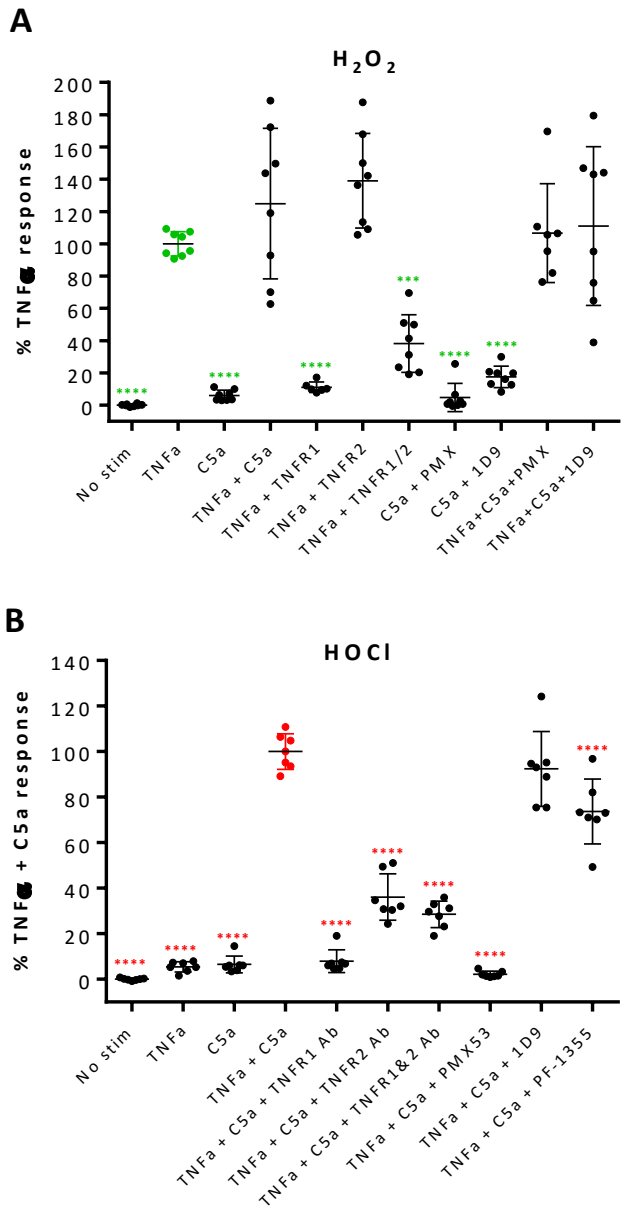

Figure 5.6. Investigating the role of TNFα and C5a in augmenting the neutrophil respiratory burst response

Neutrophil generation of H_2O_2 as detected by Amplex Red in response to TNFα and or C5a in the absence or presence of either TNFR1, TNFR2, $C5a_1$ $C5a_2$ receptor antagonists (A). Data are expressed as a percentage of the maximum H_2O_2 response to TNFα. Neutrophil generation of HOCl as detected by dihydrorhodamine-123 in response to TNFα and or C5a in the absence or presence of either TNFR1, TNFR2, $C5a_1$ or $C5a_2$ receptor antagonists or the MPO inhibitor PF-1355 (B). Data are expressed as a percentage of the maximum HOCl response to TNFα + C5a. Each datum point represents a test replicate and bars represent the mean average response ±S.D from neutrophils isolated from four separate donors. Statistical significance was determined using one-way ANOVA followed by Tukey's multiple comparison test (*** = $P < 0.001$, **** = $P < 0.0001$)

not impact the ability of C5a to contribute to the respiratory burst response. Incubation of neutrophils with the selective myeloperoxidase inhibitor PF-1355 significantly ($P < 0.0001$) but not completely inhibited the TNFα/C5a respiratory burst response. This is a surprising result as it is understood that peroxidase activity is required for production of HOCl from H_2O_2.

5.4.3. Assessing the functional response of C5a and C5a des Arg in cell lines transformed to express the C5a receptors

Next, my research focused on understanding the relative activity of C5a and C5a des Arg in activating intracellular pathways in cell lines transformed to express either the $C5a_1$ or $C5a_2$ receptor. The $C5a_1$ receptor expressing CHO cell line described in chapter 3 was used to investigate the action of each agonist on calcium mobilization, cAMP accumulation and ERK phosphorylation. In both the calcium and cAMP endpoint assays, C5a des Arg was as efficacious as C5a. A 7 fold increase in the EC_{50} value was observed for C5a in the calcium assay compared with only a 3 fold increase in the cAMP assay (figure 5.7A and B). Interestingly the absolute potencies for each agonist in the same cell line are far greater in the calcium endpoint compared with cAMP. With receptor expression remaining constant, this suggests that there is a greater degree of pathway coupling efficiency to the calcium pathway. Comparing agonist activity using $\Delta Log(E_{max}/EC_{50})$, C5a has an 8 fold greater relative activity than C5a des Arg at inducing calcium mobilization and a 3.4 fold greater relative activity at inducing cAMP accumulation.

Along with the CHO $C5a_1$ receptor expressing cell line, ERK phosphorylation was also assessed in the U2OS $C5a_2$ receptor cell line as it is thought that receptor-β-arrestin complex couples to ERK signalling. Activation of the $C5a_2$ receptor by either C5a of C5a des Arg resulted in no measurable phosphorylation of ERK (figure 5.8B). This is in contrast to the responses observed at the $C5a_1$ receptor. C5a produced a very potent ERK phosphorylation response, generating an EC_{50} value of 26 pM while C5a des Arg was 7 fold weaker generating an EC_{50} value of 180 pM (figure 5.8A). These

absolute potencies are identical to those generated in the calcium mobilization assay. Naturally this leads to a comparable $\Delta Log(E_{max}/EC_{50})$ value of -0.87 which translates to C5a displaying approximately an 8 fold greater relative activity at inducing ERK phosphorylation than C5a des Arg.

The final two cellular endpoints I investigated to determine the relative activity of C5a des Arg to C5a, made use of DiscoverX's PathHunter® assay platforms. CHO cells expressing the receptor/β-arrestin enzyme complementation technology and U2OS cells expressing the β-arrestin/endosome enzyme complementation technology were engineered to selectively express either C5a receptor. C5a des Arg was 9 fold less potent than C5a at promoting β-arrestin recruitment to the $C5a_1$ receptor but was equipotent to C5a at promoting β-arrestin recruitment the $C5a_2$ receptor (figure 5.9).

Similar results were observed in the receptor internalization assays. C5a des Arg was 6 fold weaker than C5a at inducing internalization of the $C5a_1$ receptor but equipotent to C5a at inducing $C5a_2$ receptor internalization (figure 5.10). Using the $\Delta Log(E_{max}/EC_{50})$ to assess relative agonist activity, C5a possesses 11 fold greater activity at inducing β-arrestin recruitment to the $C5a_1$ receptor, 6 fold greater relative activity at internalizing the $C5a_1$ receptor but is equiactive to C5a des Arg at inducing internalization of the $C5a_2$ receptor. C5a des Arg is marginally more active at promoting the recruitment of β-arrestin to the $C5a_2$ receptor.

A summary of all EC_{50}, E_{max}, $\Delta Log(E_{max}/EC_{50})$ values and fold relative activities values can be found in table 5.1.

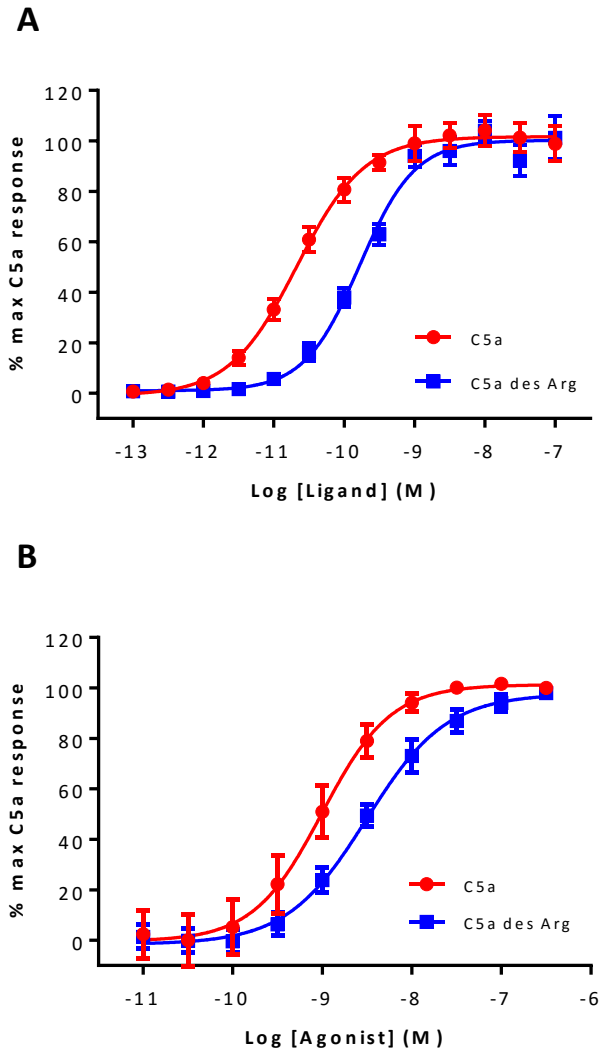

Figure 5.7. C5a and C5a des Arg induced calcium mobilization and cAMP via the $C5a_1$ receptor

Concentration response curves of human purified C5a and C5a des Arg at inducing calcium mobilization (A) and cAMP accumulation (B) in CHO cells transformed to express the $C5a_1$ receptor. All data points were expressed as a percentage of the maximal response observed to C5a. Each data point represents the mean average ±S.D. of two replicates. Data representative of four separate experiments.

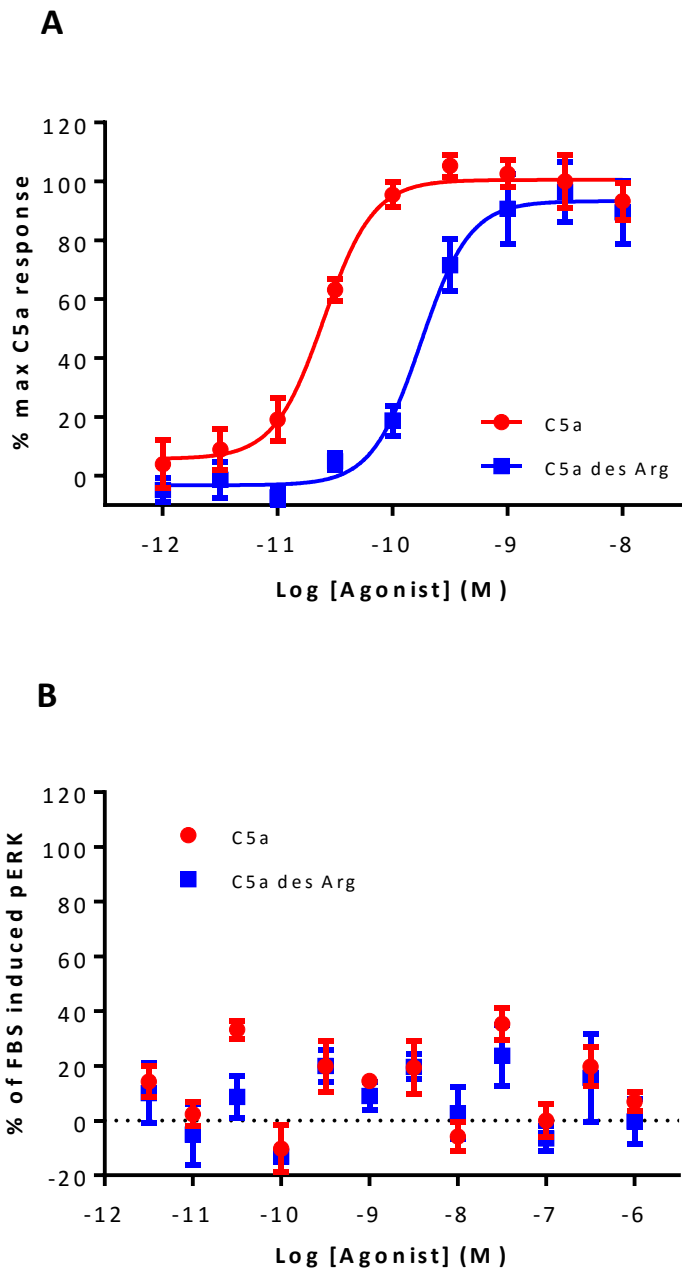

Figure 5.8. C5a and C5a des Arg induced phosphorylation of extracellular signal-regulated kinases

Concentration response curves of human purified C5a and C5a des Arg at inducing phosphorylation of extracellular signal–regulated kinases (ERK) in CHO cells expressing the $C5a_1$ receptor (A) and U2OS cells expressing the $C5a_2$ receptor (B). For responses in CHO cells all data points were expressed as a percentage of the maximal response observed to C5a. For responses in U2OS cells all data points were expressed as a percentage of the maximal response observed to 1% heat inactivated foetal bovine serum. Each data point represents the mean average ±S.D. of two replicates. Data are representative of at least four separate experiments.

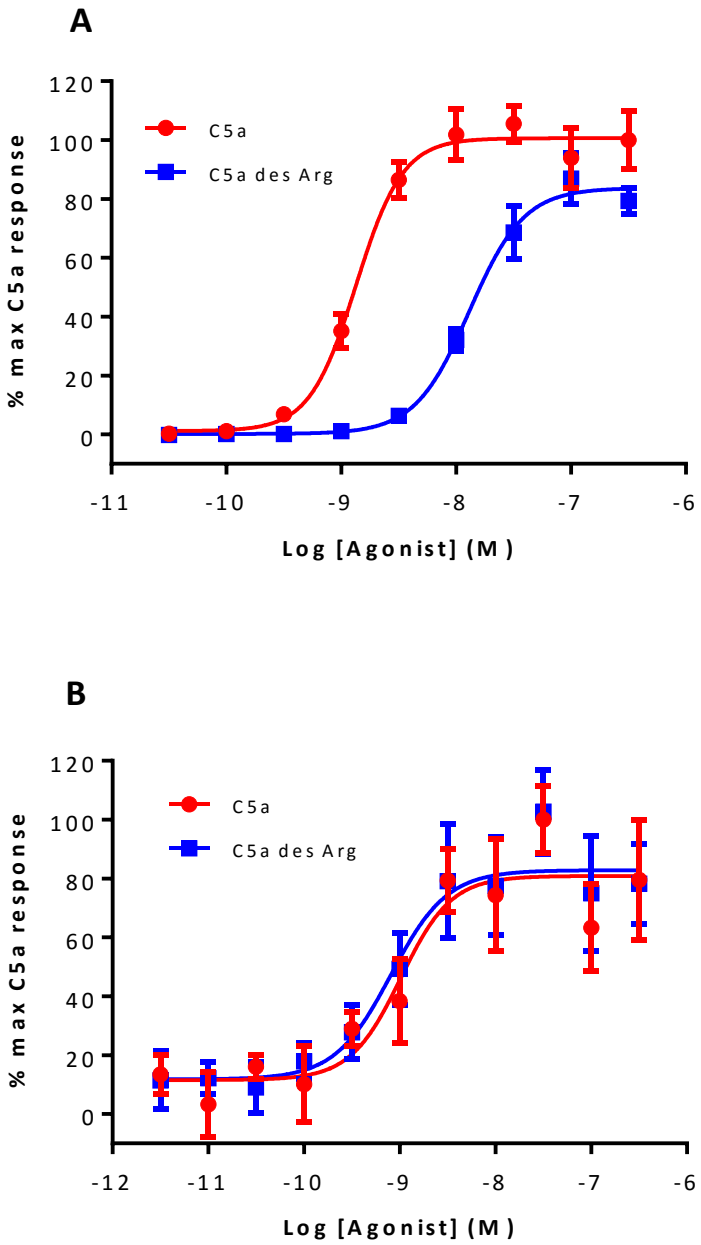

Figure 5.9. C5a and C5a des Arg promote the coupling of β-arrestin to the $C5a_1$ and $C5a_2$ receptors

Concentration response curves of human purified C5a and C5a des Arg at inducing the recruitment of β-arrestin to the $C5a_1$ receptor (A) or $C5a_2$ receptor (B) expressed in CHO cells as detected with DiscoverX PathHunter® technology. Data are expressed as a percentage of the maximum response observed to C5a and each point represents the mean average ±S.D of two replicates, data are representative of four separate experiments.

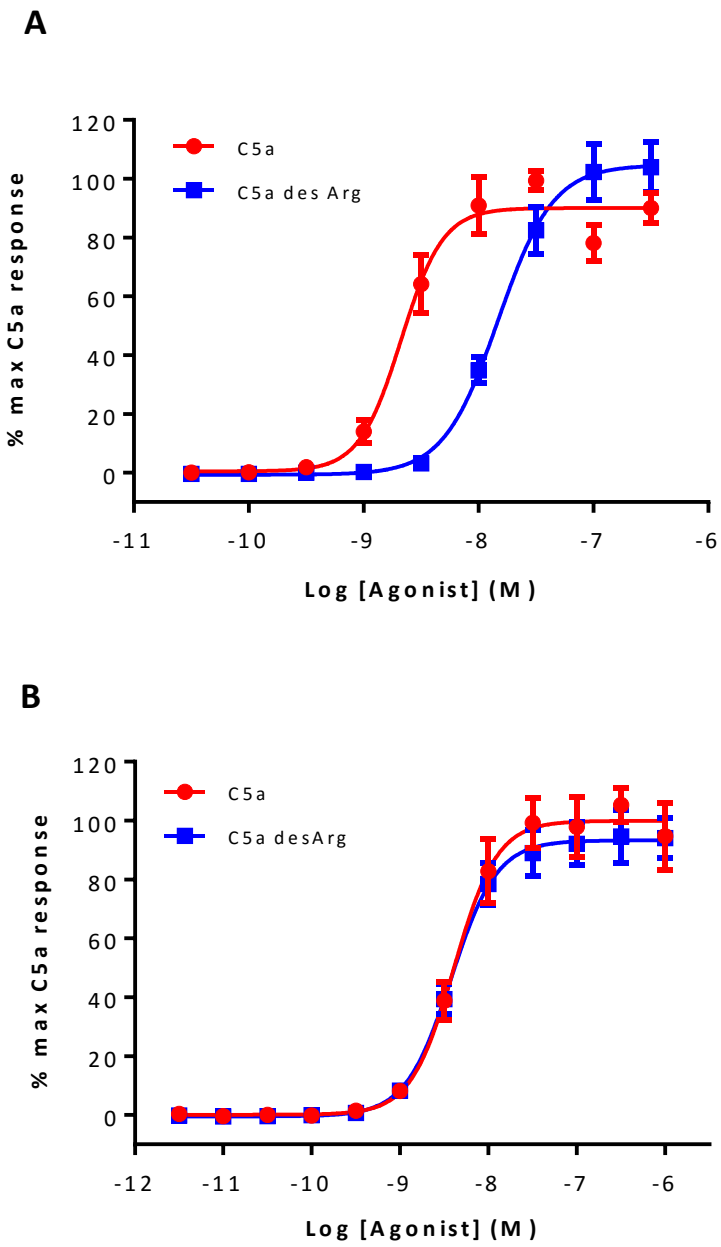

Figure 5.10. C5a and C5a des Arg promote internalization of the $C5a_1$ and $C5a_2$ receptors

Concentration response curves of human purified C5a and C5a des Arg at inducing internalization of the $C5a_1$ receptor (A) or $C5a_2$ receptor (B) expressed in U2OS cells as detected with DiscoverX PathHunter® technology. Data are expressed as a percentage of the maximum response observed to C5a and each point represents the mean average ±S.D of two replicates, data are representative of four separate experiments.

5.5. Discussion

In this research chapter, I performed an extensive analysis of the relative activity of human purified C5a and C5a des Arg in range of functional cell based assays using both human isolated neutrophils and receptor transformed cell lines. Using E_{max} and EC_{50} values from concentration response curves, I was able to determine a system independent expression of agonism for each peptide using $Log(E_{max}/EC_{50})$ and a measure of relative agonist activity using $\Delta Log(E_{max}/EC_{50})$. By plotting all $\Delta Log(E_{max}/EC_{50})$ scores together, I was able to generate a 'web of relative activity' for C5a and C5a des Arg which can be seen in figure 5.11. From the presentation of all relative activities together, it becomes clear that C5a de Arg has a strong bias for activating certain functional responses compared with others. This bias is towards promoting recruitment of β-arrestin to the $C5a_2$ receptor, internalization of the $C5a_2$ receptor and responses associated with neutrophil extravasation including chemotaxis and up regulation of cell surface adhesion molecules. Alternatively, C5a des Arg shows a reduced relative activity at inducing the antimicrobial, neutrophil respiratory burst response, a response where the relative activity of C5a des Arg is further reduced in the presence of TNFα. This reduced relative activity is also observed in cellular responses downstream of the $C5a_1$ receptor including calcium mobilization, cAMP accumulation and ERK phosphorylation.

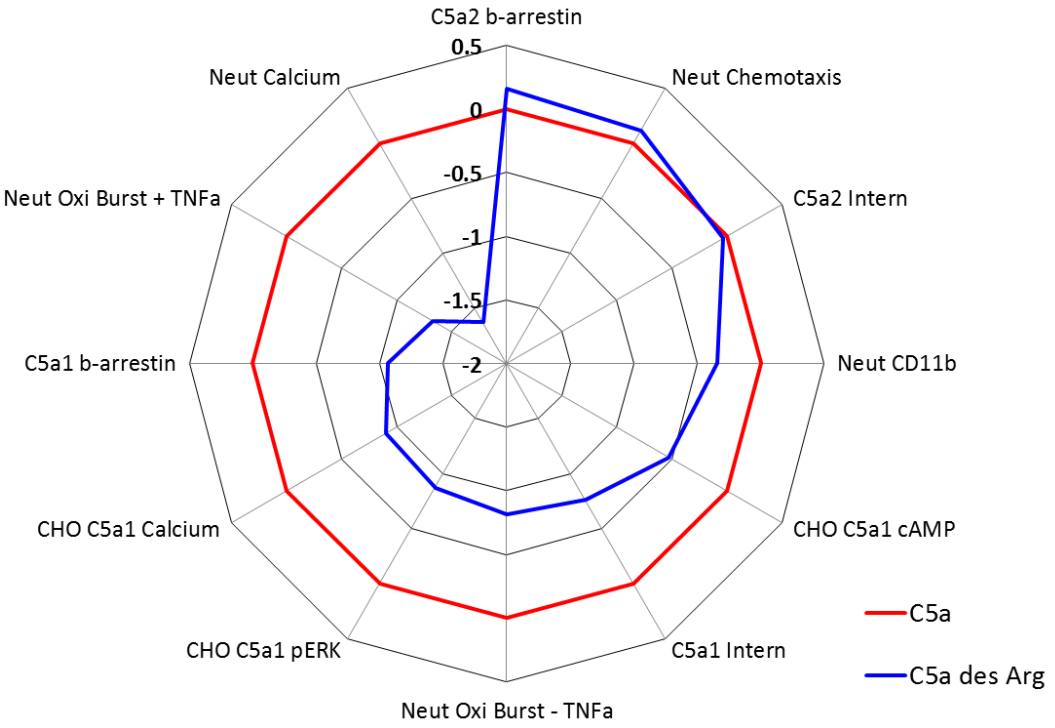

Figure 5.11. The C5a, C5a des Arg 'web of relative activity'

From quantification of the E_{max} and EC_{50} values from concentration response data, system independent expression of agonism for C5a and C5a des Arg was calculated for each *in vitro* cell based assay using $Log(E_{max}/EC_{50})$. The relative activity of C5a des Arg to C5a was determined using $\Delta Log(E_{max}/EC_{50})$. Along each *in vitro* assay axis the $\Delta Log(E_{max}/EC_{50})$ of C5a to C5a (red) or C5a des Arg to C5a (blue) is plotted generating a C5a/C5a des Arg web of relative efficacy.

		C5a				C5a des Arg					
Response	**n**	**%E_{max}**	**EC_{50} (M)**	**Log (E_{max}/EC_{50})**	**ΔLog (E_{max}/EC_{50})**	**%E_{max}**	**EC_{50} (M)**	**Log (E_{max}/EC_{50})**	**ΔLog (E_{max}/EC_{50})**	**Inv-Log**	**Fold activity**
Neutrophil Calcium	8	102.0	8.71E-11	12.2	0	85.2	8.33E-09	10.6	-1.63	0.024	42.3
Neutrophil Chemotaxis	8	95.6	4.86E-10	11.5	0	84.3	2.77E-10	11.6	0.12	1.307	0.8
Neutrophil CD11b	7	103.3	2.44E-10	11.7	0	72.6	3.57E-10	11.3	-0.35	0.452	2.2
Neutrophil Respiratory Burst + TNFa	4	97.3	2.40E-09	10.7	0	38.8	1.86E-08	9.3	-1.33	0.047	21.4
Neutrophil Respiratory Burst - TNFa	4	107.1	2.41E-09	10.7	0	80.8	1.26E-08	9.9	-0.81	0.154	6.5
CHO $C5a_1$ pERK	4	102.9	2.63E-11	12.6	0	95.0	1.80E-10	11.7	-0.87	0.134	7.5
CHO $C5a_1$ cAMP	4	101.3	1.00E-09	11.0	0	99.4	3.27E-09	10.5	-0.53	0.298	3.4
CHO $C5a_1$ Calcium	8	102.1	2.23E-11	12.7	0	100.0	1.63E-10	11.8	-0.90	0.127	7.9
$C5a_1$ B-arrestin2	4	103.3	1.39E-09	10.9	0	82.3	1.29E-08	9.8	-1.06	0.086	11.6
$C5a_2$ B-arrestin2	4	83.9	1.09E-09	10.9	0	89.9	8.24E-10	11.1	0.16	1.450	0.7
$C5a_1$ Internalization	4	108.9	2.40E-09	10.7	0	111.4	1.40E-08	9.9	-0.76	0.173	5.8
$C5a_2$ Internalization	4	101.3	3.56E-09	10.4	0	97.9	3.51E-09	10.3	-0.04	0.920	1.1

Table 5.1. The relative activity of human purified C5a des Arg to C5a in 12 *in vitro* cell based functional assays

E_{max} and EC_{50} values were extrapolated from non-linear regression fits to concentration response data for human purified C5a and C5 des in a range of in vitro cell based functional assays. A system independent expression of agonism was calculated using Log(E_{max}/EC_{50}) and the relative activity of C5a des Arg to C5a was calculated using the ΔLog(Emax/EC50). Fold activity was calculated by determining the reciprocal of the inverse Log of ΔLog(E_{max}/EC_{50}).

C5a des Arg also displayed a reduced relative activity at inducing the recruitment of β-arrestin to and internalization of the $C5a_1$ receptor, cellular processes that are considered to be important for desensitizing cellular responses during continual agonist exposure. From receptor antagonism studies I demonstrated that the $C5a_1$ receptor is responsible for mediating the chemotactic responses of both peptide agonists, yet C5a des Arg did not promote the typical desensitization response often observed in cellular migration experiments. This lack of desensitization was also observed by Yancey *et al.* (1989) who investigated the chemotactic effects of C5a and C5a des Arg on human monocytes and neutrophils. The inability of C5a des Arg to desensitize the cell migratory response is probably due to its reduced activity to switch off the $C5a_1$ receptor via β-arrestin recruitment and subsequent receptor internalization.

This apparent signalling bias of C5a des Arg towards an integrin up regulation and chemotactic phenotype and away from an antimicrobial phenotype could be considered mechanistically advantageous. When a peripheral microbial infection is detected by the complement system and tissue resident macrophages, C5a and pro-inflammatory cytokines are produced (figure 5.12). As C5a diffuses away from the site of infection and towards blood vessels it is metabolized to C5a des Arg by carboxypeptidases. With the majority of, if not all, serum C5a in the blood being C5a des Arg, this peptide needs to retain potent integrin and chemotactic activity to effectively extravasate immune cells from the blood to sites of infection. On the other hand, it would be a disadvantage if neutrophils, while migrating to the site of infection, produced antimicrobial agents such as HOCl that could potentially damage the surrounding tissue. Therefore, the fact that neutrophil generation of antimicrobial agents appears to be under the control of C5a and TNFα, agents whose concentration are at their highest at the immediate site of infection, suggests that this microbial clearance response is tightly controlled to minimize damage to the surrounding tissue.

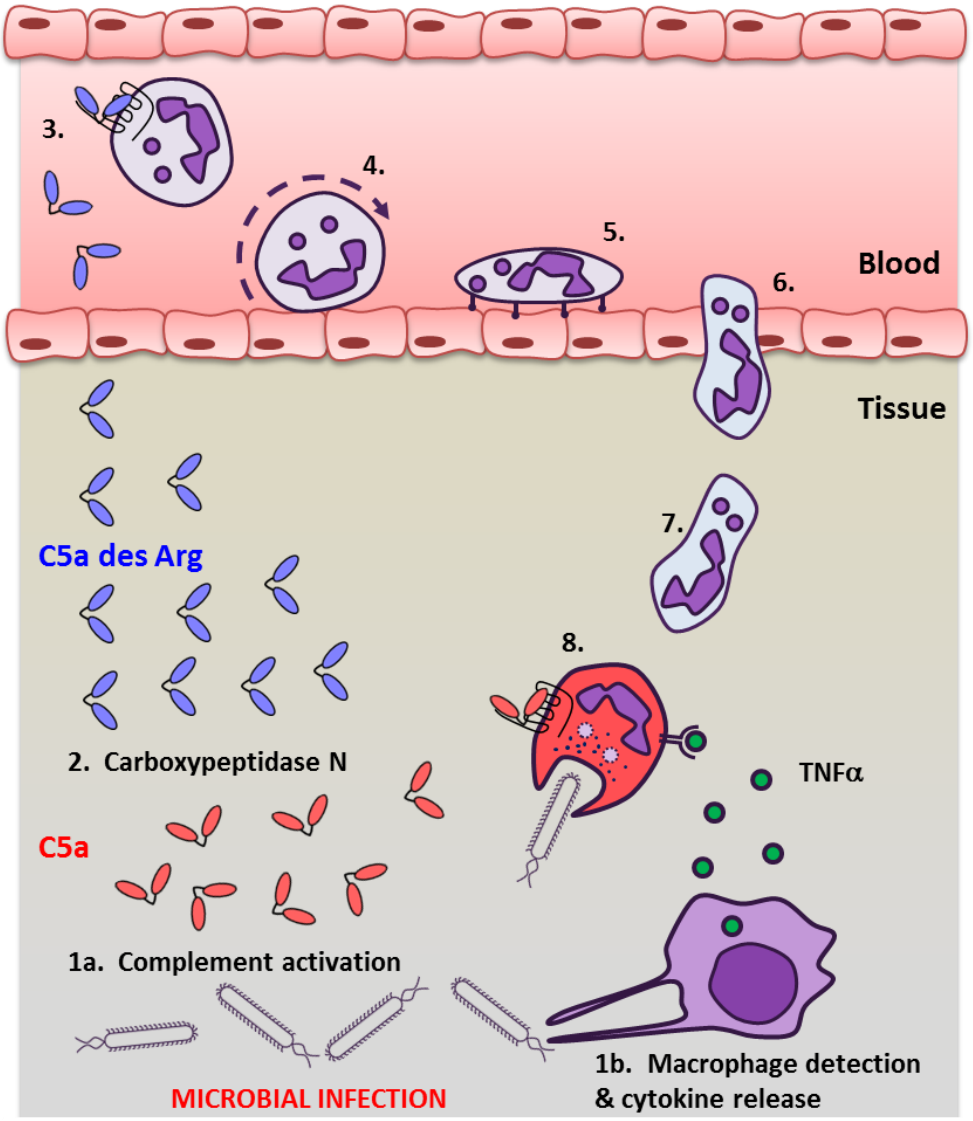

Figure 5.12. Schematic depiction of the role of C5a and C5a des Arg in elimination of a microbial infection

Peripheral microbial infection results in activation of the complements system (1a) and production of proinflammatory cytokines, including TNFα, by tissue resident macrophages (1b). As C5a diffuses away from the site of infection towards blood vessels it is rapidly converted to C5a des Arg by carboxypeptidases (2). C5a des Arg binds to $C5a_1$ receptors expressed on the surface of neutrophils (3), resulting cell activation and adhesion to endothelial cells lining the vasculature (4 & 5). Neutrophils migrate from blood vessels along the C5a des Arg / C5a gradient by chemotaxis (6 & 7) to the site of infection. Upon contact, neutrophils phagocytose pathogenic microbes, while non-metabolized C5a and TNFα ligate $C5a_1$ and TNFR1 expressed on the neutrophil surface. Dual receptor activation induces the respiratory burst response resulting in the production of the antimicrobial agent HOCl (8).

Lastly, my research in this chapter attempted to shed light on the mechanism through which TNFα and C5a control the HOCl respiratory burst response. It is well known that during respiratory burst, phagocytes generate HOCl, to destroy pathogenic microbes that have entered sterile compartments of the body (Albrich *et al.*, 1982; Pullar *et al.*, 2000). My research has demonstrated that in order to achieve a full respiratory burst response, neutrophils require both a priming and activation stimuli. This research demonstrates that TNFα provides a priming role by increasing intracellular concentrations of the oxygen radical H_2O_2, which is mediated solely through the TNFR1. Unlike TNFR2, which primarily couples to TNF receptor-associating factors (TRAFs), TNFR1 contains a death domain motif towards the carboxy-terminal of the receptor which allows it to couple to other death domain containing proteins including TNF receptor-associated death domain (TRADD) and Fas-associated death domain (FADD) (Tartaglia *et al.*, 1993; MacEwan, 2002). While FADD regulates cell death mechanisms, TRADD has been shown to recruit and activate riboflavin kinase (RFK) (Yazdanpanah *et al.*, 2009). RFK phosphorylates riboflavin to produce flavin mononucleotide (FMN) which is subsequently converted to flavin adenine dinucleotide (FAD) by FAD synthetase (Schramm *et al.*, 2014). FAD acts as an essential cofactor of the NADPH oxidases 2 (NOX2), an oxidase abundant in phagocytic immune cells (Panday *et al.*, 2015). Upon activation, NOX2 generates superoxide (O_2^-) inside the phagosome which is rapidly converted to H_2O_2 by superoxide dismutase (SOD). However H_2O_2 is unable to rapidly oxidize the ROS indicator dihydrorhodamine123 and is not the ultimate oxygen species to effectively neutralize pathogenic microbes.

It was not until neutrophils were exposed to C5a after being primed with TNFα that HOCl was generated, the effects of which were solely mediated via the $C5a_1$ receptor. C5a is known to induce neutrophil degranulation, causing release of myeloperoxidase (MPO) from azurophilic lysosomal granules (Chenoweth *et al.*, 1980). The release of MPO results in the chlorination of H_2O_2 to generate the highly reactive HOCl (figure 5.13). Although not directly measured here, there is an indication that C5a des Arg would show a bias away from inducing a degranulation-MPO release response. In fact this was observed by Chenoweth *et al.* (1983) who

showed that C5a des Arg is approximately 40 fold weaker than C5a at inducing MPO activity in neutrophils.

I believe the results described here pertaining to the dual mechanism required to generate HOCl for complete respiratory burst (TNFα inducing the intracellular production of H_2O_2 via TNFR1, and C5a promoting the release of MPO from azurophilic granules via the $C5a_1$ receptor), shed light on the true role of C5a in the respiratory burst response. C5a does not induce the production of H_2O_2, which it is often misrepresented in the literature as doing so (Lee *et al.*, 2008).

In summary, the work in this research chapter demonstrates that C5a des Arg displays a biased agonism profile. This signalling bias is towards promoting a cell phenotype required for extravasation of neutrophils from the blood to peripheral sites of microbial infection and away from a phenotype required for microbial elimination. Unfortunately the research described here was unable to shed further light as to the function of the $C5a_2$ receptor, the role of which is still largely enigmatic.

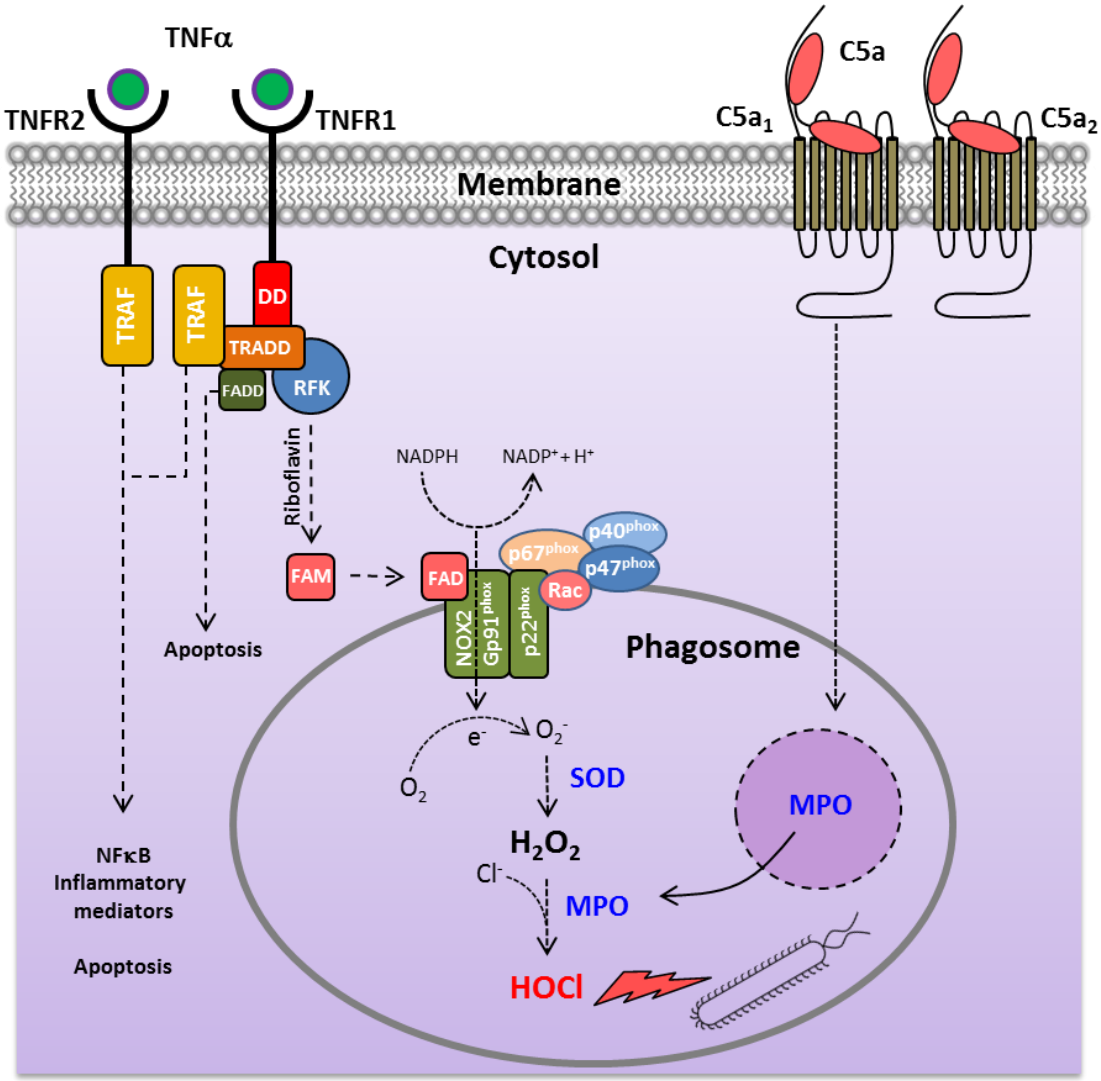

Figure 5.13. Schematic depiction of the role C5a, TNFα and their receptors in the neutrophil respiratory burst response

TNFα ligation of the TNFR1 expressed on the surface of neutrophils results in the recruitment of death domain adaptor proteins, including TNF-receptor associated death domain (TRADD) or Fas-associated death domain (FADD) to the death domain region of TNRF1 located at its carboxyl-terminal. The TNFR2 is not capable of interacting with death domain containing adaptor proteins but couples to TNF receptor-associated factors (TRAFF). TRADD recruits and activates riboflavin kinase (RFK) which phosphorylates riboflavin to produce flavin mononucleotide (FMN) which is then converted to flavin adenine dinucleotide (FAD) by FAD synthetase. FAD binds to NADPH oxidase 2 (NOX2) which further recruits the regulatory subunits $p40^{phox}$, $p47^{phox}$, $p67^{phox}$ and Rac. This leads to NOX2 activation which transfers electrons from cytosolic NADPH to oxygen (O_2) on the luminal side of the phagosome generating superoxide (O_2^-). O_2^- is converted to hydrogen peroxide (H_2O_2) by superoxide dismutase (SOD). Activation of the $C5a_1$ receptors expressed on the surface of neutrophils by C5a results in degranulation of azurophilic lysosomal granules releasing myeloperoxidase (MPO) into the phagosome. MPO chlorinates H_2O_2 resulting in the generation of the highly reactive antimicrobial agent hypochlorous acid (HOCl).

Chapter 6

Defining the mechanism of C5a des Arg induced biased agonism

Defining the mechanism of C5a des Arg induced biased agonism

6.1. Abstract

The complement system fragment peptide, C5a des Arg, retains a significant degree of the activity displayed by its parent isoform, C5a, at the $C5a_1$ receptor. The functional responses induced by C5a des Arg promote a cellular phenotype linked to immune cell extravasation. However, C5a des Arg is almost devoid of the ability to induce an immune cell response involved in the removal of a microbial infection. The work performed in this chapter attempted to elucidate the mechanism by which C5a des Arg produces its biased agonism profile.

Receptor mutagenesis and cell based functional assays were performed to understand whether there are differences in how C5a and C5a des Arg bind the transmembrane domain of the $C5a_1$ receptor. The BioSens-All^{TM} platform, offered by Domain Therapeutics, was subsequently employed to determine whether C5a des Arg produces a different G-protein and β-arrestin activation profile compared with C5a.

Both C5a and C5a des Arg electrostatically interact with the transmembrane region of the $C5a_1$ receptor. To achieve its superior affinity, C5a interacts with amino acid residue D282. C5a des Arg relies on a cluster of amino acids at the top of the fourth and fifth transmembrane domains. This difference in binding does not translate into a different G-protein activation signature but it does appear to alter the ability of C5a des Arg to promote the recruitment of β-arrestin. The lack of β-arrestin recruitment induced by C5a des Arg may be responsible for its biased agonism profile at the $C5a_1$ receptor.

6.2. Introduction

As demonstrated by the work in the previous chapter, C5a des Arg displays a biased agonism profile compared with C5a. The C-terminal arginine of C5a allows it to induce neutrophil responses, especially respiratory burst which appears to be tied to calcium mobilization and/or β-arrestin recruitment. However, the removal of the arginine appears to focus the ligand's functional activity towards neutrophil phenotypes that contribute to cellular extravasation, including integrin upregulation and chemotaxis which appear to be tied to the regulation of intracellular cAMP concentrations and possibly its actions at the $C5a_2$ receptor. Although only characterized using monoclonal antibodies, due to the lack of cell permeable reagents, results from the previous chapter suggest that the $C5a_2$ does not contribute the actions of C5a des Arg in mediating neutrophil responses. With this in mind, it is possible that C5a des Arg produces its biased agonism profile by inducing a specific conformation of the $C5a_1$ receptor that only allows activation of specific intracellular pathways.

For an agonist to produce a cellular response it must first bind to its cognate GPCR and then provide a stimulus. This stimulus leads to a change in the receptors tertiary structure resulting in an active receptor conformation. The active receptor conformation is typified by a contraction of the agonist binding pocket (orthosteric site), movement of transmembrane (TM) domains, including the shift of TM6 away from the core of the receptor, which reveals intracellular binding sites to which intracellular proteins, including G-proteins and β-arrestins, bind (Rasmussen *et al.*, 2011; Cooke *et al.*, 2016). Rather than promoting a single active receptor conformation, agonists can induce an ensemble of receptor conformations that promote the recruitment of multiple types of G-proteins, leading to the activation of several intracellular pathways (Li *et al.*, 2004). It is therefore possible that C5a des Arg, in contrast to C5a, induces a different receptor conformation that leads to the activation of only select pathways. If so, what are the mechanisms by which C5a des Arg drives conformational selectivity of the $C5a_1$ receptor and how does this influence pathway activation?

There is also a possibility that the biased agonism profile generated by C5a des Arg is due to receptor-ligand binding kinetics. From results generated earlier in this thesis, which are similar to those observed by others, C5a des Arg has a significantly reduced affinity at the $C5a_1$ receptor compared with C5a. A ligand's affinity for a receptor is a function of its association and dissociation binding kinetics, with faster association and slower dissociation kinetics increasing the affinity of a ligand for a receptor. Interestingly, the functional endpoints that C5a des Arg is biased towards have extended assay incubations times, whereas, the functional endpoints which C5a des Arg is biased away from have short experimental incubation times. However, there is an exception to this trend which is observed with the recruitment of β-arrestin 2 to the $C5a_1$ receptor. Of all experimental endpoints investigated, this assay experienced the longest assay incubation time, yet C5a des Arg failed to display comparable potency to C5a.

Numerous research groups have attempted to define the specific amino acids residues within the TM domain of the $C5a_1$ receptor that contribute to the binding affinity and efficacy of C5a and C5a des Arg (DeMartino *et al.*, 1995; Cain *et al.*, 2001; Higginbottom *et al.*, 2005). Using receptor mutagenesis, researchers discovered that a strong electrostatic interaction exists between the terminal arginine of C5a and the Asp-282 amino acid residue that lies within TM seven in the $C5a_1$ receptor. This interaction contributes to the binding affinity of C5a and helps explain the reduced affinity of C5a des Arg at the $C5a_1$ receptor. Interestingly, a cluster of charged residues at the top of TM 4 and 5 (Arg 175, Glu-199 and Arg 206) contribute heavily to the affinity and efficacy of C5a des Arg but have no impact on C5a.

With the uncertainty as to whether selective receptor conformations or receptor-ligand binding kinetics contribute to the biased agonism profile of C5a des Arg, I have decided to focus the research in this chapter on understanding the mechanism by which C5a des Arg achieves its biased agonism profile. The main objectives of are:

1. Using site directed mutagenesis, investigate the contribution of the charged amino acid residues Arg-175, Glu-180, Glu-199, Arg-206 and Asp-282 within

the transmembrane region of the $C5a_1$ receptor to the potency and efficacy of C5a and C5a des Arg.

2. Using both C5a and C5a des Arg, perform pA_2 analyses with the competitive antagonist, PMX53 and the inverse agonist, NDT9513727 (figure 6.1), to determine whether each agonist is proportionally antagonized by each antagonist and how each charged residue impacts antagonist affinity.

3. Using the BioSens-All platform offered by Domain Therapeutics, assess the G-protein and β-arrestin signalling signatures induced by C5a and C5a des Arg at the wild type $C5a_1$ receptor. Assess the impact of assay kinetics on the signalling signature of each peptide agonist.

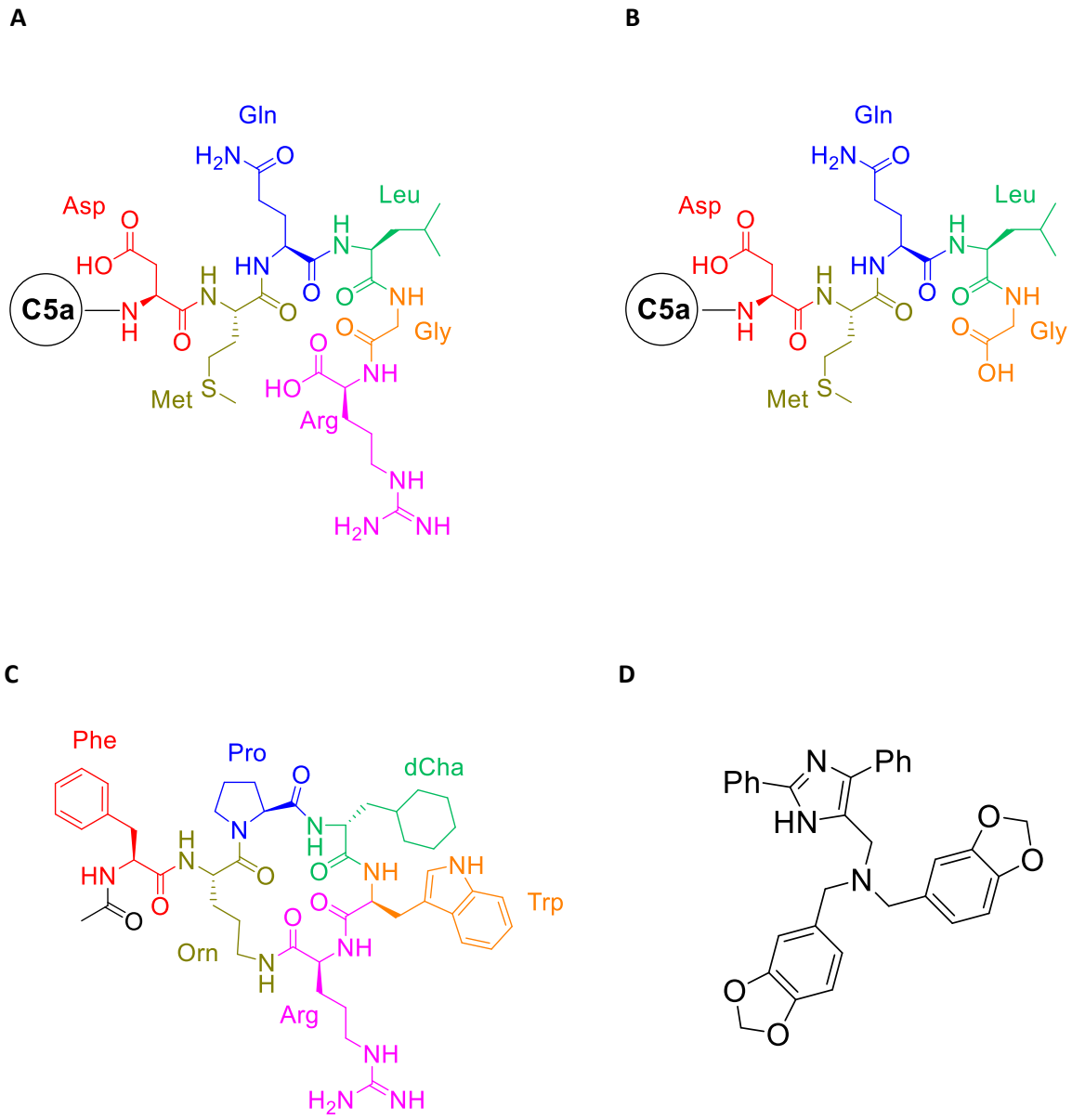

Figure 6.1. Structures of C5a, C5a des Arg, PMX53 and NDT9513727

The last six amino acids that form the C-terminus of C5a (Asp-Met-Gln-Leu-Gly-Arg) (A). The removal of the terminal arginine by carboxypeptidases generates C5a des Arg (B). The cyclic peptide $C5a_1$ receptor antagonist PMX53, (Ace-Phe-[Orn-Pro-dCha-Trp-Arg]) which resembles the C-terminus of C5a (C) and the $C5a_1$ receptor inverse agonist NDT9513727 (D).

6.3. Chapter specific methods

6.3.1. Wild type and mutant $C5a_1$ receptor expression

Codon optimized wild type and mutant $C5a_1$ receptor constructs were generated by Blue Sky BioServices Inc, Worcester, MA, USA, and expressed in pcDNA3.1 plasmid vectors. CHO cells transformed to stably overexpress the $G\alpha_{16}$ G-protein were grown to 80% confluency and separately transfected with each plasmid DNA using the MaxCyte STX electroporation apparatus. Cells from each transfection were resuspended in growth medium and either seeded into a T75 flask for assessment of receptor expression (2×10^6 cells/flask), or into black, clear bottom plates (10,000 cells/well) for functional assay assessment. Cells were left in culture for 24 hours before experimentation.

6.3.2. Flow cytometry assessment of receptor expression

On the day of experimentation, cells were harvested from the flasks and stained in FACS buffer with either the $C5a_1$ receptor specific FITC conjugated monoclonal antibody S5/1, or an equivalent concentration of IgG matched isotype control. Samples were assessed for mean fluorescence intensity in the FITC channel using flow cytometry.

6.3.3. Functional assessment of the wild type and mutant $C5a_1$ receptor constructs using pA_2 analyses

The impact of each receptor mutation on the potency and efficacy of C5a and C5a des Arg as well as the affinity of two $C5a_1$ receptor antagonists, PMX53 and NDT9513727, was assessed using calcium mobilization as described in detail in the main methods section. Concentration ranges of either C5a or C5a des Arg were tested in the absence or presence of increasing concentrations of each antagonist. To obtain estimates of potency and efficacy for each agonist condition, the four

parameter logistic equation was fit to each concentration response data set. To determine an estimate of the affinity constant for each antagonist at each receptor construct using either C5a or C5a des Arg as the agonist, equiactive agonist concentrations were extrapolated from agonist curves in the absence and presence of antagonist to calculate dose ratios (DR). Using the Schild regression (plotting the antagonist concentration (Log[B]) vs Log(DR-1)), and the pA_2 equation (equation 6.1), the concentration of antagonist that produces a 2 fold shift in agonist concentration response curve (pA_2) was calculated.

$$pA_2 = Log(DR-1) - Log[B]$$

Equation 6.1. The pA_2 equation

6.3.4. The G-protein coupling signature of C5a and C5a des Arg at the $C5a_1$ receptor

To determine the G-protein/β-arrestin signalling signature of C5a and C5a des Arg at the wild type $C5a_1$ receptor, the Domain Therapeutics BioSens-All™ platform was used. The BioSens-All™ platform uses bioluminescence resonance energy transfer (BRET) technology to determine specific G_α-protein subunit activation by measuring its proximity to a $G_{\beta\gamma}$-protein complex. At rest, in its GDP bound state, the bioluminescent, luciferase conjugated G_α subunit is in close proximity to the green fluorescent protein tagged $G_{\beta\gamma}$-protein complex, and a fluorescent signal is generated. If a particular G_α-protein is activated upon agonist induced receptor activation, GDP-GTP exchange occurs leading to its dissociation from its $G_{\beta\gamma}$-protein counterpart resulting in a diminished fluorescence signal. A similar BRET arrangement can also detect the receptor recruitment of β-arrestin.

$C5a_1$ receptor interactions with the $G_{\alpha i2}$, $G_{\alpha oB}$, and $G_{\alpha 15/16}$ as well as β-arrestin 2 biosensors were investigated in the BioSens-All platform. The potency and efficacy of both C5a and C5a des Arg were assessed using 22 point concentration response

curves. The impact of agonist kinetics on each biosensor response was assessed by reading each biosensor assay at multiple time points. The relative activity of C5 des Arg at each biosensor was compared to C5a using the previously described $\Delta Log(E_{max}/EC_{50})$ transformation.

6.3.5. Characterizing the receptor binding arrangement of the two $C5a_1$ receptor antagonists PMX53 and NDT9513727

To determine whether NDT9513727 binds to the same site on the $C5a_1$ receptor as PMX53, a competition binding study using a tritiated analogue of PMX53 was employed. CHO cells expressing the $C5a_1$ receptor were incubated with a K_d concentration of the tritiated cyclic peptide in the presence of a concentration range of either NDT9513727, PMX53 or human purified C5a or C5a des Arg. Assay was incubated for 3 hours at room temperature prior to termination via rapid filtration through PEI soaked GF/C filter plates using a Brandel Harvester. Concentration response data were expressed as a percentage of total and non-specific binding controls (defined with 1 μM PMX53) and IC_{50} values were generated using the four parameter logistic equation described earlier.

6.4. Results

6.4.1. Functionally viable expression of wild type and mutant $C5a_1$ receptors

To determine the contribution of electrostatic interactions between the $C5a_1$ receptor and C5a and C5a des Arg in driving agonist induced responses, charged residues within the transmembrane region and extracellular loops of the receptor were mutated. Single point mutations were performed at positions R175, E180, E199, R206 and D282, substituting each amino acid for a chemically inert alanine. Wild type and mutant $C5a_1$ receptors were expressed in CHO cells over-expressing the $G_{\alpha16}$-protein and receptor expression was quantified by flow cytometry. Using 40 µg of DNA, each receptor construct expressed at a comparable level in CHO cells and to within two fold of the wild type receptor. There was no detection of endogenous $C5a_1$ receptor in CHO cells using the S5/1 antibody clone. However the cross reactivity of this reagent with hamster $C5a_1$ receptor is not known (figure 6.2).

To assess the consequence of each receptor mutation on the functional activity of C5a and C5a des Arg and on the affinity of the two antagonists PMX53 and NDT9513727, a calcium mobilization assay was used. To ensure cells expressing each receptor were functionally viable and loaded with an equivalent amount of the calcium dye, plated cells were stimulated with either 100 nM of the calcium ionophore, A23187, or with a high concentration (3 µM) of human purified C5a (figure 6.3). All cells expressing $C5a_1$ receptor constructs produced robust and reproducible responses to the calcium ionophore which, were within 20% of the response produced by the parent CHO cells. Similarly, all cells expressing $C5a_1$ receptor constructs produced robust responses to C5a which were within 25% of the response produced by cells expressing the wild type receptor. Interestingly, the parent CHO cells produced a response to C5a that was approximately 15% that of the wild type receptor response. Although reproducible, this response was not considered to be large enough to impact the interpretation of agonist concentration response data.

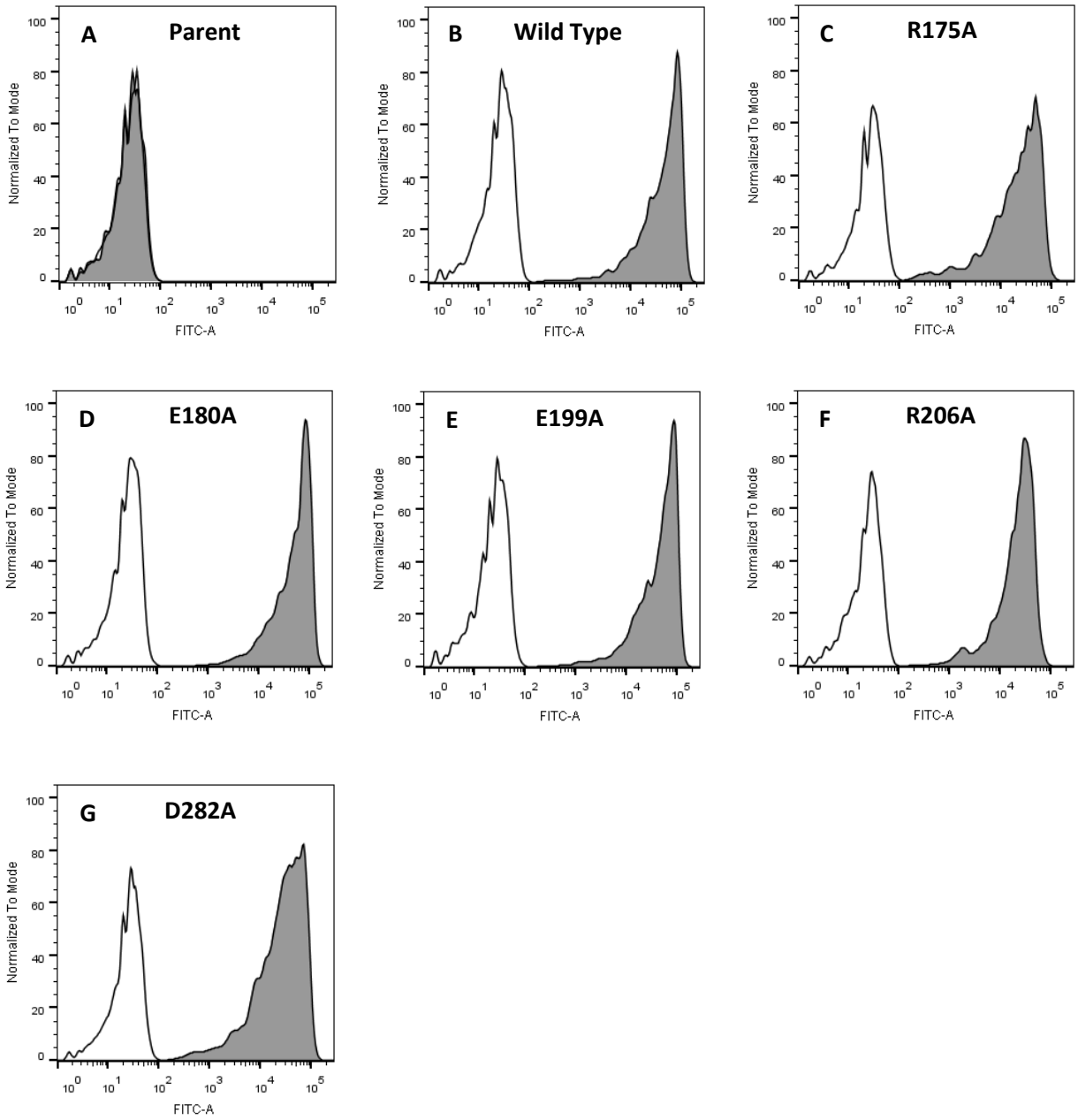

Figure 6.2. Expression of the different $C5a_1$ receptor constructs in CHO cells

Surface expression of wild type and mutant constructs of the human $C5a_1$ receptor expressed in CHO cells. Relative receptor expression was determined using flow cytometry and the FITC conjugated $C5a_1$ receptor specific antibody clone S5/1. Parent CHO cell (A), wild type $C5a_1$ receptor (B), R175A (C), E180A (D), E199A (E), R206A (F) and R282A (G). Open histogram represents concentration matched isotype control antibody staining, shaded histogram represents receptor specific antibody staining.

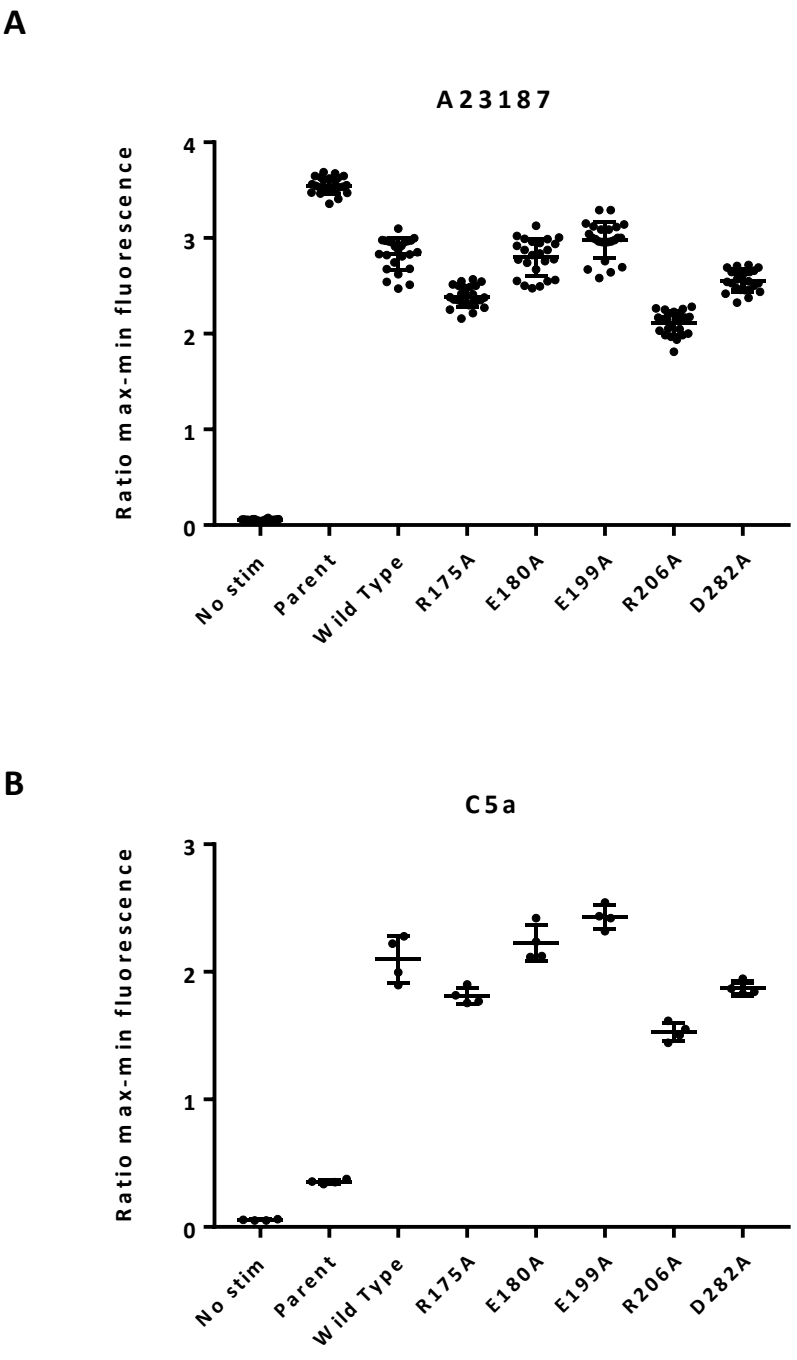

Figure 6.3. Functional responsiveness of CHO cells expressing wild type and mutant $C5a_1$ receptor constructs

Viability and functional expression of human $C5a_1$ receptor constructs in CHO cells measured by calcium mobilization using the fluorescence imaging. CHO cells loaded with calcium 3 indicator dye were stimulated with the calcium ionophore A23187 (100 nM) (A), or human purified C5a (3 µM) (B). Response is plotted as ratio of the maximum-minimum fluorescence response. Bars represent mean and S.D. from between 4-24 different replicates.

6.4.2. Charged residues within the transmembrane domain of the $C5a_1$ receptor contribute to the affinity of C5a and C5a des Arg

The impact of mutating the charged amino acid residues on the potency (EC_{50}) and efficacy (E_{max}) of C5a and C5a des Arg assessed using calcium mobilization assays. At the wild type receptor both C5a and C5a des Arg were as efficacious as each other and displayed EC_{50} values of 11 and 64 pM respectively (figure 6.4). The mutant $C5a_1$ receptor R175A, had a small impact on the EC_{50} of C5a, (3.4 fold increase) but a profound effect on the potency of C5a des Arg, reducing its EC_{50} by 170 fold to 11 nM (table 6.1). This was in contrast to the mutant E180A, a charged amino acid residue present within the second extracellular loop of the $C5a_1$ receptor. This mutation had no impact on the potency of C5a and a minor impact on the potency of C5a des Arg (2.2 fold increase in EC_{50}). Mutant E199A, located at the top to TM 5, produced a mild reduction in the EC_{50} of C5a but produced a 10 fold reduction in the EC_{50} of C5a des Arg. When mutating the $C5a_1$ receptor at position R206A, an amino acid residue also within the fifth TM, minimal impact was observed on the EC_{50} of C5a. However the mutation of this residue had the most profound effect on the EC_{50} of C5a des Arg, reducing its potency by approximately 550 fold to 35 nM. Finally, mutation D282A within the seventh TM of the $C5a_1$ receptor had no impact on the EC_{50} of C5a des Arg but had a substantial effect on the EC_{50} of C5a, reducing its EC_{50} by 6 fold to 70 pM.

Using the $\Delta Log(E_{max}/EC_{50})$ conversion, a web of efficacy for C5a and C5a des Arg at the wild type and mutant $C5a_1$ receptors was generated (figure 6.5). These data confirm the electrostatic interaction between the positively charged arginine at the C-terminal of C5a and the negatively charged Asp-282 within the seventh TM of the $C5a_1$ receptor. They also highlight the importance of the cluster of amino acids at the top of TM 5 and 6 in controlling the affinity of C5a des Arg.

Next, the effects of receptor mutagenesis were assessed on the affinity of the two $C5a_1$ receptor antagonists PMX53 and NDT9513727 using pA_2 analysis. Analyses were performed using both C5a and C5a des Arg to determine whether antagonism of each agonist was comparable. Due the lack of equilibrium achieved in calcium mobilization assays, pA_2 values were only used to compare antagonist affinity

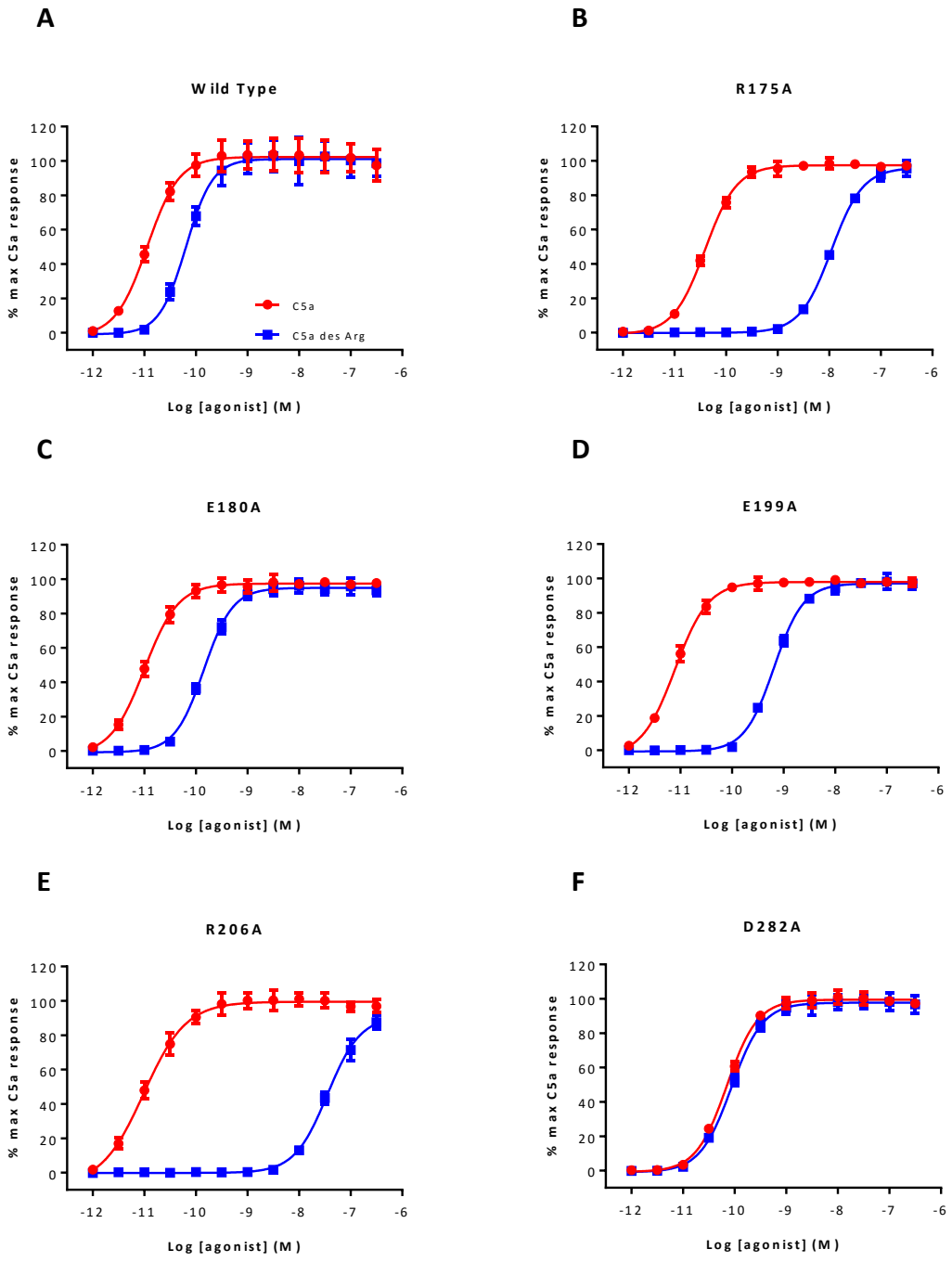

Figure 6.4. The effect of $C5a_1$ receptor mutagenesis on potency and efficacy of C5a and C5a des Arg

Calcium mobilization responses induced by concentrations of human purified C5a or C5a des Arg at human wild type and mutant $C5a_1$ receptors expressed in CHO cells. Wild type $C5a_1$ receptor (A), R175A (B), E180A (C), E199A (D), R206A (E) and R282A (F). Responses for each $C5a_1$ receptor construct were expressed as a percentage of the maximum response induced by C5a. Data points represent mean and S.D. from eight replicates.

	C5a EC_{50} (M)	C5a des Arg EC_{50} (M)	Fold difference C5a to C5a des Arg
Wild type	1.14E-11	6.46E-11	5.7
R175A	3.89E-11	1.10E-08	282.0
E180A	1.00E-11	1.41E-10	14.1
E199A	7.81E-12	6.52E-10	83.5
R206A	9.72E-12	3.54E-08	3641.2
D282A	7.08E-11	8.71E-11	1.2

	Fold difference to wild type	Fold difference to wild type
Wild type	1.0	1.0
R175A	3.4	169.9
E180A	0.9	2.2
E199A	0.7	10.1
R206A	0.9	547.9
D282A	6.2	1.3

Table 6.1. Potency of C5a and C5a des Arg at the wild type and mutant $C5a_1$ receptors

EC_{50} values of human purified C5a and C5a des Arg at the human wild type and mutant $C5a_1$ receptors expressed in CHO cells. Upper table shows EC_{50} values extrapolated from the four parameter logistic equation and the fold difference between C5a and C5a des Arg at the different $C5a_1$ receptor constructs. Lower table shows the fold difference in EC_{50} for either C5a or C5a des Arg at each mutant construct compared with wild type receptor.

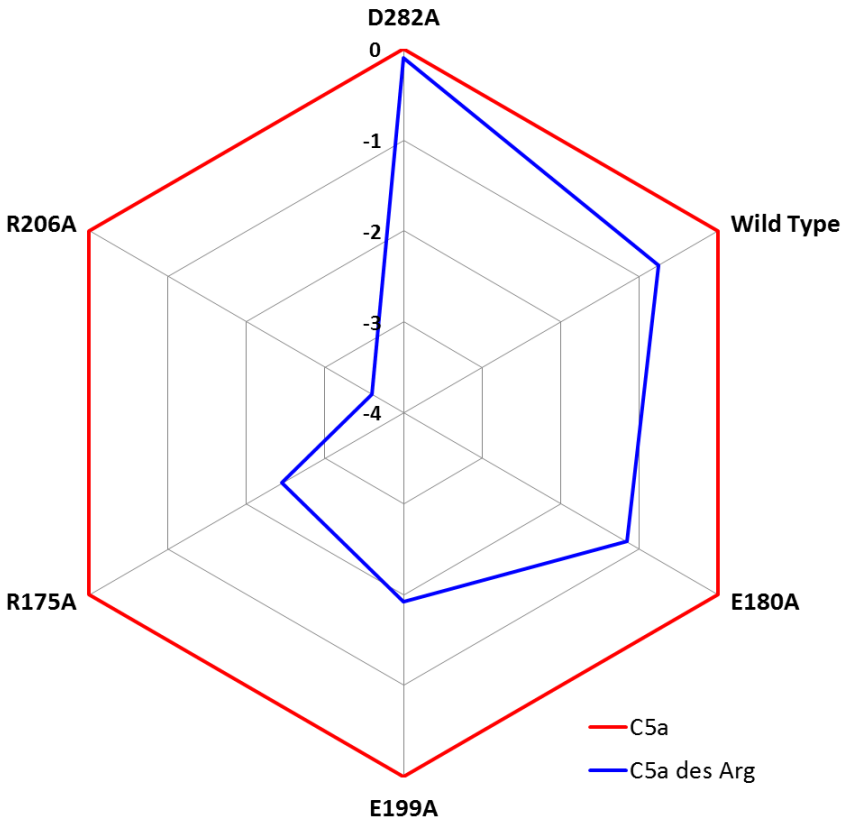

Figure 6.5. Relative agonism of C5a and C5a des Arg at each $C5a_1$ receptor construct

A radar plot showing the relative agonism of C5a des Arg (blue line) to C5a (red line) at the human wild type and mutant $C5a_1$ receptor constructs. Relative agonist activity was calculated using the $\Delta Log(E_{max}/EC_{50})$ transformation.

between receptor constructs and were not considered to be system independent measures of antagonist affinity.

Against C5a, both PMX53 and NDT9513727 produced dextral displacement of the agonist concentration response curve at the wild type $C5a_1$ receptor which were surmountable at each antagonist concentration (figure 6.6 A and C). The pA_2 values for NDT9513727 and PMX53 were comparable at 7 and 6.7 respectively (table 6.2). A very interesting observation was made from the pA_2 analyses using C5a des Arg. The dextral shifts of the C5a des Arg concentration response curves induced by both antagonists were much larger than those observed against C5a (figure 6.6 B and D). This translated into an increased affinity of both NDT9513727 and PMX53 with pA_2 values of 7.7 and 7.8 respectively. This apparent probe dependence in receptor antagonism suggests that both PMX53 and NDT9513727 bind the $C5a_1$ receptor allosterically to either one or both C5a peptides. Interestingly, at high concentrations, NDT9513727 displayed profound degree of insurmountable antagonism compared with PMX53, again further indicating an allosteric mode of action for this $C5a_1$ receptor antagonist.

At the R175A mutant receptor, both NDT9513727 and PMX53 produced greater dextral shifts in C5a concentration response curves than were seen at the wild type receptor with pA_2 values of 8.4 and 8.1 respectively (figure 6.6 E and G). In addition, NDT9513727 displayed insurmountable antagonism at the highest concentrations tested, again possibly alluding to an allosteric model of action for this antagonist. Both antagonists displayed similar antagonism profiles at C5a des Arg, with the agonist concentration response curves starting much further down the concentration range. These data confirm the observations from the agonist alone experiments, demonstrating the role of the R175 residue in controlling the affinity of C5a and C5a des Arg at the $C5a_1$ receptor. Interestingly, the addition of PMX53 to cells expressing the R175A construct, prior to the addition of agonist, resulted partial agonist response which plateaued at 50% of the response induced by C5a and with an EC_{50} 400nM. These data highlight that R175 probably forms an important electrostatic interaction with PMX53 which locks the receptor in an inactive conformation. When this interaction is absent, the cyclic peptide antagonist is able to activate the

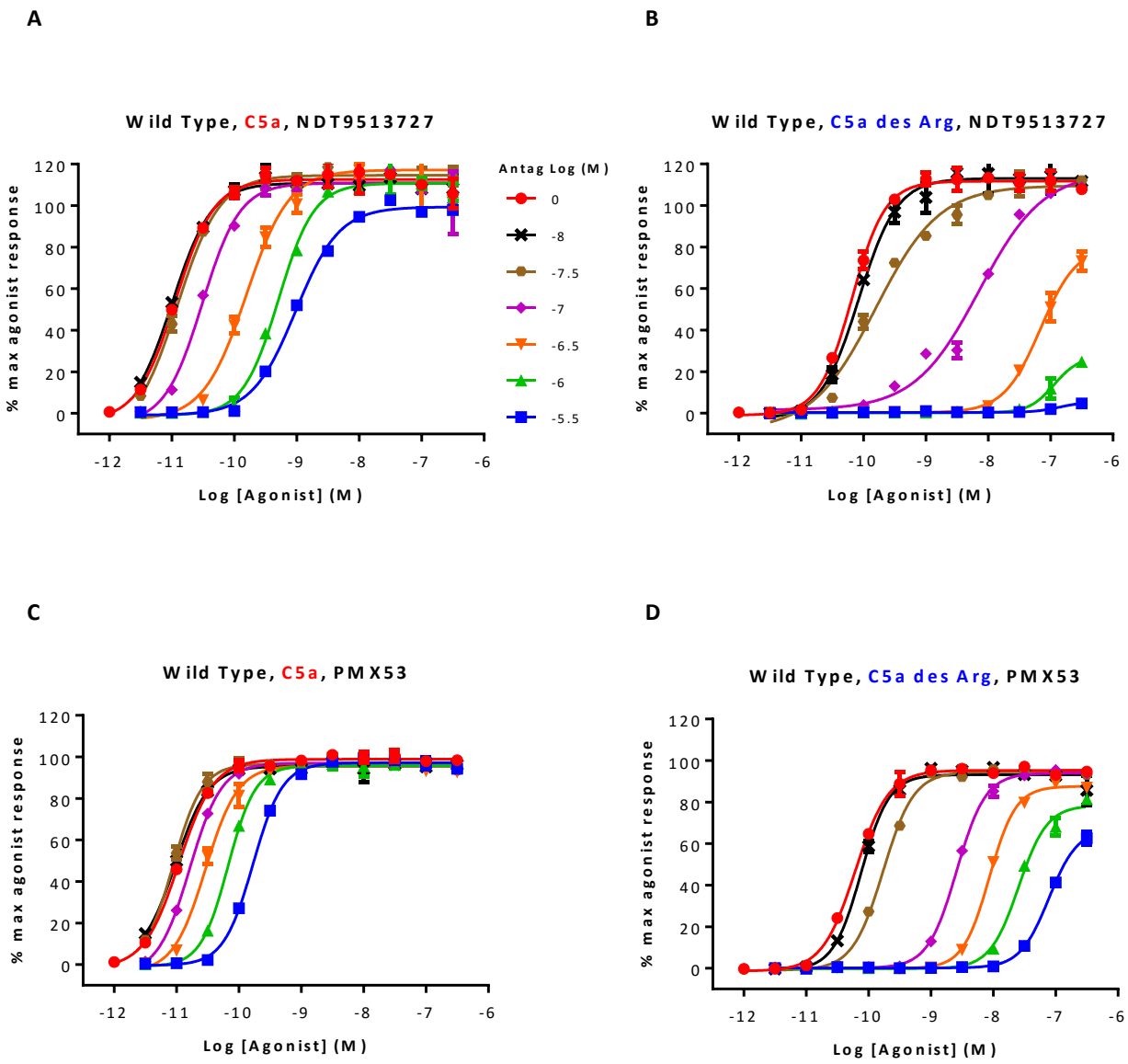

Figure 6.6. Antagonism of C5a and C5a des Arg at $C5a_1$ receptor constructs by PMX53 and NDT9513727

Concentration response curves for C5a and C5a des Arg in the absence or presence of increasing concentrations of either the cyclic peptide antagonist PMX53 or the inverse agonist NDT9513727. Wild type $C5a_1$ receptor (A-D), and mutant constructs R175A (E-H), E180A (I-L), E199A (M-P), R206A (Q-T) and D282 (U-X). All agonist responses were expressed as a percentage of the maximum agonist response. Data points are represent mean and S.D. from two replicates.

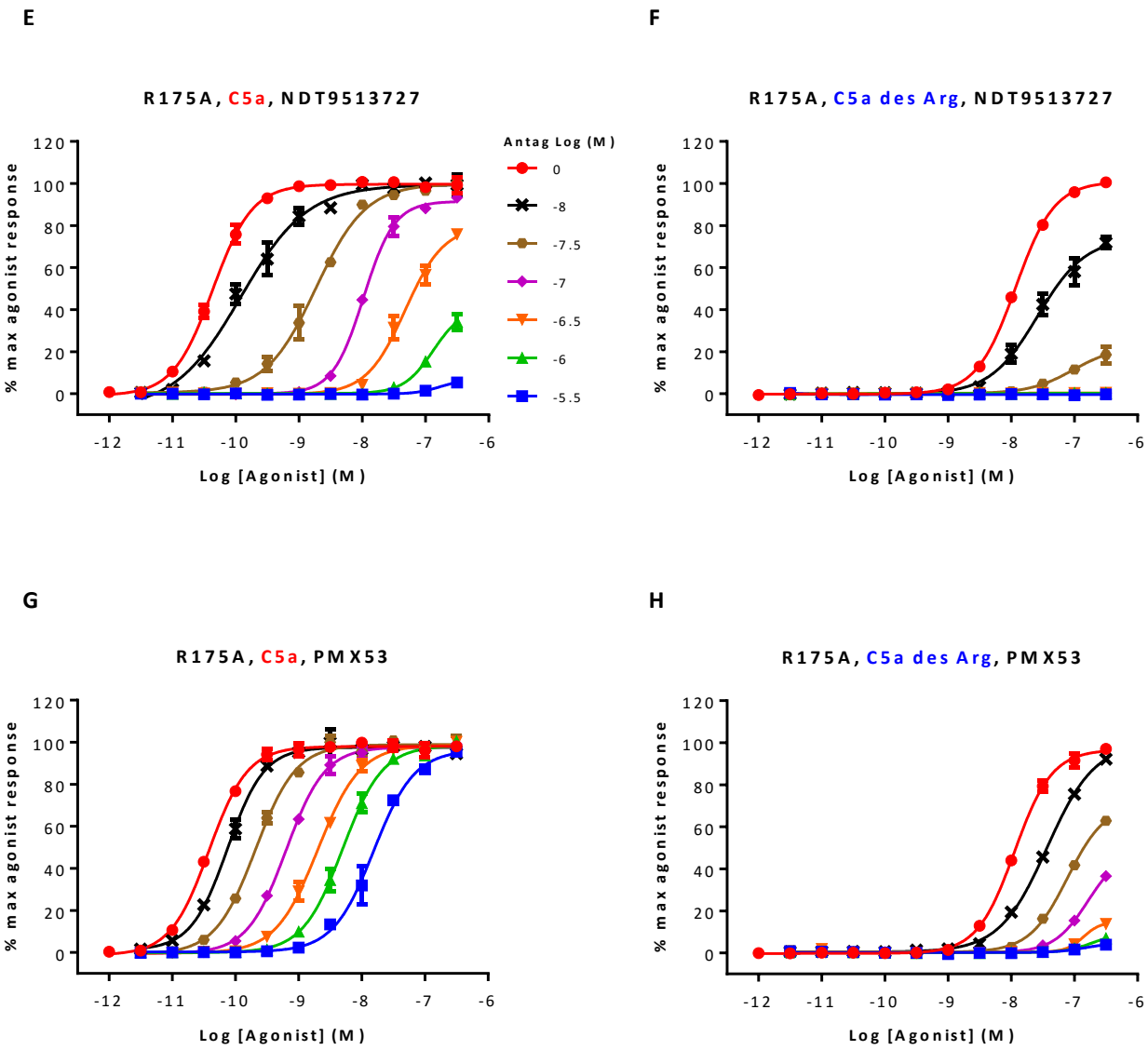

Figure 6.6. Continued

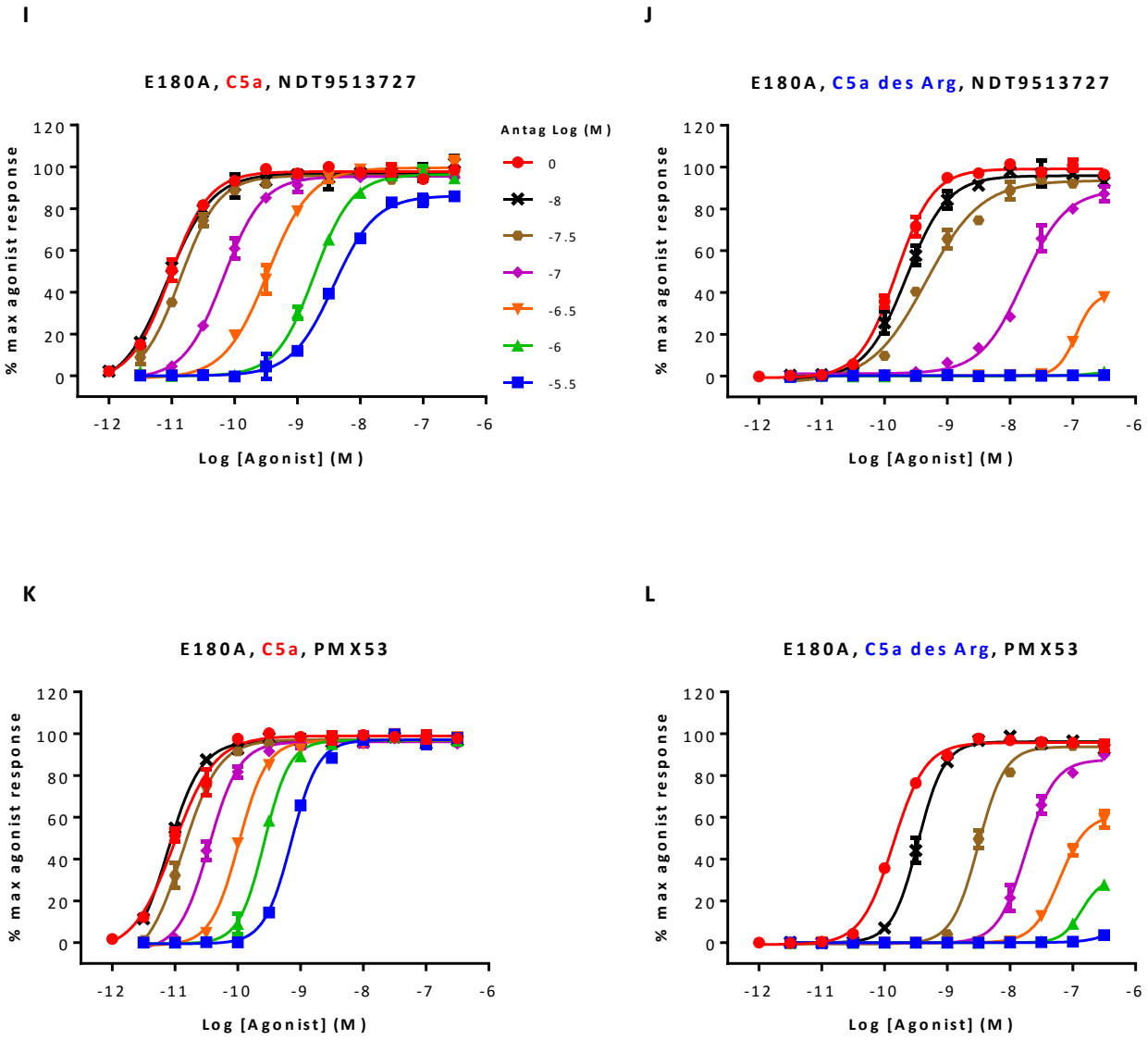

Figure 6.6. continued

M

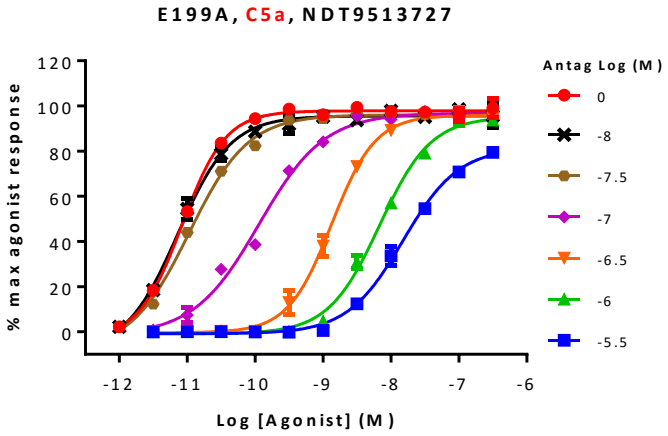

N

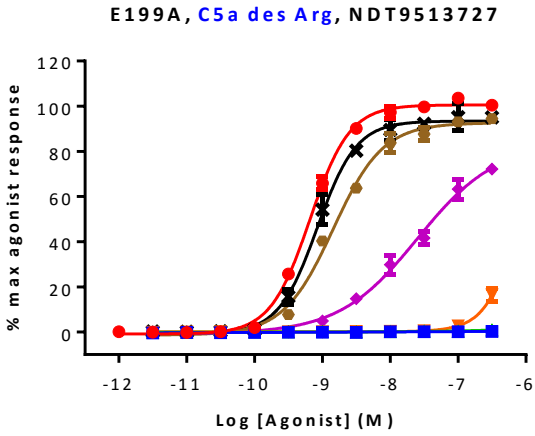

O

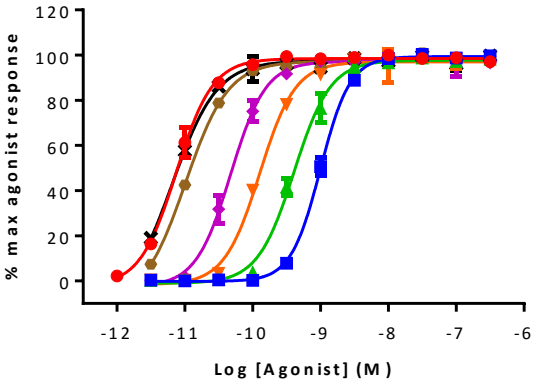

P

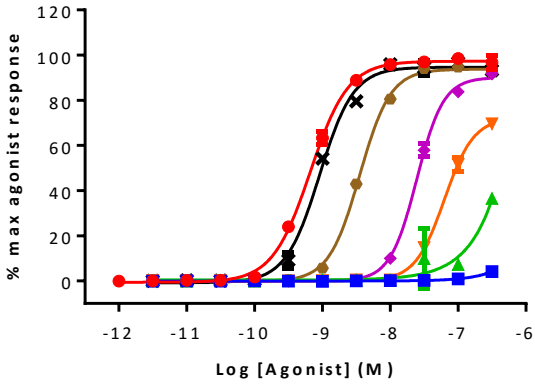

Figure 6.6. Continued

Q

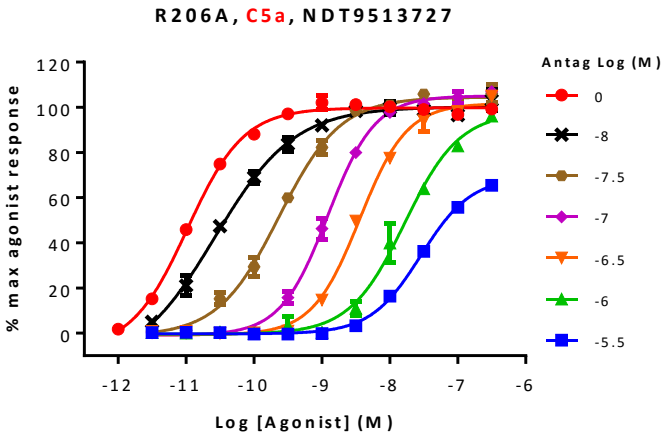

R

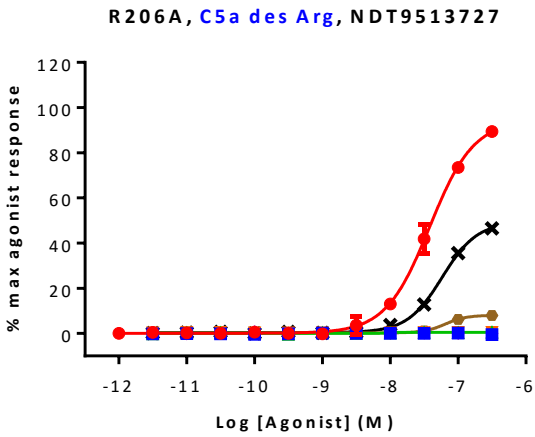

S

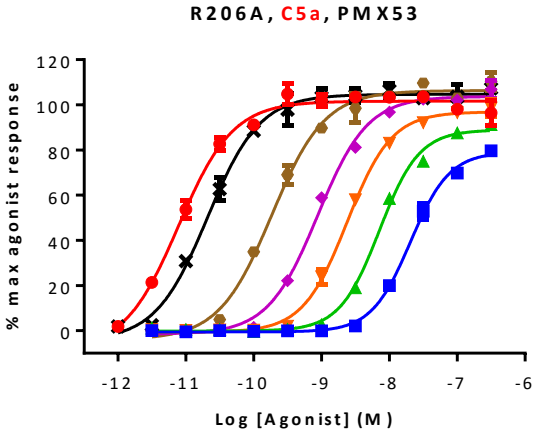

T

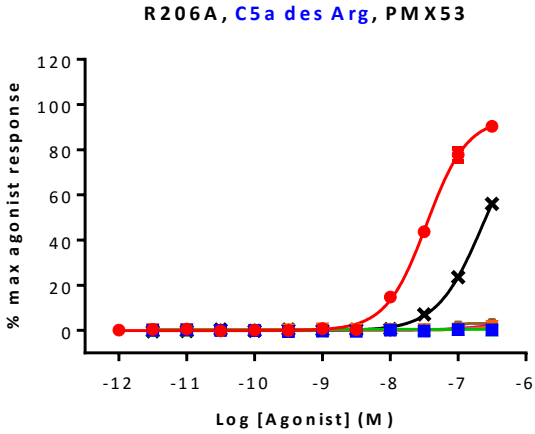

Figure 6.6. Continued

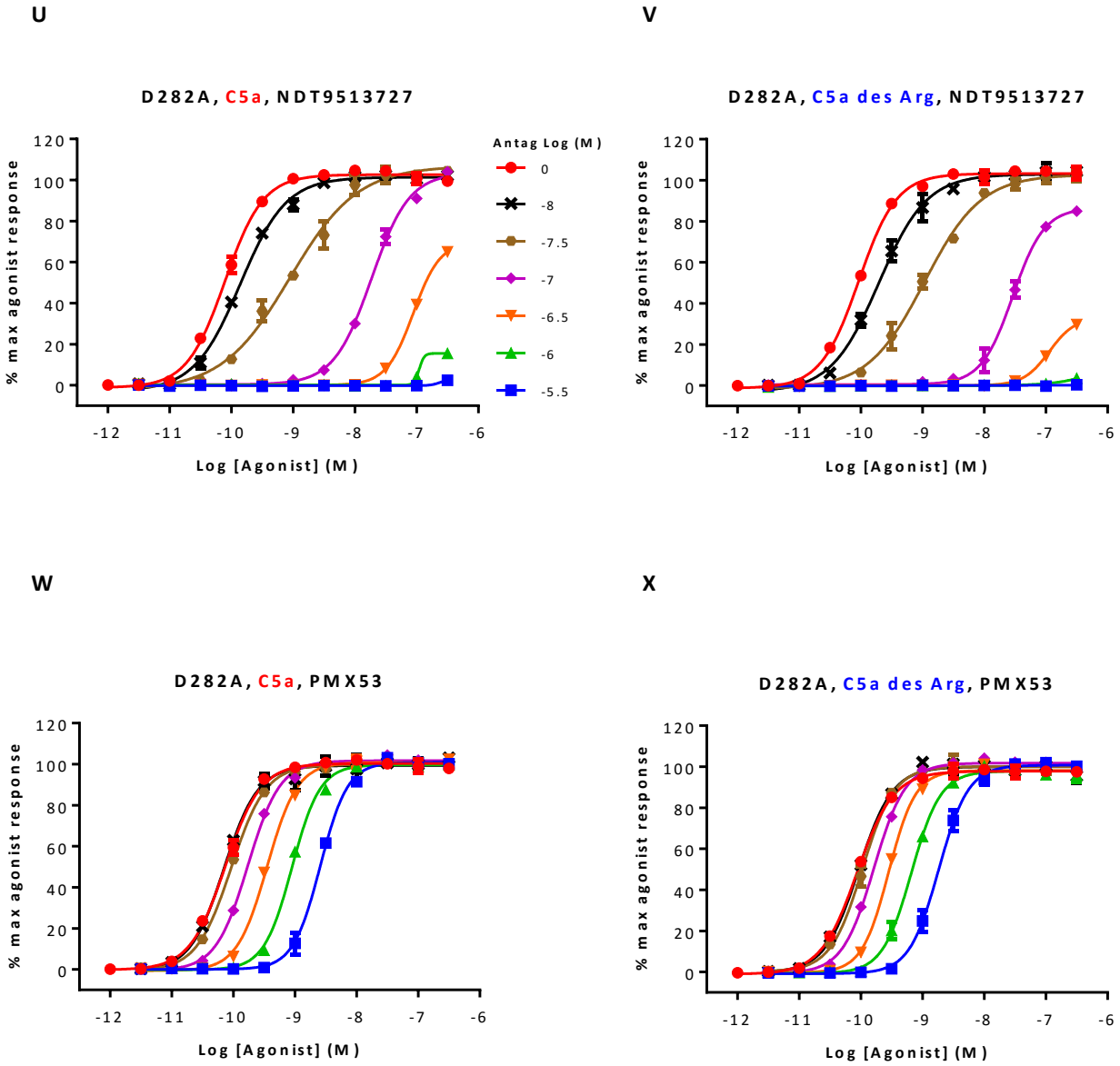

Figure 6.6. Continued

		pA_2 [M]		A_2 [M]		
$C5a_1$ receptor	**Antagonist**	**C5a**	**C5a des Arg**	**C5a**	**C5a des Arg**	**Fold A_2 C5a/C5a des Arg**
Wild Type	NDT	7.0	7.7	1.0E-07	1.9E-08	5.3
R175A	NDT	8.4	8.1	4.3E-09	8.6E-09	0.5
E180A	NDT	7.4	7.8	3.7E-08	1.7E-08	2.2
E199A	NDT	7.4	7.7	3.6E-08	2.1E-08	1.7
R206A	NDT	8.3	6.8	5.2E-09	1.5E-07	0.04
D282A	NDT	8.0	8.0	1.1E-08	9.2E-09	1.1
Wild Type	PMX53	6.7	7.8	1.9E-07	1.7E-08	11.4
R175A	PMX53	8.0	8.5	1.0E-08	3.4E-9	3
E180A	PMX53	7.3	8.3	5.5E-08	4.7E-09	11.8
E199A	PMX53	7.4	7.8	4.2E-08	1.5E-08	2.8
R206A	PMX53	8.5	7.8	3.4E-09	1.7E-08	0.2
D282A	PMX53	7.0	6.8	9.5E-08	1.4E-07	0.7

Table 6.2. pA_2 values for NDT9513727 and PMX53 at the human wild type and mutant $C5a_1$ receptors

pA_2 values for PMX53 and NDT9513727 at each $C5a_1$ receptor construct obtained from Schild analyses. pA_2 values were generated using either human purified C5a or C5a des Arg.

receptor. Neither NDT9513727 nor PMX53 produced an agonist response at the other $C5a_1$ receptor constructs.

Mutating the $C5a_1$ receptor at position E180 within the second extracellular loop, enhanced the affinity of both antagonists when profiled against C5a and C5a des Arg (figure 6.6 I-L). This was apparent by the greater dextral shifts in each agonist response curve and highlights a possible interaction between C5a and C5a des Arg at this point on the receptor. Similar concentration response curve displacement profiles were observed at the E199A mutant receptor (figure 6.6 M-P). The increase in affinity estimate for both antagonists against both agonists when compared with the wild type receptor suggest that this receptor residue contributes to the affinity of both peptides at the $C5a_1$ receptor.

As observed in the agonist alone experiment, residue R206 profoundly contributed to the affinity of C5a des Arg at the $C5a_1$ receptor but appeared to have minimal impact on C5a. However, the mutant R206A receptor caused both antagonists to produce larger dextral shifts in the concentration response curves of C5a compared with the wild type receptor and resulted in pA_2 values of 8.3 and 8.5 for NDT9513727 and PMX53 respectively (figure 6.6 Q-T).

The impact of each antagonist on the response induced by C5a des Arg was difficult to assess due to the weak potency of this agonist at the R206A mutant receptor. Although quoted in table 6.2, the pA_2 values for both antagonists against C5a des Arg at this receptor construct are probably incorrect due to the high degree of insurmountable antagonism and very few points on the Schild regression. Nevertheless, these data highlight that R206, located within the fifth TM of the $C5a_1$ contributes to the binding of both C5a and C5a des Arg.

Finally, the mutant $C5a_1$ receptor D282A, had a very interesting effect on both antagonists (figure 6.6 U-X). NDT9513727 produced much greater dextral shifts in the concentration curves produced by C5a (pA_2 of 8), which were almost identical to those generated against C5a des Arg (pA_2 of 8) and by C5a des Arg at the wild type construct (pA_2 of 7.7). This was in contrast to the shifts in concentration response curves induced by PMX53 at the R282A construct. PMX53 produced an identical

antagonism profile against C5a (pA_2 of 7) compared with C5a des Arg (pA_2 of 6.8) which was identical to that observed against C5a at the wild type receptor (pA_2 of 6.7), albeit with a change in the location of the C5a concentration response curve along the x-axis. The effect of mutating residue D282 therefore had the opposite effect on each antagonist. This mutation increased the apparent affinity of NDT9513727 yet reduced the affinity of PMX53. These data suggest that PMX53, unlike NDT9513727, uses the D282 residue for affinity, further suggesting that these two antagonists bind different sites on the $C5a_1$ receptor.

6.4.3. PMX53 and NDT9513727 bind the $C5a_1$ receptor in a non-competitive manner

The data from the pA_2 analyses suggest that cyclic peptide, PMX53, and the inverse agonist, NDT9513727 bind to different locations on the $C5a_1$ receptor. To test this hypothesis, a $C5a_1$ receptor competition binding assay using a tritiated analogue of PMX53 as the tracer ligand was employed. PMX53 displaced a K_d concentration ^{3}H-cyclic peptide analogue from the $C5a_1$ receptor in a monophasic manner with an IC_{50} of 12 nM (figure 6.7). This was in complete contrast to NDT9513727 which failed to inhibit the binding of the ^{3}H-cyclic peptide to the $C5a_1$ receptor at concentrations up to 10 µM. Although C5a displayed a greater affinity than PMX53 for the $C5a_1$ receptor (IC_{50} of 5 nM), at plateau, it was only able to able to inhibit the binding of the ^{3}H-cyclic peptide by 50%. A similar observation was made with C5a des Arg. As well as a reduced affinity (IC_{50} of 300 nM), C5a des Arg also displayed a shallow binding slope.

6.4.4. C5a des Arg does not induce G-protein bias of the $C5a_1$ receptor

To understand whether the different interactions of C5a and C5a des Arg at the $C5a_1$ receptor leads to a differences in receptor conformation and selective pathway stimulation, agonist induced G-protein activation was assessed using the BioSens-

All™ platform offered by Domain Therapeutics. Using the wild type $C5a_1$ receptor, initial experiments investigated the ability of C5a and C5a des Arg to activate the $G_{\alpha i2}$, $G_{\alpha o}$, $G_{\alpha 16}$ or β-arrestin 2 biosensors at 10 and 60 minutes. At both time points, C5a des Arg was as efficacious as C5a at each of the G_{α}-protein biosensors (figure 6.8 A-F). At the shorter assay time point, C5a produced EC_{50} values of between 50-100 pM at each of the G_{α}-protein biosensor which was approximately five fold more potent than C5a des Arg in each assay. However, at the longer assay incubation time, C5a displayed a reduced EC_{50} at each G_{α}-protein biosensor, becoming only two fold more potent than C5a des Arg (figure 6.9).

These data are in substantial contrast to those obtained with the β-arrestin 2 biosensor (figure 6.8 G&H). At both early and late time points, C5a des Arg achieved a maximal response that was only 50% of the maximal response produced by C5a. In addition, C5a des Arg displayed a reduced potency (10-20 fold) compared with C5a (figure 6.9). These data are in accordance with those generated in CHO cells using the DiscoverX PathHunter® assay technology and demonstrate that C5a des Arg displays a consistent bias away from recruiting β-arrestin to the $C5a_1$ receptor which is not due to assay kinetics.

In response to these data, a further experiment using the BioSens-All™ platform was performed to investigate the contribution of β-arrestins to the G_{α}-protein responses. As can be seen in figure 6.10, both $G_{\alpha i2}$ and $G_{\alpha 16}$ responses, induced by an EC_{50} concentration of C5a in wild type cells expressing both β-arrestin 1 and 2, decline over time. This decline in biosensor response diminishes with the double knock out of both β-arrestins. Interestingly C5a des Arg produces stable $G_{\alpha i2}$ and $G_{\alpha 16}$ response in both the presence and absence of β-arrestins. These data further confirm the reduced ability of C5a des Arg to promote β-arrestin recruitment to the $C5a_1$ receptor.

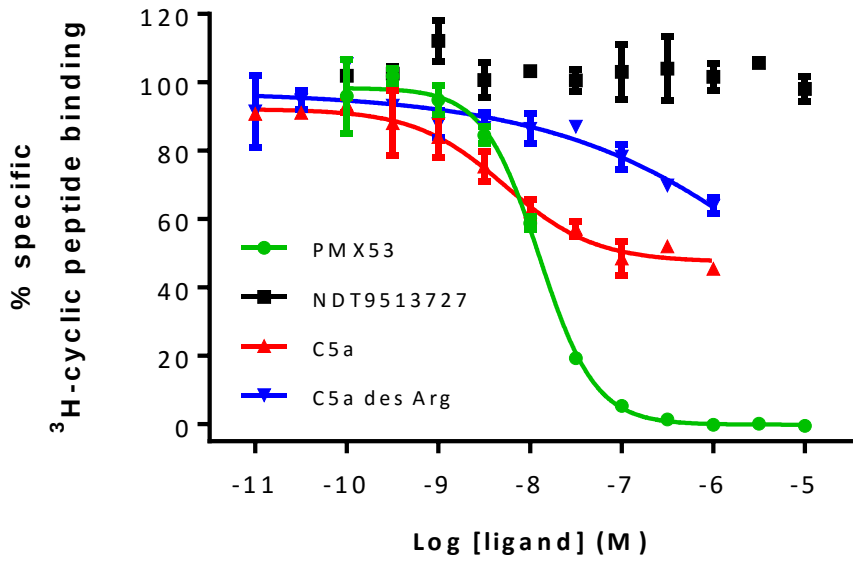

Figure 6.7 PMX53 and NDT9513727 bind separate sites on the $C5a_1$ receptor

Competition binding between human purified C5a, C5a des Arg, PMX53 or NDT9513727 and a ^{3}H-analogue of PMX53. Each ligand was tested against a K_d concentration of the ^{3}H-analogue of PMX53. Data points represent mean and S.D. from two replicates. Data are representative of two separate experiments.

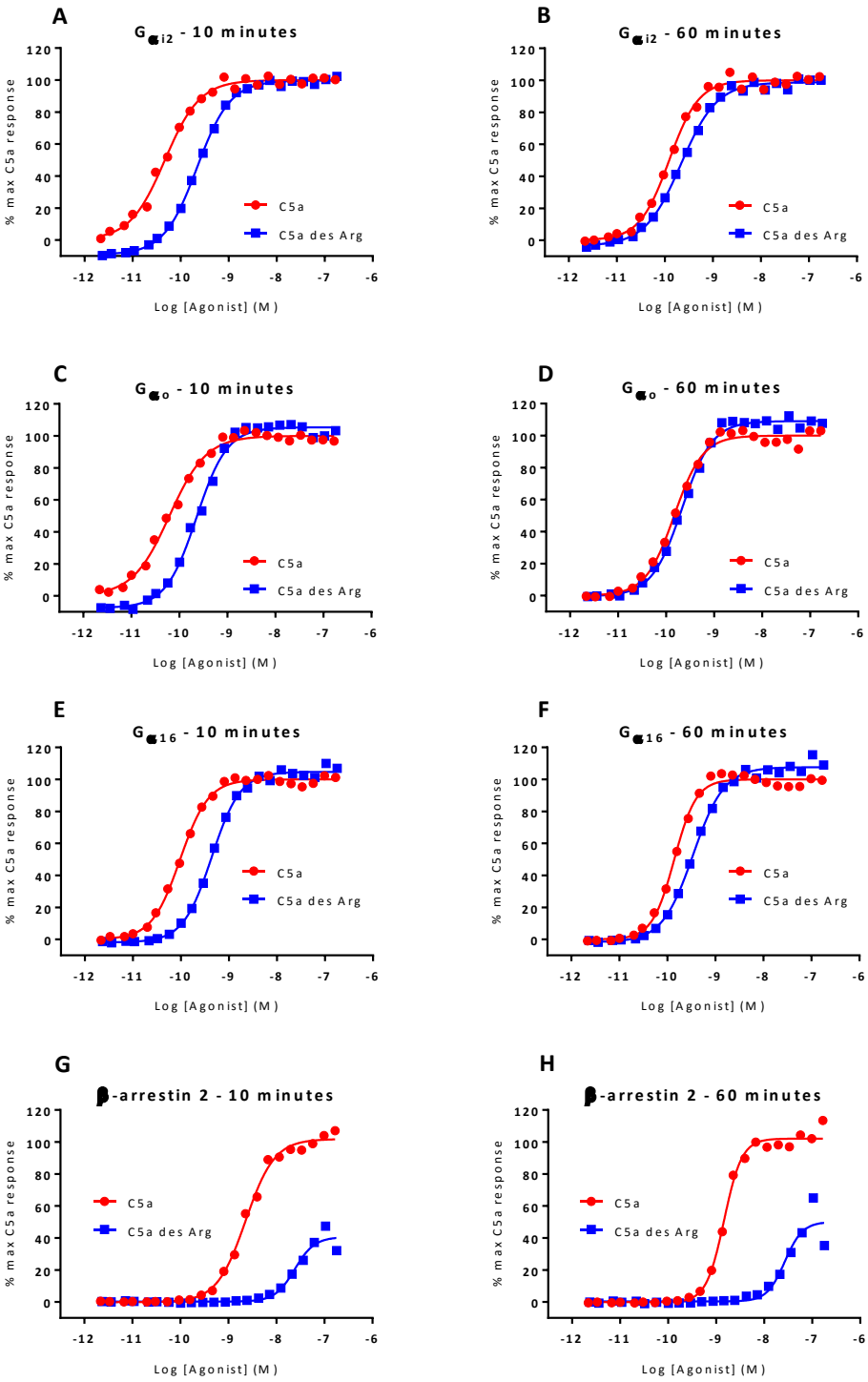

Figure 6.8. G-protein and β-arrestin signalling signatures of C5a and C5a des Arg

Activation and recruitment of G-protein and β-arrestin biosensors at the human wild type $C5a_1$ receptor by human purified C5a and C5a des Arg using the BioSens-All™ platform offered by Domain Therapeutics. Activation of $G_{\alpha i2}$ (A-B), $G_{\alpha o}$ (C-D), $G_{\alpha 16}$ (E-F) and recruitment of β-arrestin (G-H) was assessed at 10 and 60 minutes. Data points are single replicates. Data are representative of two experiments.

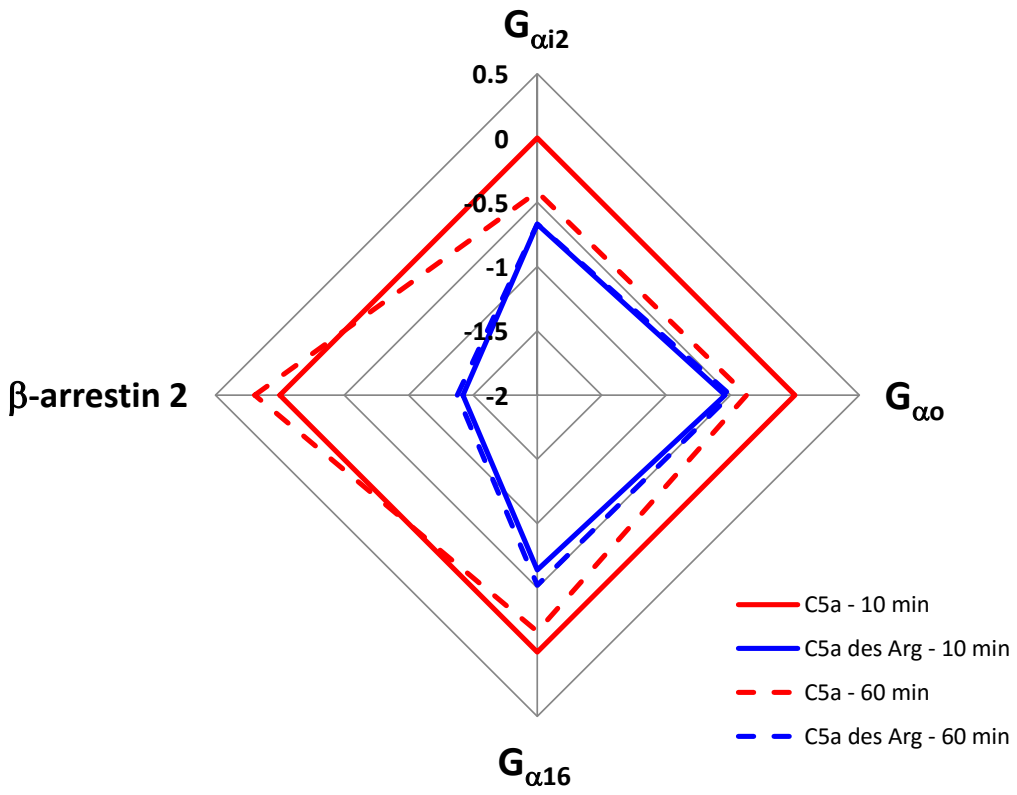

Figure 6.9. The relative G-protein and β-arrestin activity of C5a and C5a des Arg

A radar plot showing the relative activity of C5a des Arg (blue line) to C5a (red line) at inducing G-protein activation or β-arrestin recruitment via the human wild type $C5a_1$ receptor. Solid line represents response at 10 minutes, dashed line represents response at 60 minutes. Relative agonist activity was calculated using the $\Delta Log(E_{max}/EC_{50})$ transformation. All agonist responses were compared to C5a at 10 minutes.

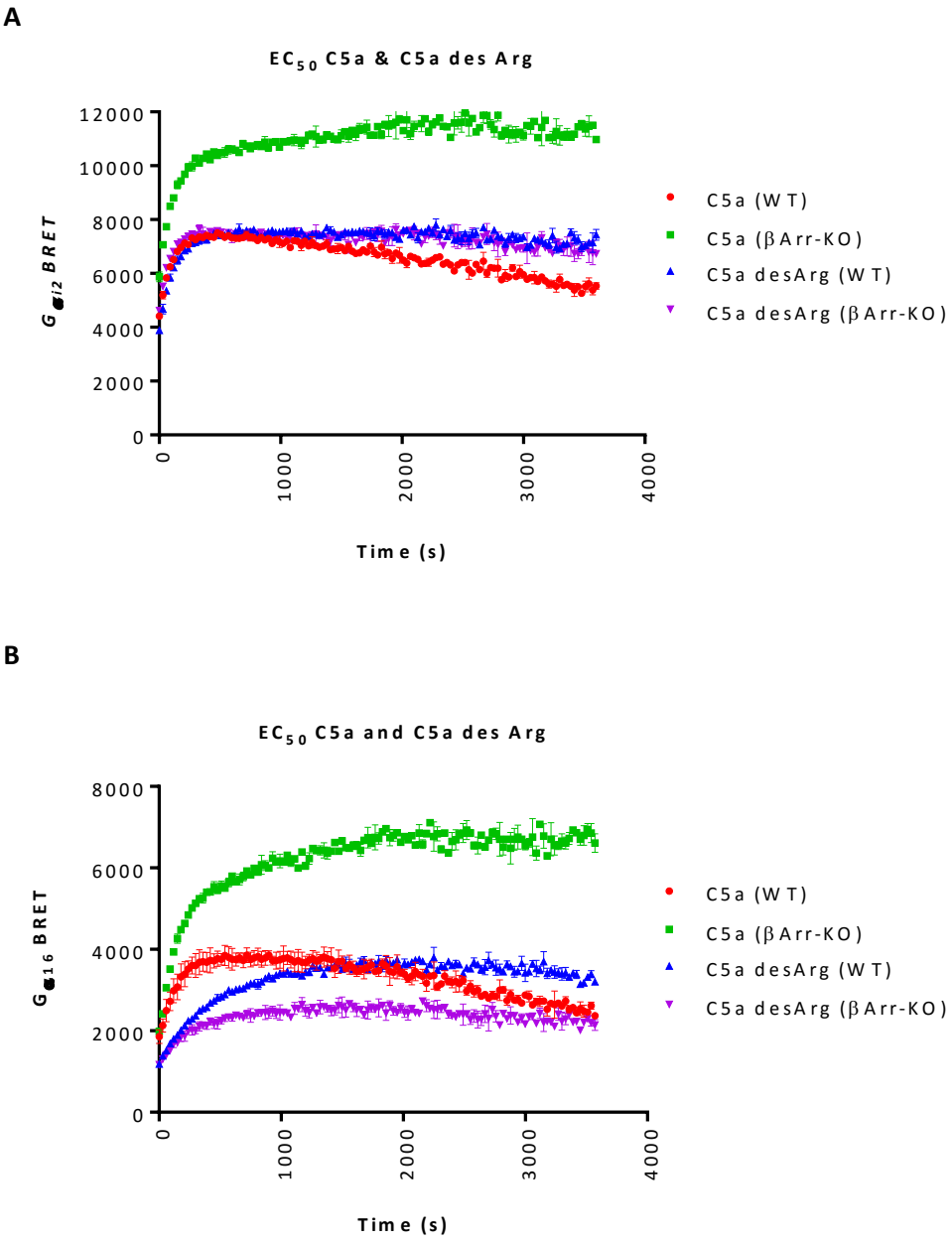

Figure 6.10. C5a induced desensitization of the G_{α}-protein biosensor response is β-arrestin dependent

Time dependent activation of the $G_{\alpha i2}$ (A) and $G_{\alpha i16}$ (B) biosensors by human purified C5a and C5a des Arg using the BioSens-All™ platform. Response assessed in cells expressing the human wild type $C5a_1$ receptor with or without endogenous β-arrestin 1 and 2. Each agonist was tested at an EC50 concentration defined at 10 minutes. Data points represent mean and S.D. from two replicates. Data are representative of two separate experiments.

6.5. Discussion

The main objective of the research outlined in this chapter was to elucidate the mechanism by which C5a des Arg produces its biased agonism response at the $C5a_1$ receptor. Two potential mechanisms were proposed. 1). C5a des Arg binds to the $C5a_1$ receptor in such a way that it induces a conformation that only allows the recruitment of certain intracellular proteins and specific pathway activation, or 2). loss of key electrostatic interactions between C5a des Arg and the $C5a_1$ receptor reduces its affinity and alters the kinetics of the C5a des Arg induced response.

By performing receptor mutagenesis coupled with a cell based calcium mobilization assay, key electrostatic interactions between charged amino acid residues within the TM region of the $C5a_1$ receptor and the two agonist peptides were detected. It was observed that the C-terminal arginine of C5a, which is missing from C5a des Arg, forms a strong electrostatic interaction with D282 on the $C5a_1$ receptor, a finding originally discovered by Cain *et al.* (2001). Receptor mutagenesis also highlighted the importance of a cluster of residues at the top of TM4 and 5, specifically R175, E199 and R206. When mutated to alanine, these residues appeared to have a mild to moderate impact on the potency of C5a but had a profound impact of the potency of C5a des Arg. Although similar to the results observed by Higginbottom *et al.* (2005), who demonstrated that mutation of these residues prevented any RBL cell degranulation induced by C5a des Arg, they observed that mutation of these residues did have a noticeable impact on the potency of C5a. These differences could in part be due to the probable high receptor reserve in the CHO cells that were used in this research, brought about by the over expression of both receptor and calcium mobilization promoting G-proteins. It could also be due to the differences in cellular endpoints that were investigated.

Subsequent pA_2 analyses using the cyclic peptide antagonist PMX53 and the inverse agonist NDT9513727 confirmed the importance of the electrostatic interaction between the arginine of C5a and D282 on the $C5a_1$ receptor. These analyses also highlighted that the C5a does in fact depend on the R175, E199 and R206 cluster of residues for affinity but not to the same degree as C5a des Arg (figure 6.11).

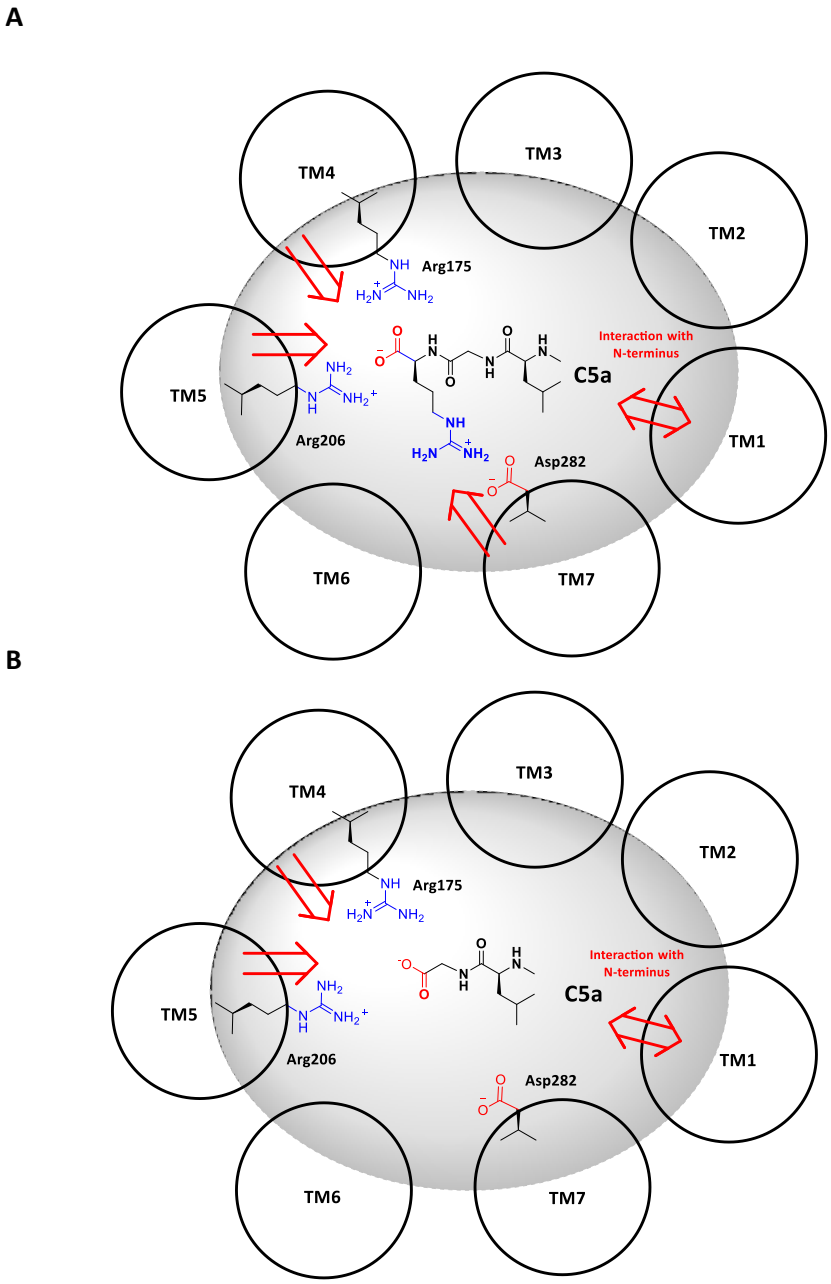

Figure 6.11. Apparent electrostatic interactions between the C5a peptide agonists and the $C5a_1$ receptor

Both C5a and C5a des Arg rely on electrostatic interactions with specific charged amino acid residues within the transmembrane (TM) region of the $C5a_1$ receptor for affinity and efficacy. The arginine of C5a interacts with aspartic acid 282 (Asp282), within the seventh TM domain (A). Both C5a and C5a des Arg interact with arginine 175 (Arg175) arginine 206 (Arg206) and glutamic acid 199 (Glu199 – residue not shown) (B).

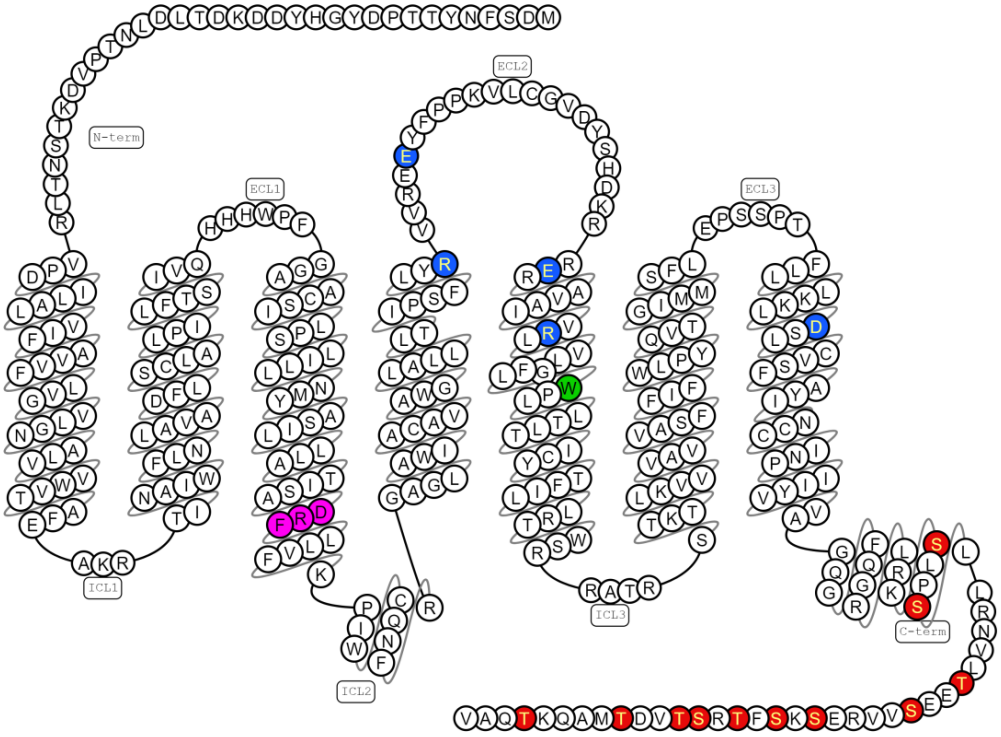

Figure 6.12. Snake plot of the $C5a_1$ receptor

Snake plot detailing the 350 amino acids that form the human $C5a_1$ receptor. Image highlights the residues that are critical for G-protein binding (pink), residues that were mutated in this thesis (blue), the serine and threonine residues that are candidates for phosphorylation by G-protein coupled receptor kinases (red) and the tryptophan residue essential for small molecule antagonist affinity (green). Image taken from www.gpcrdb.org (Isberg *et al.*, 2016).

Surprisingly, the pA_2 analyses also demonstrated that each antagonist displayed a differential capability of antagonizing either C5a or C5a des Arg, essentially giving each antagonist two different affinities depending on which agonist was used to characterize it.

With C5a and C5a des Arg relying on different receptor residues for affinity to varying degrees, it seemed plausible that each agonist may promote a different receptor conformation resulting in the differential activation of intracellular proteins, particularly G-proteins. Using the BioSens-All™ platform it was observed that C5a des Arg could induce the activation of the same set of G- proteins as C5a, with similar magnitude and potency. However, this was not the case with β-arrestin. C5a des Arg displayed weak partial agonism at promoting the recruitment of this protein to the $C5a_1$ receptor compared with C5a. The reduced ability of C5a des Arg to promote receptor recruitment of β-arrestin was further demonstrated in time course studies using cells where the arrestin proteins were knocked out. Unlike C5a, which induced a β-arrestin dependent desensitization of the G-protein biosensor response, the G-protein responses produced by C5a des were stable over time, in either the absence or presence of β-arrestin.

GPCRs recruit β-arrestin proteins upon phosphorylation of their intracellular domains by G-protein coupled receptor kinases (GRKs). This family of kinases, which includes seven members (GRK 1-7), specifically phosphorylate serine and threonine residues within the C-terminus of the receptor after activation. Different GRKs are thought to phosphorylate different serine and threonine residues on a receptor, which, is in part, considered to be regulated by the active conformational state of the receptor. This can therefore result in unique phosphorylation patterns, or barcodes, of the receptors C-terminus (Nobles *et al.*, 2011). The $C5a_1$ receptor contains 11 serine and threonine residues within its C-terminus (figure 6.12). It is, therefore, possible that the conformation of the $C5a_1$ receptor, induced by C5a des Arg, results in either the recruitment of certain GRKs that produce a different phosphorylation barcode to the one induced by C5a, or fails to recruit GRKs to the receptor at all. This latter hypothesis seems plausible, especially considering C5a des Arg does not interact with TM 7, at the tail end of which are the sites to which β-arrestin is recruited. In either

case, the actions of C5a des Arg do not lead to β-arrestin recruitment to the $C5a_1$ receptor.

Finally, using the ^{3}H-cyclic peptide competition binding assay, it was discovered that the two antagonists, PMX53 and NDT9513727, used in the pA_2 analyses bind to different locations on the $C5a_1$ receptor. This finding is in accordance with the observation set out by Waters *et al.* (2005), who demonstrated that traditional small molecules of the $C5a_1$ receptor, rely of a tryptophan residue at position 213. Based on the high lipophilicity of these small molecules, it is probable that this residue and associated binding pocket are orientated away from the hydrophilic binding pocket of C5a, where PMX53 binds, and towards the lipophilic cell membrane.

In summary, the data presented in this chapter demonstrate that key electrostatic interactions with amino acid residues in the TM region of the $C5a_1$ receptor control the affinity and efficacy of C5a and C5a des Arg. Although both peptide agonists display the same G-protein activation signature, C5a des Arg does not promote the recruitment of β-arrestin to the $C5a_1$ receptor or subsequently induce receptor desensitization. Therefore the biased agonism profile induced by C5a des Arg is probably due to both its reduced affinity for the $C5a_1$ receptor and its ability to promote a different receptor conformation to the one induced by C5a.

Chapter 7

Final discussion

7.1. Final discussion

The complement system forms an essential component of the immune system that protects multicellular organisms from microbial invasion. This complex network of soluble and membrane bound proteins orchestrates a fast and localized immune response, that is able to distinguish between host and pathogenic surfaces. However, dysregulation of the complement system can lead to it actions being directed towards the host, resulting in disease. For this reason, numerous attempts have been made to therapeutically target the effector functions of the complement system. More specifically, a great deal of effort has focused on preventing the actions of the anaphylatoxin, C5a, via the $C5a_1$ receptor. However, to date no agent targeting this axis has delivered clinical efficacy in diseases associated with over activation of the complement system.

The main objective of the research conducted in this thesis was to provide a better understanding as to functions of C5a and its cleaved isoform C5a des Arg and the precise role of their two C5a receptors in controlling neutrophil function. Such information would support future research efforts to develop therapies that target this component of the complement system to treat disease.

An important observation from the results generated early on in this thesis, is that both C5a and C5a des Arg appear to have vastly different affinities for the $C5a_1$ receptor depending on the cell in which the receptor is expressed. Both peptide agonists displayed a much greater affinity for the $C5a_1$ receptor when overexpressed in immortalized cells compared with neutrophils. Having a robust understanding of the true affinity of a peptide agonist for its receptor is of paramount importance, especially when designing a competitive receptor antagonist for the receptor to which it binds. This increase in agonist affinity is probably due to the overexpressed receptors existing in a conformation which is more energetically favourable for C5a and C5a des Arg binding. The concept of receptor conformational states and their impact on agonist binding can be explained using the two-state model of agonist-receptor interaction and an understanding that G-protein coupled receptors act as allosteric vectors that transmit signals across a cell membrane. According to the law

of mass action, an agonist (A) with affinity will bind to a receptor existing in an inactive state (R) at a rate defined by an affinity constant (K_A). Once bound, the agonist will induce a change in receptor conformation, promoting a thermodynamically distinct receptor state or active receptor state (AR*). This active receptor will now interact with intracellular G-proteins and β-arrestins subsequently activating intracellular signalling pathways (figure 4.11A) (Bridges *et al.*, 2008; Kenakin, 2012). This change in reactivity at the intracellular site of the receptor caused by energy imparted by an agonist binding to the extracellular site of the receptor is referred to as protein allosterism (Kenakin, 2009b). In this case, the receptor acts as a conduit, allowing the transfer of energy between a modulator (agonist) and a guest (G-protein or β-arrestin). This allosteric transfer of energy is considered to be bi-directional where the intracellular proteins that interact with the receptor become the modulator and the agonist becomes the guest (figure 7.1). Both the CHO cell expressing the $C5a_1$ receptor and the U2OS cell expressing the $C5a_2$ receptor were also engineered to over-express intracellular signalling proteins, $G_{\alpha 16}$ and β-arrestin-2 respectively. It is therefore probable that the overexpression of these intracellular proteins, coupled with over-expression of each receptor, artificially enhanced the active state of each receptor, a conformational state that C5a and C5a des Arg promote and one that they have increased affinity for.

One of the key objectives of this research was to shed light on the precise function of the $C5a_2$ receptor. This receptor has received much attention since its discovery 15 years ago but the role it plays in controlling the actions of C5a and C5a des Arg still remains largely enigmatic. In contrast to the observations made by Bamberg *et al.* (2010), I demonstrated that the $C5a_2$ receptor is expressed on the surface of the non-activated human neutrophils. However, although the role of this receptor in C5a and C5a des Arg mediated neutrophil responses was assessed using a validated receptor neutralizing antibody, it did not appear to contribute directly to any of the functional responses investigated. The only significant finding that was made regarding this receptor was that it appears to be removed from the surface of a neutrophil upon activation by inflammatory agents including TNFα, C5a and C5a des Arg.

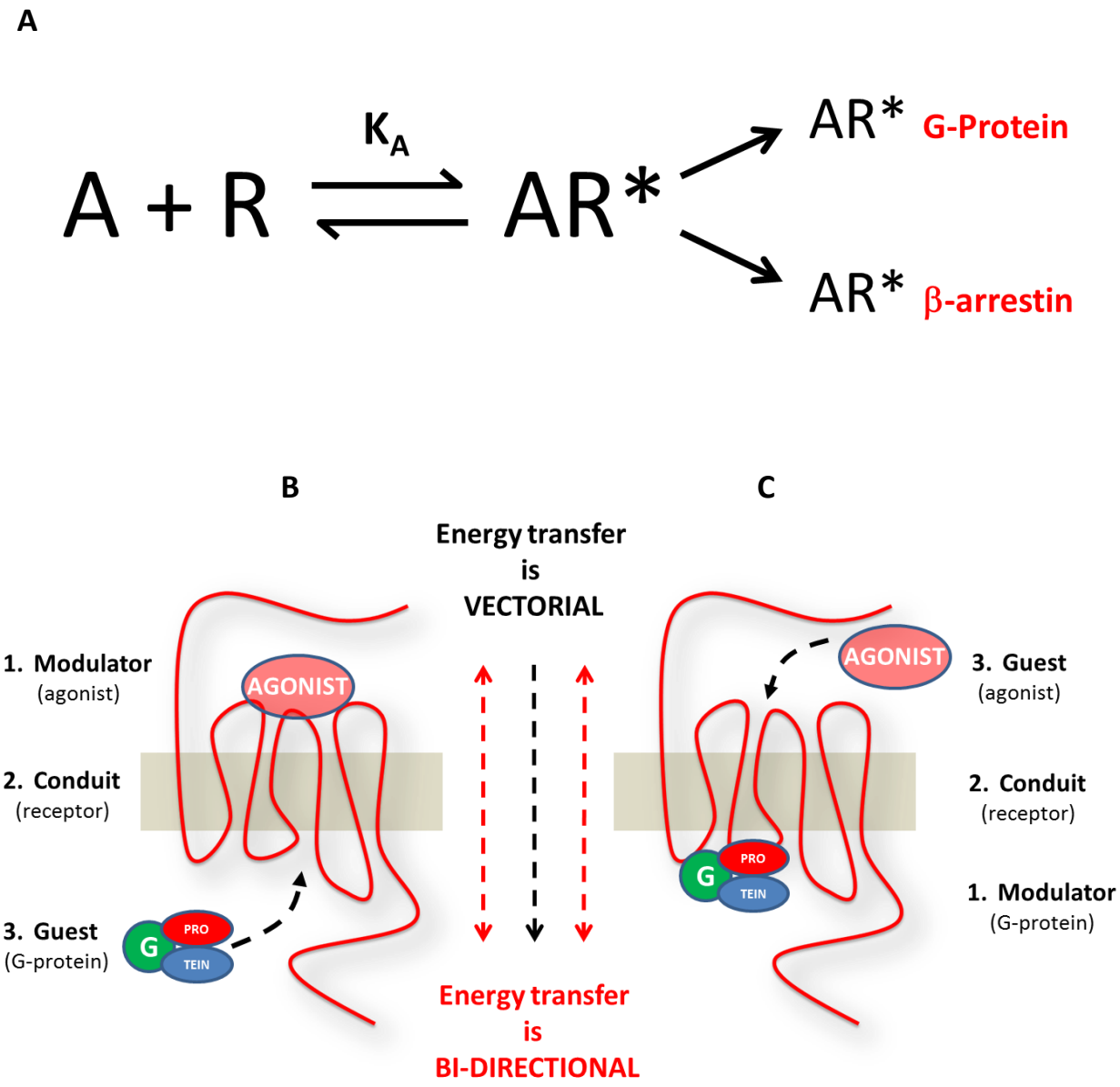

Figure 7.1. Intracellular pathway proteins and their impact on the affinity of receptor agonists

According to the 'two-state' model of agonist-receptor interactions, an agonist (A) will bind to an inactive state receptor (R) at a rate defined by an affinity constant (K_A). Once bound, the agonist will induce and conformational change in the receptor promoting an active state (AR*), which will interact with G-proteins and other proteins which subsequently activate intracellular signalling pathways (A). This flow of energy from the agonist (modulator) through the receptor (conduit) to the intracellular G-proteins (guest) is bi-directional (B). The intracellular proteins can act as the modulator, transferring energy through the conduit and inducing an active-state receptor, a state to which the guest agonist displays higher affinity for (C).

This observation may support the hypothesis set out by Scola *et al.* (2009) who claimed that the $C5a_2$ receptor serves as a recycling decoy receptor to remove extracellular C5a des Arg.

A significant amount of the research within this thesis focused on understanding how much of the functional activity of C5a is retained by C5a des Arg. By testing both peptide agonists in a range of functional cell based assays, it became apparent that C5a des Arg displays biased agonism in the favour of promoting cellular phenotypes that enhance immune cell extravasation toward sites of infection. However, its ability to induce cellular responses associated with microbial clearance and destruction, such as neutrophil respiratory burst, are significantly impaired. Although the biased response induced by C5a des Arg does not appear to be caused by the selective activation of specific G-proteins downstream of the $C5a_1$ receptor, it may in part, be due to its inability to promote the recruitment of β-arrestins to the $C5a_1$ receptor. Failure to recruit β-arrestins prevents these proteins from fulfilling their receptor desensitizing function which was observed using the BioSens-All™ platform. This result supports the observations from neutrophil chemotaxis experiments where, unlike C5a, C5a des Arg failed to produce the typical, 'bell-shaped', chemotactic response, a response often observed to chemokines. Instead, C5a des Arg's neutrophil chemotaxis profile is sustained and supports earlier observations made by Fernandez *et al.* (1978b) who demonstrated that C5a des Arg is able to recruit a greater number of human neutrophils compared with C5a.

Although C5a des Arg does not appear to induce a selective conformation of the $C5a_1$ receptor with respect to G-protein activation, it is possible that it does so with respect to the recruitment of β-arrestins. The only difference between C5a and C5a des Arg is a C-terminal arginine which was shown to electrostatically interact with Asp-282 that lies within the seventh TM domain of the $C5a_1$ receptor. It is therefore reasonable to suggest that the lack of interaction between C5a des Arg and this amino acid residue minimizes the movement of this part of the receptor. This in turn may prevent the exposure of the receptors C-terminus, that lies at the bottom of this TM domain, to GRKs which would normally phosphorylate it and promote the recruitment of β-arrestins. Further work is required to test this hypothesis.

Another objective of this research was to understand the precise contribution of C5a to the neutrophil respiratory burst response. It is often cited that C5a mediates this neutrophil response via the $C5a_1$ receptor, which serves to destroy pathogenic microbes via the generation of HOCl. Data presented here strongly suggest that C5a alone cannot produce the complete HOCl mediated respiratory response. For this to occur, neutrophils require a prime to generate the precursor to HOCl, H_2O_2. In the case of experiments described here, this prime was induced by TNFα which, via the TNFR1 presumably activates NOX_2 to generate $O_2^{\bullet-}$, which is converted to H_2O_2 by SOD. The contribution of C5a to the respiratory burst response is therefore needed to promote the release of MPO from intracellular vesicles which, in a chlorine dependent manner, generates the powerful oxidizing agent HOCl from H_2O_2.

Taken together, the results presented in this thesis suggests that a host protective mechanism has been evolutionary designed into the chemotactic capacity of the complement system. C5a, which is continually produced by complement activation at the site of infection, permeates toward blood vessels where quiescent cells of the innate immune system circulate the body. Due to the rapid actions of carboxypeptidases, the majority of this permeating trail of complement ligand is in the form of C5a des Arg. Retaining immune cell extravasation properties, but devoid of respiratory burst activity, C5a des Arg induces the long range chemotaxis of neutrophils along its gradient without promoting the release of bactericide agents. Upon approaching the epicentre of the infection, newly produced C5a hones the accuracy of cellular migration by desensitizing the chemotaxis response. Once primed with the local production of TNFα by resident macrophages, C5a promotes the destruction of the microbial infection by stimulating the neutrophil respiratory burst response. This dual mechanism required for respiratory burst focuses the release of bactericide agents at the site of infection and not along the migratory path, which if allowed to do so, would lead to tissue damage and disease. Furthermore, the apparent switching of receptor emphasis from $C5a_1$ to FPR1 by locally produced TNFα and C5a, may promote neutrophils to focus their efforts on removing host cells which have been damaged by local inflammation. Upon

inflammation induced necrosis, host cells can release DAMPs in the form of N-formyl peptides which activate the FPR1.

An overarching goal of this project was to improve the understanding of the function of the C5a/C5a des Arg-$C5a_1$ receptor axis. This in turn will support future drug discovery efforts that target this axis to treat complement associated diseases. Similar to the attempt made by Teva Pharmaceuticals Ltd, who tested the $C5a_1$ receptor cyclic peptide antagonist PMX53 in a clinical trial for RA. Unfortunately PMX53 did not show any benefit in this patient population and the sponsors of this study concluded that antagonism of the $C5a_1$ receptor does not result in reduced synovial inflammation in RA patients (Vergunst *et al.*, 2007). However, on closer inspection of the reported clinical data, it appears that this study did not adequately test the hypothesis that antagonizing the $C5a_1$ receptor would ameliorate joint inflammation associated with RA. In the published report of the findings from this study (Vergunst *et al.*, 2007), pharmacokinetic analysis of the once daily dose of PMX53 (8 mg/kg) produced a mean AUC of 40.8 nmol h/L. This concentration is four times higher than the 10 nmol h/L that they determined from *in vitro* experimentation would be sufficient to antagonise C5a at the $C5a_1$ receptor. However, the mean AUC value relates to the total exposure achieved over the 24 hour dosing interval and not the drug exposure at any one moment in time. From a crude conversion of the AUC to average exposure, the total plasma concentration of PMX53 equates to 1.7 nmol/L which is approximately 6 fold lower than the concentration required to sufficiently antagonise C5a at the $C5a_1$ receptor. The poor systemic exposure from such a dose of PMX53 was probably due to the low oral bioavailability, which from rat pharmacokinetic analysis appears to be less than 1% (Morgan *et al.*, 2008).

It therefore appears that the PMX53 clinical trial failed because fundamental pharmacokinetic and pharmacodynamic principles were not met; that is, sufficient exposure at target site of action, sufficient target binding and evidence of functional pharmacological activity (Morgan *et al.*, 2012). It is often stated that greater than 80% antagonist receptor occupancy is required to sufficiently block the effects of an agonist at a receptor (Bot *et al.*, 2017). As stated by the law of mass action, the

occupancy of a receptor by a ligand is proportional to the concentration and affinity of that ligand and can be calculated using equation 7.1. For example, using the concentration of C5a that was detected in the joints of RA patients by (Jose *et al.*, 1990) of 2 nM and the affinity of C5a at the human neutrophil $C5a_1$ receptor determined in Chapter 4 of 0.2 nM, the percentage of $C5a_1$ receptors occupied by C5a is 90%.

To determine the concentration of a competitive receptor antagonist, such as PMX53, required to reduce this agonist occupancy to 10%, the equation first described by Sir John Henry Gaddum can be used (Gaddum *et al.*, 1955) (equation 7.2). Taking the estimate of affinity for PMX53 derived in chapter 3 of 10 nM, it is not until a concentration of 1 μM PMX53 is achieved that the $C5a_1$ receptor occupancy by C5a is reduced to approximately 10%. This concentration is approximately 600 fold greater than that achieved in the PMX53 clinical trial.

The above equations assume that the functional response induced by C5a is proportional to its receptor occupancy. However, for most agonist-receptor interactions this is not the case. In fact, agonists often achieve their maximal response when they occupy only a small proportion of the receptor population. This phenomenon is known as receptor reserve (Grimwood *et al.*, 2009) and is brought about by both attributes of the agonist ligand and the system in which the agonist is tested. As well as affinity for a receptor, agonists also possess intrinsic efficacy, a property which describes the degree of stimulus that an agonist provides to a receptor. The cellular expression of that receptor and the efficiency with which the receptor couples to intracellular signalling pathways determine the proportion of receptors that need to be occupied and activated to induce a maximal response. These components of intrinsic efficacy, receptor expression and receptor pathway coupling efficiency all relate to the signal transduction capacity of the agonist and receptor system and is often described by the arbitrary factor of Tau (τ), originally described by Black *et al.* (1983).

$$P_{AR} = \frac{[A]/K_A}{[A]/K_A + 1}$$

Equation 7.1. Quantifying agonist receptor occupancy.

According to mass action, agonist receptor occupancy is proportional to its concentration and affinity. P_{AR} = proportion of receptors occupied by agonist, [A] = concentration of agonist, K_A = affinity of agonist.

$$P_{AR} = \frac{[A]/K_A}{[A]/K_A + [B]/K_B + 1}$$

Equation 7.2. Quantifying competitive receptor antagonism.

Competitive antagonism described by the Gaddum equation. P_{AR} = proportion of receptors occupied by agonist in presence of antagonist. [A] = concentration of agonist, K_A = affinity of agonist, [B] = concentration of antagonist, K_B = affinity of antagonist [B].

Therefore with the knowledge obtained from the results presented in this thesis regarding the signalling capacity of C5a des Arg and the differential affinity of a competitive receptor antagonist, with assistance from Dr Terry Kenakin, I have developed a model to predict the composite response of C5a and C5a des Arg in the absence and presence of a competitive receptor antagonist (equation 7.3). Using values of agonist affinity (K_A) and efficacy (τ) derived from the fitting of the operational model of agonism to the neutrophils functional data (appendix 2), and estimates of antagonist affinity against the two agonists, the effect of different concentrations of antagonist on the composite agonist response can be simulated.

A simulation using the composite agonist response model can be seen in figure 7.3. In this simulation, values of K_A and τ were derived for both C5a and C5a des Arg from the operational model of agonism fit to the human isolated neutrophil chemotaxis data generated in chapter 5. Affinity values of a competitive receptor antagonist were chosen so that the antagonist affinity was 10 fold greater against C5a des Arg than C5a (1 and 10 nM respectively), as observed in chapter 6. Concentrations of C5a and C5a des Arg were set at 1 and 4 nM respectively so that C5a equated to 20% of the total peptide ligand concentration. The simulations predict that C5a and C5a des Arg will produce a fractional composite chemotaxis response of 0.76 in the absence of a competitive antagonist. In the presence of 10 nM of a competitive receptor antagonist, the fractional composite chemotaxis response is only reduced to 0.75. Increasing the antagonist concentration to 100 nM further reduced the composite response to 0.53, but it is not until a concentration of 1 μM of antagonist is used, which is 100 and 1000 fold the C5a and C5a des Arg affinity respectively, that the composite chemotaxis response is reduced to approximately 0.1. These simulations, using the composite agonist response model, further suggest that the clinical exposures of PMX53 in the RA trial were not high enough to sufficiently antagonise the actions of C5a and C5a des Arg at the $C5a_1$ receptor.

The main aim of the research outlined in this thesis was to improve the understanding of the precise role of the Complement System peptide ligands C5a and C5a des Arg and their receptors, $C5a_1$ and $C5a_2$, in orchestrating neutrophil responses. Although this research was unable to shed further light on the precise function of the $C5a_2$ receptor, it did demonstrate that this receptor does not appear to regulate C5a mediated adhesion molecule expression, chemotaxis or respiratory burst responses in the human isolated neutrophil. This research did determine the precise contribution of C5a-$C5a_1$ receptor axis to the neutrophil respiratory burst response and the requirement of a neutrophil prime via the TNFR1 to induce a full respiratory burst response. It also demonstrated that the cleaved C5a peptide fragment, C5a des Arg, retains a significant degree of functional activity which appears to be aligned to the orchestration of immune cell extravasation. The biased agonist profile of C5a des Arg is due to its lack of interaction with the seventh transmembrane domain of the $C5a_1$ receptor, which promotes a receptor conformation that displays a reduced interaction with β-arrestin 2. Lastly, the results presented in this thesis have supported the development of a composite agonist model, that will enable the selection of more appropriate doses of competitive $C5a_1$ receptor antagonists to treat diseases associated with over activation of the complement system.

$$\text{Composite response} = \frac{([C_{5a}]/(K_{A\text{-}C5a}([B]/K_{B\text{-}C5a}+1)))\,\tau_{C5a} + ([C_{5a\text{-}dA}]/(K_{A\text{-}C5a\text{-}dA}([B]/K_{B\text{-}C5a\text{-}dA}+1)))\,\tau_{C5a\text{-}dA}}{([C_{5a}]/(K_{A\text{-}C5a}([B]/K_{B\text{-}C5a}+1)))(\tau_{C5a}+1) + ([C_{5a\text{-}dA}]/(K_{A\text{-}C5a\text{-}dA}([B]/K_{B\text{-}C5a\text{-}dA}+1)))(\tau_{C5a\text{-}dA}+1) + 1}$$

Equation 7.3. Model to predict a composite agonist response

[C5a] = concentration of C5a, K_{C5a} = K_A of C5a, τ_{C5a} = efficacy of C5a in a test system, [C5a-dA] = concentration of C5a des Arg, $K_{C5a\text{-}dA}$ = K_A of C5a, $\tau_{C5a\text{-}dA}$ = efficacy of C5a des Arg in a test system, [B] = concentration of antagonist, $K_{B\text{-}C5a}$ = affinity of antagonist for blocking C5a response, $K_{B\text{-}C5a\text{-}dA}$ = affinity of antagonist for blocking C5a des Arg response.

C_{5a}	
τ_{C5a}	**8**
K_{C5a}=	**0.80**
$K_{B\text{-}C5a}$=	**10.00**

$C_{5a\text{-}dA}$	
$\tau_{C5a\text{-}dA}$	**3**
$K_{C5a\text{-}dA}$=	**0.20**
$K_{B\text{-}C5a\text{-}dA}$=	**1.00**

	[C5a]	[C5a-dA]	[B]	**Fraction composite response**
1	1	4	0	**0.759**
2	1	4	10	**0.752**
3	1	4	100	**0.534**
4	1	4	1000	**0.133**

Figure 7.2. Composite agonist response model simulations

Simulation of the composite agonist response induced by C5a and C5a des Arg in the absence and presence of a competitive $C5a_1$ receptor antagonist as defined by equation 7.3. Simulations of the C5a and C5a des Arg composite response using the parameters obtained from the fitting of the operational model of agonism to the neutrophil chemotaxis data (appendix 2). All concentrations in nM.

References

Ahn S, Shenoy SK, Wei H, Lefkowitz RJ (2004). Differential kinetic and spatial patterns of beta-arrestin and G protein-mediated ERK activation by the angiotensin II receptor. *J. Biol. Chem.* **279**(34)**:** 35518-35525.

Albrich JM, Hurst JK (1982). Oxidative inactivation of Escherichia coli by hypochlorous acid. Rates and differentiation of respiratory from other reaction sites. *FEBS Lett.* **144**(1)**:** 157-161.

Alexander SP, Benson HE, Faccenda E, Pawson AJ, Sharman JL, Spedding M*, et al.* (2013). The Concise Guide to PHARMACOLOGY 2013/14: G Protein-Coupled Receptors. *Br. J. Pharmacol.* **170**(8)**:** 1459-1581.

Amara U, Flierl MA, Rittirsch D, Klos A, Chen H, Acker B*, et al.* (2010). Molecular intercommunication between the complement and coagulation systems. *J. Immunol.* **185**(9)**:** 5628-5636.

Amara U, Rittirsch D, Flierl M, Bruckner U, Klos A, Gebhard F*, et al.* (2008). Interaction between the coagulation and complement system. *Adv. Exp. Med. Biol.* **632:** 71-79.

Amatruda TT, 3rd, Gerard NP, Gerard C, Simon MI (1993). Specific interactions of chemoattractant factor receptors with G-proteins. *J. Biol. Chem.* **268**(14)**:** 10139-10144.

Asokan R, Banda NK, Szakonyi G, Chen XS, Holers VM (2013). Human complement receptor 2 (CR2/CD21) as a receptor for DNA: implications for its roles in the immune response and the pathogenesis of systemic lupus erythematosus (SLE). *Mol. Immunol.* **53**(1-2)**:** 99-110.

Azzi M, Pineyro G, Pontier S, Parent S, Ansanay H, Bouvier M (2001). Allosteric effects of G protein overexpression on the binding of beta-adrenergic ligands with distinct inverse efficacies. *Mol. Pharmacol.* **60**(5)**:** 999-1007.

Bajaj MS, Kew RR, Webster RO, Hyers TM (1992). Priming of human neutrophil functions by tumor necrosis factor: enhancement of superoxide anion generation, degranulation, and chemotaxis to chemoattractants C5a and F-Met-Leu-Phe. *Inflammation* **16**(3)**:** 241-250.

Bamberg CE, Mackay CR, Lee H, Zahra D, Jackson J, Lim YS*, et al.* (2010). The C5a receptor (C5aR) C5L2 is a modulator of C5aR-mediated signal transduction. *J. Biol. Chem.* **285**(10)**:** 7633-7644.

Barczyk M, Carracedo S, Gullberg D (2010). Integrins. *Cell Tissue Res.* **339**(1)**:** 269-280.

Bekker P, Dairaghi D, Seitz L, Leleti M, Wang Y, Ertl L*, et al.* (2016). Characterization of Pharmacologic and Pharmacokinetic Properties of CCX168, a Potent and Selective Orally Administered Complement 5a Receptor Inhibitor, Based on Preclinical Evaluation and Randomized Phase 1 Clinical Study. *PLoS One* **11**(10)**:** e0164646.

Bienaime F, Dragon-Durey MA, Regnier CH, Nilsson SC, Kwan WH, Blouin J*, et al.* (2010). Mutations in components of complement influence the outcome of Factor I-associated atypical hemolytic uremic syndrome. *Kidney Int.* **77**(4)**:** 339-349.

Black JW, Leff P (1983). Operational models of pharmacological agonism. *Proc. R. Soc. Lond. B. Biol. Sci.* **220**(1219)**:** 141-162.

Blanc C, Roumenina LT, Ashraf Y, Hyvarinen S, Sethi SK, Ranchin B*, et al.* (2012). Overall neutralization of complement factor H by autoantibodies in the acute phase of the autoimmune form of atypical hemolytic uremic syndrome. *J. Immunol.* **189**(7)**:** 3528-3537.

Bland EJ, Keshavarz T, Bucke C (2001). Using 2', 7'-dichlorodihydrofluorescein-diacetate to assess polysaccharides as immunomodulating agents. *Mol. Biotechnol.* **19**(2)**:** 125-131.

Blom AM, Villoutreix BO, Dahlback B (2004). Complement inhibitor C4b-binding protein-friend or foe in the innate immune system? *Mol. Immunol.* **40**(18)**:** 1333-1346.

Bokisch VA, Muller-Eberhard HJ (1970). Anaphylatoxin inactivator of human plasma: its isolation and characterization as a carboxypeptidase. *J. Clin. Invest.* **49**(12)**:** 2427-2436.

Bot I, Ortiz Zacarias NV, de Witte WE, de Vries H, van Santbrink PJ, van der Velden D*, et al.* (2017). A novel CCR2 antagonist inhibits atherogenesis in apoE deficient mice by achieving high receptor occupancy. *Sci. Rep.* **7**(1)**:** 52.

Boulay F, Mery L, Tardif M, Brouchon L, Vignais P (1991). Expression cloning of a receptor for C5a anaphylatoxin on differentiated HL-60 cells. *Biochemistry* **30**(12)**:** 2993-2999.

Bridges TM, Lindsley CW (2008). G-protein-coupled receptors: from classical modes of modulation to allosteric mechanisms. *ACS Chem. Biol.* **3**(9)**:** 530-541.

Brodbeck RM, Cortright DN, Kieltyka AP, Yu J, Baltazar CO, Buck ME*, et al.* (2008). Identification and characterization of NDT 9513727 [N,N-bis(1,3-benzodioxol-5-ylmethyl)-1-butyl-2,4-diphenyl-1H-imidazole-5-methanam ine], a novel, orally bioavailable C5a receptor inverse agonist. *J. Pharmacol. Exp. Ther.* **327**(3)**:** 898-909.

Buhl AM, Eisfelder BJ, Worthen GS, Johnson GL, Russell M (1993). Selective coupling of the human anaphylatoxin C5a receptor and alpha 16 in human kidney 293 cells. *FEBS Lett.* **323**(1-2)**:** 132-134.

Cain SA, Coughlan T, Monk PN (2001). Mapping the ligand-binding site on the C5a receptor: arginine74 of C5a contacts aspartate282 of the C5a receptor. *Biochemistry* **40**(46)**:** 14047-14052.

Cain SA, Monk PN (2002). The orphan receptor C5L2 has high affinity binding sites for complement fragments C5a and C5a des-Arg(74). *J. Biol. Chem.* **277**(9)**:** 7165-7169.

Carugati A, Pappalardo E, Zingale LC, Cicardi M (2001). C1-inhibitor deficiency and angioedema. *Mol. Immunol.* **38**(2-3)**:** 161-173.

Chen NJ, Mirtsos C, Suh D, Lu YC, Lin WJ, McKerlie C*, et al.* (2007). C5L2 is critical for the biological activities of the anaphylatoxins C5a and C3a. *Nature* **446**(7132)**:** 203-207.

Cheng Y, Prusoff WH (1973). Relationship between the inhibition constant (K1) and the concentration of inhibitor which causes 50 per cent inhibition (I50) of an enzymatic reaction. *Biochem. Pharmacol.* **22**(23)**:** 3099-3108.

Chenoweth DE, Goodman MG (1983). The C5a receptor of neutrophils and macrophages. *Agents Actions Suppl.* **12:** 252-273.

Chenoweth DE, Hugli TE (1980). Human C5a and C5a analogs as probes of the neutrophil C5a receptor. *Mol. Immunol.* **17**(2)**:** 151-161.

Cooke R, Congreve M (2016). Allosteric binding: structures reveal new ways to tame G protein-coupled receptors. *Future Med. Chem.*

Craddock PR, Fehr J, Jacob HS (1976). Complement-mediated granulocyte dysfunction in paroxysmal nocturnal hemoglobinuria. *Blood* **47**(6)**:** 931-939.

Croker DE, Halai R, Kaeslin G, Wende E, Fehlhaber B, Klos A*, et al.* (2014). C5a2 can modulate ERK1/2 signaling in macrophages via heteromer formation with C5a1 and beta-arrestin recruitment. *Immunol. Cell Biol.* **92**(7)**:** 631-639.

Delves PJ, Roitt IM (2000). The immune system. First of two parts. *N. Engl. J. Med.* **343**(1)**:** 37-49.

DeMartino JA, Konteatis ZD, Siciliano SJ, Van Riper G, Underwood DJ, Fischer PA*, et al.* (1995). Arginine 206 of the C5a receptor is critical for ligand recognition and receptor activation by C-terminal hexapeptide analogs. *J. Biol. Chem.* **270**(27)**:** 15966-15969.

DeMartino JA, Van Riper G, Siciliano SJ, Molineaux CJ, Konteatis ZD, Rosen H*, et al.* (1994). The amino terminus of the human C5a receptor is required for high affinity C5a binding and for receptor activation by C5a but not C5a analogs. *J. Biol. Chem.* **269**(20)**:** 14446-14450.

DiScipio RG, Smith CA, Muller-Eberhard HJ, Hugli TE (1983). The activation of human complement component C5 by a fluid phase C5 convertase. *J. Biol. Chem.* **258**(17)**:** 10629-10636.

Dodds AW (2002). Which came first, the lectin/classical pathway or the alternative pathway of complement? *Immunobiology* **205**(4-5)**:** 340-354.

Dorward DA, Lucas CD, Chapman GB, Haslett C, Dhaliwal K, Rossi AG (2015). The role of formylated peptides and formyl peptide receptor 1 in governing neutrophil function during acute inflammation. *Am. J. Pathol.* **185**(5)**:** 1172-1184.

Dranoff G (2004). Cytokines in cancer pathogenesis and cancer therapy. *Nat. Rev. Cancer* **4**(1)**:** 11-22.

Dunkelberger JR, Song WC (2010). Role and mechanism of action of complement in regulating T cell immunity. *Mol. Immunol.* **47**(13)**:** 2176-2186.

Ehlert FJ (2008). On the analysis of ligand-directed signaling at G protein-coupled receptors. *Naunyn Schmiedebergs Arch. Pharmacol.* **377**(4-6)**:** 549-577.

Ember JA, Sanderson SD, Taylor SM, Kawahara M, Hugli TE (1992). Biologic activity of synthetic analogues of C5a anaphylatoxin. *J. Immunol.* **148**(10)**:** 3165-3173.

Ennis S, Jomary C, Mullins R, Cree A, Chen X, Macleod A*, et al.* (2008). Association between the SERPING1 gene and age-related macular degeneration: a two-stage case-control study. *Lancet* **372**(9652)**:** 1828-1834.

Fernandez H, Henson P, Hugli TE (1976). A Single Scheme for C3a and C5a Isolation and Characterization of Chemotactic Behavior. *The Journal of Immunology* **116**(6)**:** 1732-1732.

Fernandez HN, Henson PM, Otani A, Hugli TE (1978a). Chemotactic response to human C3a and C5a anaphylatoxins. I. Evaluation of C3a and C5a leukotaxis in vitro and under stimulated in vivo conditions. *J. Immunol.* **120**(1)**:** 109-115.

Fernandez HN, Hugli TE (1978b). Primary structural analysis of the polypeptide portion of human C5a anaphylatoxin. Polypeptide sequence determination and assignment of the oligosaccharide attachment site in C5a. *J. Biol. Chem.* **253**(19)**:** 6955-6964.

Finch AM, Wong AK, Paczkowski NJ, Wadi SK, Craik DJ, Fairlie DP*, et al.* (1999). Low-molecular-weight peptidic and cyclic antagonists of the receptor for the complement factor C5a. *J. Med. Chem.* **42**(11)**:** 1965-1974.

Foley JH, Walton BL, Aleman MM, O'Byrne AM, Lei V, Harrasser M*, et al.* (2016). Complement Activation in Arterial and Venous Thrombosis is Mediated by Plasmin. *EBioMedicine* **5:** 175-182.

Fritsche LG, Lauer N, Hartmann A, Stippa S, Keilhauer CN, Oppermann M*, et al.* (2010). An imbalance of human complement regulatory proteins CFHR1, CFHR3 and factor H influences risk for age-related macular degeneration (AMD). *Hum. Mol. Genet.* **19**(23)**:** 4694-4704.

Gao H, Neff TA, Guo RF, Speyer CL, Sarma JV, Tomlins S*, et al.* (2005). Evidence for a functional role of the second C5a receptor C5L2. *FASEB J.* **19**(8)**:** 1003-1005.

Gerard C, Hugli TE (1981). Identification of classical anaphylatoxin as the des-Arg form of the C5a molecule: evidence of a modulator role for the oligosaccharide unit in human des-Arg74-C5a. *Proc. Natl. Acad. Sci. U. S. A.* **78**(3)**:** 1833-1837.

Gerard NP, Gerard C (1991). The chemotactic receptor for human C5a anaphylatoxin. *Nature* **349**(6310)**:** 614-617.

Gerard NP, Lu B, Liu P, Craig S, Fujiwara Y, Okinaga S*, et al.* (2005). An anti-inflammatory function for the complement anaphylatoxin C5a-binding protein, C5L2. *J. Biol. Chem.* **280**(48)**:** 39677-39680.

Gerber BO, Meng EC, Dotsch V, Baranski TJ, Bourne HR (2001). An activation switch in the ligand binding pocket of the C5a receptor. *J. Biol. Chem.* **276**(5)**:** 3394-3400.

Glass D, Raum D, Gibson D, Stillman JS, Schur PH (1976). Inherited deficiency of the second component of complement. Rheumatic disease associations. *J. Clin. Invest.* **58**(4)**:** 853-861.

Glasser L, Fiederlein RL (1990). The effect of various cell separation procedures on assays of neutrophil function. A critical appraisal. *Am. J. Clin. Pathol.* **93**(5)**:** 662-669.

Goicoechea de Jorge E, Caesar JJ, Malik TH, Patel M, Colledge M, Johnson S*, et al.* (2013). Dimerization of complement factor H-related proteins modulates complement activation in vivo. *Proc. Natl. Acad. Sci. U. S. A.* **110**(12)**:** 4685-4690.

Goicoechea de Jorge E, Harris CL, Esparza-Gordillo J, Carreras L, Arranz EA, Garrido CA*, et al.* (2007). Gain-of-function mutations in complement factor B are associated with atypical hemolytic uremic syndrome. *Proc. Natl. Acad. Sci. U. S. A.* **104**(1)**:** 240-245.

Grimwood S, Hartig PR (2009). Target site occupancy: emerging generalizations from clinical and preclinical studies. *Pharmacol. Ther.* **122**(3)**:** 281-301.

Guo RF, Ward PA (2005). Role of C5a in inflammatory responses. *Annu. Rev. Immunol.* **23:** 821-852.

Hageman GS, Anderson DH, Johnson LV, Hancox LS, Taiber AJ, Hardisty LI*, et al.* (2005). A common haplotype in the complement regulatory gene factor H (HF1/CFH) predisposes individuals to age-related macular degeneration. *Proc. Natl. Acad. Sci. U. S. A.* **102**(20)**:** 7227-7232.

Halliwell B, Clement MV, Long LH (2000). Hydrogen peroxide in the human body. *FEBS Lett.* **486**(1)**:** 10-13.

Hansen CB, Csuka D, Munthe-Fog L, Varga L, Farkas H, Hansen KM*, et al.* (2015). The Levels of the Lectin Pathway Serine Protease MASP-1 and Its Complex Formation with C1 Inhibitor Are Linked to the Severity of Hereditary Angioedema. *J. Immunol.* **195**(8)**:** 3596-3604.

Hao J, Wang C, Yuan J, Chen M, Zhao MH (2013). A pro-inflammatory role of C5L2 in C5a-primed neutrophils for ANCA-induced activation. *PLoS One* **8**(6)**:** e66305.

Harboe M, Mollnes TE (2008). The alternative complement pathway revisited. *J. Cell. Mol. Med.* **12**(4)**:** 1074-1084.

Haviland DL, McCoy RL, Whitehead WT, Akama H, Molmenti EP, Brown A*, et al.* (1995). Cellular expression of the C5a anaphylatoxin receptor (C5aR): demonstration of C5aR on nonmyeloid cells of the liver and lung. *J. Immunol.* **154**(4)**:** 1861-1869.

Hayashi F, Means TK, Luster AD (2003). Toll-like receptors stimulate human neutrophil function. *Blood* **102**(7)**:** 2660-2669.

Hellwage J, Jokiranta TS, Koistinen V, Vaarala O, Meri S, Zipfel PF (1999). Functional properties of complement factor H-related proteins FHR-3 and FHR-4: binding to the C3d region of C3b and differential regulation by heparin. *FEBS Lett.* **462**(3)**:** 345-352.

Higginbottom A, Cain SA, Woodruff TM, Proctor LM, Madala PK, Tyndall JD*, et al.* (2005). Comparative agonist/antagonist responses in mutant human C5a receptors define the ligand binding site. *J. Biol. Chem.* **280**(18)**:** 17831-17840.

Hirsch E, Katanaev VL, Garlanda C, Azzolino O, Pirola L, Silengo L*, et al.* (2000). Central role for G protein-coupled phosphoinositide 3-kinase gamma in inflammation. *Science* **287**(5455)**:** 1049-1053.

Huang H, Nguyen T, Ibrahim S, Shantharam S, Yue Z, Chen JY (2015). DMAP: a connectivity map database to enable identification of novel drug repositioning candidates. *BMC Bioinformatics* **16 Suppl 13:** S4.

Huber-Lang M, Sarma JV, Zetoune FS, Rittirsch D, Neff TA, McGuire SR*, et al.* (2006). Generation of C5a in the absence of C3: a new complement activation pathway. *Nat. Med.* **12**(6)**:** 682-687.

Huber-Lang M, Younkin EM, Sarma JV, Riedemann N, McGuire SR, Lu KT*, et al.* (2002). Generation of C5a by phagocytic cells. *Am. J. Pathol.* **161**(5)**:** 1849-1859.

Hussain A, Prasad KS, Bhattacharyya D, El-Bouri K (2007). C2 deficiency primary meningococcal arthritis of the elbow by Neisseria meningitidis serogroup Y in a 12-year old girl. *Infection* **35**(4)**:** 287-288.

Inglese J, Koch WJ, Touhara K, Lefkowitz RJ (1995). G beta gamma interactions with PH domains and Ras-MAPK signaling pathways. *Trends Biochem. Sci.* **20**(4)**:** 151-156.

Isberg V, Mordalski S, Munk C, Rataj K, Harpsoe K, Hauser AS*, et al.* (2016). GPCRdb: an information system for G protein-coupled receptors. *Nucleic Acids Res.* **44**(D1)**:** D356-364.

Jackson RL, Hirs CH (1970). The primary structure of porcine pancreatic ribonuclease. II. The amino acid sequence of the reduced S-aminoethylated protein. *J. Biol. Chem.* **245**(3)**:** 637-653.

Jagels MA, Daffern PJ, Hugli TE (2000). C3a and C5a enhance granulocyte adhesion to endothelial and epithelial cell monolayers: epithelial and endothelial priming is required for C3a-induced eosinophil adhesion. *Immunopharmacology* **46**(3)**:** 209-222.

Janeway CA, Jr. (2001). How the immune system protects the host from infection. *Microbes Infect* **3**(13)**:** 1167-1171.

Janeway CA, Jr., Medzhitov R (2002). Innate immune recognition. *Annu. Rev. Immunol.* **20:** 197-216.

Jeitner TM, Kalogiannis M, Krasnikov BF, Gomlin I, Peltier MR, Moran GR (2016). Linking Inflammation and Parkinson Disease: Hypochlorous Acid Generates Parkinsonian Poisons. *Toxicol. Sci.* **151**(2)**:** 388-402.

Johswich K, Martin M, Thalmann J, Rheinheimer C, Monk PN, Klos A (2006). Ligand specificity of the anaphylatoxin C5L2 receptor and its regulation on myeloid and epithelial cell lines. *J. Biol. Chem.* **281**(51)**:** 39088-39095.

Jose PJ, Moss IK, Maini RN, Williams TJ (1990). Measurement of the chemotactic complement fragment C5a in rheumatoid synovial fluids by radioimmunoassay: role of C5a in the acute inflammatory phase. *Ann. Rheum. Dis.* **49**(10)**:** 747-752.

Jozsi M, Prechl J, Bajtay Z, Erdei A (2002). Complement receptor type 1 (CD35) mediates inhibitory signals in human B lymphocytes. *J. Immunol.* **168**(6)**:** 2782-2788.

Kalant D, Cain SA, Maslowska M, Sniderman AD, Cianflone K, Monk PN (2003). The chemoattractant receptor-like protein C5L2 binds the C3a des-Arg77/acylation-stimulating protein. *J. Biol. Chem.* **278**(13)**:** 11123-11129.

Kaufmann SH (2008). Immunology's foundation: the 100-year anniversary of the Nobel Prize to Paul Ehrlich and Elie Metchnikoff. *Nat. Immunol.* **9**(7)**:** 705-712.

Kawai M, Quincy DA, Lane B, Mollison KW, Or YS, Luly JR*, et al.* (1992). Structure-function studies in a series of carboxyl-terminal octapeptide analogues of anaphylatoxin C5a. *J. Med. Chem.* **35**(2)**:** 220-223.

Kawakami M, Ihara I, Suzuki A, Harada Y (1982). Properties of a new complement-dependent bactericidal factor specific for Ra chemotype salmonella in sera of conventional and germ-free mice. *J. Immunol.* **129**(5)**:** 2198-2201.

Kenakin T (2002). Efficacy at G-protein-coupled receptors. *Nat Rev Drug Discov* **1**(2)**:** 103-110.

Kenakin T (2009a). Quantifying biological activity in chemical terms: a pharmacology primer to describe drug effect. *ACS Chem. Biol.* **4**(4)**:** 249-260.

Kenakin T, Christopoulos A (2013). Signalling bias in new drug discovery: detection, quantification and therapeutic impact. *Nat Rev Drug Discov* **12**(3)**:** 205-216.

Kenakin T, Watson C, Muniz-Medina V, Christopoulos A, Novick S (2012). A simple method for quantifying functional selectivity and agonist bias. *ACS Chem. Neurosci.* **3**(3)**:** 193-203.

Kenakin TP (2009b). '7TM receptor allostery: putting numbers to shapeshifting proteins. *Trends Pharmacol. Sci.* **30**(9)**:** 460-469.

Kenakin TP (2012). Biased signalling and allosteric machines: new vistas and challenges for drug discovery. *Br. J. Pharmacol.* **165**(6)**:** 1659-1669.

Kerr MA, Porter RR (1978). The purification and properties of the second component of human complement. *Biochem. J.* **171**(1)**:** 99-107.

Kjaer TR, Thiel S, Andersen GR (2013). Toward a structure-based comprehension of the lectin pathway of complement. *Mol. Immunol.* **56**(4)**:** 413-422.

Klos A, Wende E, Wareham KJ, Monk PN (2013). International Union of Pharmacology. LXXXVII. Complement peptide C5a, C4a, and C3a receptors. *Pharmacol. Rev.* **65**(1)**:** 500-543.

Kolaczkowska E, Kubes P (2013). Neutrophil recruitment and function in health and inflammation. *Nat. Rev. Immunol.* **13**(3)**:** 159-175.

Konteatis ZD, Siciliano SJ, Van Riper G, Molineaux CJ, Pandya S, Fischer P*, et al.* (1994). Development of C5a receptor antagonists. Differential loss of functional responses. *J. Immunol.* **153**(9)**:** 4200-4205.

Lachmann PJ (2009). The amplification loop of the complement pathways. *Adv. Immunol.* **104:** 115-149.

Lachmann PJ, Halbwachs L (1975). The influence of C3b inactivator (KAF) concentration on the ability of serum to support complement activation. *Clin. Exp. Immunol.* **21**(1)**:** 109-114.

Law SK (1988). C3 receptors on macrophages. *J. Cell Sci. Suppl.* **9:** 67-97.

Lee H, Whitfeld PL, Mackay CR (2008). Receptors for complement C5a. The importance of C5aR and the enigmatic role of C5L2. *Immunol. Cell Biol.* **86**(2)**:** 153-160.

Lhotta K, Janecke AR, Scheiring J, Petzlberger B, Giner T, Fally V*, et al.* (2009). A large family with a gain-of-function mutation of complement C3 predisposing to atypical hemolytic uremic syndrome, microhematuria, hypertension and chronic renal failure. *Clin. J. Am. Soc. Nephrol.* **4**(8)**:** 1356-1362.

Li F, De Godoy M, Rattan S (2004). Role of adenylate and guanylate cyclases in beta1-, beta2-, and beta3-adrenoceptor-mediated relaxation of internal anal sphincter smooth muscle. *J. Pharmacol. Exp. Ther.* **308**(3)**:** 1111-1120.

Li R, Coulthard LG, Wu MC, Taylor SM, Woodruff TM (2013). C5L2: a controversial receptor of complement anaphylatoxin, C5a. *FASEB J.* **27**(3)**:** 855-864.

Linton SM, Morgan BP (1999). Properdin deficiency and meningococcal disease--identifying those most at risk. *Clin. Exp. Immunol.* **118**(2)**:** 189-191.

Liszewski MK, Atkinson JP (2015). Complement regulator CD46: genetic variants and disease associations. *Hum Genomics* **9:** 7.

Liszewski MK, Post TW, Atkinson JP (1991). Membrane cofactor protein (MCP or CD46): newest member of the regulators of complement activation gene cluster. *Annu. Rev. Immunol.* **9:** 431-455.

Lorincz Z, Gal P, Dobo J, Cseh S, Szilagyi K, Ambrus G*, et al.* (2000). The cleavage of two C1s subunits by a single active C1r reveals substantial flexibility of the C1s-C1r-C1r-C1s tetramer in the C1 complex. *J. Immunol.* **165**(4)**:** 2048-2051.

Lu J, Teh C, Kishore U, Reid KB (2002). Collectins and ficolins: sugar pattern recognition molecules of the mammalian innate immune system. *Biochim. Biophys. Acta* **1572**(2-3)**:** 387-400.

Lublin DM, Atkinson JP (1989). Decay-accelerating factor: biochemistry, molecular biology, and function. *Annu. Rev. Immunol.* **7:** 35-58.

MacEwan DJ (2002). TNF receptor subtype signalling: differences and cellular consequences. *Cell. Signal.* **14**(6)**:** 477-492.

Maillard N, Wyatt RJ, Julian BA, Kiryluk K, Gharavi A, Fremeaux-Bacchi V*, et al.* (2015). Current Understanding of the Role of Complement in IgA Nephropathy. *J. Am. Soc. Nephrol.* **26**(7)**:** 1503-1512.

Manthey HD, Woodruff TM, Taylor SM, Monk PN (2009). Complement component 5a (C5a). *The International Journal of Biochemistry & Cell Biology* **41**(11)**:** 2114-2117.

Maqbool M, Vidyadaran S, George E, Ramasamy R (2011). Optimisation of laboratory procedures for isolating human peripheral blood derived neutrophils. *Med. J. Malaysia* **66**(4)**:** 296-299.

Marder SR, Chenoweth DE, Goldstein IM, Perez HD (1985). Chemotactic responses of human peripheral blood monocytes to the complement-derived peptides C5a and C5a des Arg. *J. Immunol.* **134**(5)**:** 3325-3331.

Martinelli S, Urosevic M, Daryadel A, Oberholzer PA, Baumann C, Fey MF*, et al.* (2004). Induction of genes mediating interferon-dependent extracellular trap formation during neutrophil differentiation. *J. Biol. Chem.* **279**(42)**:** 44123-44132.

Matsushita M, Fujita T (2001). Ficolins and the lectin complement pathway. *Immunol. Rev.* **180:** 78-85.

Meri S, Morgan BP, Davies A, Daniels RH, Olavesen MG, Waldmann H*, et al.* (1990). Human protectin (CD59), an 18,000-20,000 MW complement lysis restricting factor, inhibits C5b-8 catalysed insertion of C9 into lipid bilayers. *Immunology* **71**(1)**:** 1-9.

Mery L, Boulay F (1993). Evidence that the extracellular N-terminal domain of C5aR contains amino-acid residues crucial for C5a binding. *Eur. J. Haematol.* **51**(5)**:** 282-287.

Milligan G, Kostenis E (2006). Heterotrimeric G-proteins: a short history. *Br. J. Pharmacol.* **147 Suppl 1:** S46-55.

Mochizuki N, Ohba Y, Kiyokawa E, Kurata T, Murakami T, Ozaki T*, et al.* (1999). Activation of the ERK/MAPK pathway by an isoform of rap1GAP associated with G alpha(i). *Nature* **400**(6747)**:** 891-894.

Mollnes TE, Brekke OL, Fung M, Fure H, Christiansen D, Bergseth G*, et al.* (2002). Essential role of the C5a receptor in E coli-induced oxidative burst and phagocytosis revealed by a novel lepirudin-based human whole blood model of inflammation. *Blood* **100**(5)**:** 1869-1877.

Monk PN, Scola AM, Madala P, Fairlie DP (2007). Function, structure and therapeutic potential of complement C5a receptors. *Br. J. Pharmacol.* **152**(4)**:** 429-448.

Morgan BP, Harris CL (2015). Complement, a target for therapy in inflammatory and degenerative diseases. *Nat Rev Drug Discov* **14**(12)**:** 857-877.

Morgan M, Bulmer AC, Woodruff TM, Proctor LM, Williams HM, Stocks SZ*, et al.* (2008). Pharmacokinetics of a C5a receptor antagonist in the rat after different sites of enteral administration. *Eur. J. Pharm. Sci.* **33**(4-5)**:** 390-398.

Morgan P, Van Der Graaf PH, Arrowsmith J, Feltner DE, Drummond KS, Wegner CD*, et al.* (2012). Can the flow of medicines be improved? Fundamental pharmacokinetic and pharmacological principles toward improving Phase II survival. *Drug Discov Today* **17**(9-10)**:** 419-424.

Morris KM, Aden DP, Knowles BB, Colten HR (1982). Complement biosynthesis by the human hepatoma-derived cell line HepG2. *J. Clin. Invest.* **70**(4)**:** 906-913.

Morrison LF (1922). On the Origin and Nature of Alexin (Complement) in Guinea-Pig Blood. *The Journal of Immunology* **7**(5)**:** 435-459.

Mueller-Ortiz SL, Wang D, Morales JE, Li L, Chang JY, Wetsel RA (2009). Targeted disruption of the gene encoding the murine small subunit of carboxypeptidase N (CPN1) causes susceptibility to C5a anaphylatoxin-mediated shock. *J. Immunol.* **182**(10)**:** 6533-6539.

Muller-Eberhard HJ (1969). Complement. *Annu. Rev. Biochem.* **38:** 389-414.

Muller-Eberhard HJ, Polley MJ, Calcott MA (1967). Formation and functional significance of a molecular complex derived from the second and the fourth component of human complement. *J. Exp. Med.* **125**(2)**:** 359-380.

Murray I, Parker RA, Kirchgessner TG, Tran J, Zhang ZJ, Westerlund J*, et al.* (1997). Functional bioactive recombinant acylation stimulating protein is distinct from C3a anaphylatoxin. *J. Lipid Res.* **38**(12)**:** 2492-2501.

Nagasawa S, Stroud RM (1977). Cleavage of C2 by C1s into the antigenically distinct fragments C2a and C2b: demonstration of binding of C2b to C4b. *Proc. Natl. Acad. Sci. U. S. A.* **74**(7)**:** 2998-3001.

Nobles KN, Xiao K, Ahn S, Shukla AK, Lam CM, Rajagopal S*, et al.* (2011). Distinct phosphorylation sites on the beta(2)-adrenergic receptor establish a barcode that encodes differential functions of beta-arrestin. *Sci Signal* **4**(185)**:** ra51.

Nonaka M, Kimura A (2006). Genomic view of the evolution of the complement system. *Immunogenetics* **58**(9)**:** 701-713.

Noris M, Remuzzi G (2015). Glomerular Diseases Dependent on Complement Activation, Including Atypical Hemolytic Uremic Syndrome, Membranoproliferative Glomerulonephritis, and C3 Glomerulopathy: Core Curriculum 2015. *Am. J. Kidney Dis.* **66**(2)**:** 359-375.

O'Flaherty JT, Rossi AG, Redman JF, Jacobson DP (1991). Tumor necrosis factor-alpha regulates expression of receptors for formyl-methionyl-leucyl-phenylalanine, leukotriene B4, and platelet-activating factor. Dissociation from priming in human polymorphonuclear neutrophils. *J. Immunol.* **147**(11)**:** 3842-3847.

Ohno M, Hirata T, Enomoto M, Araki T, Ishimaru H, Takahashi TA (2000). A putative chemoattractant receptor, C5L2, is expressed in granulocyte and immature dendritic cells, but not in mature dendritic cells. *Mol. Immunol.* **37**(8)**:** 407-412.

Okinaga S, Slattery D, Humbles A, Zsengeller Z, Morteau O, Kinrade MB*, et al.* (2003). C5L2, a nonsignaling C5A binding protein. *Biochemistry* **42**(31)**:** 9406-9415.

Opal SM, Cohen J (1999). Clinical gram-positive sepsis: does it fundamentally differ from gram-negative bacterial sepsis? *Crit. Care Med.* **27**(8)**:** 1608-1616.

Oppermann M, Gotze O (1994). Plasma clearance of the human C5a anaphylatoxin by binding to leucocyte C5a receptors. *Immunology* **82**(4)**:** 516-521.

Oppermann M, Raedt U, Hebell T, Schmidt B, Zimmermann B, Gotze O (1993). Probing the human receptor for C5a anaphylatoxin with site-directed antibodies. Identification of a potential ligand binding site on the NH2-terminal domain. *J. Immunol.* **151**(7)**:** 3785-3794.

Orbai AM, Truedsson L, Sturfelt G, Nived O, Fang H, Alarcon GS*, et al.* (2015). Anti-C1q antibodies in systemic lupus erythematosus. *Lupus* **24**(1)**:** 42-49.

Panday A, Sahoo MK, Osorio D, Batra S (2015). NADPH oxidases: an overview from structure to innate immunity-associated pathologies. *Cell. Mol. Immunol.* **12**(1)**:** 5-23.

Pangburn MK, Rawal N (2002). Structure and function of complement C5 convertase enzymes. *Biochem. Soc. Trans.* **30**(Pt 6)**:** 1006-1010.

Parkin J, Cohen B (2001). An overview of the immune system. *Lancet* **357**(9270)**:** 1777-1789.

Patel AK, Campbell AK (1987). The membrane attack complex of complement induces permeability changes via thresholds in individual cells. *Immunology* **60**(1)**:** 135-140.

Payne CM, Glasser L, Tischler ME, Wyckoff D, Cromey D, Fiederlein R*, et al.* (1994). Programmed cell death of the normal human neutrophil: an in vitro model of senescence. *Microsc. Res. Tech.* **28**(4)**:** 327-344.

Perez HD, Chenoweth DE, Goldstein IM (1986). Attachment of human C5a des Arg to its cochemotaxin is required for maximum expression of chemotactic activity. *J. Clin. Invest.* **78**(6)**:** 1589-1595.

Perez HD, Goldstein IM, Chernoff D, Webster RO, Henson PM (1980). Chemotactic activity of C5ades Arg: evidence of a requirement for an anionic peptide 'helper factor' and inhibition by a cationic protein in serum from patients with systemic lupus erythematosus. *Mol. Immunol.* **17**(2)**:** 163-169.

Pickering MC, Botto M, Taylor PR, Lachmann PJ, Walport MJ (2000). Systemic lupus erythematosus, complement deficiency, and apoptosis. *Adv. Immunol.* **76:** 227-324.

Pillemer L, Blum L, Lepow IH, Ross OA, Todd EW, Wardlaw AC (1954). The properdin system and immunity. I. Demonstration and isolation of a new serum protein, properdin, and its role in immune phenomena. *Science* **120**(3112)**:** 279-285.

Pullar JM, Vissers MC, Winterbourn CC (2000). Living with a killer: the effects of hypochlorous acid on mammalian cells. *IUBMB Life* **50**(4-5)**:** 259-266.

Ramage A (2005). Problems of drug selectivity and dose--pharmacology. *J. Physiol.* **569**(Pt 2)**:** 711; author reply 712.

Rasmussen SG, DeVree BT, Zou Y, Kruse AC, Chung KY, Kobilka TS*, et al.* (2011). Crystal structure of the beta2 adrenergic receptor-Gs protein complex. *Nature* **477**(7366)**:** 549-555.

Rawal N, Pangburn MK (2001). Structure/function of C5 convertases of complement. *Int. Immunopharmacol.* **1**(3)**:** 415-422.

Regal JF, Hardy TM, Casey FB, Chakrin LW (1983). Effects of C5a on guinea pig lung: histamine release and mechanism of contraction. *Immunopharmacology* **5**(4)**:** 315-327.

Reis ES, Chen H, Sfyroera G, Monk PN, Kohl J, Ricklin D*, et al.* (2012). C5a receptor-dependent cell activation by physiological concentrations of desarginated C5a: insights from a novel label-free cellular assay. *J. Immunol.* **189**(10)**:** 4797-4805.

Riedemann NC, Guo RF, Sarma VJ, Laudes IJ, Huber-Lang M, Warner RL*, et al.* (2002). Expression and function of the C5a receptor in rat alveolar epithelial cells. *J. Immunol.* **168**(4)**:** 1919-1925.

Rittirsch D, Flierl MA, Nadeau BA, Day DE, Huber-Lang M, Mackay CR*, et al.* (2008). Functional roles for C5a receptors in sepsis. *Nat. Med.* **14**(5)**:** 551-557.

Rollins TE, Siciliano S, Kobayashi S, Cianciarulo DN, Bonilla-Argudo V, Collier K*, et al.* (1991). Purification of the active C5a receptor from human polymorphonuclear leukocytes as a receptor-Gi complex. *Proc. Natl. Acad. Sci. U. S. A.* **88**(3)**:** 971-975.

Rother RP, Rollins SA, Mojcik CF, Brodsky RA, Bell L (2007). Discovery and development of the complement inhibitor eculizumab for the treatment of paroxysmal nocturnal hemoglobinuria. *Nat. Biotechnol.* **25**(11)**:** 1256-1264.

Sacks T, Moldow CF, Craddock PR, Bowers TK, Jacob HS (1978a). Endothelial damage provoked by toxic oxygen radicals released from complement-triggered granulocytes. *Prog. Clin. Biol. Res.* **21:** 719-726.

Sacks T, Moldow CF, Craddock PR, Bowers TK, Jacob HS (1978b). Oxygen radicals mediate endothelial cell damage by complement-stimulated granulocytes. An in vitro model of immune vascular damage. *J. Clin. Invest.* **61**(5)**:** 1161-1167.

Sahu A, Lambris JD (2001). Structure and biology of complement protein C3, a connecting link between innate and acquired immunity. *Immunol. Rev.* **180:** 35-48.

Sarma JV, Ward PA (2011). The complement system. *Cell Tissue Res.* **343**(1)**:** 227-235.

Schramm M, Wiegmann K, Schramm S, Gluschko A, Herb M, Utermohlen O*, et al.* (2014). Riboflavin (vitamin B2) deficiency impairs NADPH oxidase 2 (Nox2) priming and defense against Listeria monocytogenes. *Eur. J. Immunol.* **44**(3)**:** 728-741.

Scola A-M, Johswich K-O, Morgan BP, Klos A, Monk PN (2009). The human complement fragment receptor, C5L2, is a recycling decoy receptor. *Mol. Immunol.* **46**(6)**:** 1149-1162.

Scola AM, Higginbottom A, Partridge LJ, Reid RC, Woodruff T, Taylor SM*, et al.* (2007). The role of the N-terminal domain of the complement fragment receptor C5L2 in ligand binding. *J. Biol. Chem.* **282**(6)**:** 3664-3671.

Seow V, Lim J, Cotterell AJ, Yau MK, Xu W, Lohman RJ*, et al.* (2016). Receptor residence time trumps drug-likeness and oral bioavailability in determining efficacy of complement C5a antagonists. *Sci. Rep.* **6:** 24575.

Servais A, Noel LH, Roumenina LT, Le Quintrec M, Ngo S, Dragon-Durey MA*, et al.* (2012). Acquired and genetic complement abnormalities play a critical role in dense deposit disease and other C3 glomerulopathies. *Kidney Int.* **82**(4)**:** 454-464.

Shin HS, Snyderman R, Friedman E, Mellors A, Mayer MM (1968). Chemotactic and anaphylatoxic fragment cleaved from the fifth component of guinea pig complement. *Science* **162**(3851)**:** 361-363.

Siciliano SJ, Rollins TE, DeMartino J, Konteatis Z, Malkowitz L, Van Riper G*, et al.* (1994). Two-site binding of C5a by its receptor: an alternative binding paradigm for G protein-coupled receptors. *Proc. Natl. Acad. Sci. U. S. A.* **91**(4)**:** 1214-1218.

Skerka C, Chen Q, Fremeaux-Bacchi V, Roumenina LT (2013). Complement factor H related proteins (CFHRs). *Mol. Immunol.* **56**(3)**:** 170-180.

Skidgel RA, Erdos EG (2007). Structure and function of human plasma carboxypeptidase N, the anaphylatoxin inactivator. *Int. Immunopharmacol.* **7**(14)**:** 1888-1899.

Smith LC, Chang L, Britten RJ, Davidson EH (1996). Sea urchin genes expressed in activated coelomocytes are identified by expressed sequence tags. Complement homologues and other putative immune response genes suggest immune system homology within the deuterostomes. *J. Immunol.* **156**(2)**:** 593-602.

Snyderman R, Phillips JK, Mergenhagen SE (1971). Biological activity of complement in vivo. Role of C5 in the accumulation of polymorphonuclear leukocytes in inflammatory exudates. *J. Exp. Med.* **134**(5)**:** 1131-1143.

Strobel S, Zimmering M, Papp K, Prechl J, Jozsi M (2010). Anti-factor B autoantibody in dense deposit disease. *Mol. Immunol.* **47**(7-8)**:** 1476-1483.

Stroud RM, Mayer MM, Miller JA, McKenzie AT (1966). C'2ad, an inactive derivative of C'2 released during decay of EAC'4,2a. *Immunochemistry* **3**(3)**:** 163-176.

Sumichika H, Sakata K, Sato N, Takeshita S, Ishibuchi S, Nakamura M*, et al.* (2002). Identification of a potent and orally active non-peptide C5a receptor antagonist. *J. Biol. Chem.* **277**(51)**:** 49403-49407.

Sun L, Ye RD (2012). Role of G protein-coupled receptors in inflammation. *Acta Pharmacol. Sin.* **33**(3)**:** 342-350.

Super M, Thiel S, Lu J, Levinsky RJ, Turner MW (1989). Association of low levels of mannan-binding protein with a common defect of opsonisation. *Lancet* **2**(8674)**:** 1236-1239.

Tartaglia LA, Rothe M, Hu YF, Goeddel DV (1993). Tumor necrosis factor's cytotoxic activity is signaled by the p55 TNF receptor. *Cell* **73**(2)**:** 213-216.

Tofts PS, Chevassut T, Cutajar M, Dowell NG, Peters AM (2011). Doubts concerning the recently reported human neutrophil lifespan of 5.4 days. *Blood* **117**(22)**:** 6050-6052; author reply 6053-6054.

Tonnesen MG, Smedly LA, Henson PM (1984). Neutrophil-endothelial cell interactions. Modulation of neutrophil adhesiveness induced by complement fragments C5a and C5a des arg and formyl-methionyl-leucyl-phenylalanine in vitro. *J. Clin. Invest.* **74**(5)**:** 1581-1592.

Urban CF, Ermert D, Schmid M, Abu-Abed U, Goosmann C, Nacken W*, et al.* (2009). Neutrophil extracellular traps contain calprotectin, a cytosolic protein complex involved in host defense against Candida albicans. *PLoS Pathog.* **5**(10)**:** e1000639.

Vallota EH, Muller-Eberhard HJ (1973). Formation of C3a and C5a anaphylatoxins in whole human serum after inhibition of the anaphylatoxin inactivator. *J. Exp. Med.* **137**(5)**:** 1109-1123.

Vergunst CE, Gerlag DM, Dinant H, Schulz L, Vinkenoog M, Smeets TJ*, et al.* (2007). Blocking the receptor for C5a in patients with rheumatoid arthritis does not reduce synovial inflammation. *Rheumatology (Oxford)* **46**(12)**:** 1773-1778.

Vik DP, Fearon DT (1987). Cellular distribution of complement receptor type 4 (CR4): expression on human platelets. *J. Immunol.* **138**(1)**:** 254-258.

Vogt W, Bodammer G, Lufft E, Schmidt G (1969). Formation of anaphylatoxin in human serum. *Experientia* **25**(7)**:** 744-745.

Wagner C, Ochmann C, Schoels M, Giese T, Stegmaier S, Richter R*, et al.* (2006). The complement receptor 1, CR1 (CD35), mediates inhibitory signals in human T-lymphocytes. *Mol. Immunol.* **43**(6)**:** 643-651.

Walport MJ (2001). Complement. First of two parts. *N. Engl. J. Med.* **344**(14)**:** 1058-1066.

Ward PA, Hill JH (1970). C5 chemotactic fragments produced by an enzyme in lysosomal granules of neutrophils. *J. Immunol.* **104**(3)**:** 535-543.

Waters SM, Brodbeck RM, Steflik J, Yu J, Baltazar C, Peck AE*, et al.* (2005). Molecular characterization of the gerbil C5a receptor and identification of a transmembrane domain V amino acid that is crucial for small molecule antagonist interaction. *J. Biol. Chem.* **280**(49)**:** 40617-40623.

Weber C, Kitayama J, Springer TA (1996). Differential regulation of beta 1 and beta 2 integrin avidity by chemoattractants in eosinophils. *Proc. Natl. Acad. Sci. U. S. A.* **93**(20)**:** 10939-10944.

Webster RO, Hong SR, Johnston RB, Jr., Henson PM (1980). Biologial effects of the human complement fragments C5a and C5ades Arg on neutrophil function. *Immunopharmacology* **2**(3)**:** 201-219.

Wetsel RA, Kolb WP (1983). Expression of C5a-like biological activities by the fifth component of human complement (C5) upon limited digestion with noncomplement enzymes without release of polypeptide fragments. *J. Exp. Med.* **157**(6)**:** 2029-2048.

Williams SC, Sim RB (1994). Binding sites involved in the formation of the C3 (H2O)-factor B complex of the alternative pathway of complement. *Biochem. Soc. Trans.* **22**(1)**:** 2S.

Wirthmueller U, Dewald B, Thelen M, Schafer MK, Stover C, Whaley K*, et al.* (1997). Properdin, a positive regulator of complement activation, is released from secondary granules of stimulated peripheral blood neutrophils. *J. Immunol.* **158**(9)**:** 4444-4451.

Wu C, Orozco C, Boyer J, Leglise M, Goodale J, Batalov S*, et al.* (2009). BioGPS: an extensible and customizable portal for querying and organizing gene annotation resources. *Genome Biol.* **10**(11)**:** R130.

Yancey KB, Lawley TJ, Dersookian M, Harvath L (1989). Analysis of the interaction of human C5a and C5a des Arg with human monocytes and neutrophils: flow cytometric and chemotaxis studies. *J. Invest. Dermatol.* **92**(2)**:** 184-189.

Yazdanpanah B, Wiegmann K, Tchikov V, Krut O, Pongratz C, Schramm M*, et al.* (2009). Riboflavin kinase couples TNF receptor 1 to NADPH oxidase. *Nature* **460**(7259)**:** 1159-1163.

Yih Chen J, Ling Wu Y, Yin Mok M, Jan Wu YJ, Lintner KE, Wang CM*, et al.* (2016). Effects of Complement C4 Gene Copy Number Variations, Size Dichotomy, and C4A Deficiency on Genetic Risk and Clinical Presentation of Systemic Lupus Erythematosus in East Asian Populations. *Arthritis Rheumatol* **68**(6)**:** 1442-1453.

Zhu L, Zhai YL, Wang FM, Hou P, Lv JC, Xu DM*, et al.* (2015). Variants in Complement Factor H and Complement Factor H-Related Protein Genes, CFHR3 and CFHR1, Affect Complement Activation in IgA Nephropathy. *J. Am. Soc. Nephrol.* **26**(5)**:** 1195-1204.

Zipfel PF, Skerka C (2009). Complement regulators and inhibitory proteins. *Nat. Rev. Immunol.* **9**(10)**:** 729-740.

Appendix

Appendix 1

C5a receptor sequence confirmation.

Translated amino acid sequence for the recombinant $C5a_1$ receptor (A), $C5a_2$ receptor (B) and their alignment to published amino acid sequences. Amino acid sequence alignment was performed using the Life Technologies Vector NTi application.

(A)

```
                                1                                                50
             C5a1_PCR  (1) MNSFNYTTPDYGHYDDKDTLDLNTPVDKTSNTLRVPDILALVIFAVVFLV
Human C5a1 NP_001727  (1) MNSFNYTTPDYGHYDDKDTLDLNTPVDKTSNTLRVPDILALVIFAVVFLV
           Consensus  (1) MNSFNYTTPDYGHYDDKDTLDLNTPVDKTSNTLRVPDILALVIFAVVFLV
                               51                                               100
             C5a1_PCR (51) GVLGNALVVWVTAFEAKRTINAIWFLNLAVADFLSCLALPILFTSIVQHH
Human C5a1 NP_001727 (51) GVLGNALVVWVTAFEAKRTINAIWFLNLAVADFLSCLALPILFTSIVQHH
           Consensus (51) GVLGNALVVWVTAFEAKRTINAIWFLNLAVADFLSCLALPILFTSIVQHH
                              101                                              150
             C5a1_PCR (101) HWPFGGAACSILPSLILLNMYASILLLATISADRFLLVFKPIWCQNFRGA
Human C5a1 NP_001727 (101) HWPFGGAACSILPSLILLNMYASILLLATISADRFLLVFKPIWCQNFRGA
           Consensus (101) HWPFGGAACSILPSLILLNMYASILLLATISADRFLLVFKPIWCQNFRGA
                              151                                              200
             C5a1_PCR (151) GLAWIACAVAWGLALLLTIPSFLYRVVREEYFPPKVLCGVDYSHDKRRER
Human C5a1 NP_001727 (151) GLAWIACAVAWGLALLLTIPSFLYRVVREEYFPPKVLCGVDYSHDKRRER
           Consensus (151) GLAWIACAVAWGLALLLTIPSFLYRVVREEYFPPKVLCGVDYSHDKRRER
                              201                                              250
             C5a1_PCR (201) AVAIVRLVLGFLWPLLTLTICYTFILLRTWSRRATRSTKTLKVVVAVVAS
Human C5a1 NP_001727 (201) AVAIVRLVLGFLWPLLTLTICYTFILLRTWSRRATRSTKTLKVVVAVVAS
           Consensus (201) AVAIVRLVLGFLWPLLTLTICYTFILLRTWSRRATRSTKTLKVVVAVVAS
                              251                                              300
             C5a1_PCR (251) FFIFWLPYQVTGIMMSFLEPSSPTFLLLNKLDSLCVSFAYINCCINPIIY
Human C5a1 NP_001727 (251) FFIFWLPYQVTGIMMSFLEPSSPTFLLLNKLDSLCVSFAYINCCINPIIY
           Consensus (251) FFIFWLPYQVTGIMMSFLEPSSPTFLLLNKLDSLCVSFAYINCCINPIIY
                              301                                              350
             C5a1_PCR (301) VVAGQGFQGRLRKSLPSLLRNVLTEESVVRESKSFTRSTVDTMAQKTQAV
Human C5a1 NP_001727 (301) VVAGQGFQGRLRKSLPSLLRNVLTEESVVRESKSFTRSTVDTMAQKTQAV
           Consensus (301) VVAGQGFQGRLRKSLPSLLRNVLTEESVVRESKSFTRSTVDTMAQKTQAV
```

(B)

```
                                1                                                50
             C5a2_PCR   (1) MGNDSVSYEYGDYSDLSDRPVDCLDGACLAIDPLRVAPLPLYAAIFLVGV
Human C5a2 NP_060955    (1) MGNDSVSYEYGDYSDLSDRPVDCLDGACLAIDPLRVAPLPLYAAIFLVGV
           Consensus    (1) MGNDSVSYEYGDYSDLSDRPVDCLDGACLAIDPLRVAPLPLYAAIFLVGV
                               51                                               100
             C5a2_PCR  (51) PGNAMVAWVAGKVARRRVGATWLLHLAVADLLCCLSLPILAVPIARGGHW
Human C5a2 NP_060955   (51) PGNAMVAWVAGKVARRRVGATWLLHLAVADLLCCLSLPILAVPIARGGHW
           Consensus   (51) PGNAMVAWVAGKVARRRVGATWLLHLAVADLLCCLSLPILAVPIARGGHW
                              101                                              150
             C5a2_PCR (101) PYGAVGCRALPSIILLTMYASVLLLAALSADLCFLALGPAWWSTVQRACG
Human C5a2 NP_060955 (101) PYGAVGCRALPSIILLTMYASVLLLAALSADLCFLALGPAWWSTVQRACG
           Consensus (101) PYGAVGCRALPSIILLTMYASVLLLAALSADLCFLALGPAWWSTVQRACG
                              151                                              200
             C5a2_PCR (151) VQVACGAAWTLALLLTVPSAIYRRLHQEHFPARLQCVVDYGGSSSTENAV
Human C5a2 NP_060955 (151) VQVACGAAWTLALLLTVPSAIYRRLHQEHFPARLQCVVDYGGSSSTENAV
           Consensus (151) VQVACGAAWTLALLLTVPSAIYRRLHQEHFPARLQCVVDYGGSSSTENAV
                              201                                              250
             C5a2_PCR (201) TAIRFLFGFLGPLVAVASCHSALLCWAARRCRPLGTAIVVGFFVCWAPYH
Human C5a2 NP_060955 (201) TAIRFLFGFLGPLVAVASCHSALLCWAARRCRPLGTAIVVGFFVCWAPYH
           Consensus (201) TAIRFLFGFLGPLVAVASCHSALLCWAARRCRPLGTAIVVGFFVCWAPYH
                              251                                              300
             C5a2_PCR (251) LLGLVLTVAAPNSALLARALRAEPLIVGLALAHSCLNPMLFLYFGRAQLR
Human C5a2 NP_060955 (251) LLGLVLTVAAPNSALLARALRAEPLIVGLALAHSCLNPMLFLYFGRAQLR
           Consensus (251) LLGLVLTVAAPNSALLARALRAEPLIVGLALAHSCLNPMLFLYFGRAQLR
                              301                  337
             C5a2_PCR (301) RSLPAACHWALRESQGQDESVDSKKSTSHDLVSEMEV
Human C5a2 NP_060955 (301) RSLPAACHWALRESQGQDESVDSKKSTSHDLVSEMEV
           Consensus (301) RSLPAACHWALRESQGQDESVDSKKSTSHDLVSEMEV
```

Appendix 2

Using a Microsoft Excel tool developed by Dr Terry Kenakin, the Operational Model of Agonism was fit to the neutrophil functional data from chapter 5. Estimates of affinity (K_A) agonist efficacy (τ) were obtained for both C5a and C5a des Arg in each neutrophil assay system. These parameters were used in the modified Gaddum equation, described in the final discussion, to understand the composite neutrophil response induced by combinations of C5a and C5a des Arg in the absence and presence of a competitive $C5a_1$ receptor antagonist.

The Black & Leff Operational Model of Agonism:

$$\text{Response} = \frac{[A]\cdot\tau\cdot E_{max}}{[A](\tau + 1) + K_A}$$

Where:

[A] = Agonist concentration

τ (tau) = Efficacy of an agonist which is made up of both the intrinsic efficacy of the agonist and the sensitivity of the biological system.

E_{max} = Maximal response capability of the system

K_A = The equilibrium dissociation constant for the agonist (affinity)

The Operational Model of Agonism fit to the neutrophil functional data to obtain estimates of K_A and τ.